

University of Strathclyde
Strathclyde Institute of Pharmacy and
Biomedical Sciences

Non-Ionic Surfactant Vesicles as a Delivery System
for Cisplatin

by

Manal Mohamed Alsaadi

A thesis presented in fulfilment of the requirements for the degree of
Doctor of Philosophy

October 2011

Copyright Statement

This thesis is the result of the author's original research. It has been composed by the author and has not been previously submitted for examination which has led to the award of a degree.

The copyright of this thesis belongs to the author under the terms of the United Kingdom Copyright Act as qualified by University of Strathclyde Regulation 3.50. Due acknowledgement must always be made of the use of any material contained in, or derived from, this thesis.

Signed:

Date:

I would like to dedicate this thesis to the memory of all the courageous revolutionaries of my beloved country Libya who sacrificed their lives for us to live free.

Their continuous determination and strong belief that surrender is not an option has given me the motivation and encouragement to continue writing at a very difficult and overwhelming time for all Libyans.

Acknowledgments

The opportunity to study for a PhD is the greatest gift which would not have been possible without the grace of God. I am grateful to Him for all the blessings that have led me to this.

I would first like to thank my supervisor Prof Alex Mullen who has made studying for a PhD the best experience I have ever had. His generosity, to share his knowledge, and his great support have given me the inspiration and motivation throughout my study. He was also a friend during the difficult times and gave me the encouragement I needed. He is an amazing supervisor with a great sense of humour. Alex, it was a great honour to be your student.

I would also like to thank Dr Val Ferro whom I am indebted to for her invaluable advice. She has unconditionally offered me help throughout my study despite her academic commitments. She is a great friend who has always been there for me and her door was always open to me. Val, I am privileged to know a remarkable person who is kind and has a great heart like you.

I thank all my friends and colleagues whom I have shared good times with inside and outside of university during our study. Great thanks to Heba, Jo, Ju Yen, Hibah, Issra, Gemma, Vivek, Mohammed and Guarav.

I thank the Libyan Government for funding my study.

Last but not least my greatest appreciation goes to my family who have supported me and have been there for me to achieve my ambition. I am grateful to my father, Mohamed, my mother, Sania, my sisters, Hanan and Amal, and my brothers, Yahya and Ahmed. This would not have been possible without you, thank you and love you all. I would not have done this without your encouragement.

Abstract

Cisplatin is a leading anti-cancer drug used in the treatment of various cancers. However, its clinical use is limited by its undesirable toxic side effect profile and the potential of certain tumours to be or to develop resistance to cisplatin. Encapsulation of cisplatin within a vesicular structure such as non-ionic surfactant vesicles (NIVs) was developed to overcome these limitations.

Characterisation studies showed that the size and negative surface charge of cisplatin NIVs could be exploited in enhancing their uptake by the mononuclear phagocytic system present in the lungs, liver and spleen. Physicochemical stability of the systems over a 15 month time period was demonstrated in relation to vesicle size and surface charge; the absence of colloidal aggregation and chemical stability of the lipid components.

Vesicle entrapment efficiency of cisplatin was improved with increasing cisplatin concentrations used for lipid hydration but subsequent precipitation of drug limited the usefulness of such an approach. Removal of untrapped cisplatin by the use of diafiltration and resuspension in lower concentrations of cisplatin solution overcame this problem but resulted in drug leakage from the vesicles over time.

Preliminary *in vitro* and *in vivo* studies were used to evaluate NIVs. *In vitro* studies confirmed the potential of NIVs in enhancing the anti-cancer effect of cisplatin in comparison to free drug in a murine B16-F0 murine melanoma cell line. *In vivo* rodent studies compared cisplatin NIVs with free drug solution administered as single doses by intravenous or pulmonary routes of delivery. Intravenous delivery demonstrated more representable results with greater accumulation of cisplatin in the lungs when administered as a NIVs formulation in comparison to free drug solution.

In conclusion, NIVs have great potential to be a viable delivery platform for the administration of cisplatin.

Publications

- Alsaadi, M., Carter, K., Mullen, A. The use of a vesicular delivery system in the enhancement of cisplatin bioavailability. Abstract for poster presentation at Strathclyde University Research Day (2009) and UKICRS Symposium (2010).
- Alsaadi, M., Carter, K., Mullen, A. The use of a vesicular delivery system in the enhancement of cisplatin bioavailability. Abstract for oral presentation at the Integrative Mammalian Biology Symposium (2010).
- Alsaadi, M., Carter, K., Mullen, A. The use of a vesicular delivery system in the enhancement of cisplatin bioavailability. Abstract for poster presentation at the CRS (2010).
- Alsaadi, M., Roberts, F., Vass, M., Ferro, V., Dunlop, D., Carter, K., Mullen, A. The potential of a non-ionic surfactant vesicle system to enhance cisplatin delivery to lung tumours. In preparation.
- Alsaadi, M., Carter, K., Mullen, A. The use of high performance liquid chromatography and evaporative light scattering detection in analysing the lipid content of non-ionic surfactant vesicles. In preparation.
- Alsaadi, M., Italia, J., Mullen, A., Kumar, M.N.V., Candlish, A., Williams, R., Shaw, C., Al Gawhari, F., Coombs, G., Weise, M., Thomson, A., Puig, M., Wallace, J., Sharp, A., Wheeler, L., Warn, P., Carter, K. The efficacy of aerosol treatment with non-ionic surfactant vesicles containing amphotericin B in rodent models of pulmonary aspergillus infection. In press.
- H. Mansour, F. McInnes, L-A. Hodges, M. Alsaadi, A. Mullen, *In vivo* performance of lyophilised glibenclamide capsule formulations allowing oral administration to Beagle dogs. In preparation.
- Campbell, S., Alawa, J., Doro, B., Henriquez, F., Roberts, C., Nok, A., Alawa, C., Alsaadi, M., Mullen, A., Carter, C. (2012). Comparative assessment of a DNA and protein *Leishmania donovani* gamma glutamyl cysteine synthetase

vaccine to cross-protect against murine cutaneous leishmaniasis caused by *L. major* or *L. Mexicana* infection. *Vaccine*, 30 (7), 1357-1363

Table of Contents

Acknowledgments	iii
Abstract	iv
Publications	v
List of Abbreviations	xiii
List of Figures	xv
List of Tables	xxiii
Chapter 1. Introduction	1
1.1. Cancer – an overview	1
1.1.1. History of cancer	1
1.1.2. Formation of cancer	2
1.1.3. Causes of cancer	3
1.1.4. Treatment of cancer	3
1.1.5. Classification of cancer	4
1.1.6. Cancer epidemiology	4
1.1.7. Lung cancer	6
1.1.7.1. Causes of lung cancer	7
1.1.7.2. Classification of lung cancer	8
1.1.7.3. Staging of lung cancer	10
1.1.7.4. Treatment of lung cancer	10
1.2. Delivery routes and their physiological barriers	14
1.2.1. Intravenous delivery	14
1.2.1.1. Physiology of the cardiovascular system	14
1.2.1.1.1. Physiological barriers in intravenous delivery	16
1.2.2. Pulmonary delivery	17
1.2.2.1. Physiology of the respiratory system	17
1.2.2.1.1. The upper respiratory tract and larynx	17
1.2.2.1.2. The trachea	19
1.2.2.1.3. The bronchi and bronchioles	19
1.2.2.1.4. The alveoli	20
1.2.2.2. Physiological barriers in pulmonary delivery	22
1.3. Platinum therapy	22

1.3.1. Cisplatin	24
1.3.1.1. History of cisplatin.....	24
1.3.1.2. Uses of cisplatin.....	24
1.3.1.3. Administration of cisplatin	24
1.3.1.4. Side effects of cisplatin	25
1.3.1.5. Mechanism of action of cisplatin	25
1.3.1.6. Pharmacokinetics of cisplatin	29
1.3.1.7. Resistance to cisplatin	30
1.3.1.7.1. Resistance mechanisms before DNA binding	31
1.3.1.7.2. Resistance mechanisms after DNA binding.....	32
1.3.1.8. Circumvention of cisplatin resistance	32
1.3.2. Carboplatin	34
1.3.3. Oxaliplatin.....	34
1.3.4. Picoplatin.....	34
1.3.5. Satraplatin	35
1.4. Vesicular delivery systems – liposomes and niosomes	36
1.4.1. Liposomes	37
1.4.1.1. Classification of liposomes.....	38
1.4.1.2. Implications of liposomal physical characteristics.....	39
1.4.1.3. Clinical studies of liposomes	40
1.4.2. Niosomes.....	43
1.4.2.1. Classification of niosomes	43
1.4.2.2. Implications of niosomal physical characteristics.....	44
1.4.2.3. Clinical studies of niosomes	44
1.5. Analytical methods for detecting platinum.....	46
1.6. Study outline	50
Chapter 2. Materials and Methods.....	52
2.1. Materials.....	52
2.1.1. Materials used in preparation of NIVs	52
2.1.2. Materials used in HPLC analysis of cisplatin.....	52
2.1.3. Materials used in HPLC analysis of lipids	52
2.1.4. Materials used in pilot production of empty and cisplatin NIVs.....	52
2.1.5. Materials used for <i>in vitro</i> proliferation and cytotoxicity studies	52

2.1.6. Materials used for <i>in vivo</i> studies	53
2.1.7. Animals used in the <i>in vivo</i> studies.....	53
2.2. Methods	53
2.2.1. Preparation of NIVs	53
2.2.2. Preparation of freeze-dried empty NIVs	54
2.2.3. Ultrafiltration of NIVs	54
2.2.4. Characterisation of NIVs.....	54
2.2.4.1. Entrapment efficiency of NIVs	54
2.2.4.2. Sizing and zeta potential (ZP) of NIVs	55
2.2.4.3. Freeze-fracture electron microscopic images (FFEM) of NIVs	55
2.2.4.4. Lipid content of NIVs	56
2.2.5. HPLC analysis of platinum	56
2.2.5.1. HPLC instrumentation and chromatographic conditions	56
2.2.5.2. HPLC method I.....	57
2.2.5.3. HPLC method II.....	57
2.2.5.4. HPLC method III	58
2.2.6. HPLC analysis of lipids	58
2.2.6.1. HPLC instrumentation and chromatographic conditions	58
2.2.6.2. Optimisation of evaporative light scattering detector (ELSD)	60
2.2.6.3. HPLC method	60
2.2.7. Pilot production of NIVs for stability study	61
2.2.7.1. Stability study I.....	61
2.2.7.2. Stability study II.....	64
2.2.8. <i>In vitro</i> proliferation and cytotoxicity studies	66
2.2.8.1. Cell culture	66
2.2.8.2. <i>In vitro</i> proliferation studies	66
2.2.8.3. <i>In vitro</i> cytotoxicity studies	67
2.2.9. <i>In vivo</i> studies	68
2.2.9.1. Treatment of animals.....	69
2.2.9.2. <i>In vivo</i> anti-tumour activity studies	69
2.2.9.3. <i>In vivo</i> tissue uptake studies	70
2.2.9.4. Pharmacokinetic study	70
2.2.10. Statistical analysis.....	71

Chapter 3. Characterisation studies of NIVs.....	72
3.1. Introduction	72
3.1.1. Principle theory of zeta potential (ZP)	73
3.1.2. Principle theory of size	76
3.1.3. Principle theory of freeze fracture electron microscopy (FFEM).....	78
3.2. Results	81
3.2.1. Entrapment efficiency, sizing and ZP studies	81
3.2.1.1. Non-processed and processed NIVs.....	81
3.2.1.1.1. Non-processed and processed NIVs in different volumes	81
3.2.1.1.2. Non-processed and processed NIVs in equal volumes	84
3.2.1.2. Processed NIVs prepared using different concentrations of cisplatin	87
3.2.1.3. Processed NIVs prepared using 6mg/ml cisplatin and suspended in different solutions post-manufacture	91
3.2.2. FFEM studies	94
3.2.2.1. Non-processed NIVs (150µmol) hydrated with 0.5mg/ml cisplatin	94
3.2.2.2. Non-processed NIVs hydrated with 6mg/ml cisplatin	96
3.2.2.3. Processed NIVs hydrated with 6mg/ml cisplatin	96
3.3. Discussion.....	98
3.4. Conclusion	108
Chapter 4. Development of HPLC methods for platinum and lipid quantification	109
4.1. Introduction	109
4.1.1. Quantification of platinum by HPLC.....	110
4.1.2. Quantification of lipids by HPLC.....	111
4.2. Results	112
4.2.1. Quantification of platinum by HPLC.....	112
4.2.1.1. Method I	112
4.2.1.2. Method II.....	117
4.2.1.3. Method III.....	121
4.2.3. Quantification of lipids by HPLC	129
4.3. Discussion.....	140
4.4. Conclusion	146
Chapter 5. Stability studies of NIVs produced in a pilot scale	147
5.1. Introduction	147

5.2. Results	149
5.2.1. Comparison between empty NIVs and cisplatin NIVs – Stability study I	149
5.2.1.1. Physical appearance of cisplatin NIVs	149
5.2.1.2. Cisplatin content in NIVs (entrapment efficiency, supernatant and total)...150	
5.2.1.3. Lipid content – cholesterol, surfactant VIII and dicetyl phosphate (DCP)..154	
5.2.1.3.1. Cholesterol content	154
5.2.1.3.2. Surfactant VIII content	161
5.2.1.3.3. DCP content	168
5.2.1.4. Size and zeta potential (ZP) of empty and cisplatin NIVs.....	175
5.2.1.4.1. Size results	176
5.2.1.4.2. ZP results	181
5.2.2. Comparison between NIVs of different cisplatin concentrations – stability study II.....	186
5.2.2.1. Physical appearance of NIVs prepared with different cisplatin concentrations	186
5.2.2.2. Cisplatin content in NIVs (entrapment efficiency, supernatant and total)...187	
5.2.2.3. Vesicle size and ZP of NIVs hydrated with different concentrations of cisplatin.....	193
5.2.2.3.1. Vesicle size results	193
5.2.2.3.2. ZP results	197
5.2.2.4. Lipid content	200
5.2.2.4.1. Cholesterol content	200
5.2.2.4.2. Surfactant VIII content	207
5.2.2.4.3. DCP content	213
5.3. Discussion	218
5.4. Conclusion	235
Chapter 6. <i>In vitro</i> evaluation of cisplatin NIVs – a preliminary study	236
6.1. Introduction	236
6.2. Results	239
6.2.1. <i>In vitro</i> proliferation studies	239
6.2.2. <i>In vitro</i> cytotoxicity studies	240
6.3. Discussion	244
6.4. Conclusion	246
Chapter 7. <i>In vivo</i> evaluation of cisplatin NIVs – a preliminary study	248

7.1. Introduction	248
7.1.1. Theory of vibrating plate technology in inhalation therapy	249
7.1.2. Theory of inductively coupled plasma mass spectroscopy (ICP-MS)	250
7.2. Results	252
7.2.1. <i>In vivo</i> anti-tumour activity	252
7.2.1.1. Comparison between control (0.9% w/v NaCl) solution, cisplatin solution and non-processed cisplatin NIVs	252
7.2.1.2. Comparison between control (0.9% w/v NaCl) solution, cisplatin solution and processed cisplatin NIVs over one time-point	254
7.2.1.3. Comparison between control (0.9% w/v NaCl) solution and processed cisplatin NIVs over two time-points.....	258
7.2.2. <i>In vivo</i> tissue uptake of cisplatin.....	261
7.2.2.1. Comparison between cisplatin solution and non-processed cisplatin NIVs	261
7.2.2.2. Comparison between cisplatin solution and processed cisplatin NIVs	264
7.2.3. Preliminary pharmacokinetic study	267
7.3. Discussion	269
7.4. Conclusion	285
General Conclusions and Future work	286
References	291

List of Abbreviations

AB	Alamar Blue
AmB	Amphotericin B
ATRA	All-trans-retinoic acid
CRUK	Cancer Research UK
CTR1	Copper transporter I protein
DCP	Dicetyl phosphate
DLS	Dynamic light scattering
DMEM	Dulbecco's modified eagle medium
DDTC	Sodium diethyldithiocarbamate
DNA	Deoxyribose nucleic acid
ELSD	Evaporative light scattering detector
FFEM	Freeze-fracture electron microscopy
HPLC	High performance liquid chromatography
ICP-MS	Inductively coupled plasma- mass spectroscopy
LUV	Large unilamellar vesicle
MLV	Multilamellar vesicle
MMAD	Mass median aerodynamic diameter
MMR	Mismatch mechanism repair
MPS	Mononuclear phagocytic system
MVV	Multivesicular vesicle

NER	Nucleotide excision repair
NICE	National Institute for Clinical Excellence
NIVs	Non-ionic surfactant vesicles
NP-HPLC	Normal phase-HPLC
NSCLC	Non-small cell lung cancer
PEG	Polyethylene glycol
RP-HPLC	Reverse phase-HPLC
rpm	Rotations per minute
RSD	Relative standard deviation
SCLC	Small cell lung cancer
SLPM	Standard litre per minute
SSG	Sodium stibogluconate
Surfactant VIII	Tetraethylene glycol mono-n-hexadecyl ether
SUV	Small unilamellar vesicle
UV	Ultraviolet
WHO	World Health Organisation
ZP	Zeta potential

List of Figures

Figure 1.1. Distribution of cancer incidence worldwide.	5
Figure 1.2. Distribution of cancer deaths worldwide.	5
Figure 1.3. Incidence of the most common cancers in both males and females.	6
Figure 1.4. Most common deaths due to cancer in both males and females.	7
Figure 1.5. A schematic diagram of the basic clinical classification of lung cancer.	9
Figure 1.6. Schematic diagram describing the guidelines for treating the different stages of SCLC.	11
Figure 1.7. Schematic diagram describing the guidelines for treating the different stages of NSCLC.	12
Figure 1.8. Schematic diagram describing the types of capillaries.	15
Figure 1.9. Structure of the respiratory system.	18
Figure 1.10. The anatomical structure of the bronchial tree (a), the alveoli at the termination of the respiratory bronchiole (b), the cell composition of alveoli (c) and the exchange surfaces between alveolar epithelium and capillary endothelium (d)..	21
Figure 1.11. The chemical structure of platinum anti-cancer drugs.	23
Figure 1.12. The mechanism of cisplatin entry into the cell and possible factors related to resistance.	26
Figure 1.13. The reaction of cisplatin with DNA to form 1,2-intrastrand crosslink on two adjacent guanines.	28
Figure 1.14. The structure of a unilamellar lipid vesicular delivery system.	37
Figure 3.1. The forces on particle surface that control colloidal stability as function of distance.	74
Figure 3.2. The electrochemical double layer surrounding a negatively charged particle. ...	75
Figure 3.3. Correlation function of small and large particles in DLS to determine particle size.	77
Figure 3.4. The different paths of fracture that lead to three types of replica images in FFEM.	80
Figure 3.5. Relation between time and vesicle entrapment efficiency for original and processed cisplatin NIVs prepared in different volumes (n=3).	82
Figure 3.6. The size of cisplatin NIVs with and without processing prepared in different volumes. Each point is representative of triplicate readings (n=1).	83
Figure 3.7. The ZP values of cisplatin NIVs with and without processing prepared in different volumes. Each point is representative of triplicate readings (n=1).	84
Figure 3.8. The entrapment efficiency of processed and non-processed cisplatin NIVs prepared in equal volumes over time (n=3).	85
Figure 3.9. The size of cisplatin NIVs with and without processing prepared in equal volumes (n=3).	86
Figure 3.10. The ZP results of cisplatin prepared with and without processing prepared in equal volumes. Each point is representative of triplicate readings (n=1).	87
Figure 3.11. The size of processed NIVs hydrated with 0.5mg/ml or 6mg/ml cisplatin. Each point is representative of triplicate readings (n=1).	89

Figure 3.12. The ZP results of processed NIVs hydrated with 0.5 and 6mg/ml cisplatin. Each point is representative of triplicate readings (n=1).....	90
Figure 3.13. FFEM of NIVs prepared with 150µmol lipid concentration and hydrated with 0.5mg/ml cisplatin (a) and freeze-dried empty NIVs prepared with 150µmol lipid concentration and rehydrated with 0.5mg/ml cisplatin (b).	95
Figure 3.14. FFEM of NIVs hydrated with 6mg/ml without diafiltration showing possible MLVs as indicated by white arrow (a) and multi-vesicular niosomes akin to multi-vesicular liposomes (b) – see Figures 3.16 and 3.17.....	97
Figure 3.15. FFEM of processed NIVs hydrated with 6mg/ml cisplatin suggesting presence of MLVs as indicated by white arrows and possible multi-vesicular vesicle as indicated by black arrow.....	98
Figure 3.16. FFEM images of vesosomes which is a class of multivesicular vesicle showing similarity to multivesicular niosomes shown in Figure 3.15b. Images adapted from Kisak <i>et al.</i> (2004).....	105
Figure 3.17. FFEM images of multivesicular vesicles prepared using DepoFoam [®] technology. Images are adapted from Spector <i>et al.</i> (1996).....	106
Figure 4.1. A chromatogram illustrating the separation and elution of excess DDTC, Pt(DDTC) ₂ and Ni(DDTC) ₂ at 6, 8 and 10min, respectively, using method I.	113
Figure 4.2. A typical calibration curve obtained using method I for the quantification of platinum.	114
Figure 4.3. A chromatogram illustrating the separation and elution of excess DDTC, Pt(DDTC) ₂ and Ni(DDTC) ₂ using method I.....	115
Figure 4.4. A chromatogram illustrating the separation and elution of excess DDTC, and Ni(DDTC) ₂ at 5 and 9min, respectively, using method II.	117
Figure 4.5. A chromatogram illustrating the separation and elution of excess DDTC, Pt(DDTC) ₂ and Ni(DDTC) ₂ at 5, 7 and 9min, respectively, using method II.....	118
Figure 4.6. A typical calibration curve obtained using method II for the quantification of platinum.	119
Figure 4.7. A chromatogram illustrating the separation and elution of excess DDTC, Pt(DDTC) ₂ and Ni(DDTC) ₂ at 5, 7 and 9min, respectively. Chloroform layer was injected directly but the injection volume was reduced to 10µl. The sample was prepared from a 0.9% w/v NaCl solution containing 5µg/ml cisplatin.	121
Figure 4.8. A chromatogram illustrating the separation and elution of excess DDTC and Ni(DDTC) ₂ at 5 and 8min, respectively, using method III.	123
Figure 4.9. A chromatogram illustrating the separation and elution of excess DDTC, Pt(DDTC) ₂ and Ni(DDTC) ₂ at 5, 6 and 8min, respectively, using method III.	124
Figure 4.10. A typical calibration curve obtained using method III for the quantification of platinum.	125
Figure 4.11. A typical calibration curve obtained using method III for the quantification of platinum.	127
Figure 4.12. A chromatogram illustrating the separation and elution of cholesterol, surfactant and DCP at 7, 9 and 14min, respectively. Separation was achieved using the ternary gradient elution described (Table 4.8).	130

Figure 4.13. A chromatogram illustrating the separation and elution of cholesterol, surfactant and DCP at 1, 4 and 9min, respectively. Separation was achieved using the modified ternary gradient elution (Table 4.9).....	132
Figure 4.14. A chromatogram illustrating the separation and elution of prednisolone as an internal standard at 6min.	133
Figure 4.15. Separation and elution of cholesterol, surfactant, prednisolone and DCP at 1, 4, 6 and 9min, respectively, as illustrated in the chromatogram.	134
Figure 4.16. A typical calibration curve of cholesterol obtained using the developed method for lipid analysis.....	135
Figure 4.17. A typical calibration curve of surfactant VIII obtained using the developed method for lipid analysis.	137
Figure 4.18. A typical calibration curve of DCP obtained using the developed method for lipid analysis.	139
Figure 5.1. The physical appearance of processed cisplatin NIVs 469 days post-preparation when stored at 4°C (a), 25°C/60% RH (b) and 40°C/75% RH (c) showing clear precipitation of cisplatin. Bottom picture on the left shows precipitated cisplatin pellet after the NIVs had been centrifuged at 13000rpm for 5min.	150
Figure 5.2. The entrapment efficiency of processed cisplatin NIVs stored at 4°C, 25°C/60% RH and 40°C/75% RH determined over time at 1, 28, 189, 266 and 469 days post-preparation (n=3).....	151
Figure 5.3. The concentration of total cisplatin (entrapped and unentrapped) in processed NIVs stored at 4°C, 25°C/60% RH and 40°C/75% RH determined over time at 1, 28, 189, 266 and 469 days post-preparation (n=3).	152
Figure 5.4. The concentration of unentrapped cisplatin present in the supernatant of processed NIVs stored at 4°C, 25°C/60% RH and 40°C/75% RH determined over time at 1, 28, 189, 266 and 469 days post-preparation (n=3).	153
Figure 5.5. The ratio between cholesterol and DCP weights in processed empty NIVs and processed cisplatin NIVs stored at 4°C in comparison to lyophilised processed NIVs prepared from empty NIVs over time at 1, 28, 189, 266 and 469 days post-preparation (n=3).	158
Figure 5.6. The ratio between cholesterol and DCP weights in processed empty NIVs and processed cisplatin NIVs stored at 25°C/60% RH in comparison to lyophilised processed NIVs prepared from empty NIVs over time at 1, 28, 189, 266 and 469 days post-preparation with empty NIVs not available on days 266 and 469 post-preparation (n=3).	159
Figure 5.7. The ratio between cholesterol and DCP weights in processed empty NIVs and processed cisplatin NIVs stored at 40°C/75% RH in comparison to lyophilised processed NIVs prepared from empty NIVs over time at 1, 28, 189, 266 and 469 days post-preparation with empty NIVs not available on days 266 and 469 post-preparation (n=3).	160
Figure 5.8. The ratio between surfactant VIII and DCP weights in processed empty NIVs and processed cisplatin NIVs stored at 4°C in comparison to lyophilised processed NIVs prepared from empty NIVs over time at 1, 28, 189, 266 and 469 days post-preparation (n=3).	165

Figure 5.9. The ratio between surfactant VIII and DCP weights in processed empty NIVs and processed cisplatin NIVs stored at 25°C/60% RH in comparison to lyophilised processed NIVs prepared from empty NIVs over time at 1, 28, 189, 266 and 469 days post-preparation with samples stored at 25°C/60% RH and 40°C/75% RH not available on days 266 and 469 post-preparation (n=3).	166
Figure 5.10. The ratio between surfactant VIII and DCP weights in processed empty NIVs and processed cisplatin NIVs stored at 40°C/75% RH in comparison to lyophilised processed NIVs prepared from empty NIVs over time at 1, 28, 189, 266 and 469 days post-preparation with empty NIVs not available on days 266 and 469 post-preparation (n=3).	167
Figure 5.11. The dicetyl phosphate weight ratios in processed empty NIVs and processed cisplatin NIVs stored at 4°C in comparison to lyophilised processed NIVs prepared from empty NIVs over time at 1, 28, 189, 266 and 469 days post-preparation (n=3).	172
Figure 5.12. The dicetyl phosphate weight ratios in processed empty NIVs and processed cisplatin NIVs stored at 25°C/60% RH in comparison to lyophilised processed NIVs prepared from empty NIVs over time at 1, 28, 189, 266 and 469 days post-preparation with empty NIVs not available on days 266 and 469 post-preparation (n=3).	173
Figure 5.13. The dicetyl phosphate weight ratios in processed empty NIVs and processed cisplatin NIVs stored at 40°C/75% RH in comparison to lyophilised processed NIVs prepared from empty NIVs over time at 1, 28, 189, 266 and 469 days post-preparation with empty NIVs not available on days 266 and 469 post-preparation (n=3).	174
Figure 5.14. The size of empty processed NIVs stored at 4°C, 25°C/60% RH and 40°C/75% RH determined over time at 1, 28, 189, 266 and 469 days post-preparation with samples stored at 25°C/60% RH and 40°C/75% RH not available on days 266 and 469 post-preparation (n=3 except for day 1 post-preparation where n=1).	176
Figure 5.15. The size of processed cisplatin NIVs stored at 4°C, 25°C/60% RH and 40°C/75% RH determined over time at 1, 28, 189, 266 and 469 days post-preparation (n=3 except for day 1 post-preparation where n=1).	177
Figure 5.16. The size of processed empty NIVs and processed cisplatin NIVs stored at 4°C in comparison to lyophilised NIVs prepared from empty NIVs over time at 1, 28, 161, 235 and 534 days post-preparation (n=3 except for day 1 post-preparation where n=1).	178
Figure 5.17. The size of processed empty NIVs and processed cisplatin NIVs stored at 25°C/60% RH in comparison to lyophilised NIVs prepared from empty NIVs over time at 1, 28, 189, 266 and 469 days post-preparation with empty NIVs not available on days 266 and 469 post-preparation (n=3 except for day 1 post-preparation where n=1).	179
Figure 5.18. The size of processed empty NIVs and processed cisplatin NIVs stored at 40°C/75% RH in comparison to lyophilised NIVs prepared from empty NIVs over time at 1, 28, 189, 266 and 469 days post-preparation with empty NIVs not available on days 266 and 469 post-preparation (n=3 except for day 1 post-preparation where n=1).	180
Figure 5.19. The ZP of processed empty NIVs stored at 4°C, 25°C/60% RH and 40°C/75% RH determined over time at 1, 28, 189, 266 and 469 days post-preparation with	

samples stored at 25°C/60% RH and 40°C/75% RH not available on days 266 and 469 post-preparation (n=3 except for day 1 post-preparation where n=1).	181
Figure 5.20. The ZP of processed cisplatin NIVs stored at 4°C, 25°C/60% RH and 40°C/75% RH determined over time at 1, 28, 189, 266 and 469 days post-preparation (n=3 except for day 1 post-preparation where n=1).	182
Figure 5.21. The ZP of processed empty NIVs and processed cisplatin NIVs stored at 4°C in comparison to lyophilised NIVs prepared from empty NIVs over time at 1, 28, 189, 266 and 469 days post-preparation (n=3 except for day 1 post-preparation where n=1).	183
Figure 5.22. The ZP of processed empty NIVs and processed cisplatin NIVs stored at 25°C/60% RH in comparison to lyophilised NIVs prepared from empty NIVs over time at 1, 28, 189, 266 and 469 days post-preparation with empty NIVs not available on days 266 and 469 post-preparation (n=3 except for day 1 post preparation where n=1).	184
Figure 5.23. The ZP of processed empty NIVs and processed cisplatin NIVs stored at 40°C/75% RH in comparison to lyophilised NIVs prepared from empty NIVs over time at 1, 28, 189, 266 and 469 days post-preparation with empty NIVs not available on days 266 and 469 post-preparation (n=3 except for day 1 post-preparation where n=1).	185
Figure 5.24. The physical appearance of NIVs hydrated with 6mg/ml (a), 3mg/ml (b) and 1mg/ml (c) cisplatin 97 days post-preparation and stored at 4°C showing signs of precipitation in a and b.	186
Figure 5.25. The entrapment efficiency of NIVs, hydrated with 3 and 6mg/ml cisplatin, stored at 4°C, 25°C/60% RH and 40°C/75% RH determined at 97 and 168 post-preparation (n=3).	187
Figure 5.26. The concentration of untrapped and entrapped cisplatin in NIVs hydrated with 3mg/ml cisplatin and stored at 4°C, 25°C/60% and 40°C/75% RH determined at 97 and 168 post-preparation (n=3).	189
Figure 5.27. The concentration of untrapped and entrapped cisplatin in NIVs hydrated with 6mg/ml cisplatin and stored at 4°C, 25°C/60% and 40°C/75% RH determined at 97 and 168 post-preparation (n=3).	190
Figure 5.28. The concentration of cholesterol and ratio between cholesterol and DCP weights in processed NIVs hydrated with 1mg/ml cisplatin and stored at 4°C, 25°C/60% RH and 40°C/75% RH determined on days 3, 97 and 168 post-preparation (n=3).	201
Figure 5.29. The concentration of cholesterol and ratio between cholesterol and DCP weights in processed NIVs hydrated with 3mg/ml cisplatin and stored at 4°C, 25°C/60% RH and 40°C/75% RH determined on days 3, 97 and 168 post-preparation (n=3).	202
Figure 5.30. The concentration of cholesterol and ratio between cholesterol and DCP weights in processed NIVs hydrated with 6mg/ml cisplatin and stored at 4°C, 25°C/60% RH and 40°C/75% RH determined on days 3, 97 and 168 post-preparation (n=3).	203

Figure 5.31. The concentration of cholesterol in processed NIVs hydrated with different cisplatin concentrations of 1, 3 and 6mg/ml and stored at 4°C determined on days 3, 97 and 168 post-preparation (n=3).	204
Figure 5.32. The concentration of cholesterol in processed NIVs hydrated with different cisplatin concentrations of 1, 3 and 6mg/ml and stored at 25°C/60% RH determined on days 3, 97 and 168 post-preparation (n=3).	205
Figure 5.33. The concentration of cholesterol in processed NIVs hydrated with different cisplatin concentrations of 1, 3 and 6mg/ml and stored at 40°C/75% RH determined on days 3, 97 and 168 post-preparation (n=3).	206
Figure 5.34. The concentration of surfactant VIII and ratio between surfactant VIII and DCP weights in processed NIVs hydrated with 1mg/ml cisplatin and stored at 4°C, 25°C/60% RH and 40°C/75% RH determined on days 3, 97 and 168 post-preparation (n=3).	207
Figure 5.35. The concentration of surfactant VIII and ratio between surfactant VIII and DCP weights in processed NIVs hydrated with 3mg/ml cisplatin and stored at 4°C, 25°C/60% RH and 40°C/75% RH determined on days 3, 97 and 168 post-preparation (n=3).	208
Figure 5.36. The concentration of surfactant VIII and ratio between surfactant VIII and DCP weights in processed NIVs hydrated with 6mg/ml cisplatin and stored at 4°C, 25°C/60% RH and 40°C/75% RH determined on days 3, 97 and 168 post-preparation (n=3).	209
Figure 5.37. The concentration of surfactant VIII in processed NIVs hydrated with different cisplatin concentrations of 1, 3 and 6mg/ml and stored at 4°C determined on days 3, 97 and 168 post-preparation (n=3).	210
Figure 5.38. The concentration of surfactant VIII in processed NIVs hydrated with different cisplatin concentrations of 1, 3 and 6mg/ml and stored at 25°C/60% RH determined on days 3, 97 and 168 post-preparation (n=3).	211
Figure 5.39. The concentration of surfactant VIII in processed NIVs hydrated with different cisplatin concentrations of 1, 3 and 6mg/ml and stored at 40°C/75% RH determined on days 3, 97 and 168 post-preparation (n=3).	212
Figure 5.40. The concentration of dicetyl phosphate and dicetyl phosphate weight ratios in processed NIVs hydrated with 1mg/ml cisplatin and stored at 4°C, 25°C/60% RH and 40°C/75% RH determined on days 3, 97 and 168 post-preparation (n=3).	213
Figure 5.41. The concentration of dicetyl phosphate and dicetyl phosphate weight ratios in processed NIVs hydrated with 3mg/ml cisplatin and stored at 4°C, 25°C/60% RH and 40°C/75% RH determined on days 3, 97 and 168 post-preparation (n=3).	214
Figure 5.42. The concentration of dicetyl phosphate and dicetyl phosphate weight ratios in processed NIVs hydrated with 6mg/ml cisplatin and stored at 4°C, 25°C/60% RH and 40°C/75% RH determined on days 3, 97 and 168 post-preparation (n=3).	215
Figure 5.43. The concentration of dicetyl phosphate in processed NIVs hydrated with different cisplatin concentrations of 1, 3 and 6mg/ml and stored at 4°C determined on days 3, 97 and 168 post-preparation (n=3).	216
Figure 5.44. The concentration of dicetyl phosphate in processed NIVs hydrated with different cisplatin concentrations of 1, 3 and 6mg/ml and stored at 25°C/60% RH determined on days 3, 97 and 168 post-preparation (n=3).	217

Figure 5.45. The concentration of dicetyl phosphate in processed NIVs hydrated with different cisplatin concentrations of 1, 3 and 6mg/ml and stored at 40°C/75% RH determined on days 3, 97 and 168 post-preparation (n=3).	218
Figure 6.1. The proliferation of B16-F0 using AB after a 24hr incubation period with a starting seeding density of 1.25×10^6 cells/ml serially diluted down to 4882 cells/ml (n=6).	240
Figure 6.2. The effect of cisplatin solution with a starting concentration of 1.667mM serially diluted down to 0.026mM on the proliferation of B16-F0 seeded at a density of 1.88×10^5 cells/ml incubated for 24hr with AB as represented by a sigmoidal dose-response curve (experiment performed once with n=6 for each concentration level).	241
Figure 6.3. Comparison between the effect of cisplatin NIVs, cisplatin solution and empty NIVs at a starting concentration of 1.667mM and serially diluted down to 0.052mM on the proliferation of B16-F0 seeded at a density of 1.88×10^5 cells/ml and incubated for 24hr with AB (n=6).	242
Figure 6.4. The effect of cisplatin NIVs, cisplatin solution and empty NIVs at a starting concentration of 1.667mM and serially diluted down to 0.052mM on the proliferation of B16-F0 seeded at a density of 1.88×10^5 cells/ml and incubated for 24h with AB represented by a sigmoidal dose-response curve (experiment performed once with n=6 for each concentration level).	243
Figure 7.1. Tumour burdens in lungs and livers of BALB/c mice inoculated with 2.7×10^5 B16-F0 cells and administered 7 days post-inoculation by inhalation a single dose of control (0.9% w/v NaCl) solution, cisplatin solution or non-processed cisplatin NIVs hydrated with 6mg/ml and diluted to 0.5mg/ml (n=8).	253
Figure 7.2. Tumour burdens in lungs and livers of BALB/c mice inoculated with 3.33×10^5 B16-F0 cells and administered 7 days post-inoculation by inhalation a single dose of control (0.9% w/v NaCl) solution, cisplatin solution or processed cisplatin NIVs (n=5).	255
Figure 7.3. Tumour burdens in lungs of BALB/c mice inoculated with 1×10^5 B16-F0 cells and administered 7 days post-inoculation by inhalation a single dose of control (0.9% w/v NaCl) solution or processed cisplatin NIVs (n=6).	259
Figure 7.4. Tumour burdens in livers of BALB/c mice inoculated with 1×10^5 B16-F0 cells and administered 7 days post-inoculation by inhalation a single dose of control (0.9% w/v NaCl) solution or processed cisplatin NIVs (n=6).	260
Figure 7.5. The accumulation of cisplatin solution, non-processed cisplatin NIVs hydrated with 0.5mg/ml and non-processed NIVs hydrated with 6mg/ml and diluted to 0.5mg/ml following a single intravenous injection to BALB/c mice (n=5).	262
Figure 7.6. The accumulation of cisplatin solution, non-processed cisplatin NIVs hydrated with 0.5mg/ml and non-processed NIVs hydrated with 6mg/ml and diluted to 0.5mg/ml following inhalation treatment of BALB/c mice (n=5).	263
Figure 7.7. The accumulation of cisplatin solution and processed cisplatin following single intravenous injection to BALB/c mice (n=5).	265
Figure 7.8. The accumulation of cisplatin solution and processed cisplatin administered by inhalation to BALB/c mice (n=5).	266

Figure 7.9. Pharmacokinetic profile of platinum in plasma of Sprague-Dawley rats following a single intravenous injection of cisplatin solution or inhalation administration of processed cisplatin NIVs (n=3).	268
Figure 7.10. Pharmacokinetic profile of platinum in lungs of Sprague-Dawley rats following a single intravenous injection of cisplatin solution or inhalation administration of processed cisplatin NIVs (n=3).	269

List of Tables

Table 2.1. Gradient elution sequence used in lipid analysis using 100% isohexane (A), 100% ethyl acetate (B) and a mixture of 60% propan-2-ol, 30% acetonitrile and 10% methanol, 142µl/100ml glacial acetic acid and 378µl/100ml triethylamine (C).	59
Table 2.2. The weighed amount of lipids used to prepare 200ml empty NIVs and 500ml cisplatin NIVs.	61
Table 2.3. The weight of lipids that would be present in 1ml of empty and cisplatin NIVs calculated from the actual weights used to prepare the batches.....	63
Table 2.4. The weighed amount of lipids used in the preparation of NIVs hydrated with 1, 3 and 6mg/ml cisplatin in batches of 100ml.	64
Table 3.1. Corresponding Pdl values of cisplatin NIVs with and without processing sized in Figure 3.5. Each point is representative of triplicate readings (n=1).	83
Table 3.2. Corresponding Pdl values of cisplatin NIVs with and without processing sized in Figure 3.8. Each point is representative of triplicate readings (n=3).	86
Table 3.3. Entrapment efficiency of processed NIVs hydrated with 6mg/ml cisplatin over time. Each result is representative of a single measurement.....	88
Table 3.4. Corresponding Pdl values of processed NIVs hydrated with 0.5 and 6mg/ml cisplatin sized in Figure 3.10. Each point is representative of triplicate readings (n=1).	89
Table 3.5. The size, Pdl and ZP values of 1mg/ml cisplatin NIVs subjected to diafiltration without a dilution and concentration step. Each point is representative of triplicate readings (n=3 for size and Pdl results and n=1 for ZP results).....	91
Table 3.6. The entrapment efficiency of processed NIVs hydrated with 6mg/ml cisplatin then separated from untrapped cisplatin and re-suspended in 0.9% w/v NaCl, 0.5mg/ml and 1mg/ml cisplatin (n=3).	92
Table 3.7. The size of processed NIVs hydrated with 6mg/ml cisplatin then separated from untrapped drug and re-suspended in 0.9% w/v NaCl, 0.5mg/ml and 1mg/ml cisplatin. Each point is representative of triplicate readings (n=1).	92
Table 3.8. Corresponding Pdl values of processed NIVs hydrated with 6mg/ml cisplatin then separated from entrapped drug and re-suspended in 0.9% w/v NaCl, 0.5mg/ml and 1mg/ml cisplatin sized in Table 3.6. Each point is representative of triplicate readings (n=1).	93
Table 3.9. The ZP of processed NIVs hydrated with 6mg/ml cisplatin then separated from untrapped drug and re-suspended in 0.9% w/v NaCl, 0.5mg/ml and 1mg/ml cisplatin. Each point is representative of triplicate readings (n=3).	93
Table 4.1. Comparison of peak properties obtained by direct injection of chloroform layer in a 10µl volume (A) and 20µl injection of a sample reconstituted in 75% v/v acetonitrile in water following evaporation of the chloroform layer (B).	116
Table 4.2. The intra-day and inter-day precision of method II as represented by %RSD values. Two sets of standards were analysed in triplicates for intra-day precision and three sets of standards were analysed in triplicates for inter-day precision.	120
Table 4.3. Peak characteristics of DDTC, Pt(DDTC) ₂ and Ni(DDTC) ₂ when elution was carried out at 40°C at different flow rates.	122

Table 4.4. The intra-day and inter-day precision of method III in the analysis of cisplatin standard concentrations in 0.9% w/v NaCl. Values are representative of %RSD. Two sets of standards were analysed in triplicates for intra-day precision and three sets of standards were analysed in triplicates for inter-day precision.	126
Table 4.5. Accuracy of method III in the detection of platinum using three concentrations prepared in 0.9% w/v NaCl and analysed in triplicates.	126
Table 4.6. The intra-day and inter-day precision of method III in the analysis of cisplatin standard concentrations in 0.9% w/v NaCl. Values are representative of %RSD. Two sets of standards were analysed in triplicates for intra-day precision and three sets of standards were analysed in triplicates for inter-day precision.	128
Table 4.7. Accuracy of method III in the detection of platinum using three concentrations prepared in 0.9% w/v NaCl and analysed in triplicates.	128
Table 4.8. The ternary gradient elution sequence used in the analysis of lipid ingredients as indicated from the unpublished method. Solvent channels consisted of 100% isohexane (A), 100% ethyl acetate (B) and a mixture of 60% propan-2-ol, 30% acetonitrile and 10% methanol, 142µl/100ml glacial acetic acid and 378µl/100ml triethylamine (C).	129
Table 4.9. Gradient elution sequence used in lipid analysis using 100% isohexane (A), 100% ethyl acetate (B) and a mixture of 60% propan-2-ol, 30% acetonitrile and 10% methanol, 142µl/100ml glacial acetic acid and 378µl/100ml triethylamine (C).	131
Table 4.10. The intra-day and inter-day precision of the developed method in the analysis of cholesterol standard concentrations. Values are representative of %RSD. Two sets of standards were analysed in triplicates for intra-day precision and three sets of standards were analysed in triplicates for inter-day precision.	136
Table 4.11. The intra-day and inter-day precision of the developed method in the analysis of surfactant VIII standard concentrations. Values are representative of %RSD. Two sets of standards were analysed in triplicates for intra-day precision and three sets of standards were analysed in triplicates for inter-day precision.	138
Table 4.12. The intra-day and inter-day precision of the developed method in the analysis of DCP standard concentrations. Values are representative of %RSD. Two sets of standards were analysed in triplicates for intra-day precision and three sets of standards were analysed in triplicates for inter-day precision.	140
Table 5.1. The concentration of cholesterol in processed empty NIVs stored at 4°C, 25°C/60% RH and 40°C/75% RH determined over time at 1, 28, 189, 266 and 469 days post-preparation with samples stored at 25°C/60% RH and 40°C/75% RH not available on days 266 and 469 post-preparation (n=3).	154
Table 5.2. The ratio between cholesterol and DCP weights in processed empty NIVs stored at 4°C, 25°C/60% RH and 40°C/75% RH determined over time at 1, 28, 189, 266 and 469 days post-preparation with samples stored at 25°C/60% RH and 40°C/75% RH not available on days 266 and 469 post-preparation (n=3).	155
Table 5.3. The concentration of cholesterol in processed cisplatin NIVs stored at 4°C, 25°C/60% RH and 40°C/75% RH determined over time at 1, 28, 189, 266 and 469 days post-preparation (n=3).	156

Table 5.4. The ratio between cholesterol and DCP weights in processed empty NIVs stored at 4°C, 25°C/60% RH and 40°C/75% RH determined over time at 1, 28, 189, 266 and 469 days post-preparation (n=3).	157
Table 5.5. The concentration of surfactant VIII in processed empty NIVs stored at 4°C, 25°C/60% RH and 40°C/75% RH determined over time at 1, 28, 189, 266 and 469 days post-preparation with samples stored at 25°C/60% RH and 40°C/75% RH not available on days 266 and 469 post-preparation (n=3).....	161
Table 5.6. The ratio between surfactant VIII and DCP weights in processed empty NIVs stored at 4°C, 25°C/60% RH and 40°C/75% RH determined over time at 1, 28, 189, 266 and 469 days post-preparation with samples stored at 25°C/60% RH and 40°C/75% RH not available on days 266 and 469 post-preparation (n=3).....	162
Table 5.7. The concentration of surfactant VIII in processed cisplatin NIVs stored at 4°C, 25°C/60% RH and 40°C/75% RH determined over time at 1, 28, 189, 266 and 469 days post-preparation (n=3).	163
Table 5.8. The ratio between surfactant VIII and DCP weights in processed cisplatin NIVs stored at 4°C, 25°C/60% RH and 40°C/75% RH determined over time at 1, 28, 189, 266 and 469 days post-preparation (n=3).	164
Table 5.9. The concentration of dicetyl phosphate in processed empty NIVs stored at 4°C, 25°C/60% RH and 40°C/75% RH determined over time at 1, 28, 189, 266 and 469 days post-preparation with samples stored at 25°C/60% RH and 40°C/75% RH not available on days 266 and 469 post-preparation (n=3).....	168
Table 5.10. The dicetyl phosphate weight ratios in processed empty NIVs stored at 4°C, 25°C/60% RH and 40°C/75% RH determined over time at 1, 28, 189, 266 and 469 days post-preparation with samples stored at 25°C/60% RH and 40°C/75% RH not available on days 266 and 469 post-preparation (n=3).....	169
Table 5.11. The concentration of dicetyl phosphate in processed cisplatin NIVs stored at 4°C, 25°C/60% RH and 40°C/75% RH determined over time at 1, 28, 189, 266 and 469 days post-preparation (n=3).	170
Table 5.12. The dicetyl phosphate weight ratios in processed cisplatin NIVs stored at 4°C, 25°C/60% RH and 40°C/75% RH determined over time at 1, 28, 189, 266 and 469 days post-preparation (n=3).	171
Table 5.13. The concentration of total cisplatin (entrapped and unentrapped) in NIVs hydrated with 1mg/ml cisplatin and stored at 4°C, 25°C/60% and 40°C/75% RH determined on days 97 and 168 days post-preparation (n=3).	191
Table 5.14. The concentration of total cisplatin (entrapped and unentrapped) in NIVs hydrated with 3mg/ml cisplatin and stored at 4°C, 25°C/60% and 40°C/75% RH determined on days 97 and 168 post-preparation (n=3).	192
Table 5.15. The concentration of total cisplatin (entrapped and unentrapped) in NIVs hydrated with 6mg/ml cisplatin and stored at 4°C, 25°C/60% and 40°C/75% RH determined on days 97 and 168 post-preparation (n=3).	192
Table 5.16. The size of processed NIVs hydrated with 1mg/ml cisplatin and stored at 4°C, 25°C/60% RH and 40°C/75% RH determined on days 97 and 168 post-preparation (n=3).....	193

Table 5.17. The size of processed NIVs hydrated with 3mg/ml cisplatin and stored at 4°C, 25°C/60% RH and 40°C/75% RH determined on days 97 and 168 post-preparation (n=3).	194
Table 5.18. The size of processed NIVs hydrated with 6mg/ml cisplatin and stored at 4°C, 25°C/60% RH and 40°C/75% RH determined on days 97 and 168 post-preparation (n=3).	194
Table 5.19. The size of processed NIVs hydrated with 1, 3 and 6mg/ml cisplatin and stored at 4° determined on days 97 and 168 post-preparation (n=3).	195
Table 5.20. The size of processed NIVs hydrated with 1, 3 and 6mg/ml cisplatin and stored at 25°C/60% RH determined on days 97 and 168 post-preparation (n=3).	196
Table 5.21. The size of processed NIVs hydrated with 1, 3 and 6mg/ml cisplatin and stored at 40°C/75% RH determined on days 97 and 168 post-preparation (n=3).	196
Table 5.22. The ZP of processed NIVs hydrated with 1mg/ml cisplatin and stored at 4°C, 25°C/60% RH and 40°C/75% RH determined on days 97 and 168 post-preparation (n=3).	197
Table 5.23. The ZP of processed NIVs hydrated with 3mg/ml cisplatin and stored at 4°C, 25°C/60% RH and 40°C/75% RH determined on days 97 and 168 post-preparation (n=3).	197
Table 5.24. The ZP of processed NIVs hydrated with 6mg/ml cisplatin and stored at 4°C, 25°C/60% RH and 40°C/75% RH determined on days 97 and 168 post-preparation (n=3).	198
Table 5.25. The ZP of processed NIVs hydrated 1, 3 and 6mg/ml cisplatin and stored at 4°C determined on days 97 and 168 post-preparation (n=3).	199
Table 5.26. The ZP of processed NIVs hydrated with 1, 3 and 6mg/ml cisplatin and stored at 25°C/60% RH determined on days 97 and 168 post-preparation (n=3).	199
Table 5.27. The ZP of processed NIVs hydrated with 1, 3 and 6mg/ml cisplatin and stored at 40°C/75% RH determined on days 97 and 168 days post-preparation (n=3).	200
Table 7.1. Amount of cisplatin contained in a 0.5ml dose of cisplatin solution or non-processed NIVs administered by inhalation.	252
Table 7.2. Amount of cisplatin contained in a 0.5ml dose of cisplatin solution or processed NIVs administered by inhalation.	254
Table 7.3. Incidence of tumour metastasis in lungs of BALB/c mice inoculated with 3.33×10^5 B16-F0 cells and administered 7 days post-inoculation by inhalation a single dose of saline control (0.9% w/v NaCl) solution, cisplatin solution or processed cisplatin NIVs (n=5).	256
Table 7.4. Incidence of tumour metastasis in livers of BALB/c mice inoculated with 3.33×10^5 B16-F0 cells and administered 7 days post-inoculation by inhalation a single dose of control (0.9% w/v NaCl) solution, cisplatin solution or processed cisplatin NIVs (n=5).	257
Table 7.5. Amount of cisplatin contained in 0.5ml dose of processed cisplatin NIVs administered by inhalation.	258
Table 7.6. Amount of cisplatin contained in 0.2ml and 0.5ml dose of cisplatin solution and processed NIVs administered by intravenous injection and inhalation, respectively.	264

Table 7.7. Amount of cisplatin contained in 0.2ml of cisplatin solution administered by intravenous injection and 0.5ml of processed cisplatin NIVs administered by inhalation.	267
---	-----

Chapter 1. Introduction

1.1. Cancer – an overview

Cancer is the leading cause of death worldwide. Most recent statistics indicated that in 2008, 13% of all deaths were cancer-related and a further increase is expected in the future (WHO, 2011). Lung cancer tops the cancer mortality rate as it is considered an aggressive type of cancer with a low survival rate (WHO, 2011). Cancer arises from genetic mutations and the longer we live the more susceptible our genes are to mutations, which could explain higher cancer incidence in the elderly. Furthermore, living in a developed world and lifestyle habits are associated with greater risk factors that contribute to genetic mutations (Pecorino, 2008a). It is suggested that 30% of cancers can be prevented by avoiding key risk factors (WHO, 2011). However, this indicates that the remaining 70% may be difficult to prevent. Therefore, it is essential to develop efficient treatment which starts by understanding the behaviour of cancer, its types, its complications and then choosing the best way(s) to eradicate it.

1.1.1. History of cancer

Cancer is a disease that has existed long before humans even walked the planet where evidence of cancer was found in dinosaur fossils from 70 to 80 million years ago (Rothschild *et al.*, 2003). In humans, the earliest case of cancer was found in the fossilised bones of mummies in Egypt and Peru dating back to nearly five thousand years ago (Almeida and Barry, 2010a). However, the disease remained nameless until it was first named by the Greek physician Hippocrates (460-370 BC) as *carcinus* or *carcinoma*, which are Greek words for a crab due to the extensions that often radiate from the tumour mass which resembles a crab shape (Almeida and Barry, 2010a).

In those early ages, cancer treatments were primarily palliative and incurable. The earliest description of cancer was found in a scroll dating back to 3000 BC in ancient Egypt called the Edwin Smith Papyrus. The scroll documented cases of breast cancer that were treated by cauterisation as palliative care (Hajdu, 2011a). The belief that cancer was incurable was the reason behind the slow progress in understanding and

treating cancer for many centuries (Hajdu, 2011a). Despite that, our knowledge about cancer today would not have been possible without the discoveries and the enormous work done by our predecessors. Many important historical milestones played an important role in our current knowledge. To highlight a few, the founder of pathological anatomy Giovanni Morgagni (1682-1771) performed autopsies relating post-mortem pathological findings to the cause of death and laid the foundations for cancer study in 1761 (Hajdu, 2011c). The founder of cellular pathology Rudolf Virchow (1821-1902) laid the scientific foundations for modern pathological cancer study in the 19th century allowing the development of cancer surgery and the birth of scientific oncology (Hajdu, 2011c). In 1953, the greatest discovery of all times was the revelation of the DNA structure by Francis Crick and James Watson. This historic discovery revolutionised the understanding of cell biology and cancer at the molecular level, which helped in developing treatment (Almeida and Barry, 2010a).

1.1.2. Formation of cancer

The discovery of the DNA structure led to understand that cancer starts from an accumulated mutation in the DNA of a single cell leading to its transformation to an abnormal cell that divides uncontrollably to form daughter cells and so on until a tumour mass is formed accompanied with severe complications. Any mutated genes involved in cell growth, differentiation or death can give rise to cancer (Pecorino, 2009a). Specifically speaking, two major classifications of genes have been identified to result in cancer if they become mutated. They are oncogenes and tumour suppressor genes. Both these types of genes are normally present and under reciprocal control. However, once irreparable mutations occur, the activity of both genes is reversed resulting in carcinogenesis (Patrick, 2009). Currently, over 100 oncogenes and at least 15 tumour suppressor genes have been identified (Pecorino, 2008b). Normal cells are usually subjected to mutations in their DNA, but these mutations are usually controlled by cell repair mechanisms that either repair the defect or command the cell to die by programmed death (apoptosis) in order to prevent the alteration from passing onto the daughter cells. However, the problem is initiated when cellular repair mechanisms permit mutations to occur. Cumulative mutations can subsequently cause cells to lose their normal functionality and become

cancerous (Pecorino, 2008a). Six fundamental abnormalities characterise cancer and are “hallmarks”: abnormal signalling pathways and cell cycle regulation; insensitivity to growth inhibitor signals; evasion of apoptosis; immortality through limitless cell division; ability to develop new blood vessels (angiogenesis) and tissue invasion & metastasis (Hanahan and Weinberg, 2000).

1.1.3. Causes of cancer

Cancer can be induced by carcinogens present in chemicals or due to lifestyle factors including diet, smoking and drinking. Carcinogens may also be present in the environment e.g. air pollution and ultraviolet radiation. Infectious agents have also been linked to 15% of cancer related deaths (Patrick, 2009). The association of human papillomavirus with cervical cancer, Epstein-Barr virus with nasopharyngeal carcinoma and Burkitt’s lymphoma, Kaposi’s sarcoma-associated herpesvirus with Kaposi’s sarcoma and primary effusion lymphoma, human T-cell leukaemia virus with T-cell leukaemia, hepatitis B virus with hepatocellular carcinoma and *Helicobacter pylori* with gastric cancer have been verified (Pagano *et al.*, 2004).

1.1.4. Treatment of cancer

Understanding cancer cell biology and contributory factors leading to carcinogenesis has assisted in the development of cancer therapy. The emergence of surgical treatment in cancer can be traced back between 1500 and 1750 (Hajdu, 2011b). For many years, surgery was the only known treatment for cancer which meant that not all types of cancer were curable. By the beginning of the 20th century, radiotherapy was introduced and its combination with surgery was the mainstay of cancer treatment into the 1960s (DeVita and Chu, 2008). During World War II, an incident occurred in 1943 where a ship carrying mustard bombs was destroyed. Survivors exposed to the gas developed bone marrow hypoplasia, lymphoid tissue involution and most severely low white blood cell counts (DeVita and Chu, 2008; Muggia, 2009). The anti-cancer effect of nitrogen mustards against lymphomas was realised and a major breakthrough in cancer therapy began with the birth of chemotherapy (Muggia, 2009). Various chemotherapeutics were subsequently discovered, including those that targeted DNA, RNA, or proteins (Patrick, 2009). Enhanced understanding

of the molecular biology of cancer has driven the continued availability of more precise anti-cancer agents (DeVita and Chu, 2008).

1.1.5. Classification of cancer

Tumours, whether benign or malignant, are classified according to the type of cell that has transformed into four types: epithelial, mesenchymal, haematopoietic and neuroectodermal. Epithelial cancers are the most common cancers and are known as carcinomas and account for over 80% of cancer deaths. They can be sub-classified as squamous cell carcinomas or adenocarcinomas, depending on whether the epithelial cell functions solely as a lining layer or has secretory functions. Mesenchymal cells, in connective tissues, form sarcomas. This type of cancer represents about 1% of cancer cases. Haematopoietic cell cancers affect blood and lymphatic cells. Cancer that affects cells comprising the central and peripheral nervous system are called neuroectodermal tumours. These types of cancer represent 1.3% of cancer cases. Very few tumours can become dedifferentiated. They are referred to as anaplastic tumours as they cannot be traced back to their originating tissues (Weinberg, 2007).

1.1.6. Cancer epidemiology

A report released by the World Health Organization's International Agency for Research on Cancer (IARC) showed the incidence and mortality rate of all types of cancers and for every population for the year 2008. It reported that the incidence of all cancers except for non-melanoma cancers in 2008 reached 12.7 million and 7.6 million deaths. In 2030 it is expected that incidence will rise to 21.3 million and 13 million deaths, which is about a 73% increase in the mortality rate. The distribution of the incidence (Figure 1.1) and mortality rate (Figure 1.2) of cancer worldwide are represented indicating that the majority of cancer cases and related deaths occurred in the Asian continent (Ferlay *et al.*, 2010).

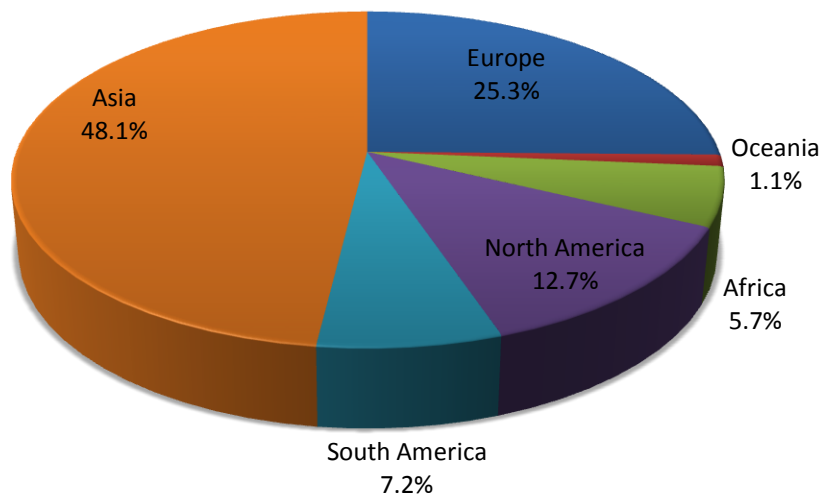


Figure 1.1. Distribution of cancer incidence worldwide (accessed and reconstituted from <http://globocan.iarc.fr> on 24-08-2011).

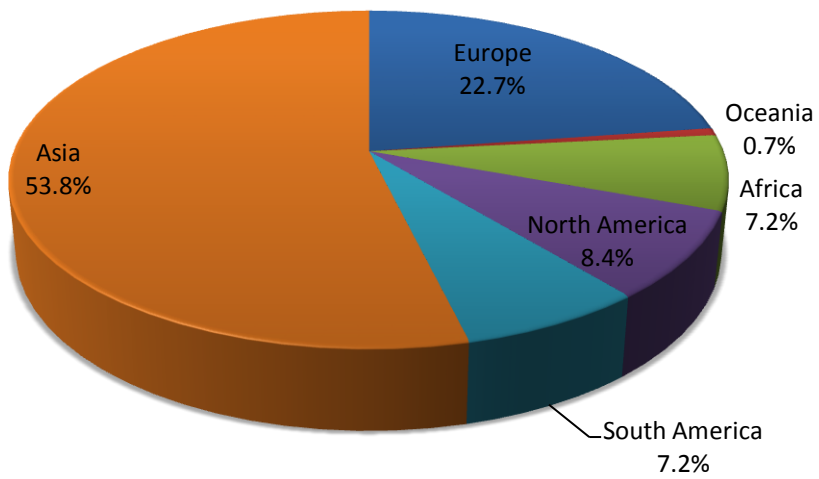


Figure 1.2. Distribution of cancer deaths worldwide (accessed and reconstituted from <http://globocan.iarc.fr> on 24-08-2011).

1.1.7. Lung cancer

Lung cancer is the most common type of cancer in men (16.5% of all cases) and the fourth most common cancer in women (8.5% of all cases) worldwide. It is the leading cause of cancer death. Lung cancer alone comprised 18.2% of all cancer deaths worldwide with 1.38 million deaths estimated in 2008. The incidence (Figure 1.3) and mortality rate (Figure 1.4) of the most common cancers in both sexes are represented (Ferlay *et al.*, 2010).

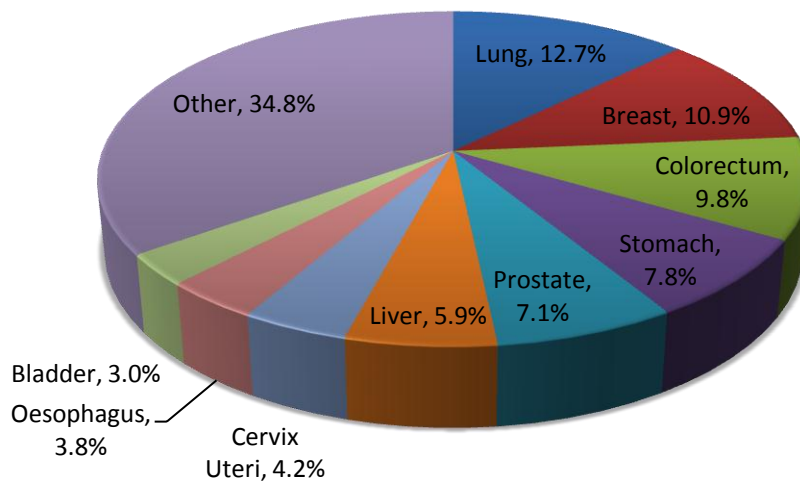


Figure 1.3. Incidence of the most common cancers in both males and females (accessed and reconstituted from <http://globocan.iarc.fr> on 24-08-2011).

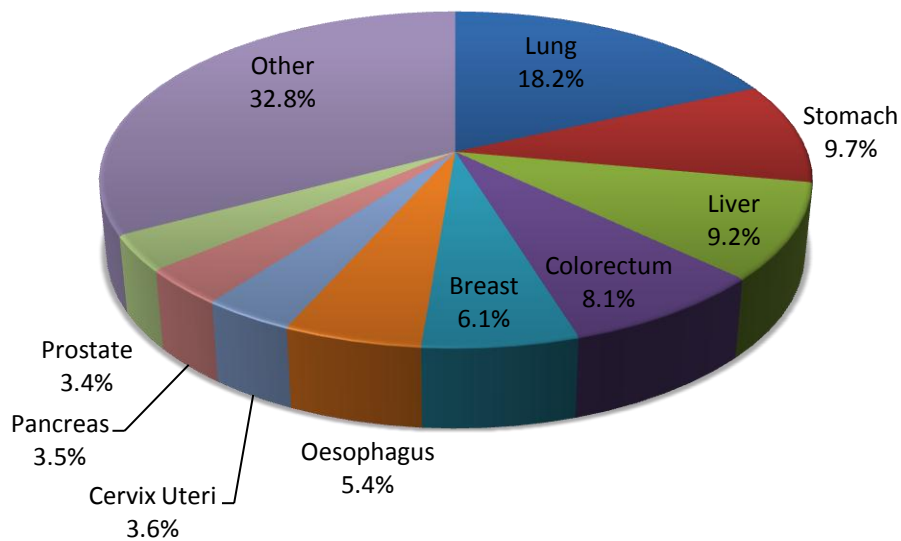


Figure 1.4. Most common deaths due to cancer in both males and females (accessed and reconstituted from <http://globocan.iarc.fr> on 24-08-2011).

In the UK, 2007 figures indicated that lung cancer was the second most common cancer in men and the third most common cancer in women. It topped the mortality rate accounting for 22% of all cancer deaths with average annual death rates over a 3 year period being greater than 34,600 deaths. Patients aged 65 years and above accounted for more than 75% of the lung cancer deaths (CRUK, 2010).

1.1.7.1. Causes of lung cancer

There is strong evidence indicating that tobacco is a major cause of lung cancer in 87% of all cases whether it was through active or passive smoking. Cigarettes contain over 40 known carcinogens and 4000 chemicals that can cause a variety of cancers including lung, mouth, throat, oesophagus, cervix, kidney, pancreas, stomach and bladder cancer. Exposure to asbestos, chemicals, solvents, coal products, air pollution and radon gas produced from uranium rich soil can also be associated with lung cancer (Almeida and Barry, 2010b).

1.1.7.2. Classification of lung cancer

Lung cancer is classified into small cell lung cancer (SCLC) and non-small cell lung cancer (NSCLC), both of which are epithelial tumours (Herbst *et al.*, 2008). NSCLC is further sub-classified into squamous cell carcinoma, adenocarcinoma and large cell carcinoma (Triano *et al.*, 2010). A more detailed classification of lung tumours based on histological studies was provided by the World Health Organization/International Association for the Study of Lung Cancer, which listed 8 classifications in order to provide an international basis for unifying treatment (Brambilla *et al.*, 2001). In the report, the eight classes of lung tumours were epithelial, soft tissue, mesothelial, miscellaneous, lymphoproliferative disease, secondary, unclassified, and tumour-like lesions. SCLC and all three types of NSCLC were categorised under malignant tumours under the epithelial tumour class along with other types such as adenosquamous carcinoma, carcinomas with pleomorphic; sarcomatoid; or sarcomatous elements, carcinoid tumour, carcinomas of salivary-gland type and unclassified carcinomas. However, when it comes to treatment, they are stratified as either SCLC or NSCLC (Figure 1.5).

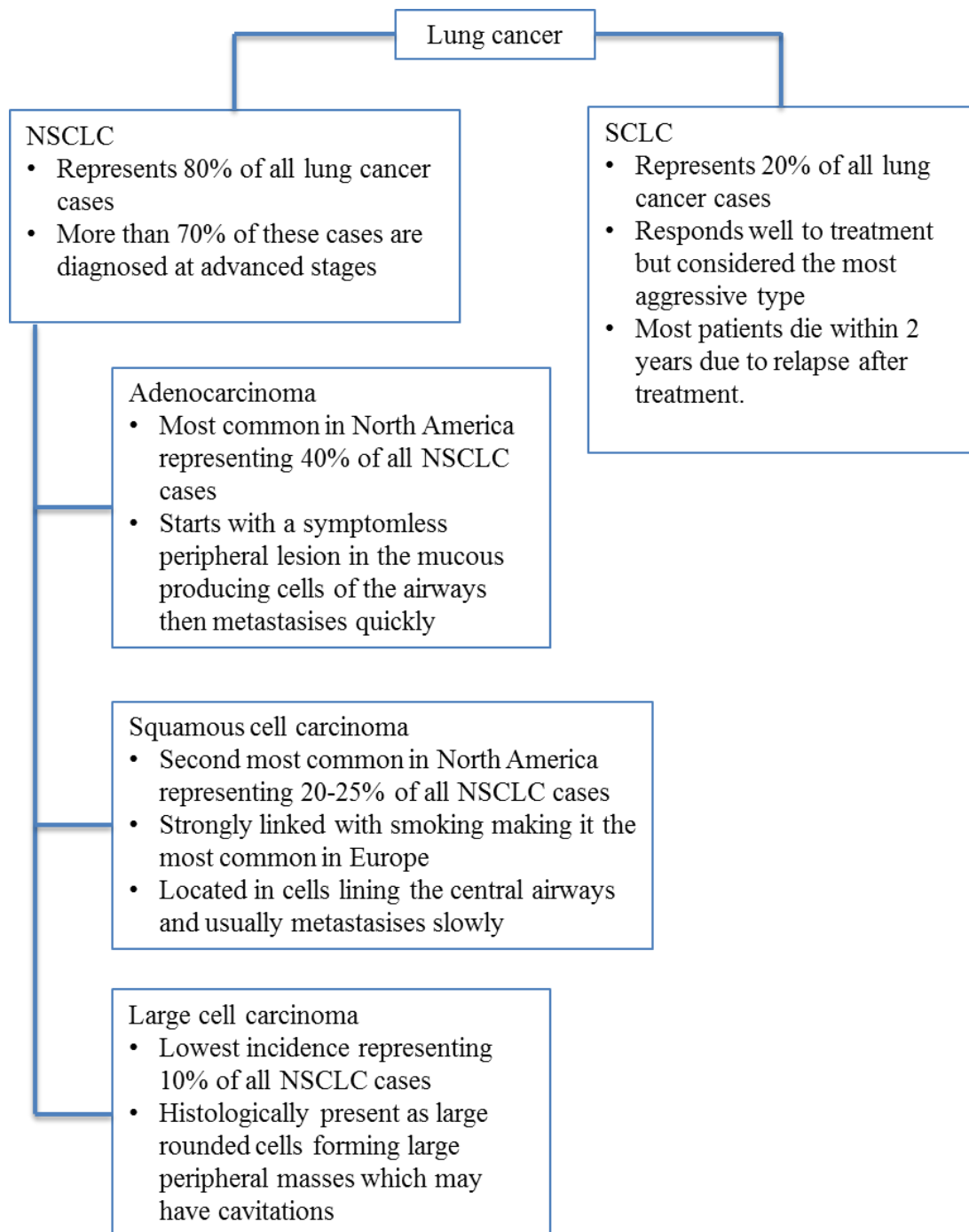


Figure 1.5. A schematic diagram of the basic clinical classification of lung cancer as described (Hoffman *et al.*, 2000).

1.1.7.3. Staging of lung cancer

The clinical stages of SCLC according to the Veterans Administration Lung Study Group are limited-stage and extensive-stage disease. Limited-stage disease is treated with curative intent, and has a 5 year survival rate of 15-25%. Palliative chemotherapy is given to those with extensive-stage disease to ameliorate symptomatology (Sher *et al.*, 2008). In limited-stage disease, the tumour is usually confined to one hemithorax and can be accompanied with hilar and mediastinal nodes that can be controlled in one tolerable radiotherapy portal (Rosti *et al.*, 2006). Wider anatomical distribution is considered to be an extensive-stage disease. This accounts for 60-70% of the patients diagnosed with SCLC (Jackman and Johnson, 2005). The 5 year survival rate for extensive-stage cases is around 2% (Jackman and Johnson, 2005).

The clinical stages of NSCLC according to the International Staging System for Lung Cancer are different from that of SCLC. The type of staging used in NSCLC is called TNM (tumour, node, metastases) staging system. This depends on the size and location of the primary tumour, the presence or absence of metastasis in regional lymph nodes and its extent and the presence or absence of distant metastasis and its extent. Accordingly, NSCLC is divided into four stages with the first three stages subdivided into A and B and the fourth stage involving metastases and considered to be an advanced stage (Nair *et al.*, 2011). The TNM staging system can be used in SCLC, but is rarely used as most patients are rarely diagnosed with SCLC that is sufficiently localised for tumour resection (Jackman and Johnson, 2005)

1.1.7.4. Treatment of lung cancer

Treatment of lung cancer depends on its type and stage. SCLC is considered to be more responsive to chemotherapy unlike NSCLC which is considered to be more responsive to surgery (Hoffman *et al.*, 2000). The National Institute for Clinical Excellence (NICE) submitted a guideline for treating lung cancer depending on its type and stage. Treatment recommendations for SCLC (Figure 1.6) and NSCLC (Figure 1.7) according to NICE (2011) are represented.

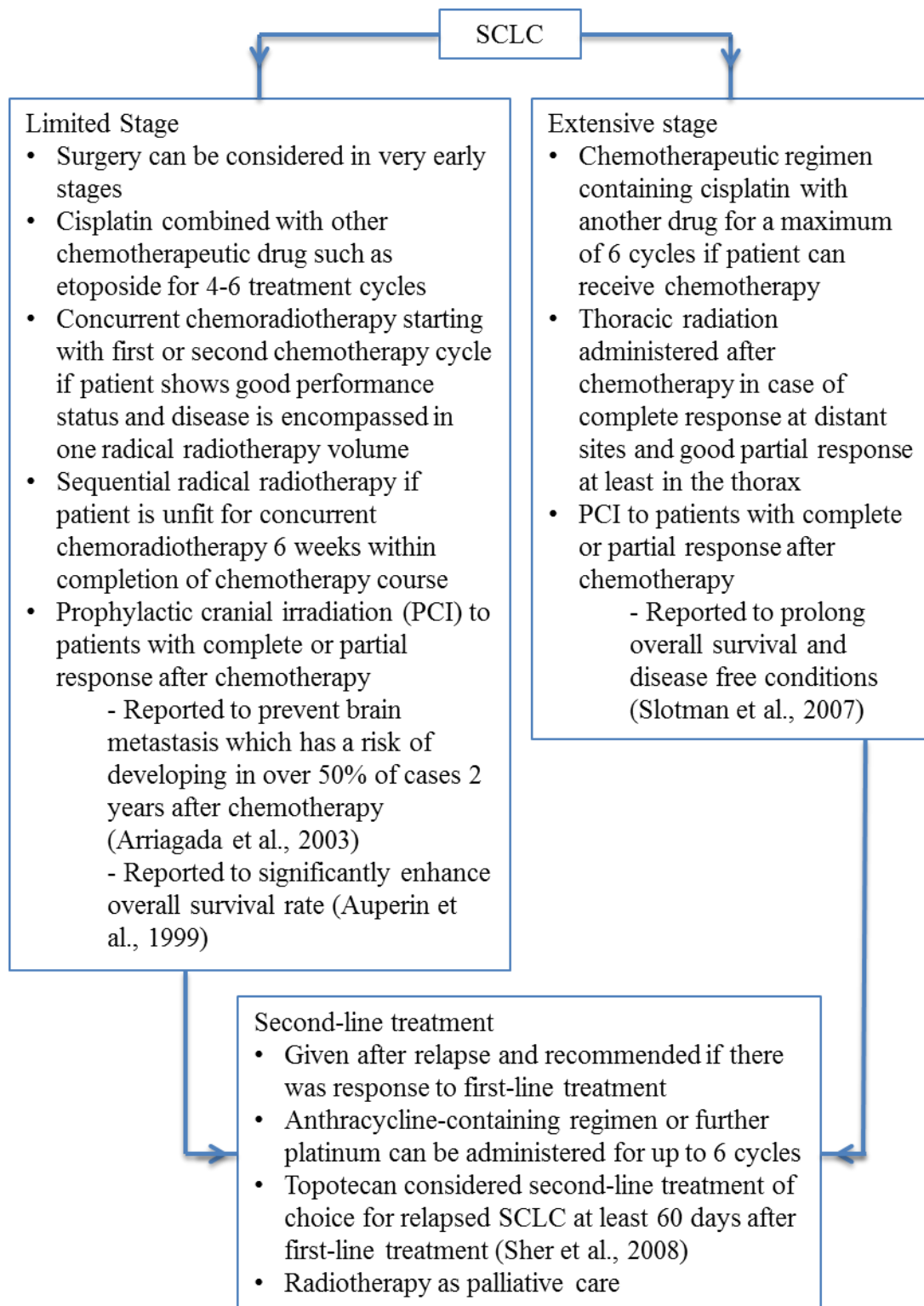


Figure 1.6. Schematic diagram describing the guidelines for treating the different stages of SCLC as provided by NICE (2011) unless otherwise cited.

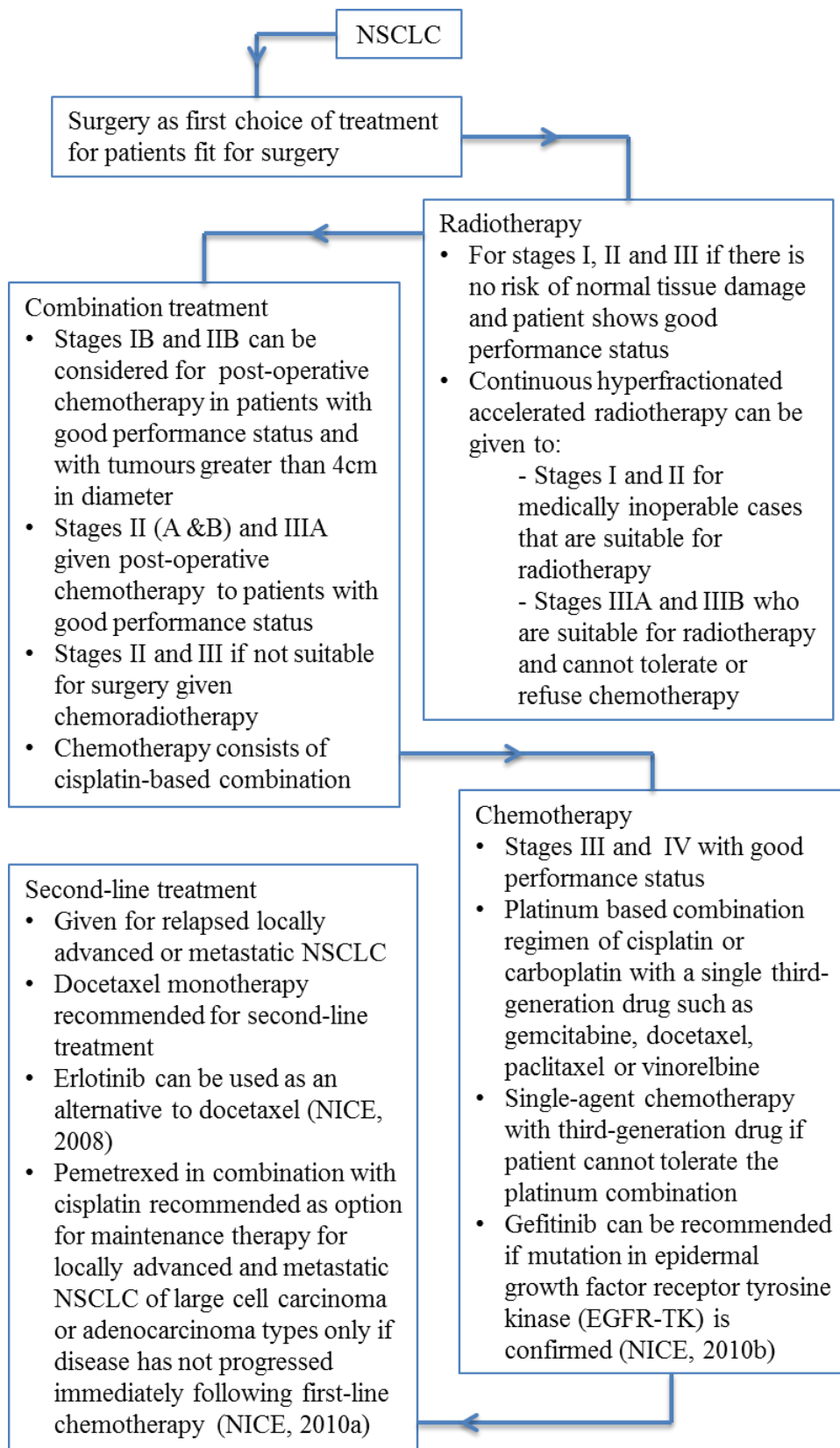


Figure 1.7. Schematic diagram describing the guidelines for treating the different stages of NSCLC as provided by NICE (2011) unless otherwise cited.

Recent advances in cancer treatment focus on targeting abnormal signalling pathways in cancer cells. By identifying molecular changes that occur within cancer cells, it is hypothesised that drugs can be developed to circumvent these changes without jeopardising the activity of normal (non-cancerous) cells which do not possess these pathways.

The gene abnormalities associated with lung cancer have been defined, and so far three drugs that target these abnormalities have shown outstanding outcomes (Herbst *et al.*, 2008). In 2006, bevacizumab was approved by the FDA for treating inoperable, locally advanced, recurrent or metastatic non-squamous NSCLC in combination with carboplatin and paclitaxel (Triano *et al.*, 2010). Bevacizumab works by targeting the vascular endothelial growth factor (VEGF), associated with angiogenesis (Di Costanzo *et al.*, 2008). Erlotinib and gefitinib are also FDA approved drugs that act on molecular targets (Dancey, 2007; Sanford and Scott, 2009). These agents target the epidermal growth factor receptor gene (EGFR), which is associated with proliferation, reduced apoptosis, invasion and angiogenesis characteristic of cancer cells, by inhibiting tyrosine kinase (Dancey, 2007; Herbst *et al.*, 2008). However, because of tumour molecular heterogeneity, patients with similar clinical stages and tumour histology of NSCLC can have dramatically different clinical outcomes and responses to treatment (Herbst *et al.*, 2008).

Novel targeted delivery has been suggested for the treatment of SCLC as this might permit therapy of patients whose cancers are chemo-resistant to first line treatments for advanced disease. A recent report by Kim and Mishima (2011) stated that drugs targeting molecular pathways have not shown effectiveness against SCLC. Accordingly, there is strong support that chemotherapy will still remain indispensable despite the successful discovery of novel drugs targeting the molecular pathways, as they will not be completely efficient in treating cancer and will need to be used in combination with mainstay chemotherapeutic drugs such as platinum agents (Kelland, 2007). Therefore, until further progress is made, platinum drugs will remain prominent in treating many cancers including lung cancer.

1.2. Delivery routes and their physiological barriers

As mentioned (Section 1.1.7.4), cisplatin is the cornerstone of chemotherapy in lung cancer and involves the intravenous route of administration. However, anti-cancer drugs are currently being considered for localised pulmonary delivery for the purpose of reducing systemic exposure associated with systemic intravenous delivery (Carvalho *et al.*, 2011a). In both cases it is important to know the physiological barriers that are associated with the selected route of administration that may impede drug absorption.

1.2.1. Intravenous delivery

Intravenous delivery is one of the many routes involved in parenteral delivery and is the dominant route for general chemotherapy administration. Other parenteral routes that have been used to deliver chemotherapy locally include intraarterial, intraperitoneal, and intrathecal. Following intravenous delivery, drug is distributed by the cardiovascular system to the organs (Washington *et al.*, 2001a).

1.2.1.1. Physiology of the cardiovascular system

The heart serves to distribute blood to and from organs. Blood is transported through a network of vessels consisting of arteries, capillaries and veins which together form the circulatory network. In normal circulation, blood is pumped from the left ventricle of the heart to the aorta which branches to the arteries, arterioles and capillaries carrying oxygenated blood and nutrients throughout the tissues of the whole body. Deoxygenated blood and waste products are then collected by the capillaries and carried through venules to veins and ultimately the superior and inferior vena cava to the right atrium then right ventricle of the heart. This blood is then distributed to the lungs to be oxygenated and then collected again, through the pulmonary circulation, in the left atrium then the left ventricle for the cycle to be repeated. However the functional importance of the cardiovascular system as one structural unit completely depends on the capillaries. Despite the contribution of veins and arteries in delivering blood carrying nutrients and oxygen, it is only through the capillaries where gas exchange and nutrient diffusion can occur (Martini and Nath, 2009a).

The human body is permeated with about 10 billion capillaries that if combined together would exceed 25,000 miles. They are very tiny and have an average diameter, almost to that of a red blood cell, of about 8 μ m. Capillary structure differs from the basic structure of veins and arteries and consists of a delicate basal lamina lined by an endothelium. Depending on the lining endothelium structure, capillaries are classified into continuous or fenestrated where fenestrated capillaries are further sub-classified into sinusoids (Figure 1.8) (Martini and Nath, 2009b).

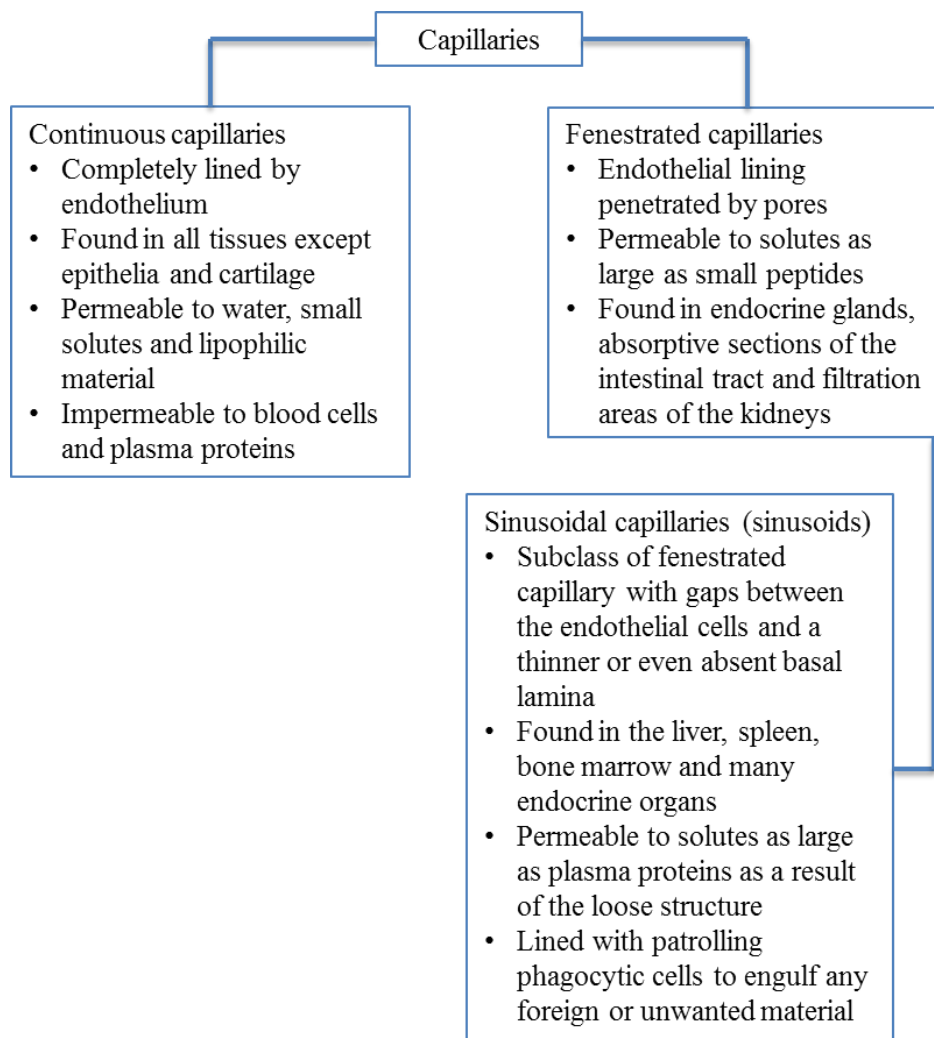


Figure 1.8. Schematic diagram describing the types of capillaries (Martini and Nath, 2009b).

1.2.1.1. Physiological barriers in intravenous delivery

Intravenous delivery has the advantage of rapid onset of action, avoidance of first-pass metabolism and that the drug can be diluted to achieve a desired response. Intravenous delivery in the form of infusions also has the advantage of terminating administration in case unwanted effects develop. Intravenous delivery is considered the most suitable method of delivery when it comes to studying new drugs and their pharmacokinetics (Washington *et al.*, 2001a).

Systemic exposure occurs very quickly following intravenous delivery where it has been reported that it takes 20-30 seconds for an injected solution in the arm to circulate and reach the leg (Washington *et al.*, 2001a). Pulmonary exposure to drug is significant following intravenous delivery and this can be exploited to target the lungs (Smola *et al.*, 2008). Intravenously injected particles of about 5 μ m or more tend to be retained in the small pulmonary capillary beds and particles of a wide size range have the opportunity to be taken up by fixed tissue macrophages of the lungs, liver and spleen (Washington *et al.*, 2001a). Collectively these contribute to the mononuclear phagocytic system (MPS).

The MPS participates in the rapid uptake of particles and leads to appreciable accumulation in these tissues. Uptake by MPS is governed by the process of phagocytosis which is initiated by the adsorption of certain serum proteins called opsonins onto the surface of a foreign particle. These opsonins interact with specific receptors on the surface of macrophages leading to engulfment of particles coated by the opsonins (Malmsten, 2002). The MPS consists of the circulating blood monocytes and macrophages, which can be fixed or free. Fixed macrophages are found in the liver, spleen, lungs, bone marrow and lymph nodes; whereas free macrophages are found in blood and tissues (Crommelin *et al.*, 2001; Hillery, 2001). Factors that contribute to enhanced uptake of particles by the MPS are discussed further (Section 1.4).

1.2.2. Pulmonary delivery

The respiratory system is responsible for providing our bodies with the necessary oxygen required to produce the energy used for cell maintenance, growth, defence and division. Through the process of respiration or breathing, oxygen is inhaled in the lungs and during pulmonary circulation carbon dioxide is replaced with oxygen through gaseous exchange leading to exhalation of carbon dioxide. The respiratory system is also responsible for protecting itself against pathogenic attacks, maintaining a well hydrated and warm inner environment, phonation and assisting the smelling sense (Martini and Nath, 2009c).

1.2.2.1. Physiology of the respiratory system

From an anatomical point of view, the respiratory system is divided into two major parts the upper respiratory tract and the lower respiratory tract (Figure 1.9). The upper respiratory tract consists of the nose, nasal cavity, paranasal sinuses and pharynx. The lower respiratory tract consists of the larynx, trachea, bronchi, bronchioles and alveoli. However, functionally the respiratory tract is divided into two parts the conducting zone (proximal) and the respiratory zone (peripheral). The conducting area starts from the nasal cavity all the way down to the relatively larger bronchioles. The conducting area is lined by respiratory mucosa, which consists of an epithelial layer supported by an areolar tissue called lamina propria. From the nose until the bronchi, the lamina propria secretes mucous from mucous glands present in the layer. The respiratory area consists of the small bronchioles and alveoli (Martini and Nath, 2009c).

1.2.2.1.1. The upper respiratory tract and larynx

The primary site of air entrance is the nose where air enters through the nostrils (external nares) into the nasal cavity. The epithelium within the nostrils contains coarse hair to prevent large contaminants from entering the nasal cavity. The nasal cavity contains regions lined with olfactory epithelium which provide the sense of smell. The paranasal sinuses produce mucous secretions that help maintain moist and clean conditions within the nasal cavity along with the tears produced by the nasolacrimal ducts. On the sides of the nasal cavity are three projections called nasal

conchae (Figure 1.9). The narrow space in-between them provides turbulence within the cavity during inhalation that enhances filtration. It also helps along with the rich vascularisation of the conchae in the warming and humidification of air. The lining epithelium of the nasal cavity consists of pseudostratified ciliated columnar epithelium and many mucous cells (Martini and Nath, 2009c).

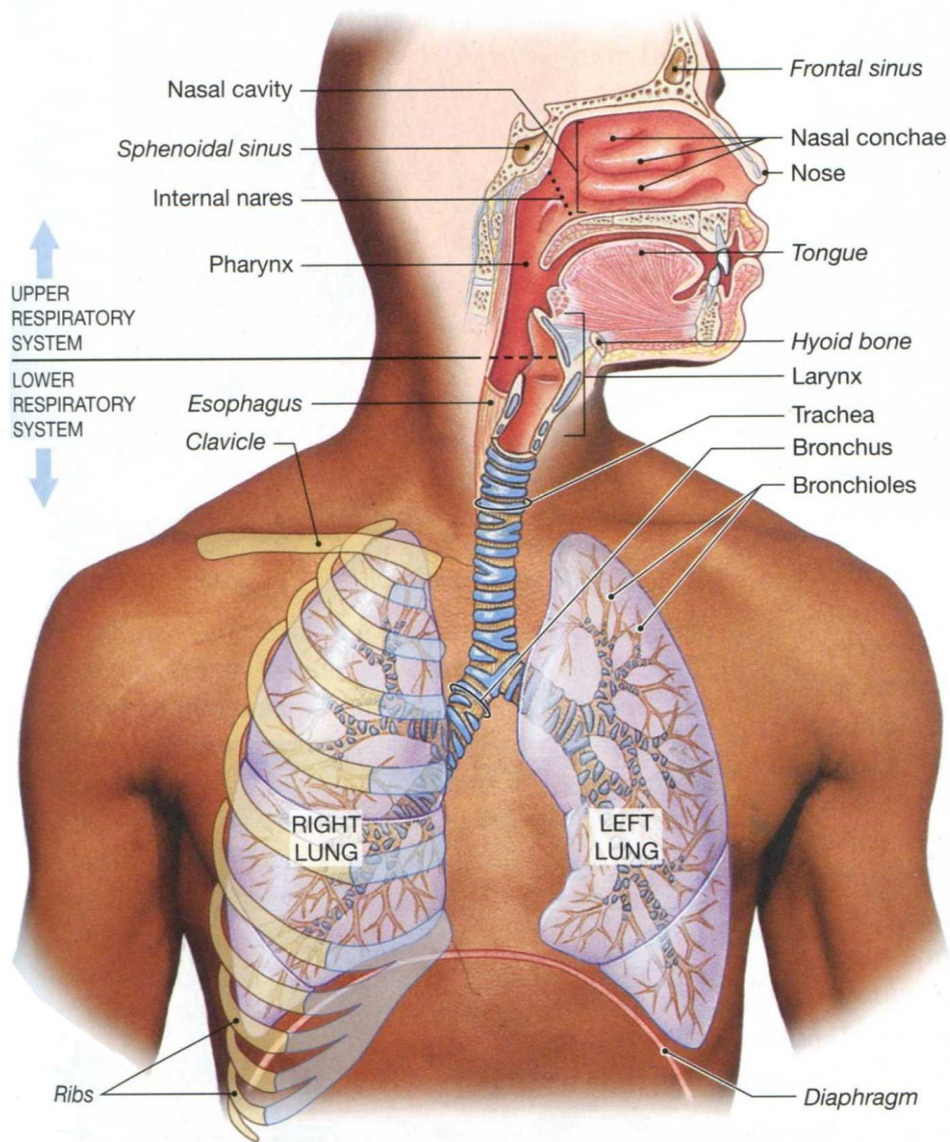


Figure 1.9. Structure of the respiratory system, reproduced from Martini and Nath (2009c).

The pharynx is connected to the nasal cavity through the internal nares. The pharynx serves respiratory and digestive functions. In addition to conducting air between the nasal cavity and the lower respiratory tract, it also plays a role in conveying chewed food from the mouth down to the oesophagus. The pharynx is divided into three portions nasopharynx, oropharynx and laryngopharynx. The lining epithelium of the nasopharynx is the same as that of the nasal cavity, whereas in the oropharynx and laryngopharynx the lining epithelium consists of stratified squamous epithelium which plays a protective role against abrasion and pathogens.

The larynx is a cartilaginous structure that connects between the pharynx and the trachea through a tiny opening it contains called the glottis. The larynx prevents the entrance of food and liquid into the trachea during swallowing by covering the glottis with the epiglottis. The larynx also contains vocal folds surrounding the glottis which vibrate when air passes through the glottis to produce sound. The lining epithelium of the larynx is pseudostratified columnar epithelium (Martini and Nath, 2009c).

1.2.2.1.2. The trachea

The trachea connects the larynx to the bronchi and is lined with the same epithelium as the larynx. Its length is about 11cm and diameter about 2.5cm. The trachea is surrounded by 15-20 incomplete tracheal cartilage rings, which are open at the posterior side facing the oesophagus. These cartilages aid in enforcing the structure of the trachea without it collapsing from pressure changes during respiration (Martini and Nath, 2009c).

1.2.2.1.3. The bronchi and bronchioles

The structural unit of the bronchi starting from the primary bronchi until the formation of the minute respiratory bronchioles through multiple branching is known as the bronchial tree (Figure 1.10a). The trachea branches into two primary bronchi, left and right, which are also surrounded by incomplete cartilage rings. Before entering the lungs, the primary bronchi branch into secondary bronchi, known as lobular bronchi. According to the number of lobes of each lung, the left and right primary bronchi branch correspondingly into two and three secondary bronchi, respectively. These further divide forming ten tertiary bronchi or segmental bronchi.

Each segmental bronchus provides air to a bronchopulmonary segment of the lung. Within each segment tertiary bronchi undergoes multiple branching to form bronchioles, terminal bronchioles until finally the formation of respiratory bronchioles. It is estimated that one tertiary bronchus can give rise to 6500 tiny terminal bronchioles with an internal diameter of 0.3-0.5mm, with each terminal bronchiole delivering air to one pulmonary lobule. These lobules are also supplied by pulmonary veins and arteries and arise from the subdivision of the pulmonary lobes into tiny compartments by interlobular septa composed of connective tissue continuous to that of the visceral pleura. Each lobule contains many respiratory bronchioles which are connected to the alveoli the site of gas exchange. The cartilage surrounding the secondary and tertiary bronchi is plate shaped and decreases as progression occurs down the bronchi until they disappear on the walls of bronchioles. The supporting structure of the bronchioles is attributed to the surrounding smooth muscle tissue instead of cartilage (Martini and Nath, 2009c).

1.2.2.1.4. The alveoli

The alveoli exist individually and in groups of 15-20 forming an alveolar sac and together are connected to the respiratory bronchiole via alveolar duct. About 150 million alveoli are present in each lung (Smola *et al.*, 2008) providing a total absorptive surface area of about 70-140m² (Groneberg *et al.*, 2003). Adequate blood supply is provided by the capillaries surrounding each alveolus to assist gas exchange (Figure 1.10b). Alveoli are very thin and delicate structures lined with two types of pneumocytes (Figure 1.10c). Type I pneumocytes are of simple squamous type, about 0.1-0.2µm thick and are the most abundant. Type II pneumocytes or septal cells are found less abundantly, are larger and protect the alveoli from collapsing by producing surfactant necessary for reducing the surface tension (Siekmeier and Scheuch, 2008). This alveolar epithelium is one of the structural components of the respiratory membrane in addition to the endothelial cells lining the alveolus and the fused basal lamina lying between epithelial and endothelial layers. The thickness of the respiratory membrane can range between 0.1-0.5µm, thereby allowing rapid gas exchange between alveolar air and capillary blood (Figure

1.10d). Also, oxygen and carbon dioxide are both lipophilic therefore easily penetrate the lining cells (Washington *et al.*, 2001b).

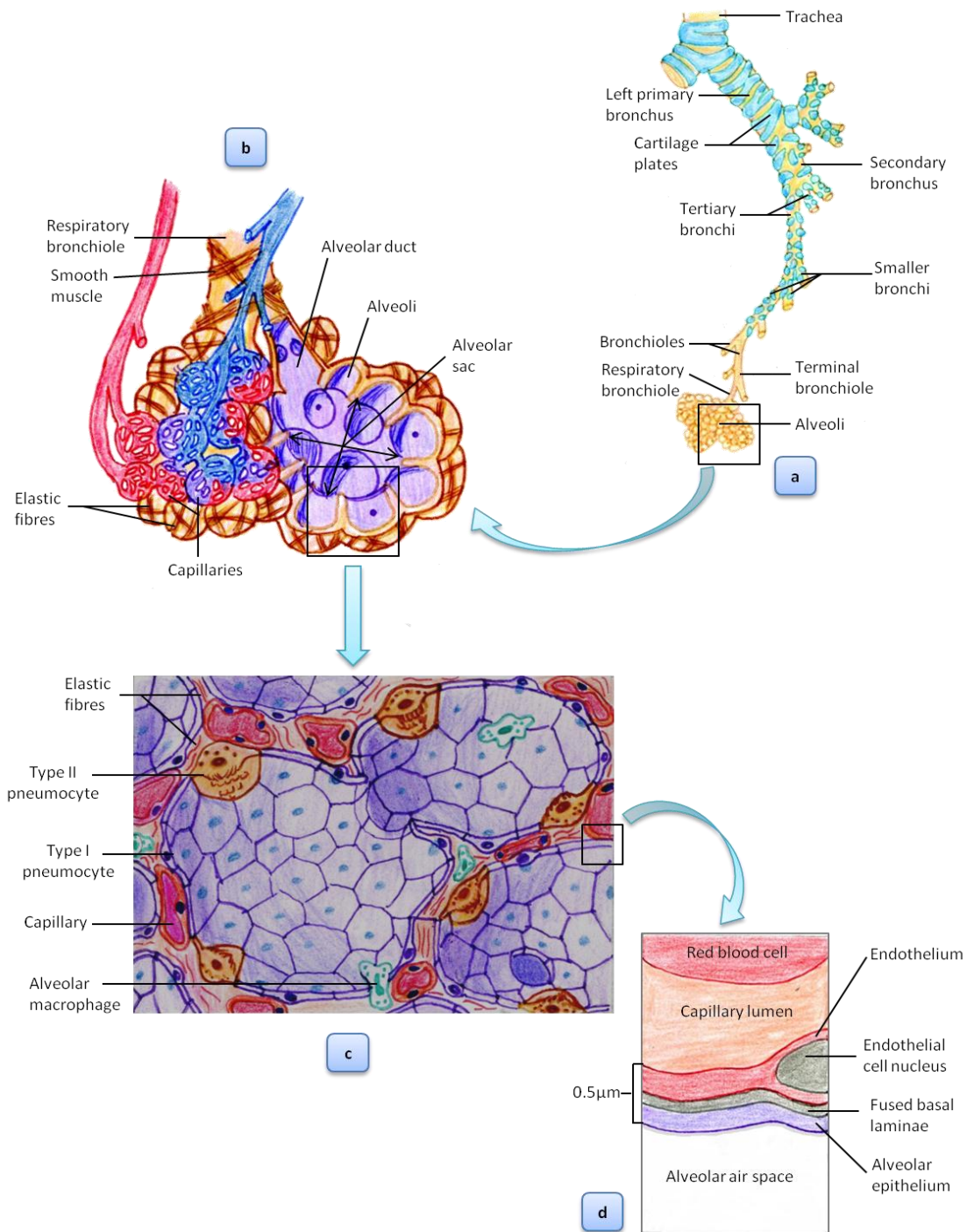


Figure 1.10. The anatomical structure of the bronchial tree (a), the alveoli at the termination of the respiratory bronchiole (b), the cell composition of alveoli (c) and the exchange surfaces between alveolar epithelium and capillary endothelium (d). Modified and reproduced from Martini and Nath (2009c).

1.2.2.2. Physiological barriers in pulmonary delivery

Inhalation therapy is considered to be a non-invasive method of drug delivery that can provide both local as well as systemic effects (Bailey and Berkland, 2009). The main requirement in inhalation therapy is for the drug particles to deposit within the periphery of the lungs in sufficient quantities to produce an effect without being expelled by the defence mechanisms of the respiratory tract (Taylor and Kellaway, 2001). A number of factors influence the deposition of drug particles in the lungs. Physiological factors include the lung's defence system. In the nose, particles over about 10 μ m are captured by the hair lining the vestibular space. Evading particles are trapped in the mucous lining the nasal cavity and nasopharynx. Particles reaching the conducting parts of the lower respiratory tract and larger than 5 μ m are trapped in the lining mucous of the tracheobronchial region (Washington *et al.*, 2001b). Trapped particles in both regions are then cleared by the mucociliary escalator where the ciliated epithelium moves the mucous towards the pharynx to be swallowed and destructed by the stomach acid and enzymes (Schreier *et al.*, 1993). Particles between 1-5 μ m are able to evade the mucous escalator and deposit in the periphery, but are mainly engulfed by alveolar macrophages (Schreier *et al.*, 1993). Particles 0.5 μ m or smaller are considered to be too small to deposit and are exhaled (Oberdörster, 1993). Other physiological factors include the respiratory rate and volume, diameter of airway passages, presence of excess mucous. Physical properties of the aerosol cloud produced also plays a role in the deposition of the drug particles such as particle size, velocity, charge, density and hygroscopicity. The patient's technique in using inhalation devices also affects deposition if not used properly (Taylor and Kellaway, 2001).

1.3. Platinum therapy

Anti-tumour platinum compounds are distinguished from other anti-cancer drugs in that they are coordination structures. These agents exert their anti-cancer effect through their action on cellular DNA in a similar way to alkylating agents. Cisplatin was the first and remains the leading clinically used platinum compound (Abrams, 1990). Intensive development of platinum compounds was investigated and carboplatin was approved in 1989 for the treatment of ovarian cancer by the FDA.

Oxaliplatin was then developed with the intent to overcome the cross-resistance to cisplatin and carboplatin, and in 2002 was granted approval by the FDA for treating colorectal cancer. The addition of picoplatin and satraplatin to the platinum therapeutic family is anticipated, where they are still undergoing clinical trials (Kelland, 2007). The benefits that newer platinum compounds will contribute to therapy are anticipated to be substantial, with satraplatin offering the potential oral administration of a platinum compound for the first time. The structures of these platinum compounds are illustrated (Figure 1.11).

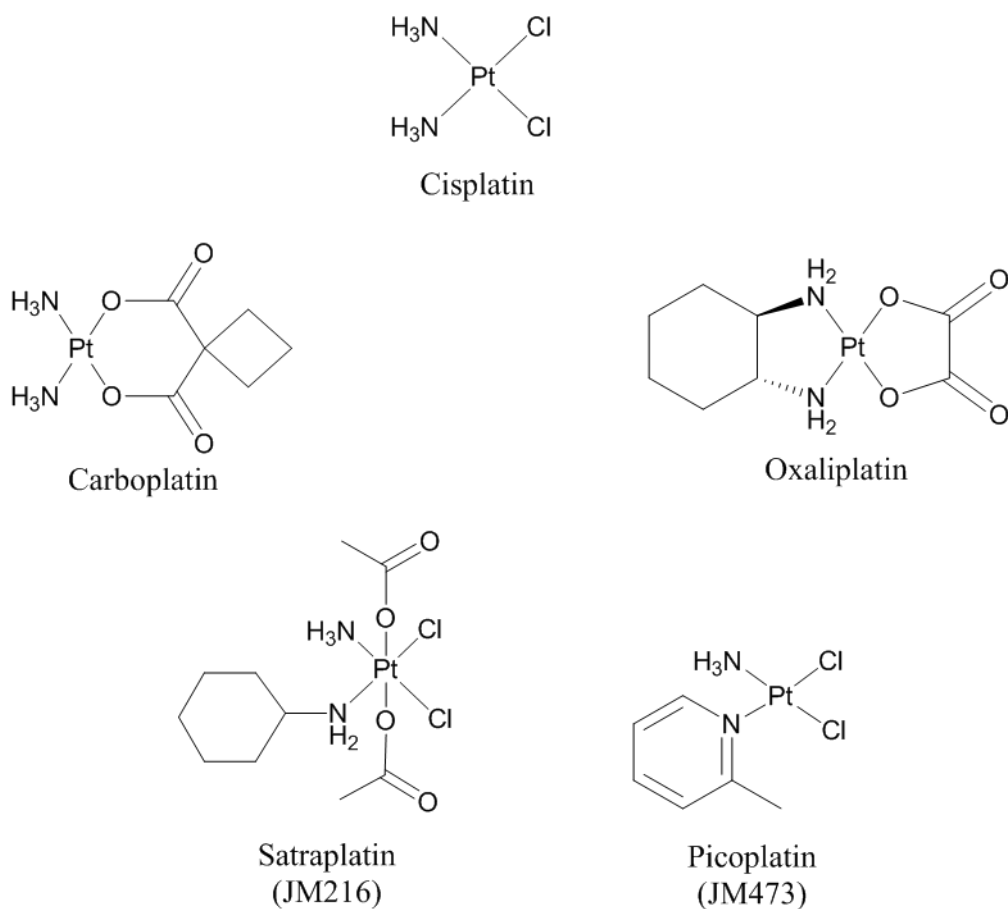


Figure 1.11. The chemical structure of platinum anti-cancer drugs.

1.3.1. Cisplatin

Cisplatin (*cis*-diamminedichloroplatinum (II)) is a water-soluble compound that consists of a central platinum atom connected to two chloride atoms and two ammonia molecules in the “*cis*” configuration.

1.3.1.1. History of cisplatin

Cisplatin was discovered accidentally in 1965 when Barnett Rosenberg was exploring if the division of bacteria was enhanced by an electrical field using platinum electrodes. The unexpected result was that the electrolysis products inhibited the division of *Escherichia coli* bacteria but without affecting their growth where the cells continued to elongate. The products responsible were found to be cisplatin, *cis*-diamminetetrachloroplatinum and transplatin (Rosenberg *et al.*, 1965). Cisplatin was already known as Peyrone’s chloride and was originally synthesised and described in 1845, so technically cisplatin was just a rediscovery. Then in 1968 its anti-cancer effect was confirmed (Rosenberg *et al.*, 1969) and further human clinical trials in 1971 by the National Cancer Institute confirmed its value in testicular and bladder cancers resulting in FDA approval in 1978 (Kelland, 2007).

1.3.1.2. Uses of cisplatin

Cisplatin is used to treat many malignancies either alone or in combination with other compounds. The most treated cancers are testicular, ovarian, head and neck, bladder, cervical and lung cancer (Patrick, 2009).

1.3.1.3. Administration of cisplatin

Cisplatin is administered as a 6-8 hour intravenous infusion in a chloride-containing solution in doses of up to 100mg/m²/course. It is rarely given at higher doses due to unacceptable side effect to benefit ratios. Before commencing treatment patients are pre-hydrated with 1-2 litres of fluid for 8-12 hours to minimise the risk of nephrotoxicity. Mannitol may also be given with the intravenous infusion to maximise urine flow (O’Dwyer *et al.*, 2000). Nausea and vomiting is typically severe and treated by a 5-HT₃ antagonist combined with a glucocorticoid steroid (Gralla *et*

al., 1999). Sometimes a post-hydration fluid is also given in a minimum of 1 litre depending on the dose of the treatment course (O'Dwyer *et al.*, 2000).

1.3.1.4. Side effects of cisplatin

The most important dose-limiting side effects resulting from cisplatin chemotherapy (at single doses of 50mg/m² or above) include nephrotoxicity, ototoxicity, neuropathy, nausea, vomiting and myelosuppression. Rare effects include visual impairment, seizures and arrhythmias. Even with the intensive prophylactic protocols undertaken to maintain kidney function, nephrotoxicity is sometimes inevitable as a result of cumulative renal damage to both glomeruli and tubules (O'Dwyer *et al.*, 2000). Acute renal toxicity has been estimated to develop in 20-30% of cisplatin-treated patients (Hartmann *et al.*, 1999). Ototoxicity resulting from inner ear damage is also cumulative and irreversible, whereas neuropathy is considered to be reversible (O'Dwyer *et al.*, 2000)

1.3.1.5. Mechanism of action of cisplatin

Cellular DNA is believed to be the major target for cisplatin's therapeutic effect. Cisplatin enters the cell either by passive diffusion or protein-mediated transport (Binks and Dobrota, 1990; Andrews *et al.*, 1991; Gately and Howell, 1993; Johnson *et al.*, 1998; Pereira-Maia and Garnier-Suillerot, 2003; Beretta *et al.*, 2004). Most studies indicate that the most popular route of protein-mediated transport is through the copper transporter 1 protein CTR1 (Ishida *et al.*, 2002; Holzer *et al.*, 2004; Howell *et al.*, 2010).

Cisplatin itself is intact and non-reactive until at least one of its chloride ligands is hydrolysed. Due to the high chloride concentration present in the extracellular fluid cisplatin exists in the non-reactive form. After entering the cell the intracellular concentration of chloride ions is lower relative to plasma (Figure 1.12) resulting in the activation of cisplatin by sequential formation of the mono-aqua and diaqua species (Berners-Price and Appleton, 2000).

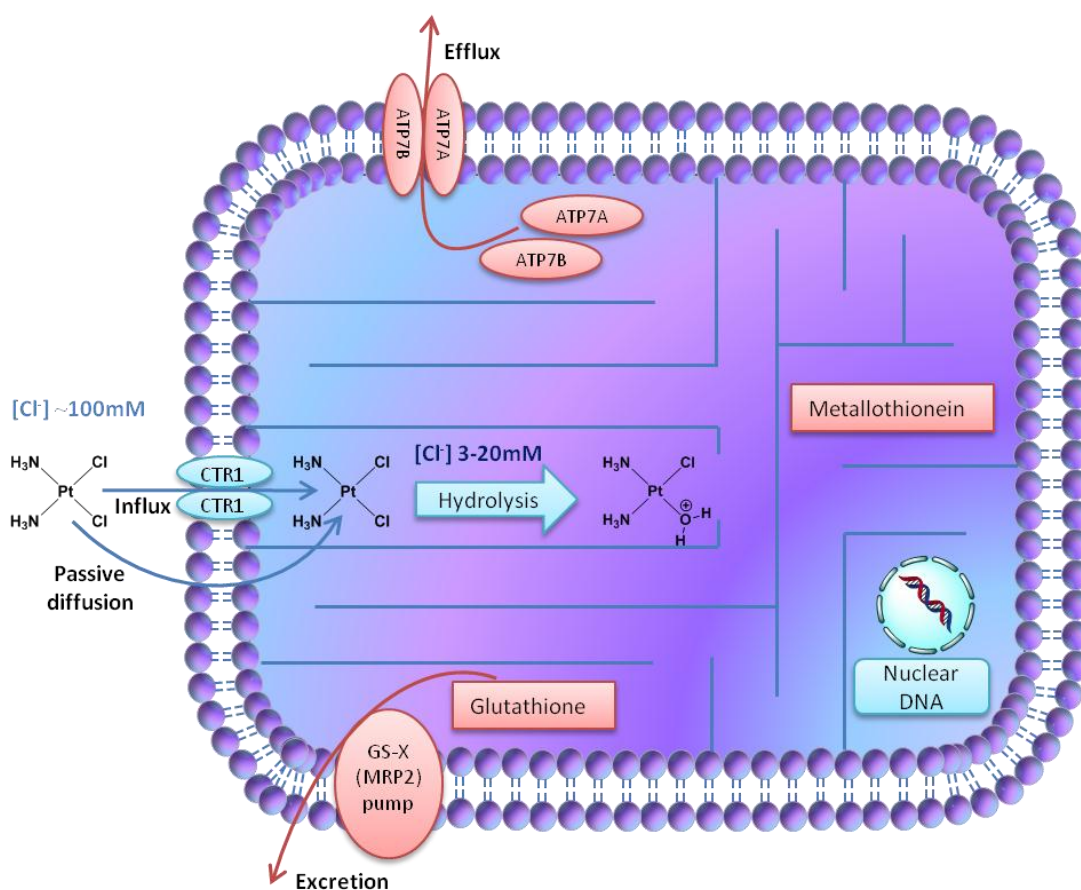


Figure 1.12. The mechanism of cisplatin entry into the cell and possible factors related to resistance.

As illustrated (Figure 1.13), activation starts by the separation of one chloride ion and replacement with a water molecule to form an active positively charged mono-aqua complex. The complex binds to DNA forming a monofunctional adduct preferably at the N7 position of a guanine residue (Prestayko, 1981b; Brabec, 2000). The second chloride ion then undergoes hydrolysis and the resultant aquated compound attacks and binds to the DNA forming a bifunctional lesion. The most common Pt-DNA bindings result from the cross-linking between the diammine platinum unit and the N-7 positions on adjacent guanines. This type of binding is believed to have the most cytotoxic effect (Sherman and Lippard, 1987). Some studies indicated that the types of cisplatin-DNA adducts formed are 65% 1,2-intrastrand crosslinks at a (GG) sequence, about 20% 1,2-intrastrand crosslinks at an (AG) sequence, 9% 1,3-intrastrand crosslink at a (GNG) sequence; where N indicates

any nucleoside and <1% interstrand adducts between two guanines on opposite strands (Eastman, 1999). However, other studies reported that 1,2-intrastrand crosslinks form about 90% of all cisplatin-DNA adducts and the minor adducts formed were interstrand crosslinks (representing 5-10%) between two guanines, 1,3-intrastrand crosslinks and monofunctional adducts (Hansson and Wood, 1989; Jones *et al.*, 1991; Brabec and Leng, 1993). However, it is clear from all studies that the 1,2 intrastrand crosslink between two deoxyguanosines is the dominant type of adduct formed. It was suggested that the increased negative charge in the DNA regions containing the (GG) sequence renders it stronger in attracting the positively charged monoaquated cisplatin species (Pullman and Pullman, 1981).

When cisplatin binds to guanosine, the hydrogen bonds are broken between guanosine and cytidine leading to bending of the DNA double helix at the site of platination towards the major groove followed by unwinding. The Pt-DNA complex inhibits transcription by blocking RNA polymerase II passage at the lesion site (Ang *et al.*, 2010). It is suggested that the alterations in the DNA from platination attract specific proteins containing a high mobility group (HMG) domain (Toney *et al.*, 1989; Bruhn *et al.*, 1992; Pil and Lippard, 1992). The HMG-domain proteins then bind to the site of platination shielding the nucleotide excision repair (NER) system from identifying and repairing the lesion eventually leading to cell death (Prestayko, 1981b; Chaney and Sancar, 1996; Sancar, 1996).

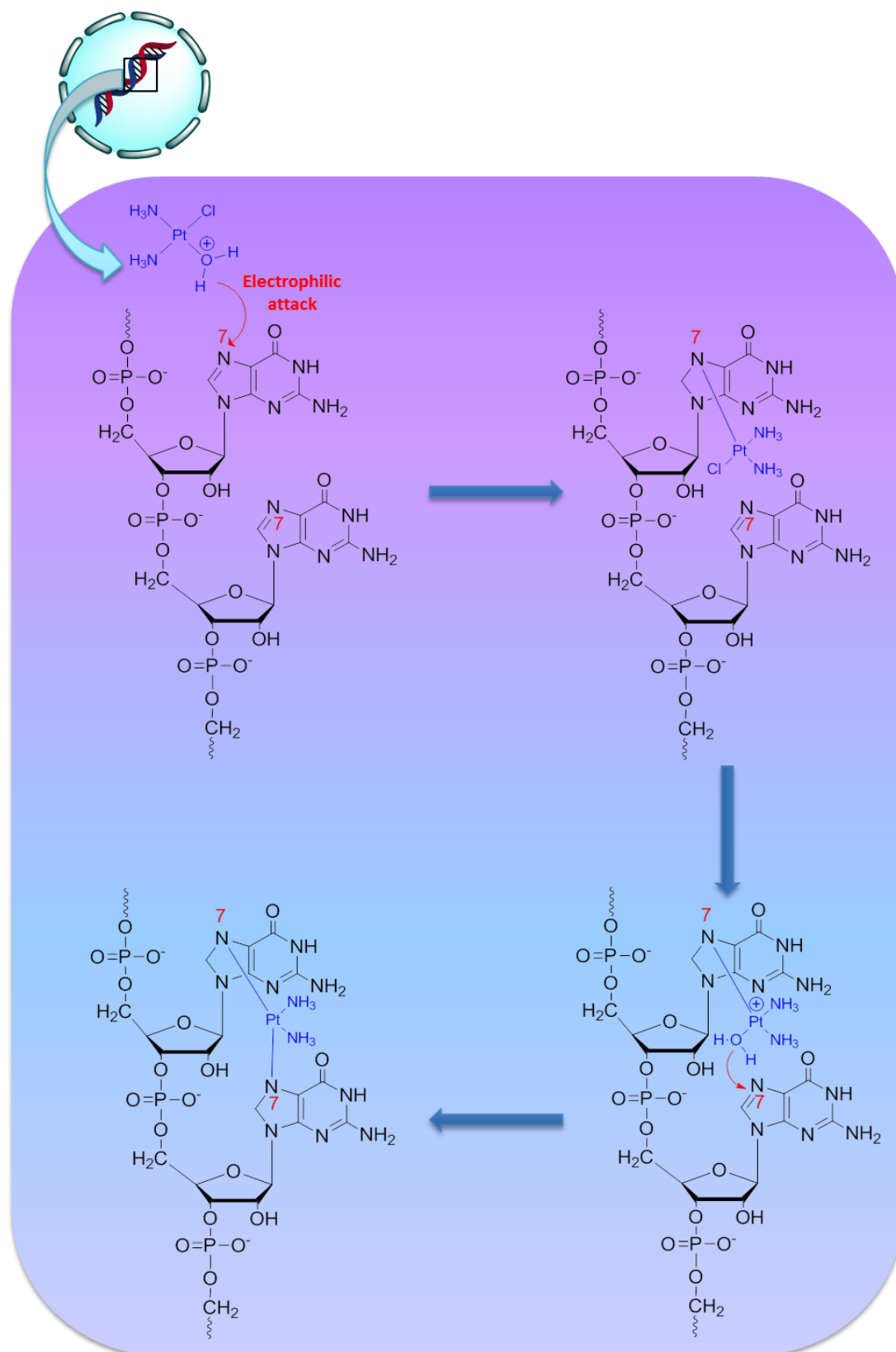


Figure 1.13. The reaction of cisplatin with DNA to form 1,2-intrastrand crosslink on two adjacent guanines.

1.3.1.6. Pharmacokinetics of cisplatin

Plasma clearance of cisplatin following a single intravenous dose was found to follow a biphasic model when radiolabelled $^{193\text{m}}\text{Pt}$ was counted using gamma scintigraphy (DeConti *et al.*, 1973). The initial half-life ($t_{1/2\alpha}$) ranged between 25-49min and the secondary phase ($t_{1/2\beta}$) ranged from 58-73h. Cisplatin urine levels increased with time and the highest level released in the urine was about 50% after 5 days. Cisplatin is excreted mainly by the kidneys but biliary excretion is also possible (Prestayko, 1981a). The binding of cisplatin to plasma protein occurs very fast, where about 90% of platinum is bound to serum proteins within 3hs of dosing (Prestayko, 1981a).

Unbound platinum is cleared rapidly from the plasma after administration, where $t_{1/2\beta}$ for unbound platinum was 40-45 minutes and for protein-bound cisplatin $t_{1/2\beta}$ was 67 hours (De Conti *et al.*, 1973). It is not clear what effect protein bound cisplatin has, but some studies suggest that they are responsible for cisplatin's side effects (Gullo *et al.*, 1980; Appleton, 1997), while others propose that they are crucial for cisplatin's activity (Espinosa *et al.*, 1995) since patients do not respond sufficiently to cisplatin when their serum albumin levels are low. In a study supporting the importance of albumin in cisplatin response, it was found that patients with low levels of albumin (< 40g/L) had a median survival time of 133 days. This survival time was significantly lower than that of the patients with normal levels of albumin (> 40g/L) where their median survival time was 768 days (Holding *et al.*, 1991).

Treatment with cisplatin as a continuous infusion has advantages over a single dose. When 80mg/m² of cisplatin was given in a 24h continuous infusion, about 14% of the dose was excreted in the 24h period (Jacobs *et al.*, 1978), in contrast to the 18-30% that was reported to be excreted after a rapid infusion. Also continuous infusion can lower the side effects without affecting its cytotoxic action (Prestayko, 1981a). Some have attributed this to the non-selective targeting of cisplatin to rapidly proliferating cancer cells regardless of where they are in their individual cell cycles (Patrick, 2009). However, others have related reduced cisplatin toxicity and enhanced tolerability to dosing time. Studies have suggested that the plasma and/or pharmacokinetic profile of cisplatin following a short intravenous infusion depends

on dosing time (Lévi *et al.*, 2007). This is known as cancer chronotherapy where the tolerability and/or efficacy of anti-tumour drugs can be improved by adjusting drug delivery according to the circadian rhythm (Lévi, 2006). Accordingly, the survival rate can vary by 50% or more depending on the circadian dosing time (Lévi, 2006). Platinum complexes including cisplatin, carboplatin and oxaliplatin have been reported to be best tolerated near the middle of the nocturnal activity span of mice or rats (Mormont and Lévi, 2003). Optimal tolerance of cisplatin associated with low renal toxicity in mice was achieved during the activity span of mice at approximately 16 hours after light onset (HALO) (Boughattas *et al.*, 1990), which is equivalent to optimum dosing at 1800 hours in human beings (Lévi *et al.*, 2007). The optimal tolerance of cisplatin during the circadian cycle was found to be related to lower glutathione levels (Mormont and Lévi, 2003). This timing was found to be effective even if cisplatin was administered in combination with other drugs such as gemcitabine (Li *et al.*, 2005), which was suggested as a treatment schedule for lung cancer. However, the circadian rhythm can be altered in cases of malignancy depending on the type, level of differentiation and growth rate of the tumour (Mormont and Lévi, 2003). Rapidly growing cancers and advanced stages show loss of the circadian rhythm and are replaced by an ultradian rhythm (Lévi *et al.*, 2007). This can be associated with reduced effectiveness to cancer chronotherapy. Patients with advanced NSCLC in particular were shown with greatly distorted circadian rhythms (Levin *et al.*, 2005). Furthermore, the application of cancer chronotherapy would require treatment to be tailored to the circadian rhythm of each individual patient. Also the benefits obtained with cancer chronotherapy in terms of increased survival in clinical trials remains to be demonstrated (Lévi, 2006).

1.3.1.7. Resistance to cisplatin

Resistance of tumours to cisplatin is an observed clinical problem. Resistance to cisplatin could occur before or after it binds to DNA. Low accumulation of cisplatin in cells and high levels of glutathione and metallothionein are considered as causes of resistance that occur before the binding of cisplatin to DNA. Enhanced NER mechanism, downregulation of mismatch mechanism repair (MMR) and enhanced

replicative bypass are associated with resistance after the binding of cisplatin to DNA.

1.3.1.7.1. Resistance mechanisms before DNA binding

The factors that could lead to development of cisplatin resistance before binding to DNA are illustrated (Figure 1.12)

The most likely reason for resistance development before binding of cisplatin to DNA could be insufficient drug levels at the tumour site to cause a cytotoxic effect (Gately and Howell, 1993). The transporter, CTR1 is considered to be the main active uptake route for cisplatin but this transporter can also play a role in cisplatin resistance. Damage to the transporter would minimise cisplatin entry into the cell thereby causing resistance. Cisplatin can cause degradation of CTR1 (Holzer *et al.*, 2004; Howel *et al.*, 2010) or copper-induced damage can lead to cross-resistance to cisplatin (Safaei *et al.*, 2004).

Cisplatin accumulation can also be reduced by increased efflux of cisplatin from a cell. ATP7A and ATP7B are efflux proteins involved in copper transport and may play a role in cisplatin efflux (Samimi *et al.*, 2004; Safaei *et al.*, 2004; Safaei and Howell, 2005).

High expression levels of sulphur-containing compounds such as glutathione (Lewis *et al.*, 1988) and metallothionein (Kelley *et al.*, 1988) could be responsible for cisplatin resistance before it binds to DNA. The high levels of glutathione and metallothionein enhance cisplatin resistance once it enters the cell by binding to cisplatin and preventing its interaction with DNA because of the high affinity of cisplatin to sulphur (Mistry *et al.*, 1991; Timmer-Brosscha *et al.*, 1992). Furthermore, multidrug resistance proteins (MRP) can mediate the ATP-dependant export of glutathione S-conjugates (Keppler, 1999). In particular, ATP-dependant glutathione S-conjugate export pump MRP2 has been suggested to play a role in efflux of the cisplatin-glutathione compound thereby resistance (Cui *et al.*, 1999).

1.3.1.7.2. Resistance mechanisms after DNA binding

The first possible reason for developing resistance after binding of cisplatin to DNA could be the enhanced ability of NER proteins to repair DNA damaged by cisplatin (Perez *et al.*, 1990). In particular, the increased expression of the NER endonuclease protein, excision repair cross-complementing-1 (ERCC1), is associated with cisplatin resistance (Ferry *et al.*, 2000).

Loss of MMR function could contribute to resistance after cisplatin has bound to DNA (Aebi *et al.*, 1996). The MMR mechanism normally identifies mismatches in the DNA and attempts to repair it if possible or otherwise triggers an apoptotic response (Fink *et al.*, 1996). However, cisplatin-DNA adducts can cause mutations leading to inactivation of proteins that initiate MMR mechanisms thereby leading to resistance (Helleman *et al.*, 2006).

Enhanced replicative bypass of cisplatin-DNA adducts by DNA polymerases β and η through translesion synthesis also contribute to resistance (Bassett *et al.*, 2002).

Finally, loss of apoptotic signalling pathways also plays a role in cisplatin resistance after binding to DNA. These pathways are controlled by p53, anti-apoptotic and pro-apoptotic members of the BCL2 family and JNK (Anthony *et al.*, 1996; Gadducci *et al.*, 2002).

1.3.1.8. Circumvention of cisplatin resistance

Platinum drugs are an integral part of chemotherapy and have played a major role in treating many cancers. Despite the incidence of resistance, cisplatin remains indispensable as a chemotherapeutic agent in the treatment of a range of cancers. Therefore, the main strategic clinical objective is to develop ways to minimise or prevent resistance to cisplatin (Timmer-Bosscha *et al.*, 1992). By studying the factors that contribute to resistance, approaches to combat resistance were proposed. These solutions include enhancing cisplatin delivery, using platinum resistance modulators, combining cisplatin with novel molecularly targeted drugs, or developing novel platinum drugs that are clinically effective against cisplatin-resistant tumours (Kelland, 2007).

Enhancing the delivery of cisplatin to tumours can be achieved by local delivery of cisplatin. Favourable results were obtained using intraperitoneal administration of cisplatin in combination with paclitaxel in a phase III clinical trial of ovarian cancer (Armstrong *et al.*, 2006). Drug delivery systems such as liposomes e.g. Lipoplatin[®] (Devarajan *et al.*, 2004) or polymers e.g. ProLindac[™] (Howell, 2009; Serova *et al.*, 2009) have been shown to enhance the delivery of platinum drugs. ProLindac is a nanopolymer consisting of the active moiety of oxaliplatin linked to a hydrophilic biocompatible polymer of hydroxypropylmethacrylamide (HPMA; Wheate *et al.*, 2010). It has showed molecular and cellular effects similar to oxaliplatin and is currently in phase II trials for ovarian cancer, a new indication for oxaliplatin (Nowotnik and Cvitkovic, 2009).

Drugs that target resistance modulators could minimise cisplatin resistance. One of these drugs targets the glutathione-metabolizing enzyme GST pi-1 (GSTP1), which is expressed in high levels within cisplatin-resistant cells. GSTP1 can activate the prodrug TER286 to the active TLK286 that releases a nitrogen mustard alkylating agent (Morgan *et al.*, 1998). TLK286, now known as canfosfamide HCl or TELCYTA[®], has shown promising results in combination with pegylated liposomal doxorubicin in a phase II trial for the treatment of refractory or resistant epithelial ovarian cancer (Kavanagh *et al.*, 2010). The use of DNA demethylating agent which targets the hypermethylated MutL gene (MLH1) responsible for loss of MMR pathway and resistance could also reverse platinum resistance. One such drug is decitabine which is predicted to be used in combination with a platinum drug (Plumb *et al.*, 2000). A phase I trial using low doses of decitabine in combination with carboplatin for patients with recurrent platinum-resistant epithelial ovarian cancer, has recently been reported with primary results indicated tolerability and favourable activity (Fang *et al.*, 2010).

Combination therapy with molecular targeting agents could also minimise cisplatin resistance. Bevacizumab in combination with carboplatin and paclitaxel to treat metastatic or advanced non-squamous NSCLC has been encouraging (Triano *et al.*, 2010).

1.3.2. Carboplatin

Carboplatin (diammine [1,1-cyclobutanedicarboxylato(2-)-*O,O'*] platinum (II)) is a second generation drug in the platinum class. It has the same activity as cisplatin but with less toxic side effects (Dabrowiak and Bradner, 1987) except for myelosuppression which is more severe and dose-limiting. Carboplatin contains a cyclobutanedicarboxylate ligand as the leaving group instead of the chloride ligands in cisplatin. The leaving group in carboplatin is considered to be less labile than that in cisplatin, which may explain its lower toxicity. Carboplatin is widely used to treat advanced ovarian cancer and lung cancer, but some types of cancer are more responsive to cisplatin than carboplatin such as testicular and head & neck cancers. It can be given intravenously on an out-patient setting and no pre-hydration treatment is necessary. Nevertheless, even though carboplatin is better tolerated, cross-resistance between carboplatin and cisplatin is typical (O' Dwyer *et al.*, 1999).

1.3.3. Oxaliplatin

Oxaliplatin ([oxalate(2-)-*O,O'*][*(1R,2R)*-cyclohexanediamine-*N,N'*] platinum (II)) is a 1,2-diaminocyclohexane derivative (DACH) and has shown activity against several cisplatin-resistant tumour cell lines (Kraker and Moore, 1988). Oxaliplatin is used in the treatment of metastatic colorectal cancer in combination with fluorouracil and folinic acid, and is administered as an intravenous infusion. It causes less nephrotoxic effects than cisplatin but its dose-limiting toxicity is sensory neuropathy which characterises all DACH-containing platinum species (O' Dwyer *et al.*, 1999).

1.3.4. Picoplatin

Picoplatin (*cis*-amminedichloro, 2-methylpyridine, platinum (II)), which is also referred to as JM473, AMD473 or ZD0473, is a platinum compound that has been designed with improved efficacy against cisplatin and carboplatin resistant tumours (Judson and Kelland, 2000). The structural design of picoplatin designated in the picoline ring increases the steric bulk of picoplatin (Eckardt *et al.*, 2009), which can prevent its interaction with thiol-containing groups, one of the common causes of platinum resistance (Kelland, 2000).

Preliminary studies indicated the effectiveness of picoplatin in NSCLC, head & neck, mesothelioma and ovarian cancer (Judson and Kelland, 2000). Phase II clinical trials of picoplatin have demonstrated effectiveness against mesothelioma (Giaccone *et al.*, 2002), NSCLC and SCLC (Treat *et al.*, 2002), prostate cancer (Tyrrell *et al.*, 2001) and ovarian cancer (Gore *et al.*, 2002). A better toxicity profile was also observed in these studies, where nephrotoxicity, ototoxicity and neurotoxicity were not apparent. Picoplatin's dose limiting toxicity was myelosuppression resulting in haematological toxicities.

In a follow-up phase II study, the use of picoplatin as second line therapy in refractory or progressive SCLC demonstrated favourable results with enhanced median overall survival. The study also reported haematological toxicities being predominant (Eckardt *et al.*, 2009). Results of a phase III study supported the use of picoplatin as second line therapy for progressive SCLC in combination with best supportive care (Ciuleanu *et al.*, 2010).

Picoplatin is also being considered for treatment of NSCLC, where the outcomes of an ongoing phase II trial using picoplatin as second line treatment in progressive NSCLC after cisplatin therapy is awaited (Chang, 2010).

1.3.5. Satraplatin

Satraplatin (*bis*-[acetate]-ammine dichloro-[cyclohexylamine] platinum (IV)), also referred to as JM216, was developed with the ambition of creating an orally active platinum drug with low toxicity and no cross-resistance to clinically used platinum complexes (Weiss and Christian, 1993). Its octahedral Pt (IV) structure distinguishes it from the rest of the square planar Pt (II) structure of cisplatin, carboplatin, oxaliplatin and picoplatin (McKeage *et al.*, 2007). The presence of the two axial acetate groups enhances its lipophilicity and oral bioavailability. *In vivo*, satraplatin is metabolised into JM113 (*cis*-ammine dichloro (cyclohexylamine) platinum (II)) and other metabolites. JM113 is considered to be an active metabolite of satraplatin that can also bind and react with DNA (Choy *et al.*, 2008). The main toxicity related to satraplatin therapy is haematological with no evidence of nephrotoxicity or neurotoxicity observed (Choy *et al.*, 2008).

Clinical studies have investigated satraplatin in patients with hormone-refractory prostate cancer (HRPC) combined with prednisone as a second line treatment in a large phase III trial, called ‘Satraplatin and Prednisone against Refractory Cancer (SPARC) trial’ (Sternberg *et al.*, 2007). Although this study reported an improved progression-free response, follow-up analysis indicated that there was no significant difference in the overall survival rate between patients treated with satraplatin combined with prednisone and those treated with prednisone alone. Further analysis studies were reported to be underway to determine if improved survival is likely to be present in a subset of patients (Sternberg *et al.*, 2007; Choy *et al.*, 2008). Satraplatin in combination with prednisone was also investigated in multinational double-blind phase III (SPARC trial) in patients with castrate-refractory prostate cancer (CRPC) as second-line treatment (Sternberg *et al.*, 2009). The study showed that disease progression and associated pain were delayed with the combination treatment although overall survival was not improved.

In a study reported by Ricart *et al.* (2009), the effect of food on the pharmacokinetics of satraplatin compared to the fasted state was reviewed. In this study, the presence of food affected the pharmacokinetics of satraplatin causing a reduction in its C_{max} and AUC_{0-24} . Therefore, satraplatin should be administered in the fasting state, although it was not clear whether this significant change in pharmacokinetics ultimately leads to reduced anti-cancer effects.

1.4. Vesicular delivery systems – liposomes and niosomes

The use of vesicular delivery systems is one of the proposed methods to enhance cisplatin delivery, minimise toxic side effects and possibly hinder the threat of resistance (Section 1.3.1.8). Lipid vesicles are structures composed of one or more lipid bilayer surrounding an aqueous core (Figure 1.14). Liposomes have been proven to enhance the bioavailability and minimise the toxicity of the anti-cancer drugs doxorubicin and daunorubicin (Park, 2002). Niosomes are lipid vesicles structurally and functionally similar to liposomes (Uchegbu and Vyas, 1998). However, niosomes are cheaper alternatives to liposomes, less likely to become toxic and more stable thereby easier to store and handle as they are formed from synthetic

lipids unlike the biologically derived phospholipids used to prepare liposomes (Uchegbu and Florence, 1995).

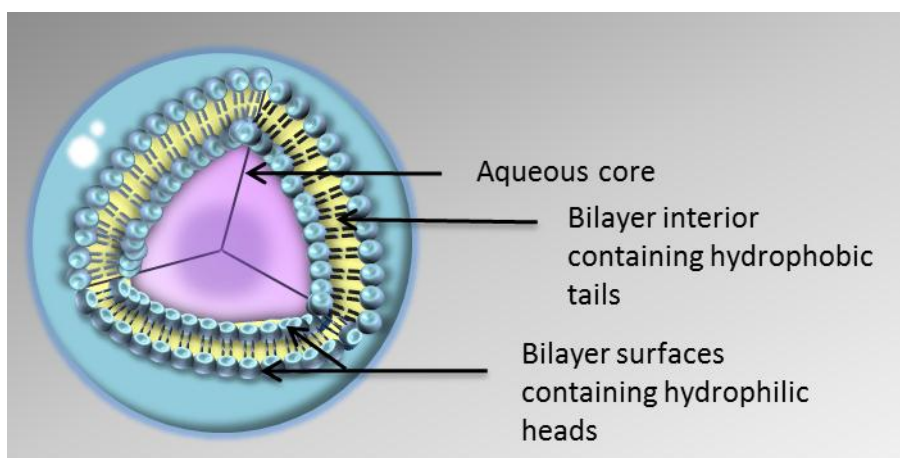


Figure 1.14. The structure of a unilamellar lipid vesicular delivery system.

1.4.1. Liposomes

Liposomes were first described in 1965 to share many of the dimensional, structural and functional properties of biological membranes (Bangham *et al.*, 1965). This initiated the idea to use liposomes as drug delivery vehicles, but it took 30 years for the clinical use of liposomes to be applied in reality (Lian and Ho, 2001).

Upon hydration of lipids, liposomes spontaneously form in the shape of spherical enclosed vesicular structures. These structures form from the self-assembly of lipids into colloidal particles composed of a lipid bilayer surrounding an aqueous core (Figure 1.14). The lipid bilayer is arranged in a way that the hydrophilic head groups face the aqueous medium on both sides and protect the hydrophobic tail moieties contained in the bilayer space (Lasic and Papahadjopoulos, 1995; Ranson *et al.*, 1996). Phospholipids are the main lipid composition of liposomes especially in the form of phosphatidylcholine as well as phosphatidylglycerol and phosphatidylethanolamine (Crommelin *et al.*, 2001). Drugs may be entrapped in the

aqueous core, within the bilayer or at the bilayer interface depending on their physicochemical properties (Goyal *et al.*, 2005).

1.4.1.1. Classification of liposomes

Liposomes were classified based on lamellarity and size by Perez-Soler into two classes, unilamellar and multilamellar vesicles (Perez-Soler, 1989). Unilamellar vesicles "UVs" could be small "SUVs" ranging from 0.05-0.1 μ m in diameter or large "LUVs" ranging from 0.1-0.25 μ m in diameter. Their aqueous cores are large relative to the whole vesicle and thereby suitable for entrapping water-soluble compounds. Multilamellar vesicles "MLVs" range from 1-5 μ m in diameter. Their aqueous cores are relatively small (<10%) thereby limiting the entrapment efficiency of hydrophilic drugs unlike hydrophobic drugs which can be entrapped efficiently in their multiple lipid bilayers (Harrington *et al.*, 2000a).

Liposomes have also been classified based on functionality into a number of classes mainly; conventional liposomes, long-circulating liposomes, immunoliposomes and pH-sensitive liposomes (Sharma and Sharma, 1997). Conventional liposomes can be anionic, cationic or neutral and are used for passive targeting through subsequent opsonisation and uptake by the MPS. This is beneficial in targeting organs rich in the MPS. Cationic liposomes have shown potential in gene therapy as carriers for the negatively charged plasmid DNA (Wasungu and Hoekstra, 2006) and efficiently transfer genes (Maitani *et al.*, 2007). Long-circulating liposomes, also known as sterically stabilised liposomes, have a hydrophilic polymer such as polyethylene glycol (PEG) attached onto their surfaces. The conjugated polymer increases surface hydration in order to delay recognition and uptake by the MPS as much as possible hence prolong their circulation time (Lasic and Needham, 1995). Immunoliposomes have specific antibody(s) attached to their surface to facilitate cellular targeting (Sapra and Allen, 2003; Völkel *et al.*, 2004). pH-sensitive liposomes are transformed from stable to destabilised structures in acidic conditions and acquire fusogenic properties leading to the release of entrapped material (Simões *et al.*, 2004). This can be useful in targeting sites with acidic environment such as tumours (Drummond *et al.*, 2008). Other types of liposomes include temperature-sensitive (Sullivan and Huang, 1986) and target-sensitive magnetic liposomes (Elmi and Sarbolouki, 2001).

This indicates that liposomes of preferable qualities can be obtained by modulating the bilayer composition (Voinea and Simionescu, 2002).

1.4.1.2. Implications of liposomal physical characteristics

The physical characteristics of a vesicular delivery system such as surface charge, bilayer fluidity and vesicle size control its stability and *in vivo* behaviour. The surface charge of liposomes affects their stability as well as their fate inside the body (Drummond *et al.*, 2008). Liposomes bearing a neutral charge are less likely to be cleared by the MPS, but this advantage is compromised by their propensity to aggregate (Lian and Ho, 2001). Using charged liposomes may overcome the dilemma of aggregation, yet risk rapid clearance. Anionic liposomes face recognition by macrophage receptors as well as other cell receptors. Cationic liposomes are also taken up by the MPS because of their great reactivity with serum proteins (Lian and Ho, 2001). Fidler *et al.*, (1980) indicated the greater uptake of negatively charged liposomes by the MPS followed by positively charged and then neutral liposomes.

Fluidity of the lipid bilayer is determined by the transition temperature (T_c). T_c is defined as the temperature in which a liposomal system exists in two states of equal proportion, gel state and liquid state (Ranade *et al.*, 1989). Above T_c , the liposomal system becomes less organised and below T_c becomes well organised (Sharma and Sharma, 1997). The fate of entrapped drugs depends on the fluidity of the bilayer, where a less organised liposomal system is more likely to leak its entrapped drug. It has been reported that maximum leakage is reached at the T_c of a particular liposomal system (Risbo *et al.*, 1997). T_c of a liposomal system depends on the type of lipids used in terms of the length of their fatty acid chains and whether the chains are saturated or not (Gray and Morgan, 1991). Therefore, using a combination of lipids can help maintain the fluidity of the liposomal bilayer. Cholesterol, for instance, increases transmembrane permeability at low concentrations while at higher concentrations (above 30mol%) phase transition is eliminated and membrane permeability is reduced at temperatures above T_c (Lian and Ho, 2001). Inclusion of cholesterol can improve bilayer fluidity, reduce permeability and reduce liposomal identification by plasma proteins (Vemuri and Rhodes, 1995).

Liposomal size is also of great relevance to its properties where the greater the size the greater the clearance (Drummond *et al.*, 2008). Even with the design of pegylated liposomes to minimise opsonisation, their size should not exceed the range of about 150-200nm for their circulation to be extended (Lian and Ho, 2001).

1.4.1.3. Clinical studies of liposomes

When drugs are encapsulated into liposomes, the plasma pharmacokinetics and tissue distribution could become dependent on the liposome itself rather than the entrapped drug (Voinea and Simionescu, 2002). As a result the therapeutic index of the entrapped drug can be enhanced by increasing efficacy and reducing toxicity from undesirable exposure (Newman *et al.*, 1999; Park, 2002; Júnior *et al.*, 2007a).

This theory was proven by the enhanced bioavailability and reduced toxicity in the form of liposomal doxorubicin (Caelyx™ and Myocet™), daunorubicin (DaunoXome™), and amphotericin B (AmBisome™) which are administered intravenously. Caelyx™ is a pegylated liposomal preparation of doxorubicin hydrochloride used in the treatment of AIDS patients with Kaposi's sarcoma and metastatic breast cancer and as second line therapy for advanced ovarian cancer and progressive multiple myeloma. Myocet™ is used in the treatment of metastatic breast cancer in combination cyclophosphamide. DaunoXome™ is used to treat advanced Kaposi's sarcoma in AIDS patients. AmBisome™ is used in the treatment of severe fungal infections and visceral leishmaniasis (Felnerova *et al.*, 2004). Therefore, encapsulation of cisplatin into liposomes could overcome the drawbacks of conventional cisplatin therapy and be used to enhance clinical responsiveness to this agent.

In one study, stealth pH-sensitive liposomes containing cisplatin (spHL-CDDP) were used since tumour tissues have a pH lower than that of healthy ones. These liposomes were composed of dioleoylphosphatidylethanolamine (DOPE), cholesteryl hemisuccinate (CHEMS), and distearoylphosphatidylethanolamine-polyethyleneglycol₂₀₀₀ (DSPE-PEG₂₀₀₀). It was assumed that these liposomes would release their contents in an acidic medium, as a result of protonation of CHEMS, and rupture of liposomal structure. Free or liposomal cisplatin in doses of 6mg/kg were

administered to Ehrlich tumour-bearing Swiss mice by a single intravenous injection. Treatment with spHL-CDDP was more effective than free cisplatin, achieving higher blood concentrations and accumulation in the liver and spleen. Liposomal cisplatin partitioned less into renal tissues, thereby reducing nephrotoxicity. Another benefit reported was the longer bloodstream retention of these liposomes compared to free cisplatin leading to extensive accumulation within tumour tissues (Júnior *et al.*, 2007a). A continuation of this study was reported by Leite *et al.* (2009) who used the same liposomal formulation to compare free cisplatin and spHL-CDDP toxicities in Swiss mice following intraperitoneal administration. The study revealed that 10-20mg/kg free cisplatin showed significant myelosuppression and nephrotoxicity, unlike 30mg/kg spHL-CDDP suggesting that liposomes could minimise cisplatin toxicity.

Ongoing research has resulted in some liposomal cisplatin preparations managing to enter clinical studies. This includes Stealth[®] liposomes (SPI-77[™]), SLIT[™] and Lipoplatin[®]. However regulatory approval has not been granted to any of these formulations.

SPI-77 was developed by ALZA Pharmaceuticals[®], formerly known SEQUUS Pharmaceuticals. These Stealth liposomes are sterically stabilised with the pegylated lipid [*N*-(carbamoyl-methoxypolyethylene glycol 2000)-1,2-distearoyl-*sn*-glycero-3-phosphoethanolamine sodium salt (MPEG-DSPE). They also contain cholesterol and fully hydrogenated soy phosphatidylcholine (HSPC). The cisplatin concentration in the liposomal suspension is 1mg/ml with an encapsulation efficiency of 90% and particle diameter of approximately 110nm (Vail *et al.*, 2002). It was postulated that, with the liposomes being sterically stabilised and small, their circulation time would be prolonged by evading opsonisation mechanisms and uptake by the MPS (Kim *et al.*, 2001). When SPI-77 entered many phase I and II clinical trials, for patients suffering from lung, ovarian, head and neck cancer as well as paediatric tumours, the concept was proven. Results from the trials demonstrated a desirable pharmacokinetic profile for the liposomal cisplatin compared to free cisplatin with no nephrotoxicity and ototoxicity observed. However, cisplatin was not released easily from the liposomal vehicle resulting in low plasma levels of ultrafiltered platinum

and relatively poor accumulation of cisplatin in tumours even after doses reaching 420mg/m². This was interpreted as insufficient anti-tumour activity and further studies were discontinued (Harrington *et al.*, 2001; Kim *et al.*, 2001; Meerum Terwoeg *et al.*, 2002; White *et al.*, 2006).

Transave has developed an inhaled cisplatin complex (Sustained release Liposomal Inhalation Therapy “SLIT™” Transave, Inc.) and evaluated its performance in patients suffering from bronchoalveolar carcinoma and lung cancer metastasised from recurrent osteosarcoma. Phase II clinical trials, published as an abstract in the 2006 meeting of the American Society of Clinical Oncology indicated promising results. In 18 patients with metastasised osteosarcoma to the lungs receiving 24 or 36mg/m² of drug by inhalation every two weeks for six cycles, two patients became disease free with no myelosuppression, nephrotoxicity or neurotoxicity reported (Transave, 2010).

Lipoplatin, similarly to SPI-77, is another pegylated liposomal cisplatin preparation developed by Regulon Inc. (Froudarakis *et al.*, 2008). The lipid composition of Lipoplatin includes dipalmitoyl phosphatidyl glycerol (DPPG), soy phosphatidylcholine, and cholesterol; which are conjugated with methoxypolyethylene glycol distearoyl phosphatidylethanolamine (mMPEG2000-DSPE). The liposomes have an average size of 110nm and are reported to contain 3mg/ml cisplatin (Devarajan *et al.*, 2004). In a preclinical study, Devarajan *et al* investigated the nephrotoxic effect of Lipoplatin in comparison to cisplatin solution on a mouse and rat model. Mice and rats were administered 20mg/kg and 5mg/kg, respectively, of cisplatin or Lipoplatin intraperitoneally as a single injection. The results indicated that Lipoplatin when compared to an equal dose of cisplatin showed no evidence of nephrotoxicity and maintenance of normal kidney function following Lipoplatin administration (Devarajen *et al.*, 2004). Lipoplatin in combination with gemcitabine has reached phase I clinical trials as a second line treatment for NSCLC (Froudarakis *et al.*, 2008) and phase II trials in inoperable (stage III/IV) NSCLC (Mylonakis *et al.*, 2009). In both studies it was reported that the Lipoplatin gemcitabine combination was well tolerated and nephrotoxicity was not observed. Phase III studies using this combination are ongoing and results are awaited.

1.4.2. Niosomes

In the 1970's, niosomes were used by researchers in the cosmetic industry. In fact, they were the first to report the self-assembly of non-ionic surfactants into vesicles (Handjani-Vila *et al.*, 1979). With the discovery of liposomes and their potential as drug carriers, this prompted the motivation to also use niosomes in drug delivery.

Niosomes or non-ionic surfactant vesicles (NIVs) are formed in the same way that liposomes are formed. Upon lipid hydration, niosomes are formed in the shape of spherical enclosed vesicular structures. These structures form from the self-assembly of non-ionic amphiphiles into colloidal particles composed of a lipid bilayer enclosing an aqueous core (Uchegbu and Vyas, 1998). The hydrophilic heads of the component amphiphiles in the lipid bilayer are oriented towards the aqueous phase with the hydrophobic tails shielded from the aqueous environment within the interior of the bilayer (Florence, 1993a). The various types of vesicle forming non-ionic surfactants include: alkyl ethers, alkyl esters, alkyl amides, fatty acid and amino acid compounds (Ozer *et al.*, 1991; Florence, 1993b; Uchegbu and Florence, 1995). As with liposomes, drugs can be entrapped in the aqueous core, within the bilayer or at the bilayer interface depending on their physicochemical properties.

1.4.2.1. Classification of niosomes

Niosomes can also be classified based on size and lamellarity as liposomes. Niosomes can be unilamellar in the form of SUVs and LUVs and can be multilamellar in the form of MLVs (Florence, 1993a).

Niosomes can also be classified based on functionality as liposomes. Conventional niosomes can carry a negative, positive or neutral charge. This can be beneficial in targeting organs rich in the MPS such as the liver and spleen (Baillie *et al.*, 1986). Cationic niosomes have been used in gene therapy (Huang *et al.*, 2008; Manosroi *et al.*, 2010). Sterically stabilised niosomes can also be produced by attaching hydrophilic polymers such as PEG onto their surfaces (Shi *et al.*, 2006; Hong *et al.*, 2009). The design and application of immunoniosomes (Hood *et al.*, 2007), pH-sensitive niosomes (Di Marzio *et al.*, 2011) and temperature-sensitive niosomes (Kato *et al.*, 2008) are also under investigation.

1.4.2.2. Implications of niosomal physical characteristics

The physical factors which affect a liposome's characteristics also affect niosomes. Surface charge, is usually conferred on the niosomes to prevent aggregation and increase stability. Adding a surfactant such as stearylamine renders the vesicle positively charged; whereas inclusion of dicetyl phosphate renders it negatively charged (Uchegbu and Vyas, 1998). Similarly to liposomes, clearance is the fastest in negatively charged niosomes followed by positively charged then neutrally charged niosomes (Erdogan *et al.*, 1996). In cases where the entrapped drug is hydrophobic, a steric stabiliser must be added to prevent aggregation because the presence of the drug within the bilayer alters the membrane's electrophoretic mobility (Uchegbu *et al.*, 1995). Bilayer fluidity can be controlled by cholesterol addition to eliminate phase transition and reduce membrane permeability at temperatures above T_C (Rogerson *et al.*, 1987). Moreover, the more rigid a niosomal bilayer is the greater will be its entrapment efficiency (Uchegbu and Duncan, 1997). As with liposomes, size is another important factor that plays a role in a niosomal system's distribution after administration (Uchegbu and Vyas, 1998).

1.4.2.3. Clinical studies of niosomes

Niosomes also have the ability to manipulate the pharmacokinetic profile of an entrapped drug and improve its therapeutic index (Florence, 1993a). The wide application of niosomes in drug delivery by various administration routes has been studied. Many of the studies have shown promising results and future studies to endorse the initial findings are strongly recommended. However, to date, no commercially available niosomal preparation of any drug has been reported. A few examples illustrating the successful possibilities of niosomes as drug carriers, each with a different route of administration, are presented below.

Sodium stibogluconate (SSG) is an antimony compound used in the treatment of visceral leishmaniasis (VL). The delivery of SSG in tetraethylene mono-n-hexadecyl ether niosomes through a single intravenous injection had greater effectiveness than free SSG in reducing parasite burdens in the spleen and bone marrow when given as a single intravenous dose to BALB/c mice (Banduwardene *et al.*, 1997). The same

formulation was compared with three commercially available amphotericin B (AmB) products used to treat VL by Mullen *et al.* (1998) in BALB/c mice. The AmB formulations used were AmBisome[®], Abelcet[®] and Amphocil[®]. Although SSG and AmB have different physicochemical and pharmacokinetic properties, vesicular delivery proved to protect entrapped drug and alter its pharmacokinetics, so that drugs were active 18 days post-administration in a pre-treatment course. From comparison studies it was concluded that niosomal SSG was highly effective in reducing parasite burdens in the liver, spleen and bone marrow at an activity comparable to the clinically available AmB formulations.

Rifampicin encapsulated in Span 85 niosomes showed a potential in enhancing tuberculosis treatment in comparison to free drug following intravenous administration. The vesicles were found to accumulate to a greater extent in the lungs of mice due to their considerably large size ranging between 8-15 μ m (Jain and Vyas, 1995a).

All-trans retinoic acid (ATRA) has been reported to exhibit anti-cancer effects and is a potential therapeutic agent in lung cancer (Kalemkerian *et al.*, 1994; Athanasiadis *et al.*, 1995; Lokshin *et al.*, 1999). Pulmonary delivery of ATRA encapsulated in niosomes has been considered as a possible candidate to overcome toxicities associated with chronic use of ATRA solution (Desai and Finlay, 2002). Initial *in vitro* studies indicated that ATRA can be efficiently encapsulated in niosomes composed of a combination of Span 20 or Span 60 with Tween 80. Analysis of nebulised niosomes showed entrapment efficiency exceeding 50% and aerodynamic diameter suitable for pulmonary delivery around 3.7 μ m for the Span 20/Tween 80 formulation and 3.58 μ m for the Span 60/Tween 80 formulation (Desai and Finlay, 2002).

Bayindir and Yuksel (2010) performed *in vitro* studies to identify the best niosomal composition for oral delivery of paclitaxel. The study indicated that niosomes containing Span 40 was optimal with respect to size, zeta potential (ZP), entrapment efficiency (96.6%) and potential gastro-intestinal stability during simulations in gastric and intestinal fluids containing enzymes.

The use of niosomes in the delivery of other anti-cancer agents has been reported such as; methotrexate (Jain and Vyas, 1995b), doxorubicin (Uchegbu *et al.*, 1995), *N*-(2-hydroxypropyl) methacrylamide copolymer-doxorubicin (PK1) (Uchegbu and Duncan, 1997; Gianasi *et al.*, 1997), vincristine (Parthasarathi *et al.*, 1994) and bleomycin (Naresh and Udupa, 1996).

Most importantly, the niosomal delivery of cisplatin is largely undocumented compared to liposomes. A single study has been found regarding the effectiveness of niosomal cisplatin in comparison to free cisplatin in a murine B16-F10 melanoma model following a single intravenous injection (Gude *et al.*, 2002). The niosomes were prepared from Span 60 and contained a cisplatin concentration of 1mg/ml. The study suggested significant efficacy of niosomal cisplatin in inhibiting lung tumour nodules, with lower associated toxicity in the form of myelosuppression and weight loss. However, they did not report nephrotoxicity, which is main dose-limiting side effect of cisplatin. Furthermore, no follow-up studies have been reported since then.

1.5. Analytical methods for detecting platinum

It is important to understand the pharmacokinetics, pharmacodynamics and metabolism of anti-cancer drugs in biological systems as this has an important bearing on their clinical use. In addition, with respect to platinum-containing anti-cancer agents, measurement of metals originating from anti-cancer agents is relevant to assess occupational exposure of health care personnel (Brouwers *et al.*, 2008a). Therefore, rapid and reliable analytical tools for detecting intact cisplatin and its biotransformation products is a basic requirement in systematic cancer chemotherapy, with the objectives of dose optimisation and clinical application (Huang *et al.*, 2006a). Of course, a detailed description of each analytical method is not within the scope of the present research, but a brief overview of methods for analysing platinum levels and their sensitivity and ease of application will be undertaken.

Cisplatin is an active drug which undergoes ligand exchange reactions *in vivo* (Daley-Yates and McBrien, 1983). It reacts with nitrogen, oxygen and sulphur residues on other biomolecules such as plasma proteins leading to the production of

multiple platinum species post-administration of cisplatin (Bell *et al.*, 2006). Such species include high and low molecular weight protein bound species and non-protein bound species including soluble transformation products and unchanged cisplatin (Daley-Yates and McBrien, 1983). The transformation of cisplatin *in vivo* was studied by Daley-Yates and McBrien (1984) who identified nine platinum species in the plasma ultrafiltrate of rats following intraperitoneal administration of cisplatin solution. Cisplatin rapidly binds to plasma proteins either irreversibly rendering it inactive or reversibly thereby allowing sustained release (Bannister *et al.*, 1977).

The methods involved in platinum analysis can be divided into non-selective methods and selective methods. Non-selective methods of quantification do not discriminate between the active and inactive forms of cisplatin. Selective methods are able to detect the active forms of cisplatin. In an early review by Riley (1988), different methods applied in the biological analysis of cisplatin were described. Non-selective methods reported included X-ray fluorescence, proton-induced X-ray emission platinum, flameless atomic absorption spectroscopy as well as the radioactive detection of $^{193\text{m}}\text{Pt}$ -labeled cisplatin using γ scintillation counting (DeConti *et al.*, 1973; Jones, 1976; Pera and Harder, 1977). However, non-selective methods would provide an overestimation of the cytotoxic forms of platinum available and can therefore be misleading. The complexity associated with these analytical techniques can make access limited, throughput low and sample analysis expensive (Riley, 1988).

Differentiation between bound and unbound platinum species by solvent precipitation of proteins or ultrafiltration prior to analysis can allow more clinically relevant information to be gathered (Bell *et al.*, 2006).

Bannister *et al.* (1977) detected free cisplatin in plasma by application of ultrafiltration followed by X-ray fluorescence. The method was influenced by sample composition; showed low detection sensitivity with the limit of detection reported to be 240 $\mu\text{g/L}$ and linear fluorescence intensity between 570-5700 $\mu\text{g/l}$.

In an attempt to overcome the disadvantages associated with X-ray fluorescence detection of platinum, flameless atomic absorption spectroscopy methodology was developed (Bannister *et al.*, 1978). The method was reported to show high reproducibility and sensitivity in contrast to X-ray fluorescence with a 10-fold increase in sensitivity and a limit of detection of 35µg/l.

However, in a pharmacokinetic study comparing platinum content of ultrafiltered plasma by flameless atomic absorption with HPLC analysis [post-derivatisation with sodium diethyldithiocarbamate (DDTC)], an improved estimation of platinum content by HPLC was reported (Goel *et al.*, 1990). The AUCs obtained by both methods were equivalent up to 4h post-dosing in 11 patients who received 100mg/m² as a 2h infusion. After this period the AUC resulting from HPLC analysis decreased by 45% compared to the AUC resulting from atomic absorption spectroscopy analysis. This indicated that although ultrafiltration was employed to separate protein bound platinum prior to detection with atomic absorption spectroscopy, the method was sensitive to the presence of inactive platinum species with longer half-lives that appeared later on in plasma ultrafiltrate.

The use of atomic absorbance spectroscopy has its disadvantages. Hull *et al.* (1981) demonstrated great variations in platinum detection following direct injection of the samples into the graphite furnace due to sample splatter, indicating sample pre-treatment is necessary. Atomic absorbance spectroscopy also requires optimisation of optical and furnace alignment each day before commencing analysis and frequent maintenance required to ensure optimal performance. Furthermore, sample throughput is low. Pera and Harder (1977) described the use of flameless atomic absorption spectroscopy as time consuming with 6-8h required to analyse 15-20 samples. The presence of matrix effect affected accuracy and precision.

HPLC may therefore be considered the method of choice for selective detection of intact compounds, allowing sample fractionation and off- or on-line detection (Riley, 1988).

Off-line detection using flameless atomic absorption spectroscopy combined with HPLC was reported to be advantageous in being selective and minimising matrix

effects leading to enhanced precision and accuracy. However, this method is also tedious in terms of time consumption and the difficulty related to fraction collection (Marsh *et al.*, 1984; Verschraagen *et al.*, 2002).

HPLC in combination with on-line detection systems including UV detection, electrochemical detection, inductively coupled plasma atomic emission spectrometric detection (ICP-AES), inductively coupled plasma-mass spectroscopy (ICP-MS) or electrospray ionisation mass spectrometry (ESI-MS) have been reported with UV then ICP-MS methods predominating (Bosch *et al.*, 2008).

The greater availability of UV detection, its stability towards temperature changes and gradient elution and its great sensitivity has prompted it to be the most used detection system (Christian, 1994). However, the low molecular absorptivity of cisplatin had limited its UV detection, thereby necessitating pre-column or post-column derivatization reactions resulting in platinum complexes with high absorptivity in the UV region (Bosch *et al.*, 2008). Many compounds have been used as derivatizing reagents, for example bis(salicylaldehyde)tetramethylenediimine (Khuhawar *et al.*, 1997), bis(isovalerylacetone)ethylenediimine (Khuhawar and Langwani, 1998), 8-hydroxyquinoline (Sanchez *et al.*, 2000), quinoxaline-2,3-dithiol (Memon and Dalziel, 2001), 2-acetylpyridine-4-phenyl-3-thiosemicarbazone (Khuhawar and Arain, 2005) and N,N'-bis(salicylidene)-1,2-propanediamine (Lanjwani *et al.*, 2006). However, the derivatizing agent mostly reported in complex formation with cisplatin is DDTc, as a pre-column derivatizing agent (Bannister *et al.*, 1979; Drummer *et al.*, 1984; Andrews *et al.*, 1984; Goel *et al.*, 1990; Aughey *et al.*, 1995; Lopez-Flores *et al.*, 2005) or a post-column derivatizing agent (Andersson and Ehrsson, 1994; Andersson *et al.*, 1996).

ICP-MS is another detecting system that has gained popularity in detecting trace elements in environmental, biological and clinical samples of different chemical species (Montes-Bayón *et al.*, 2003). It is a very sensitive method capable of multi-elemental detection and can discriminate between individual elemental isotopes thereby improving precision and accuracy (García Sar *et al.*, 2010). ICP-MS is a highly sensitive method for platinum detection (Brouwers *et al.*, 2008a) and when combined with HPLC it can achieve specific and sensitive detection with little

background interference from complex biological matrices (Bosch *et al.*, 2008). Many studies have reported the sensitivity of ICP-MS in detecting platinum either alone (Brouwers *et al.*, 2008b; Brouwers *et al.*, 2008c) or following HPLC separation as an on-line detection system (Falter and Wilken, 1999; Hann *et al.*, 2003; Hann *et al.*, 2005; Falta *et al.*, 2011).

Other analytical methods reported for detecting platinum include gas chromatography (Khuhawar *et al.*, 1999; Laghari *et al.*, 2008), capillary electrophoresis (Huang *et al.*, 2006a) and microflow injection chemiluminescence (Wang *et al.*, 2010).

In the present study, the simplicity and selectivity of HPLC combined with the feasibility of UV as an on-line detection system was adapted in the determination of platinum levels in biological samples. Ultrafiltration of samples was utilised in the separation of proteins and pre-column derivatisation with DDTc was involved to enhance UV absorption of cisplatin. The basis for this method and the attempts to develop and modify this method will be further discussed (Chapter 4, Section 4.2.1).

ICP-MS will also be employed in analysing biological samples in order to determine the pharmacokinetic profile of cisplatin when delivered in NIVs in comparison to free drug, which will further be discussed (Chapter 7, Section 7.2.3).

1.6. Study outline

Cisplatin still remains the mainstay of cancer therapy especially in the treatment of lung cancer. However the dose-related toxic side effects and the possibility of developing resistance are barriers to successful chemotherapy with cisplatin. This has encouraged many to develop ways to enhance cisplatin bioavailability, reduce unwanted toxic side effects and circumvent the threat of chemo-resistance. Vesicular delivery systems are one approach to achieve this especially after the successful approval of liposomal doxorubicin and daunorubicin in treating cancer. However, the same liposomal system successfully used for doxorubicin has failed with cisplatin. Therefore, other vesicular systems of different compositions and functions are being studied as possible candidates for cisplatin delivery. The advantages that niosomes offer as cheaper, less toxic and more stable alternatives to liposomes can possibly

allow them to have the potential as cisplatin carriers. In the present thesis it is anticipated to study the use of non-ionic surfactant vesicles (NIVs) as vehicles for cisplatin. The same NIVs composition has been used successfully as carriers for sodium stibogluconate and amphotericin B and has shown promising *in vivo* results. The aim of the present thesis is to study the suitability of these NIVs as carriers for cisplatin through:

- Formulation of cisplatin NIVs and developing ways to enhance cisplatin loading into NIVs then characterisation of the different formulations (Chapter 3).
- Development of previously reported analytical methods used in the characterisation of the cisplatin NIVs in terms of determining cisplatin content and lipid content (Chapter 4).
- Characterisation studies on the NIVs over the long term to investigate the influence of different storage conditions on the stability of the delivery system with and without cisplatin and with different concentrations of cisplatin in a long-term stability study (Chapter 5).
- A preliminary *in vitro* study to investigate the effectiveness of niosomal cisplatin in enhancing the cytotoxic effect of cisplatin on the proliferation of B16-F0 murine melanoma cell line in comparison to cisplatin solution (Chapter 6).
- A preliminary *in vivo* study to investigate the effectiveness of niosomal cisplatin administered by two routes of administration in enhancing the anti-cancer effect of cisplatin by reducing tumour burdens through efficient accumulation at required sites in comparison to cisplatin solution in a murine model of metastatic lung cancer. A preliminary pharmacokinetic study comparing pharmacokinetic profile of niosomal cisplatin to cisplatin solution (Chapter 7).

Chapter 2. Materials and Methods

2.1. Materials

2.1.1. Materials used in preparation of NIVs

Tetra-ethylene glycol mono n-hexadecyl ether (surfactant VIII) was obtained from Nikko Chemicals Co., Ltd. through Jan Dekker UK Ltd. (Hampshire, UK). Cholesterol was obtained from Croda Chemicals Ltd. (East Yorkshire, UK). Dicetyl phosphate (DCP) and *cis*-diammineplatinum (II) dichloride (cisplatin) were obtained from Sigma-Aldrich Inc. (Dorset, UK).

2.1.2. Materials used in HPLC analysis of cisplatin

Sodium diethyldithiocarbamate trihydrate (DDTC), nickel II chloride anhydrous powder (NiCl_2) and nickel II chloride hexahydrate ($\text{NiCl}_2 \cdot 6\text{H}_2\text{O}$) were obtained from Sigma-Aldrich Inc. (Dorset, UK). Sodium chloride (NaCl) and sodium hydroxide (NaOH) were obtained from VWR International Ltd. (UK). HPLC grade water, methanol, acetonitrile, and chloroform were obtained from Fisher Scientific (Leicestershire, UK).

2.1.3. Materials used in HPLC analysis of lipids

HPLC grade propan-2-ol, isohexane, ethyl acetate and glacial acetic acid were obtained from Fisher Scientific (Leicestershire, UK). Triethylamine, prednisolone and HPLC grade chloroform stabilised with ethanol were obtained from Sigma-Aldrich Inc. (Dorset, UK).

2.1.4. Materials used in pilot production of empty and cisplatin NIVs

Cisplatin was obtained from Medex (Northants, UK). Sterile water for irrigation and 0.9% w/v sodium chloride solution for irrigation were obtained from Baxter (UK).

2.1.5. Materials used for *in vitro* proliferation and cytotoxicity studies

Alamar Blue™ Solution was purchased from Biotium, Inc. through Cambridge BioScience (Cambridge, UK). Dulbecco's Modified Eagle Medium (DMEM) and

TrypLE™ Express were obtained from Invitrogen (Paisley, UK). Penicillin-Streptomycin and Trypan blue were obtained from Sigma-Aldrich (Dorset, UK). L-Glutamine was obtained from Lonza Wokingham Ltd. (Berkshire, UK). Foetal bovine serum was obtained from Biosera Ltd. (East Sussex, UK). B16-F0 melanoma cell line was obtained from American Type Culture Collection (ATCC, Middlesex, UK).

2.1.6. Materials used for *in vivo* studies

Formalin solution, neutral buffered, 10% was obtained from Sigma-Aldrich (Dorset, UK). Phosphate buffered saline (PBS) was obtained from Lonza Wokingham Ltd. (Berkshire, UK). Euthatal containing 200mg/ml pentobarbital sodium was obtained from Merial Animal Health Ltd. (Essex, UK).

2.1.7. Animals used in the *in vivo* studies

Male BALB/c mice 8-10 weeks old weighing 20-25g were obtained from Harlan Olac (Bicester, UK) or bred in-house. Male Sprague-Dawley rats weighing 200-260g were bred in-house. All procedures carried out on the animals complied with the project license approved by the UK Home Office.

2.2. Methods

2.2.1. Preparation of NIVs

Lipid constituents including surfactant VIII, cholesterol and DCP were weighed in a 3:3:1 molar ratio, respectively, to prepare 750µmol/5ml. The contents were melted at 130°C in an oil bath for 5min. The temperature was then reduced to 70°C and hydrated with 0.5 or 6mg/ml cisplatin in 0.9% w/v NaCl preheated to 70°C in a water bath. The mixture was then homogenised at 8000rpm for 15min using a Silverson L4R SU rotor fitted with a five-eighth inch tubular work head (Chesham, Buckinghamshire, UK). These NIVs will be referred to as original or non-processed NIVs.

2.2.2. Preparation of freeze-dried empty NIVs

Empty NIVs were prepared in the same way as mentioned (Section 2.2.1), except that 150µmol/5ml of lipids were weighed in the same ratio and distilled water was used for hydrating the lipids. Once prepared, the NIVs were aliquoted into 1ml volumes and frozen at -80°C for at least 2h then lyophilised for at least 9h using Modulyo freeze-drier. Lyophilised samples were then stored at -20°C until further use.

2.2.3. Ultrafiltration of NIVs

This process is also known as diafiltration. Based on the concentration of untrapped cisplatin, NIVs hydrated with 6mg/ml cisplatin were diluted 1:12 v/v with 0.9% w/v NaCl to obtain a 0.5mg/ml concentration. To maintain uniform conditions, NIVs hydrated with 0.5mg/ml were diluted the same way with 0.5mg/ml cisplatin. The diluted suspensions were then ultrafiltered by a peristaltic pump through a Vivaflow 50 Sartorius Stedim Biotech GmbH (Epson, UK) incorporating a 30,000 MWCO polyethersulphone membrane approximately back to their original starting volumes. These NIVs will be referred to as processed NIVs.

2.2.4. Characterisation of NIVs

2.2.4.1. Entrapment efficiency of NIVs

Untrapped drug was first separated from entrapped (intravesicular) drug. From the NIVs suspension 0.5ml was taken and suspended in 4.5ml 0.9% w/v NaCl then ultracentrifuged at 60000rpm for an hour using XL-90 ultracentrifuge (Beckman optima, U.S.A.). The supernatant containing untrapped drug was discarded unless otherwise stated. Pellet was resuspended in 0.1N NaOH to disrupt the vesicles and release their entrapped contents. Suitable dilutions within the range of the calibration curve were prepared using 0.1N NaOH. Samples were analysed for entrapment efficiency by one of the described HPLC methods (Section 2.2.5).

Entrapment efficiency was calculated using the following equation:

$$\% \text{ entrapment} = \frac{\text{concentration of cisplatin entrapped (mgml}^{-1}\text{)}}{\text{initial hydrating concentration of cisplatin (mgml}^{-1}\text{)}} \times 100$$

The concentration of untrapped cisplatin was determined in studies related to stability (Chapter 5). The supernatant following ultracentrifugation of the NIVs was collected and a sample was diluted to a suitable concentration within the calibration range using 0.9% w/v NaCl. Samples were then analysed for platinum content by HPLC (Section 2.2.5).

Total cisplatin concentration (entrapped and untrapped) in NIVs was also determined in stability studies (Chapter 5). NIVs were disrupted and diluted with 0.1N NaOH to release entrapped contents and prepare a suitable concentration within the calibration range, respectively. Samples were then analysed for platinum content by HPLC (Section 2.2.5).

2.2.4.2. Sizing and zeta potential (ZP) of NIVs

Approximately 0.1ml of the niosomal preparation was suspended in 2.5ml distilled water. The suspension was sampled in a cuvette and measurement of size and ZP was performed once, unless otherwise stated, using Nano ZS[®] (Malvern, UK) at 25°C. Each measurement was the average of three runs. These measurements were taken on the same days as entrapment efficiency.

2.2.4.3. Freeze-fracture electron microscopic images (FFEM) of NIVs

FFEM images of the different cisplatin NIVs formulations were carried out at the Integrated Microscopy Facility at the University of Glasgow by Dr Laurence Tetley. Formulations were sandwiched between 2 copper support plates (Leica Mikrosysteme GmbH), plunge-frozen in a cryogen mixture of propane:isopentane (3:1) at -190°C, and transferred cold to the stage of a cryo-fracture unit at -150°C. Fracturing was done at -110°C under a vacuum less than or equal to 10⁻⁶ torr. The exposed fracture face was then replicated with platinum and carbon at a 45° to create a shadow effect. Replicas were then carbon backed at 90°. Replicas were cleaned in acetone and collected on 300 mesh grids, dried and viewed using a Zeiss 912AB transmission electron microscope operating at 120kV. Images were captured digitally by 2k × 2K Slow Scan CCD camera.

2.2.4.4. Lipid content of NIVs

Individual NIVs formulations in 1ml volumes were freeze-dried to remove water. Briefly, samples were frozen at -80°C for at least 2h then lyophilised for approximately 36h using Modulyo freeze-drier. Lyophilised samples were then stored at -20°C pending analysis.

At the time of analysis, the resultant lyophilised samples were dissolved in 10ml chloroform and then 0.5ml was taken and further diluted by a factor of 20 to prepare 10ml. In the case of empty NIVs an accurate volume of 1ml could not be measured for freeze-drying due to high viscosity. Therefore, the NIVs were lyophilised and a known weight was diluted in the same way. In case of cisplatin NIVs, 1ml was taken after the first dilution step and centrifuged at 13000rpm at 4°C for 10min in order to pellet the cisplatin and obtain clear supernatant containing the dissolved lipids for the second dilution step. Samples were prepared for analysis (Section 2.2.6.3.) and analysed by HPLC (Section 2.2.6.1.).

2.2.5. HPLC analysis of platinum

The analysis of cisplatin in biological samples and formulations was assessed using an isocratic reverse-phase high performance liquid chromatography (HPLC) method adapted and modified from Lopez-Flores *et al.* (2007). NIVs formulations were prepared for analysis as described (Section 2.2.4.1) and biological samples were prepared for analysis as described (Section 2.2.9.3).

2.2.5.1. HPLC instrumentation and chromatographic conditions

The HPLC system consisted of a Gynkotek[®] HPLC pump series P580 and autosampler model GINA 50 (Macclesfield, Cheshire, UK) operated by Chromeleon[™] software version 6.30 SP3 Build 594, Dionex (Surrey, UK). Separation was carried out on a Luna C18 (150 × 4.6mm i.d. and 3µm particle size) Phenomenex[®] column (Macclesfield, Cheshire, UK) connected to a UV detector set at 254nm.

Mobile phase was pumped through the system at a flow rate of 1.6ml/min and consisted of water, acetonitrile and methanol in a ratio of 29:31:40 v/v/v,

respectively. Solvents were measured separately, mixed and degassed by vacuum filtration using Millipore vacuum filtration kit (Watford, UK) and Phenomenex[®] 0.22µm membrane filters (Macclesfield, Cheshire, UK).

In each of the described methods, a calibration curve was established from the standard concentrations of cisplatin used. Area under the curve (AUC) ratio was plotted against the concentration of cisplatin. AUC was calculated by dividing the AUC of detected platinum by the AUC of the internal standard used.

2.2.5.2. HPLC method I

This method was employed in the analysis of platinum content of all NIVs preparations in the characterisation study (Chapter 3) and in the detection of tissue uptake of platinum *in vivo* (Chapter 7, Section 7.2.2).

Standard concentrations of cisplatin ranging from 0.125-50µg/ml were prepared in serial dilutions from a freshly prepared 1mg/ml solution of cisplatin in 0.9% w/v NaCl. A 0.1mg/ml solution of the internal standard NiCl₂ was prepared from a freshly prepared 1mg/ml solution in 0.9% w/v NaCl. The chelating agent DDTC was prepared in a concentration of 100mg/ml in 0.1N NaOH.

From each standard concentration or unknown sample, 85µl was spiked with 5µl of NiCl₂ and reacted with 10µl of DDTC reagent in a 37°C water bath for 30min. A blank sample using 85µl 0.9% w/v NaCl solution was prepared in the same way. The reactant material was extracted with 80µl chloroform by vortexing for 1min and then the chloroform layer was separated by centrifugation at 13000rpm and 4°C for 5min in a Biofuge fresco centrifuge, obtained from DJB labcare Ltd. (Buckinghamshire, UK). The chloroform layer was retained for HPLC analysis where 20µl was injected directly onto the column.

2.2.5.3. HPLC method II

This method was employed in the analysis of platinum content of cisplatin NIVs prepared for the stability studies (Chapter 5). The only exception was platinum content of cisplatin NIVs from the first stability study on day 469 post-preparation which was not analysed by this method.

This method is similar to method I except that the standard concentrations of cisplatin ranged from 2-100µg/ml and NiCl₂.6H₂O was used as the internal standard. Samples of standards, unknowns and blank were prepared as in method I but after separation of the chloroform layer by centrifugation, the layer was centrifuge evaporated at 35°C under normal atmospheric pressure using SpeedVac™ (UK) for approximately 20min until complete dryness of the samples. Samples were then reconstituted in 80µl of 75% acetonitrile in water and 20µl was injected onto the column.

2.2.5.4. HPLC method III

This method was employed in the analysis of platinum content of cisplatin NIVs on day 469 post-preparation only from the first stability study (Chapter 5).

This method is similar to method I except that two standard concentration ranges of cisplatin were used, 0.125-10µg/ml or 2-100µg/ml. Samples of standards, unknowns and blank were prepared as method I but spiked with either 5µl or 10µl of NiCl₂ for the low or high calibration range, respectively. After separation of the chloroform layer by centrifugation, 10µl was injected directly onto the column. The column was heated to 30°C using a column oven.

2.2.6. HPLC analysis of lipids

The lipid content of NIVs was analysed using a gradient normal phase HPLC method developed and modified (unpublished method, personal communication Prof Alex Mullen, University of Strathclyde). Lipid content was studied as part of the stability studies carried out on NIVs formulations prepared in large scale batches (Chapter 5). NIVs were prepared for lipid analysis as described (Section 2.2.4.4).

2.2.6.1. HPLC instrumentation and chromatographic conditions

The same HPLC system described (Section 2.2.5.1) consisting of the pump and autosampler were used. Separation was carried out on a YMC-PVA Silica column (100 × 3.0mm i.d. and 5µm particle size) from Hichrom Limited (Berkshire, UK) attached to a guard column packed the same as the column with PVA-Sil (10 × 3.0mm i.d. and 5µm particle size) from Hichrom Limited (Berkshire, UK). Detection

was facilitated by an evaporative light scattering detector model 500 (Alltech, UK) supplied with 5l of nebulisation gas by a compressor and optimised at 80°C and gas flow rate of 2.90 standard litres per minute (SLPM).

A gradient ternary elution was used for separation of the lipids, where solvent A was isohexane, solvent B was ethyl acetate and solvent C was 60% propan-2-ol, 30% acetonitrile, 10% methanol, 142µl/100ml glacial acetic acid and 378µl/100ml triethylamine (Table 2.1). The gradient elution was run for 15min at a flow rate of 1ml/min where ingredients eluted within 10min and the final 5min was for column regeneration.

Table 2.1. Gradient elution sequence used in lipid analysis using 100% isohexane (A), 100% ethyl acetate (B) and a mixture of 60% propan-2-ol, 30% acetonitrile and 10% methanol, 142µl/100ml glacial acetic acid and 378µl/100ml triethylamine (C).

Time (min)	Solvent channel		
	A	B	C
0	80	20	-
2	72	25	3
3	64	30	6
4	56	35	9
5	48	40	12
6	35	45	20
7	35	45	20
8	35	45	20
9	72	25	3
10	80	20	-
15	80	20	-

2.2.6.2. Optimisation of evaporative light scattering detector (ELSD)

The standard conditions for operating the ELSD were optimised prior to any analysis according to the manufacturer's instructions. Firstly, the drift tube temperature was optimised by starting at 100°C and reducing the temperature by 5°C until a baseline with minimum noise was obtained. Accordingly, the temperature with lowest baseline noise was 80°C. Afterwards, the detector was operated at the selected temperature and the gas flow rate was optimised starting at 2.50 SLPM with 0.2 increments until a noticeable decrease in baseline noise. Accordingly, the flow rate that showed lowest baseline noise at 80°C was approximately 2.90 SLPM.

2.2.6.3. HPLC method

Standard concentrations of the lipid mixture containing cholesterol, surfactant VIII and DCP were prepared ranging from 0.025-0.25mg/ml. Each lipid was dissolved separately in chloroform stabilised with ethanol to prepare a 1mg/ml solution. From each lipid solution (1mg/ml), 12ml were taken and mixed together and additional 12ml chloroform was added to prepare 0.25mg/ml lipid mixture solution. Serial dilutions were performed to prepare the rest of the standard concentrations and 10ml volumes were taken from each concentration.

To each 10ml volume of prepared standard or unknown sample, 400µl of prednisolone (2mg/ml in methanol) as the internal standard was added. Efficient mixing was performed to ensure complete miscibility. Internal standard was similarly added to a 10ml volume of chloroform to act as a blank. From each sample, 100µl was withdrawn and centrifugally evaporated at 35°C under normal atmospheric pressure using SpeedVac™ (UK) for approximately 40min. Dried samples were reconstituted in 100µl chloroform and 20µl of the resultant solution was injected onto the column.

Calibration curves for each lipid ingredient were established separately by plotting the AUC ratio against the standard concentration of the lipid of interest. AUC ratio was calculated by dividing the AUC of the lipid of interest by the AUC of the internal standard.

2.2.7. Pilot production of NIVs for stability study

A large scale production of NIVs was carried out for the purpose of conducting a one year stability study (Chapter 5). NIVs were prepared under aseptic conditions where all procedures were performed using a class II safety cabinet except for weighing and lipid melting processes. The large size of the oil bath used in melting the lipids made it impossible to fit it inside the safety cabinet. All glassware, apparatus, vials, stopper and homogeniser head were sterilised either by autoclaving at 121° for 15min or by dry heat at 160° for 2h.

2.2.7.1. Stability study I

In this study empty and cisplatin NIVs were prepared in batches of 200ml and 500ml, respectively. Surfactant VIII, cholesterol and DCP were weighed in a 3:3:1 molar ratio, respectively, to prepare 750µmol/5ml (Table 2.2).

Table 2.2. The weighed amount of lipids used to prepare 200ml empty NIVs and 500ml cisplatin NIVs.

Material	Theoretical wt. in 5ml	Empty NIVs		Cisplatin NIVs	
		Theoretical wt. in 200ml	Actual wt. in 200ml	Theoretical wt. in 500ml	Actual wt. in 500ml
VIII	134.4mg	5.376g	5.370g	13.44g	13.426g
Cholesterol	124.4mg	4.976g	4.974g	12.44g	12.459g
DCP	58.6mg	2.344g	2.335g	5.86g	5.900g

Weighed lipids were transferred into sterile glass bottles inside a class II safety cabinet and securely closed. Lipids were melted in an oil bath for 5min at 130°C then cooled down to 70°C. The bottle containing the lipid ingredients was cleaned to remove excess oil from the outside and placed in a 70°C water bath inside the safety cabinet. Lipids were then then hydrated with either 200ml distilled water or 500ml cisplatin (6mg/ml in 0.9% w/v NaCl) both preheated to 70°C to prepare empty or

cisplatin NIVs, respectively. The mixture was homogenised at 8000rpm for 30min at 70°C using an Ultra-turrax T25 homogenizer fitted with an S25N-25G dispersing tool (IKAWerke GmbH, Staufen, Germany). NIVs were ultrafiltered whilst inside the safety cabinet as previously described (Section 2.2.3). Prepared empty and cisplatin NIVs were diluted 1:12 v/v using distilled water or 0.9% w/v NaCl, respectively and transferred to a sterile Flexboy® bag Sartorius Stedim Biotech GmbH (Epson, UK) by means of a peristaltic pump. The diluted suspension was then ultrafiltered back to its starting volume by a Vivaflow 200 incorporating a 30,000 MWCO polyethersulphone membrane obtained from Sartorius Stedim Biotech GmbH (Epson, UK).

The following day processed empty and cisplatin NIVs were sampled into sterile 10ml vials and a sample from processed cisplatin NIVs was characterised for entrapment efficiency, size and ZP. Processed cisplatin NIVs were dispensed into 3ml volumes whereas empty NIVs were sampled into approximately 2ml volumes as their high viscosity impeded their accurate measurement. A number of the vials containing processed empty NIVs were lyophilised as described previously (Section 2.2.2). The other vials were closed with stoppers and sealed by metal caps using a crimper. Sealed vials containing processed empty and cisplatin NIVs were temporarily stored at 4°C.

Two days later, vials of processed empty NIVs and cisplatin NIVs were labelled and subdivided into 4°C, 25°C/60% RH and 40°C/75% RH storage conditions. Vials containing lyophilised empty NIVs were also sealed, labelled and stored at -20°C to be used as a reference.

At 28, 189, 266 and 469 days post-preparation, three vials of each product from each storage condition were withdrawn and analysed for entrapment efficiency (in case of cisplatin NIVs only), lipid content, size and ZP. Results are presented in Chapter 5 (Section 5.2.1)

For size and ZP studies, lyophilised NIVs were rehydrated with 2ml distilled water preheated to 70°C and vortexed for 1min. Samples from rehydrated lyophilised

NIVs, empty and cisplatin NIVs were then measured for size and ZP as described (Section 2.2.4.2).

Lipid content studies were performed as described (Sections 2.2.4.4 and 2.2.6). Due to the high viscosity of processed empty NIVs, an accurate measurement of the required volume was difficult prior to lyophilisation. Therefore, the weight of lyophilised empty NIVs was taken prior to analysis and that weight was used to determine lipid concentrations actually present in a weight containing 1ml NIVs (Table 2.3). Lipid content of cisplatin NIVs on the other hand was calculated directly as the lipid concentration was already determined in a 1ml volume.

Table 2.3. The weight of lipids that would be present in 1ml of empty and cisplatin NIVs calculated from the actual weights used to prepare the batches.

Material	Theoretical wt. in 1ml	Actual wt. of empty NIVs in 1ml	Actual wt. of cisplatin NIVs in 1ml
VIII	26.88mg	26.85mg	26.85mg
Cholesterol	24.88mg	24.87mg	24.92mg
DCP	11.72mg	11.67mg	11.80mg
Total wt.	63.48mg	63.39mg	63.57mg

Processed cisplatin NIVs were characterised for entrapment efficiency, untrapped cisplatin concentration and total cisplatin concentration (entrapped and untrapped) in the NIVs (Section 2.2.4.1). Prior to analysis 1ml from the cisplatin NIVs formulations were centrifuged at 13000rpm at 4°C for 5min to separate precipitated cisplatin from the NIVs suspension. Post-centrifugation supernatant free from precipitate was prepared as described (Section 2.2.4.1) for analysis by HPLC (Section 2.2.5.1) of NIVs platinum content on days 1, 28, 189 and 266 post-preparation using HPLC method II (Section 2.2.5.3). HPLC method III was used to analyse NIVs on day 469 post-preparation (Section 2.2.5.4). Size and ZP analysis was performed on the centrifuged NIVs samples.

2.2.7.2. Stability study II

In this study, 100ml batches of cisplatin NIVs were prepared using different concentrations of cisplatin 1, 3 and 6mg/ml as described below. Surfactant VIII, cholesterol and DCP were weighed in 3:3:1 molar ratio, respectively, to prepare 750 μ ml/5ml (Table 2.4).

Table 2.4. The weighed amount of lipids used in the preparation of NIVs hydrated with 1, 3 and 6mg/ml cisplatin in batches of 100ml.

Material	Theoretical weight in 5ml	Theoretical weight in 100ml	Actual weight in 100ml		
			1mg/ml	3mg/ml	6mg/ml
VIII	134.4mg	2.688g	2.692g	2.691g	2.689g
Cholesterol	124.4mg	2.488g	2.488g	2.490g	2.490g
DCP	58.6mg	1.172g	1.175g	1.175g	1.174g

The three batches of cisplatin NIVs using 1, 3 or 6mg/ml cisplatin were prepared the same way as in stability study I. Each NIVs formulation was diluted in sterile glass bottles to produce an external cisplatin concentration of 0.5mg/ml. Accordingly, NIVs hydrated with 1mg/ml, 3mg/ml and 6mg/ml cisplatin were diluted 1:2 v/v, 1:6 v/v and 1:12v/v, respectively with 0.9% w/v NaCl. NIVs were kept in the diluted (0.5mg/ml cisplatin solution) state overnight to prevent cisplatin precipitation as a result of increased untrapped cisplatin concentration beyond its solubility limit due to vesicle leakage.

The following day, NIVs were ultrafiltered starting with the 6mg/ml cisplatin NIVs. The processing time required for the NIVs hydrated with 6mg/ml cisplatin to return to their original starting volume was recorded. Due to the smaller volumes of NIVs hydrated with 3 and 1mg/ml cisplatin, ultrafiltration was carried out until formulations returned to their original starting volumes of 100ml. Then the NIVs were recycled through the membrane filters without ultrafiltration in order to process them for the same amount of time as NIVs hydrated with 6mg/ml cisplatin.

The following day, NIVs were dispensed into sterile 10ml vials in volumes of 2ml. Vials were sealed and labelled. From each concentration vials were subdivided into 4°, 25°C/60% RH and 40°C/75% RH storage conditions.

On days 97 and 168 post-preparation, sample vials from each storage condition were withdrawn and analysed for cisplatin content, lipid content, size and ZP. Results of this study are presented in Chapter 5 (Section 5.2.2)

For cisplatin content studies, 1ml from the cisplatin NIVs formulations were first centrifuged at 13000rpm at 4°C for 5min to separate any precipitated cisplatin. The post-centrifugation supernatant free from precipitate was used to prepare analytical samples (Section 2.2.4.1) using HPLC analysis (Section 2.2.5.1) method II (Section 2.2.5.3). NIVs hydrated with 1mg/ml cisplatin only had total platinum content analysed due to separation difficulties that prevented determination of entrapped and untrapped drug levels.

For size and ZP studies, NIVs were sampled from the centrifuged NIVs suspension used in cisplatin content studies. Samples were prepared and analysed as described (Section 2.2.3.2).

Lipid content studies were carried out for days 3, 97 and 168 post-preparation as described (Sections 2.2.4.4. and 2.2.6).

2.2.8. *In vitro* proliferation and cytotoxicity studies

2.2.8.1. Cell culture

The B16-F0 cell line stored in liquid nitrogen was allowed to defrost and then added to 5ml of complete DMEM containing 5ml/500ml of each Penicillin-Streptomycin (5,000 U penicillin and 5mg streptomycin/ml) and L-Glutamine (200mM in 0.85% NaCl solution) and sufficient volume of heat inactivated foetal bovine serum to produce a 10% final concentration. The cell suspension was centrifuged at 2000rpm for 5min using a Heraeus Multifuge 3 S-R supplied by DJB Labcare Ltd. (Buckinghamshire, UK). The medium was discarded and the pellet was washed twice with fresh medium. After the washing process the pellet containing the cells was resuspended in 15ml complete DMEM, seeded in a 200ml sterile flask and incubated in a 37°C incubator supplied with 5% carbon dioxide. Once the cells grew sufficiently, usually after 2-3 days, they were harvested and passaged. To harvest the cells, culture medium was removed and cells were detached by incubating with 5ml TrypLE™ Express for 5min. The solution was then centrifuged, TrypLE™ Express was discarded and the pellet was then washed twice with complete DMEM. After washing, the pellet was resuspended in 5ml complete DMEM and 15µl of the cell suspension was mixed with 15µl Trypan blue to be counted under the microscope using a haemocytometer. In every passage a volume from the cell suspension containing 2.5×10^6 cells were seeded in a 200ml sterile flask. The volume was made to 15ml with complete DMEM and the flask was incubated.

2.2.8.2. *In vitro* proliferation studies

Alamar Blue (AB) assay was used to study the proliferation of B16-F0 murine melanoma cell line. In a 96-well plate, 200µl of 2.5×10^5 cells/ml were seeded in the first column and doubling serial dilutions were performed down the plate with 100µl DMEM. The volumes were completed to 200µl with a mixture of 1:9 v/v AB: complete DMEM. The last column was used as the negative control which contained complete DMEM only. After a 24h incubation period, absorbance was measured spectrophotometrically at 570 and 600nm. To determine proliferation of cells the percentage reduction in AB by the cells was calculated using the following equation:

$$\% \text{ reduction} = \frac{(\varepsilon_{OX})\lambda_2 A\lambda_1 - (\varepsilon_{OX})\lambda_1 A\lambda_2}{(\varepsilon_{RED})\lambda_1 A'\lambda_2 - (\varepsilon_{RED})\lambda_2 A'\lambda_1} \times 100$$

Where:

$(\varepsilon_{OX})\lambda_1 = 80,586$ which is the molar extinction coefficient of the oxidised form of AB at 570nm

$(\varepsilon_{OX})\lambda_2 = 117,216$ which is the molar extinction coefficient of the oxidised form of AB at 600nm

$(\varepsilon_{RED})\lambda_1 = 155,677$ which is the molar extinction coefficient of the reduced form of AB at 570nm

$(\varepsilon_{RED})\lambda_2 = 14,652$ which is the molar extinction coefficient of the reduced form of AB at 600nm

$A\lambda_1$ = the absorbance reading of the test well at 570nm

$A\lambda_2$ = the absorbance reading of the test well at 600nm

$A'\lambda_1$ = the absorbance reading of the negative control well at 570nm

$A'\lambda_2$ = the absorbance reading of the negative control well at 600nm

Results of this study are shown in Chapter 6 (Section 6.2.1).

2.2.8.3. *In vitro* cytotoxicity studies

Proliferation studies showed that the optimum concentration of B16-F0 cells in the log phase was 1.88×10^5 /ml for cytotoxicity studies. Cisplatin solution was prepared and filter-sterilised for the assay where its limited solubility required that its concentration not to exceed 1mg/ml or 3.33mM in 0.9% w/v NaCl. In the cytotoxicity study, 200 μ l of filter sterilised cisplatin solution was pipetted into the wells of a column and doubling serial dilutions were subsequently performed down the plate with 100 μ l DMEM. Cell suspension in 50 μ l was added to the 96-well plate with one column containing cells to be used as the positive control. All wells were made up to 200 μ l with a mixture of AB and complete DMEM in a ratio of 1:4 v/v, respectively. After 24h incubation, spectrophotometric absorbance at 570 and 600nm was measured. The cytotoxic effect of cisplatin on the proliferation of cells was determined by calculating the percentage difference in AB reduction between treated and control cells using the following equation:

$$\frac{(\varepsilon_{OX})\lambda_2 A \lambda_1 - (\varepsilon_{OX})\lambda_1 A \lambda_2}{(\varepsilon_{OX})\lambda_2 A^\circ \lambda_1 - (\varepsilon_{OX})\lambda_1 A^\circ \lambda_2} \times 100$$

Where:

$(\varepsilon_{OX})\lambda_1 = 80.586$ which is the molar extinction coefficient of the oxidised form of AB at 570nm

$(\varepsilon_{OX})\lambda_2 = 117,216$ which is the molar extinction coefficient of the oxidised form of AB at 600nm

$A\lambda_1$ = the absorbance reading of the test well at 570nm

$A\lambda_2$ = the absorbance reading of the test well at 600nm

$A^\circ\lambda_1$ = the absorbance reading of the positive control well at 570nm

$A^\circ\lambda_2$ = the absorbance reading of the positive control well at 600nm

Results of this study are presented in Chapter 6 (Section 6.2.2)

AB assay to compare the cytotoxicity of free cisplatin, cisplatin NIVs and empty NIVs was performed in the same way. Empty and cisplatin NIVs were prepared by hydrating previously prepared freeze-dried NIVs (Section 2.2.2) with 0.9% w/v NaCl or 3mM cisplatin in 0.9% w/v NaCl, respectively. Formulations were then filter sterilised through Millex[®] 0.22µm sterile syringe driven membrane filter units (Millipore, Watford, UK). Results of this study are presented in Chapter 6 (Section 6.2.3).

Dose-response curves in the *in vitro* cytotoxicity study were established using sigmoidal dose-response (variable slope) by GraphPad Prism Software version 5.00 (California, USA).

2.2.9. *In vivo* studies

In vivo studies are presented in Chapter 7. The procedures carried out in this section were a collaboration of efforts and not all performed personally. The personal responsibility in the present section lay in the preparation and characterisation of cisplatin formulations used in treatment (except the formulations used in section 7.2.2.1), preparation of biological samples for *in vivo* uptake studies (Section 2.2.9.3), determination of *in vivo* tissue uptake of platinum by HPLC (Sections 2.2.5

and 7.2.2) and occasional assistance in the sacrifice of animals and extraction of organs. The planning and process of carrying out *in vivo* studies and related issues such as maintenance of cancer cells used for inoculation and decisions regarding inoculum number, dose administered, time periods from inoculation to dosing to sacrifice of animals and requested anti-tumour studies were the responsibility of the second academic supervisor Dr Katharine Carter. Procedures for histological anti-tumour activity and pharmacokinetic studies were carried out in-house up to the point of extraction of the required biological samples. Samples were then shipped for histological anti-tumour activity studies at the Pathology Department in Glasgow Western Infirmary and for pharmacokinetic studies at Intertek Ltd. in Manchester. Procedures not performed personally are indicated as described.

2.2.9.1. Treatment of animals

Animals in all studies were dosed by single intravenous injection or single inhalation dose. Intravenous injection was performed by injecting 0.2ml of the intended formulation at once through the tail vein of the animal. Inhalation therapy was performed through an AERONEB[®] Lab nebuliser (Aerogen[®] Inc., Ireland) operated by Buxco[®] nebulisation system. The AERONEB[®] Lab nebuliser was connected to a Volumatic[™] Spacer (Allen and Hanbury, Middlesex, UK) containing 2-3 mice or 1 rat, where 0.5ml of the intended formulation was nebulised for 1.5min and the animal(s) was kept for a further 5min inside the spacer to inhale the resulting aerosol.

2.2.9.2. *In vivo* anti-tumour activity studies

Mice used in the anti-tumour studies were inoculated with $1-3.33 \times 10^5$ B16-F0 murine melanoma cells through an intravenous injection to the tail vein 7 days prior to dose administration in order to induce metastatic lung and liver cancer. Mice were weighed and sacrificed 14 or 21 days post-inoculation by cervical dislocation. The lungs and livers were removed, weighed and stored in 10% formal-saline until analysed.

Histological studies were carried out at the Western Infirmary's Pathology Department in Glasgow by Dr Fiona Roberts. The organs were cut into longitudinal slices and placed on a tissue cassette. After routine processing in paraffin wax, 5 μ m

sections were mounted on a glass slide, dewaxed in 100% xylene and serially hydrated in graded ethanol to water. Sections were then stained with haematoxylin and eosin (H&E) and examined by light microscopy. For each organ the presence of tiny (immeasurable), the number of small; medium and large tumours and the size of the largest tumour deposit were determined in one H&E section. The characterisation of tumours into small, medium and large was based on the dimensions 0.5-1.0mm, 1.1-1.7mm or greater than 1.7mm, respectively. Results are presented in Chapter 7 (Section 7.2.1)

2.2.9.3. *In vivo* tissue uptake studies

Mice were weighed and sacrificed 5min after treatment termination by cervical dislocation. Lungs, livers, spleens, and right kidneys were dissected along with blood and lung lavages. Blood was left to clot for 2h at 4°C and then centrifuged at 13000rpm for 5min at 4°C to separate the serum. Lung lavages were obtained by inflating the lungs with 0.8ml phosphate buffered saline (PBS) pH 7.4 twice and combining both washes together. The isolated biological samples were stored at -20°C pending analysis for platinum levels.

Defrosted organs were firstly weighed either as a whole or a portion then suspended in 0.5ml of saline and homogenized with IKA[®] T10 basic (Ultra-turrax[®], Germany) homogenizer. The homogenized material as well as defrosted serum and lung lavage samples were ultrafiltered at 4000rpm for 15min in Amicon[®] Ultra-4 centrifugal filter devices 30,000 MWCO (Millipore, Watford, UK). The obtained filtrate was analysed by HPLC (Section 2.2.5.1) using method I (Section 2.2.5.2). Results of this study are presented in Chapter 7 (Section 7.2.2).

2.2.9.4. Pharmacokinetic study

Rats were weighed and sacrificed by a lethal dose (0.1mg/100gm body weight) of euthatal administered intraperitoneally at different time points after treatment termination (5, 30, 240 and 480min). Blood was collected via cardiac puncture into heparinised tubes, and plasma isolated from cellular components by centrifugation at 13000rpm for 5min at 4°C. Lungs were removed, weighed and stored along with the plasma samples at -20°C pending analysis.

Platinum levels in lungs and plasma of rats were detected by inductively coupled plasma mass spectroscopy (ICP-MS), which was carried out by Intertek Analytical Services in Manchester. The standards for the lung samples range (0, 1, 5, 10, 100, 200ppb w/v) were prepared in 100ml volumetric flasks containing 8ml concentrated nitric acid, 2ml hydrogen peroxide and 5ppb w/v ^{193}Ir (internal standard) and finished to volume with deionised water. Standards for the plasma samples were prepared in the same concentration range in 25ml volumetric flasks containing 2.5ml concentrated nitric acid and 5ppb w/v ^{193}Ir then finished to volume with deionised water. The lung samples were first digested by adding to them 8ml concentrated nitric acid and 2ml hydrogen peroxide in a microwave digestion vessel. The microwave was ramped to 210°C over 15min and kept at that temperature for 40min then cooled down for 20min. Digested samples were then transferred to 100ml volumetric flasks containing 5ppb w/v ^{193}Ir and made to volume with deionised water. Plasma samples were analysed by placing 150µl of the sample in a plastic capped tube containing 300µl concentrated nitric acid and 5ppb w/v ^{193}Ir then made to 3ml with deionised water. Samples were then aspirated into an Agilent 7500c ICP-MS, where ^{195}Pt was the mass of interest detected with the internal standard. Results of this study are presented in Chapter 7 (Section 7.2.3).

2.2.10. Statistical analysis

Minitab version 15 software package was used in the statistical analysis of data. Data that showed normal distribution was analysed by parametric student's 2 t-test or one way analysis of variance (ANOVA) combined with Newman-Keuls Multiple range test. As for data with abnormal distribution, statistical analysis was performed using non-parametric Mann Whitney test or Kruskal Wallis test. A p value ≤ 0.05 was considered to be significant.

Chapter 3. Characterisation studies of NIVs

3.1. Introduction

The concept of using a vesicular delivery system is to provide a carrier vehicle that can retain the entrapped drug, and deliver the payload at its intended site to enhance therapeutic outcomes (Jadon *et al.*, 2009). The ability to achieve this relies on the physicochemical characteristics of the vesicular delivery system such as size, lamellarity, surface charge, surface hydration and bilayer fluidity (Sharma and Sharma, 1997).

By controlling these properties, the intended indication profile of a vesicular system can be optimised (Voinea and Simionescu, 2002). For instance, intravenous administration of vesicles would subject them to engulfment by the mononuclear phagocytic system (MPS) following opsonisation by plasma proteins (Allen and Chonn, 1987). This could be advantageous in some cases where it is required to target the specific organs rich in the MPS such as the liver and spleen (Harrington *et al.*, 2000a). In other instances, evasion of MPS uptake to prolong vesicle circulation and target tumours elsewhere is required (Harrington *et al.*, 2000a). Modification of the physicochemical characteristics of vesicles such as increasing surface hydration could achieve this (Sharma and Sharma, 1997).

However, the ability of a vesicular system to efficiently entrap a drug and its ability to maintain stable entrapment efficiency is arguably by far the most important characteristic. Otherwise, there is little justification in targeting vesicles if insufficient drug reaches the target through poor entrapment or leaky vesicles. Lasic *et al.* (1995) emphasised that high entrapment efficiency with low leakage rates is essential for efficient liposomal therapy in order to achieve a sustainable therapeutic index.

The present research is intended to exploit the MPS, to direct cisplatin NIVs, particularly in the lungs. It is essential to characterise cisplatin NIVs post-preparation to permit *in vitro* and *in vivo* correlation. It is also crucial to demonstrate physicochemical stability of the formulation. Characterisation studies involved measurement of entrapment efficiency, surface charge, vesicle size and morphology.

These parameters have been the foundation of countless studies on vesicular delivery systems ever since their discovery.

3.1.1. Principle theory of zeta potential (ZP)

A vesicular system is considered to be a colloidal structure where vesicles are dispersed in an aqueous medium (Roy *et al.*, 1998). Therefore, surface charge is important in defining the physical state of the vesicles and predicting their *in vivo* performance. By measuring surface charge, the stability of a colloidal system can be estimated by the ability of the particles to overcome aggregation through repulsion. This phenomenon was first described by Derjaguin, Landau, Verwey, and Overbeek and is known as the DLVO theory (Derjaguin and Landau, 1941; Verwey and Overbeek, 1948).

DLVO theory suggests that the net balance of two forces on a particle surface control the stability of a colloidal system, London-van der Waals attractive forces and electric double layer repulsive forces resulting in potential energies of attraction (V_A) and repulsion (V_R), respectively (Kayes, 1988). When particles come close to each other due to Brownian motion these forces determine whether the particles will repulse or aggregate. At a moderate inter-particle distance, a high potential barrier of repulsion exists when V_R is high. This potential barrier prevents collision of the particles and aggregation. However, if the repulsive forces are not strong enough to overcome the attractive forces the particles may collide with sufficient energy to overcome the potential barrier and enter a deep potential of attraction, also known as primary minimum, where the particles aggregate irreversibly (Figure 3.1) (Martin *et al.*, 1983a).

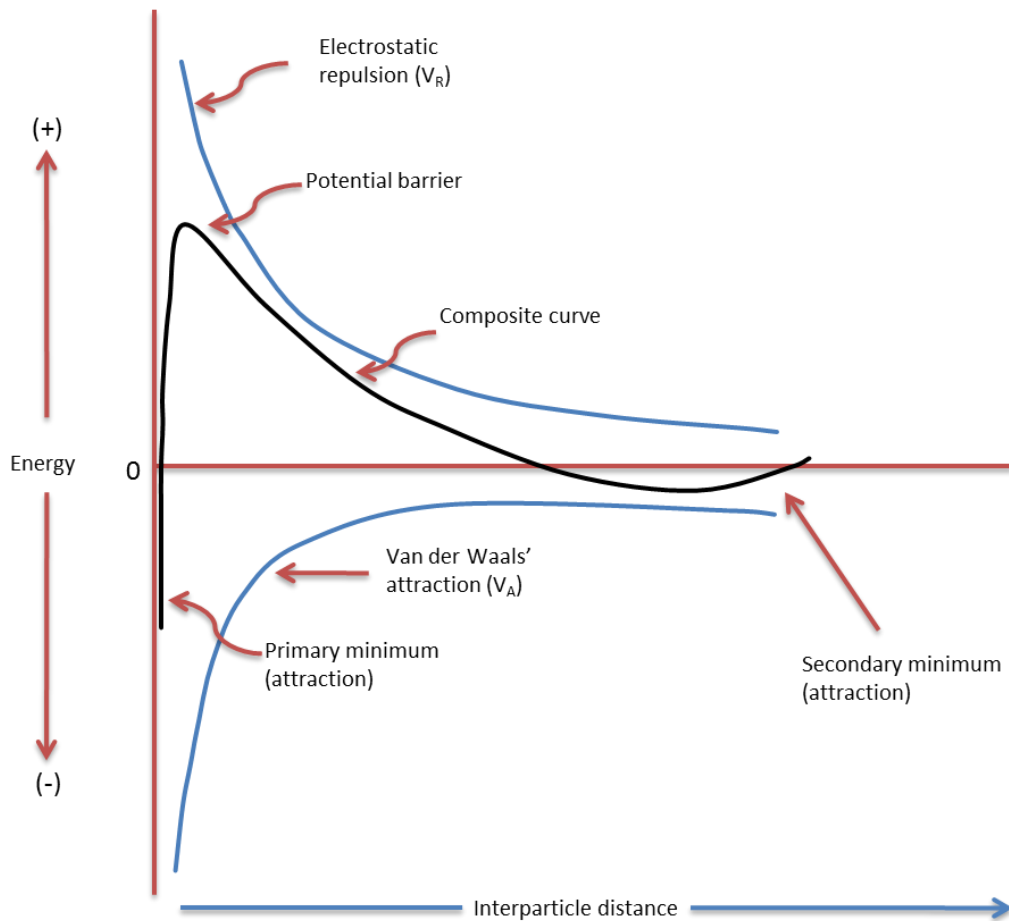


Figure 3.1. The forces on particle surface that control colloidal stability as function of distance (re-constituted from Martin *et al.*, 1983a).

To maintain colloidal stability, V_R should be dominant. This can be obtained by conferring a charge to the particles. When particles are suspended in an aqueous medium the surface charge of the particles will attract counterions by electric forces. These counterions will be distributed into two layers forming the electric double layer (Figure 3.2). The first layer consists of counterions tightly bound to the charged surface of the particles known as the stern layer. The second layer consists of less tightly bound counterions with a few ions known as the diffuse layer (Tandon *et al.*, 2008). The tight bondage between the stern layer and the charged particle allows it to move with the particle unlike the diffuse layer. The boundary between these two layers is known as the shear plane and it is the potential at the shear plane which

determines the net charge of the particle known as ZP. ZP depends on the number of counterions in the stern layer in comparison to the surface charge of the particle itself. Assuming the particle is negatively charged (Figure 3.2), ZP is neutral if the numbers are equal. ZP is negative if the number of counterions is less and positive if the numbers are more (Martin *et al.*, 1983b).

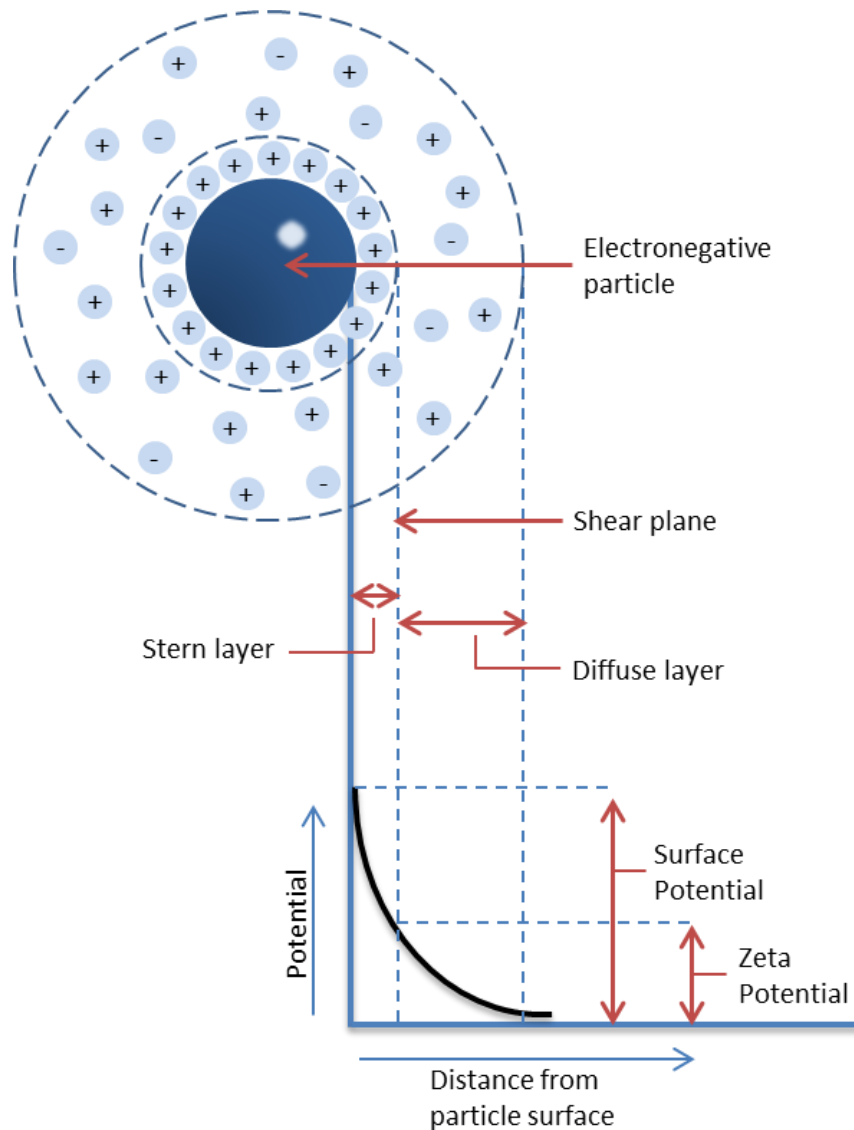


Figure 3.2. The electrochemical double layer surrounding a negatively charged particle.

Therefore, the degree of repulsion between particles is determined by the ZP. The magnitude of ZP should be high enough to prevent aggregation. A ZP value $\geq 30\text{mV}$ or $\leq -30\text{mV}$ is generally considered to provide enough repulsion (Malvern, 2004). ZP is determined by measuring the electrophoretic mobility of particles when an electric field is applied to a colloidal system. This leads to migration of the particles to the electrode of the opposite charge. Since the net charge of a particle depends on the ZP, the direction and rate of migration of the particle can be used to determine the sign and magnitude of the ZP (Martin *et al.*, 1983a). By determining the electrophoretic mobility ZP can be calculated using the Henry correction of Smoluchowski's equation:

$$\mu = \frac{2\varepsilon\zeta f(Ka)}{3\eta}$$

Where (μ) is the particle electrophoretic mobility, (ε) is the dielectric constant, (ζ) is the ZP, ($f(Ka)$) is the Henry coefficient and (η) is the viscosity.

In this project the ZP of the vesicles was detected by the Malvern Nano ZS. Using this device, the electrophoretic mobility of the vesicles is measured using a combination of laser Doppler velocimetry (LDV) and phase analysis light scattering (PALS), which allows the accurate measurement of particles with low electrophoretic mobility where it is 1000 times more sensitive than the limit of detection using LDV (Riley, 2005).

3.1.2. Principle theory of size

The characterisation of a vesicular delivery system on the basis of size and size distribution is another property that can have a profound effect in predicting its *in vivo* distribution and stability (Vemuri and Rhodes, 1995). Size and size distribution are preferably determined by dynamic light scattering (DLS) also known as photon correlation spectroscopy (PCS) or quasi-elastic light scattering (QELS) (Barth and Sun, 1991; Pencer and Hallett, 2003). The technique is popular as it is simple and rapid to perform (Mattison *et al.*, 2003).

DLS is a measurement of the time fluctuations in scattered light (Kralchevsky *et al.*, 2009) When a beam of light is passed through a dispersed medium, the

electromagnetic energy impacts the charge of the particles causing it to accelerate and radiate or scatter light (Berne and Pecora, 1976). The energy of a photon scattered from a particle will shift because of the small exchange of energy between the photon and the particle, which could be due to the particle gaining energy from or losing energy to the photon (Richardson, 2005), resulting in fluctuations in the intensity of the scattered light. The fluctuation is a result of the random movement of particles in the dispersion medium as a consequence of bombardment by solvent molecules, which is known as Brownian motion (Martin *et al.*, 1983a). Depending on the size of the particle, the intensity of the scattered light will fluctuate at different rates. As the particle size decreases the Brownian motion velocity increases and leads to an increased fluctuation rate of scattered light.

The Malvern Nano ZS employs DLS in determining particle size and size distribution by measuring the rate of intensity fluctuation using a digital correlator, where the signal intensity over time is compared to the intensity taken at (t_0). The more similar the signal intensity at a different time to that at (t_0) the stronger the correlation is where perfect correlation is equal to 1. This correlation will decrease as a result of particle movement until no similarity in intensity to the original is found, where correlation is zero. As a result of particle size, the decay rate of the correlation function will be quicker for small particles compared to large ones (Figure 3.3).

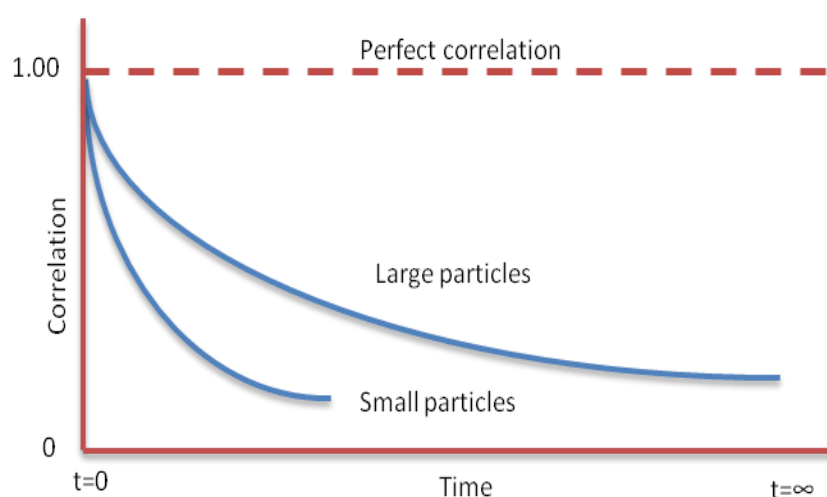


Figure 3.3. Correlation function of small and large particles in DLS to determine particle size (re-constituted from Malvern, 2004).

The ZS software uses the correlation function to calculate the size distribution using algorithms to extract the decay rates for a number of size classes to produce a size distribution (Malvern, 2004). Particle size is indicated by the hydrodynamic diameter where the intensity correlation function is used to determine the diffusion coefficient of the Brownian particle and accordingly the particle's hydrodynamic radius can be calculated using Stokes-Einstein equation:

$$a = \frac{KT}{6\pi\eta D}$$

Where (a) is the hydrodynamic radius (η) is the viscosity, (K) is Boltzman's constant, (T) is the absolute temperature and (D) is the diffusion coefficient.

The extent of homogeneity in size distribution is indicated by the polydispersity index (PdI) value. The scale of PdI ranges from 0-1 and the closer PdI to zero is the more homogenous the size distribution is (Roy *et al.*, 1998; Gaumet *et al.*, 2008).

3.1.3. Principle theory of freeze fracture electron microscopy (FFEM)

Although size measurements can give an indication of the vesicle size range and homogeneity of size distribution, a main disadvantage is that it does not discriminate between individual vesicles and aggregates. Also the ability to characterise the vesicles based on their morphology such as bilayer organisation is not provided by such a technique (Bibi *et al.*, 2011). Therefore, the visualisation of vesicles is an important process in gaining further knowledge about the physical state of individual vesicles.

FFEM is a widely used technique that can offer a key tool in revealing a detailed description of vesicles based on lamellarity and tightness of bilayer packing in case of multilamellar vesicles (Bibi *et al.*, 2011). FFEM can also provide information on phase transitions of lipids such as the rippled effect, which results from some disordered transitions of the acyl chains (Meyer and Richter, 2001).

In FFEM four essential steps are required to produce a three dimensional replica of the sample. The first is rapid freezing of the sample to limit the formation of ice crystals and preserve the vesicle structure. The sample is then fractured at a

temperature of -100°C or less and usually under vacuum where the bilayer is split into half membrane leaflets. Therefore, a three-dimensional vesicle structure with an en face membrane interior will be obtained. The third step involves rendering these structures visible under the microscope via vacuum deposition of platinum and carbon to produce a replica of the exposed frozen surface from fracture. A fine layer of platinum-carbon is sputtered onto the surface at an angle to create a shadowing effect which is then strengthened by evaporating a layer of electron-lucent carbon immediately following the shadowing step. Thus, depending on the topography of the fractured surface, platinum is deposited in varying thicknesses accordingly. In the final step, after the replica is allowed to reach room temperature and atmospheric pressure, it is then cleaned of biological material and mounted on a grid for electron microscopy examination (Severs, 2007; Robenek and Severs, 2008).

The appearance of vesicles in a FFEM image as protruding, hollow or flat structures are dependent on the fracture path (Figure 3.4). Basically there are three fracture paths through which these appearances are obtained. If the fracture splits the bilayer and travels upwards above the vesicle then a convex fracture is obtained where the vesicle will protrude. If the fracture splits the bilayer and travels downwards below the vesicle then a concave fracture is obtained where the vesicle is removed in the complementary fragment leaving a hollow space. A cross-sectional fracture is obtained if the fracture breaks through the bilayer and divides the vesicle into two halves, thereby revealing its internal structure. Any structures within a cross-sectional fracture may also appear as convex, concave or cross-sectional fractures (Severs, 2007).

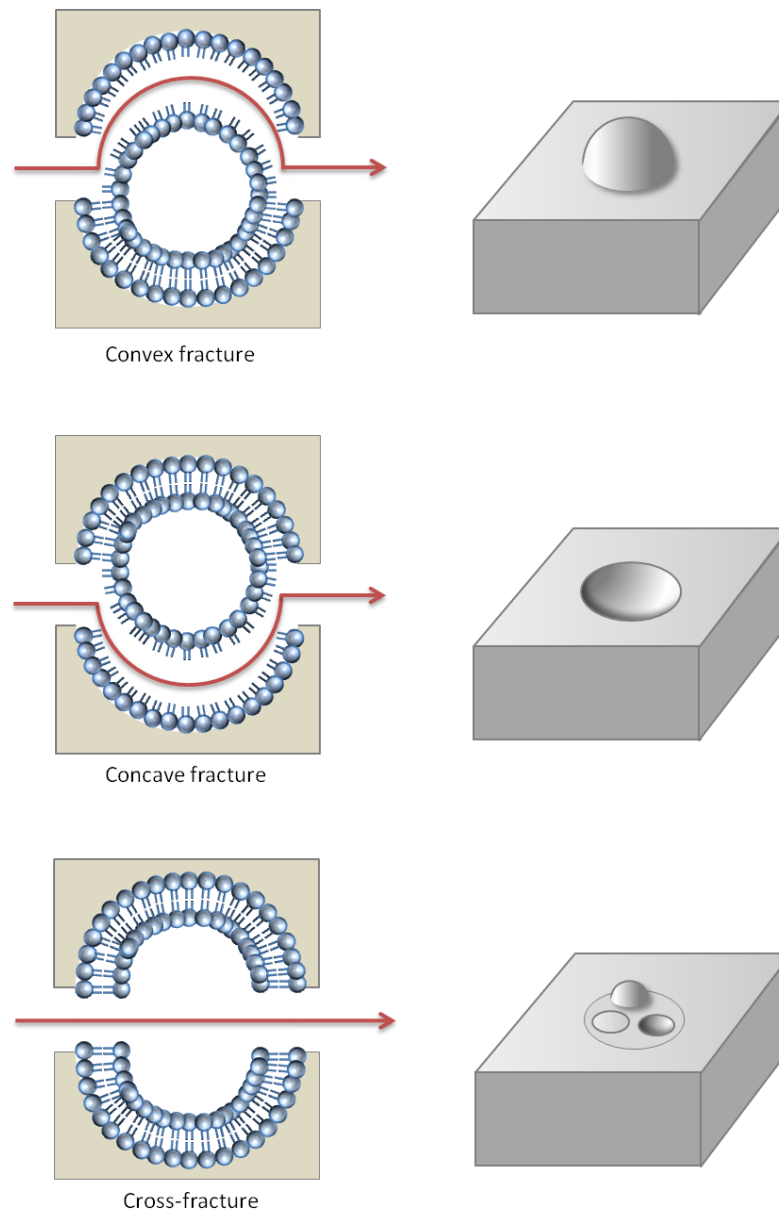


Figure 3.4. The different paths of fracture that lead to three types of replica images in FFEM.

3.2. Results

3.2.1. Entrapment efficiency, sizing and ZP studies

The entrapment efficiency for all the formulations was determined as described (Section 2.2.4.1) by HPLC (Section 2.2.5.1) using method I (Section 2.2.5.3). Size and ZP results were determined as described (Section 2.2.4.2).

3.2.1.1. Non-processed and processed NIVs

The characteristics of processed and non-processed cisplatin NIVs were compared in this section. In the first part of the present section the volumes of processed and non-processed NIVs differed from each other. In the second part of the present section the volumes of processed and non-processed were unified for characterisation studies.

3.2.1.1.1. Non-processed and processed NIVs in different volumes

As described (Section 2.2.1), a 5 and 10ml NIVs formulations were prepared with 6mg/ml cisplatin. The 5ml formulation was then processed as described (Section 2.2.3). The formulations were characterised on the basis of entrapment efficiency, size and ZP on days 0, 1, 3 and 7 post-preparation.

The % entrapment results over time (Figure 3.5) showed greater entrapment efficiency of original NIVs in comparison to processed NIVs. The only exception was on day 1 post-preparation where the entrapment efficiency (\pm SD) of the original NIVs plummeted to $5.17 \pm 1.90\%$, which was even lower than the entrapment efficiency of processed NIVs at $20.33 \pm 3.28\%$. The entrapment efficiency of processed NIVs remained stable over time. Original NIVs did not differ between days 0 and 7 post-preparation.

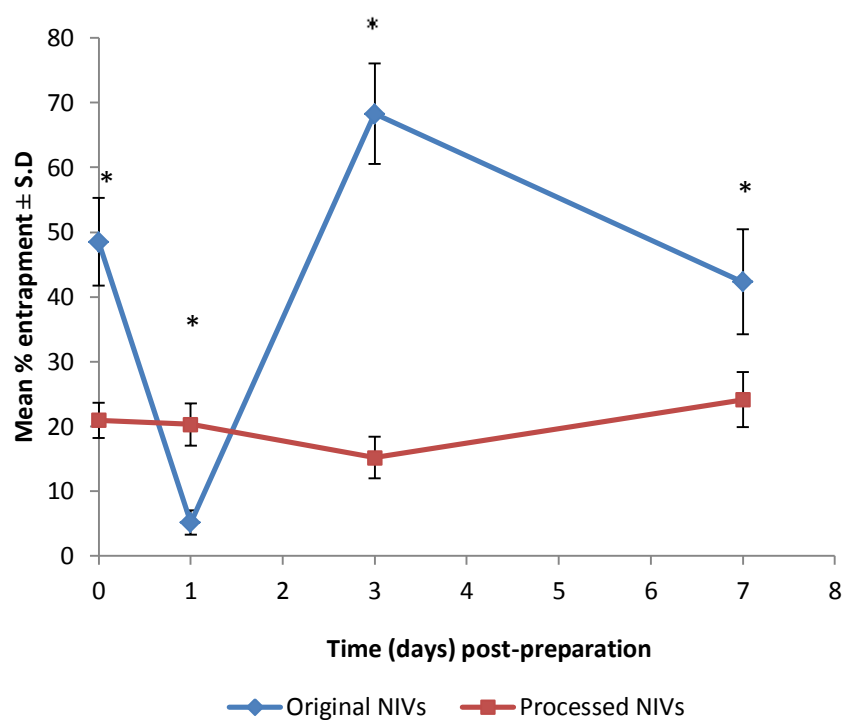


Figure 3.5. Relation between time and vesicle entrapment efficiency for original and processed cisplatin NIVs prepared in different volumes (n=3). * indicates significant difference between original and processed NIVs.

The sizing results of both formulations (Figure 3.6) showed that processing significantly reduced vesicle size. The size ranged from 1500-2000nm for non-processed NIVs to 600-850nm for the processed NIVs, representing an approximate 50% reduction in size range. Over time, size of processed NIVs appeared stable up to day 7 post-preparation where the size increased, whereas the original NIVs appeared to show similar vesicle size between days 0, 1 and 7 post-preparation. The PDI values (Table 3.1) indicated that both formulations have a heterogeneous size distribution but the processed NIVs were less heterogeneous.

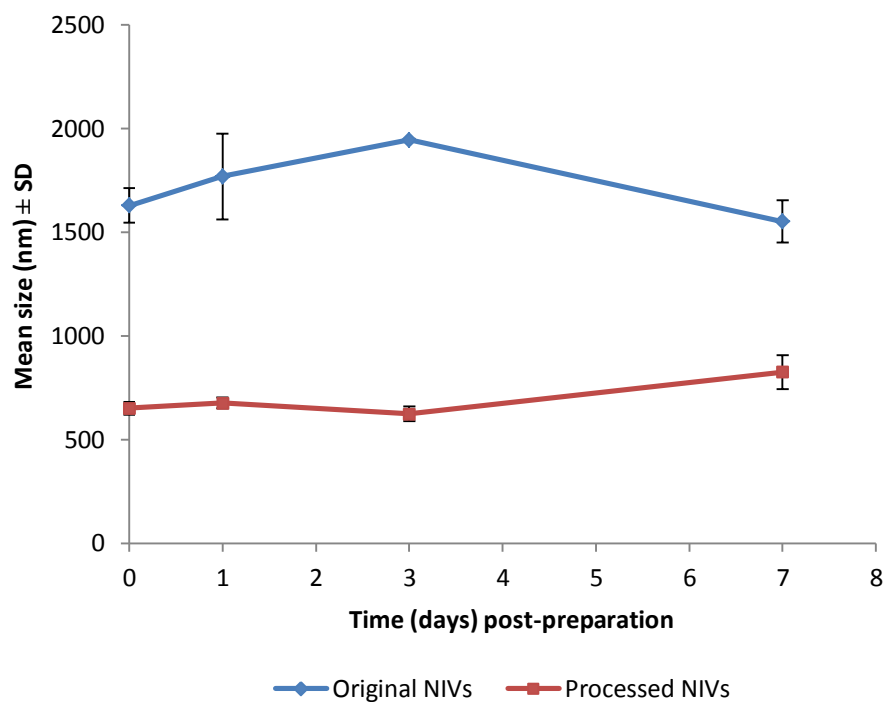


Figure 3.6. The size of cisplatin NIVs with and without processing prepared in different volumes. Each point is representative of triplicate readings (n=1).

Table 3.1. Corresponding PDI values of cisplatin NIVs with and without processing sized in Figure 3.5. Each point is representative of triplicate readings (n=1).

Days post-preparation	Mean PDI ± SD	
	Original NIVs	Processed NIVs
0	0.89 ± 0.05	0.49 ± 0.01
1	0.95 ± 0.03	0.53 ± 0.02
3	0.97 ± 0.03	0.60 ± 0.08
7	0.82 ± 0.05	0.61 ± 0.05

In the ZP results (Figure 3.7), both NIVs formulations showed a surface charge well below -30mV. The ZP range for processed NIVs lay between -85 to -100mV and for the non-processed NIVs between -65 to -85mV. The ZP of the formulations appeared different between each other on days 0 and 3 post-preparation. The ZP of processed NIVs appeared similar from days 1 to 7 post-preparation, whereas the non-processed NIVs showed similarity between days 0, 1 and 7 post-preparation.

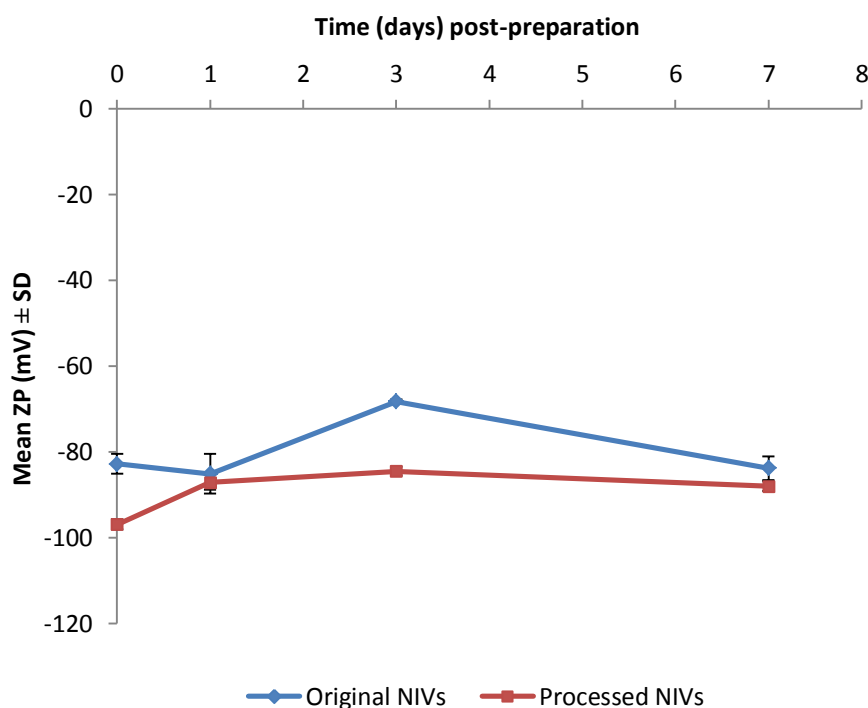


Figure 3.7. The ZP values of cisplatin NIVs with and without processing prepared in different volumes. Each point is representative of triplicate readings (n=1).

3.2.1.1.2. Non-processed and processed NIVs in equal volumes

To standardise the formulation effects on the sizing results, a 10ml NIVs formulation was prepared with a 6mg/ml cisplatin concentration (Section 2.2.1). The NIVs were divided into two 5ml volumes, one portion was kept non-processed and the other portion was processed (Section 2.2.3). Both formulations were assessed for entrapment efficiency, size and ZP. For size measurements, 3 aliquots from each

formulation were analysed in triplicates representing a mean \pm SD value of nine runs instead of three runs for a single aliquot analysed before.

The same trend was observed in the entrapment efficiency results (Figure 3.8), where original NIVs showed significantly higher entrapment efficiency than processed NIVs. The entrapment efficiency of original NIVs was stable over time, whereas for the processed NIVs a significant reduction was observed on day 7 post preparation.

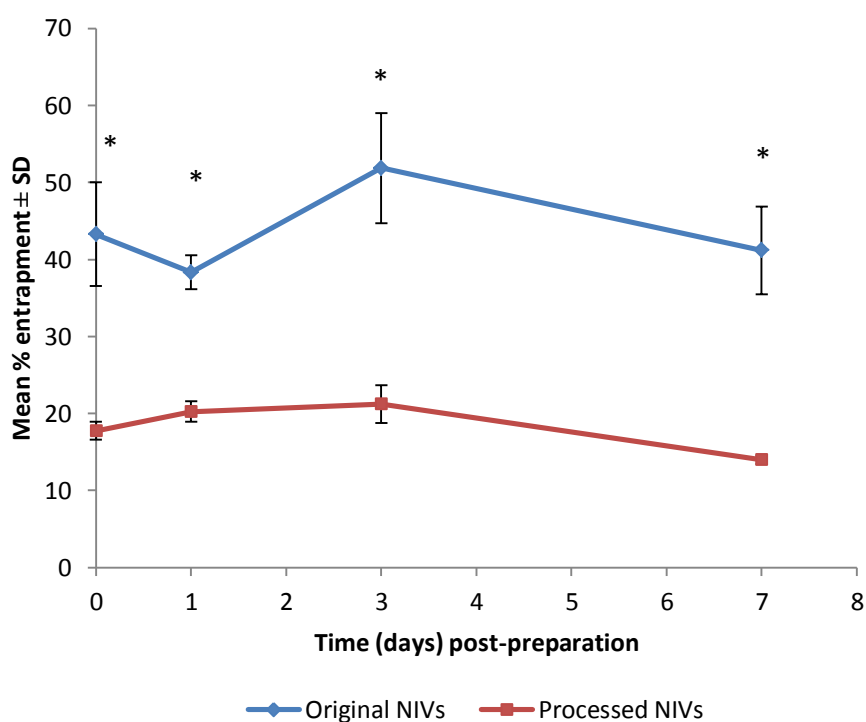


Figure 3.8. The entrapment efficiency of processed and non-processed cisplatin NIVs prepared in equal volumes over time (n=3). * indicates a significant difference between original and processed NIVs (p \leq 0.05).

Even though equal volumes were subjected to the same homogenisation settings, a significant difference in size between both formulations was still observed (Figure 3.9). The size range fell significantly (p \leq 0.05) by approximately 2-fold from 1500-2200nm for original NIVs to 650-950nm for processed NIVs. Furthermore, the

extent of size distribution heterogeneity was minimised in processed NIVs in comparison to non-processed NIVs (Table 3.2).

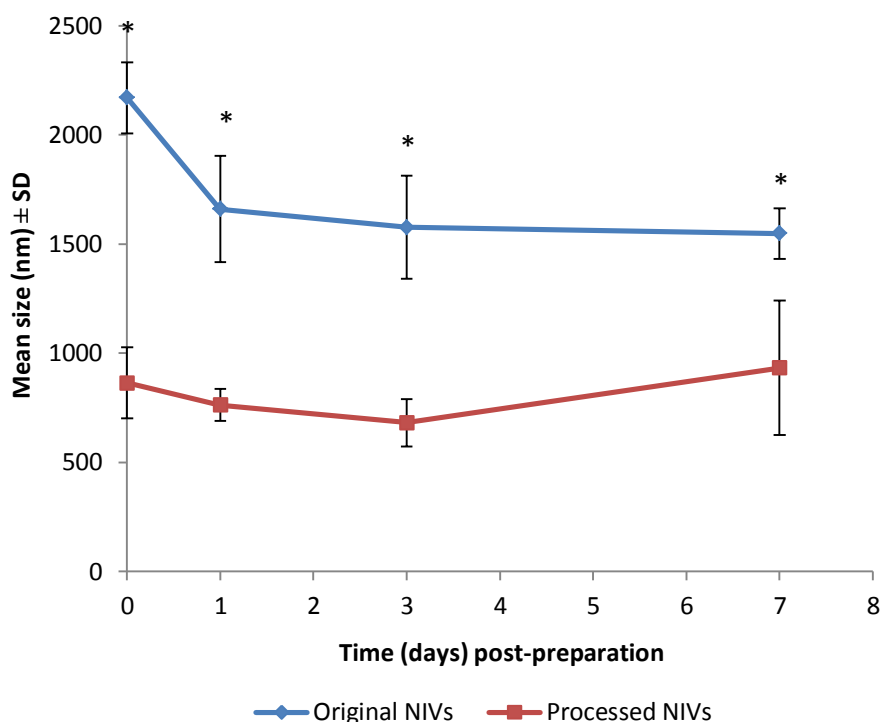


Figure 3.9. The size of cisplatin NIVs with and without processing prepared in equal volumes. Each point is representative of triplicate readings (n=3). * indicates significant difference in size between original and processed NIVs ($p \leq 0.05$).

Table 3.2. Corresponding PDI values of cisplatin NIVs with and without processing sized in Figure 3.8. Each point is representative of triplicate readings (n=3).

Days post-preparation	Mean PDI ± SD	
	Original NIVs	Processed NIVs
0	0.99 ± 0.00	0.67 ± 0.07
1	0.94 ± 0.07	0.61 ± 0.05
3	0.93 ± 0.06	0.58 ± 0.04
7	0.91 ± 0.05	0.67 ± 0.12

The original NIVs showed lower negativity than processed NIVs (Figure 3.10). The ZP values appeared reasonably consistent throughout the study from day 0 to 7 post-preparation.

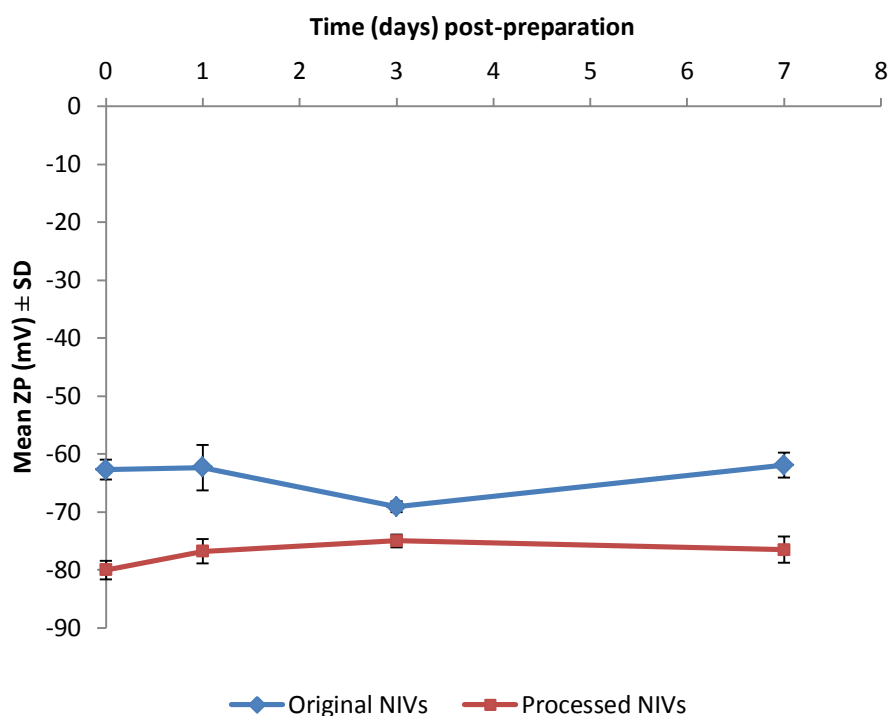


Figure 3.10. The ZP results of cisplatin prepared with and without processing prepared in equal volumes. Each point is representative of triplicate readings (n=1).

3.2.1.2. Processed NIVs prepared using different concentrations of cisplatin

In this study two processed NIVs of different concentrations were prepared as described (Section 2.2.1) with a 0.5 and 6mg/ml cisplatin concentration. Both formulations were processed as described (Section 2.2.3) and characterised for entrapment efficiency, size and ZP.

In the entrapment efficiency, processed NIVs hydrated with 0.5mg/ml cisplatin could not be quantified as it was not possible to pellet the formulation by ultracentrifugation using the procedures described (Section 2.2.4.1) to separate

entrapped from unentrapped drug. Therefore, only the processed NIVs hydrated with 6mg/ml cisplatin were quantified for entrapment efficiency (Table 3.3). The entrapment efficiency was the highest on the day of preparation, then fell significantly on day 1 and remained stable throughout the whole time period.

Table 3.3. Entrapment efficiency of processed NIVs hydrated with 6mg/ml cisplatin over time. Each result is representative of a single measurement.

% Entrapment	Day 0	Day 1	Day 4	Day 7	Day 32
1	37.2%	17.0%	15.6%	17.7%	9.5%
2	35.2%	21.9%	19.6%	25.0%	18.4%
3	40.9%	21.0%	16.9%	21.7%	9.7%
Mean	37.7%	20.0%	17.4%	21.5%	12.5%
S.D	2.87	2.61	2.00	3.69	5.08

The sizing results appeared different between the processed NIVs hydrated with 0.5 and 6mg/ml only on day 4 post-preparation (Figure 3.11). The size of processed NIVs hydrated with 6mg/ml cisplatin was unusually high on day 4 post-preparation, which is also demonstrated by its corresponding unexpectedly higher PdI in comparison to the other time points (Table 3.4). Overall, the formulation was stable over time with only day 4 post-preparation being the outlier. The processed NIVs hydrated with 0.5mg/ml cisplatin showed a fluctuated size distribution over the week. As both formulations were subjected to diafiltration their PdI values were in the same range.

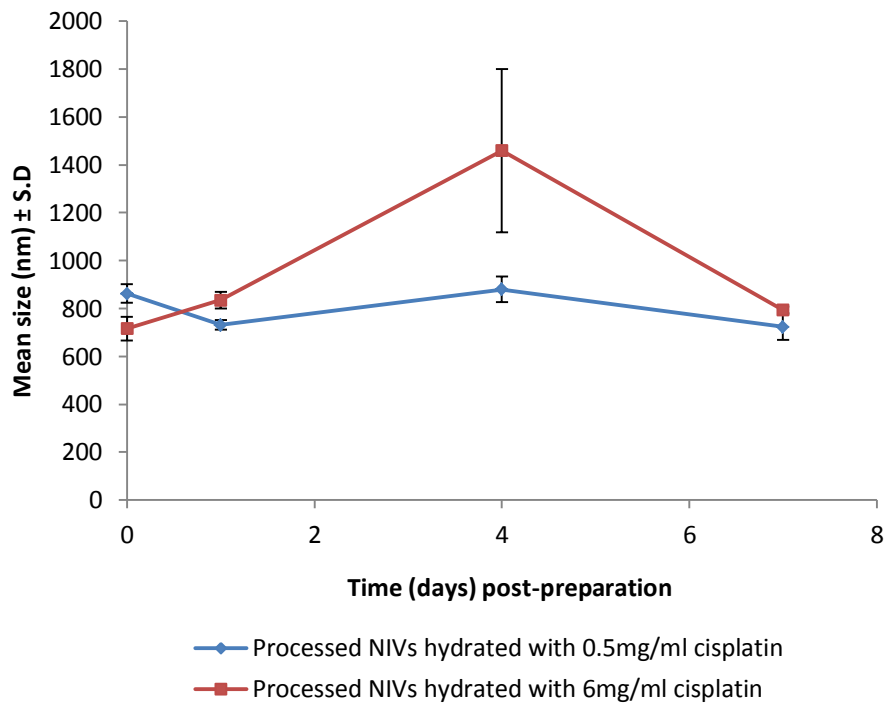


Figure 3.11. The size of processed NIVs hydrated with 0.5mg/ml or 6mg/ml cisplatin. Each point is representative of triplicate readings (n=1).

Table 3.4. Corresponding PDI values of processed NIVs hydrated with 0.5 and 6mg/ml cisplatin sized in Figure 3.10. Each point is representative of triplicate readings (n=1).

Days post-preparation	Mean PDI ± SD	
	Processed NIVs hydrated with 0.5mg/ml cisplatin	Processed NIVs hydrated with 6mg/ml cisplatin
0	0.66 ± 0.03	0.58 ± 0.03
1	0.52 ± 0.10	0.64 ± 0.03
4	0.67 ± 0.03	0.89 ± 0.10
7	0.64 ± 0.05	0.61 ± 0.00

ZP for both formulations did not appreciably differ from each other and were also stable over time (Figure 3.12).

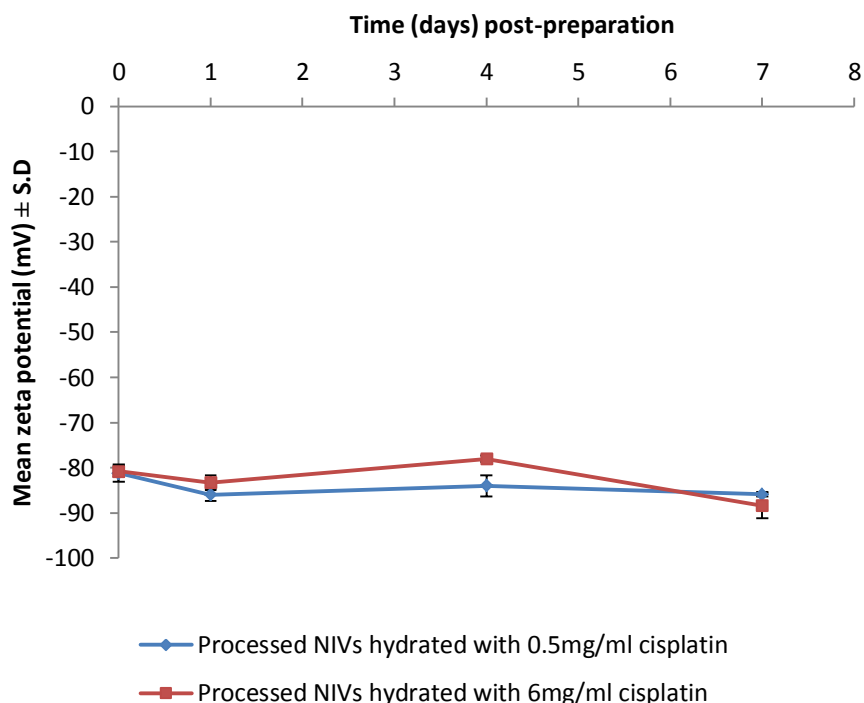


Figure 3.12. The ZP results of processed NIVs hydrated with 0.5 and 6mg/ml cisplatin. Each point is representative of triplicate readings (n=1).

As it was not possible to separate untrapped from entrapped drug in the processed 0.5mg/ml cisplatin NIVs, another study using NIVs hydrated with 1mg/ml cisplatin was performed. These NIVs were prepared using 1mg/ml cisplatin as described (Section 2.2.1) but then without additional dilution the NIVs were processed whilst maintaining the same volume for the same amount of time it would take to process a diluted suspension back to its original volume, which was approximately 15min. This process was performed in order to maintain the same size distribution as a result of the diafiltration process. Unfortunately, these NIVs also lacked the ability to pellet upon ultracentrifugation; therefore it was not possible to measure the entrapment

efficiency. However, they were only characterised on the basis of size and ZP over a one week period (Table 3.5).

Table 3.5. The size, PdI and ZP values of 1mg/ml cisplatin NIVs subjected to diafiltration without a dilution and concentration step. Each point is representative of triplicate readings (n=3 for size and PdI results and n=1 for ZP results).

Mean parameter measured \pm SD		Size (nm)	PdI	ZP (-mV)
Time (days) post-preparation	0	727.6 \pm 89.3	0.62 \pm 0.05	-69.7 \pm 1.1
	1	754.6 \pm 110.6	0.66 \pm 0.04	-67.6 \pm 1.8
	3	1017 \pm 147.2	0.73 \pm 0.05	-66.9 \pm 1.3
	7	974.2 \pm 107.2	0.80 \pm 0.09	-72.6 \pm 8.4

3.2.1.3. Processed NIVs prepared using 6mg/ml cisplatin and suspended in different solutions post-manufacture

From the same processed NIVs hydrated with 6mg/ml cisplatin (Section 3.2.1.2), three 3ml aliquots were taken on day 1 post-preparation suspended in 3ml solution of 0.9%w/v NaCl and ultracentrifuged at 60000 rpm at 4°C for 2h. The supernatant containing untrapped drug was discarded and each pellet was re-suspended in either 3ml of 1mg/ml cisplatin, 0.5mg/ml cisplatin or 0.9% w/v NaCl. The NIVs were then assessed for entrapment efficiency, size and ZP.

The entrapment efficiency did not differ whether processed NIVs were re-suspended in different concentrations of cisplatin solutions or 0.9% w/v NaCl. All formulations managed to maintain stable entrapment efficiencies over time until significant reduction was observed on day 32 post-production (Table 3.6).

Table 3.6. The entrapment efficiency of processed NIVs hydrated with 6mg/ml cisplatin then separated from untrapped cisplatin and re-suspended in 0.9% w/v NaCl, 0.5mg/ml and 1mg/ml cisplatin (n=3).

Days post-preparation	Mean entrapment efficiency (%) \pm SD		
	1mg/ml	0.5mg/ml	Saline
1	16.5 \pm 0.7	29.3 \pm 6.1	36.8 \pm 3.7
4	12.7 \pm 0.2	22.5 \pm 1.7	22.2 \pm 2.8
7	12.2 \pm 4.5	28.3 \pm 6.8	35.9 \pm 3.3
32	6.1 \pm 2.3	10.5 \pm 3.1	4.8 \pm 5.6

The re-suspending of processed NIVs in different concentrations of cisplatin solutions or 0.9% w/v NaCl also did not affect the size or the ZP of the NIVs. The size measurements did not appear different from each other (Table 3.7) and showed a similar heterogeneity in size distribution (Table 3.8), as well as the ZP results (Table 3.9).

Table 3.7. The size of processed NIVs hydrated with 6mg/ml cisplatin then separated from untrapped drug and re-suspended in 0.9% w/v NaCl, 0.5mg/ml and 1mg/ml cisplatin. Each point is representative of triplicate readings (n=1).

Days post-preparation	Mean size (nm) \pm SD		
	1mg/ml	0.5mg/ml	Saline
1	665.1 \pm 42.3	804.8 \pm 60.5	693.3 \pm 32.5
4	856.8 \pm 50.6	814.6 \pm 22.1	689.8 \pm 6.4
7	544.4 \pm 50.9	654.3 \pm 20.4	506.7 \pm 8.1
32	610.8 \pm 44.3	590.0 \pm 18.1	697.0 \pm 60.7

Table 3.8. Corresponding PdI values of processed NIVs hydrated with 6mg/ml cisplatin then separated from entrapped drug and re-suspended in 0.9% w/v NaCl, 0.5mg/ml and 1mg/ml cisplatin sized in Table 3.6. Each point is representative of triplicate readings (n=1).

Days post-preparation	Mean PdI \pm SD		
	1mg/ml	0.5mg/ml	Saline
1	0.59 \pm 0.07	0.61 \pm 0.05	0.60 \pm 0.05
4	0.66 \pm 0.05	0.63 \pm 0.02	0.53 \pm 0.07
7	0.57 \pm 0.09	0.57 \pm 0.02	0.61 \pm 0.07
32	0.55 \pm 0.07	0.54 \pm 0.02	0.56 \pm 0.02

Table 3.9. The ZP of processed NIVs hydrated with 6mg/ml cisplatin then separated from unentrapped drug and re-suspended in 0.9% w/v NaCl, 0.5mg/ml and 1mg/ml cisplatin. Each point is representative of triplicate readings (n=3).

Days post-preparation	Mean ZP (mV) \pm SD		
	1mg/ml	0.5mg/ml	Saline
1	-86.2 \pm 2.4	-84.6 \pm 1.8	-86.4 \pm 2.2
4	-83.6 \pm 1.2	-85.5 \pm 2.3	-87.8 \pm 1.4
7	-96.5 \pm 2.5	-94.6 \pm 0.9	-95.0 \pm 1.2
32	-96.5 \pm 0.1	-94.3 \pm 2.9	-93.4 \pm 1.8

3.2.2. FFEM studies

The characterisation studies of niosomes using FFEM was performed employing the described method (Section 2.2.4.3).

3.2.2.1. Non-processed NIVs (150 μ mol) hydrated with 0.5mg/ml cisplatin

These NIVs were prepared by the same method of preparation described (Section 2.2.1) except that the lipid concentration used was 150 μ mol instead of 750 μ mol in a molar ratio of 3:3:1 of surfactant VIII: cholesterol: DCP, respectively.

FFEM images of the NIVs show vesicles with a size range of 50-300nm (Figure 3.13.a). Images suggest a mixture of unilamellar vesicles. Freeze-dried empty vesicles of the same lipid concentration, (Section 2.2.2), when hydrated with a concentration of 0.5mg/ml cisplatin showed a noticeable increase in size and a possible wider distribution in size range (Figure 3.13.b).

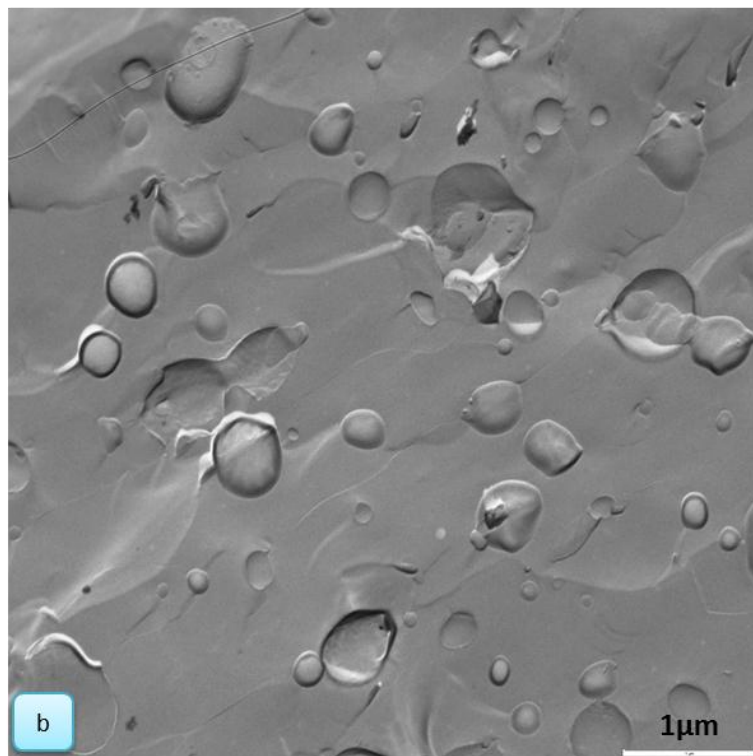
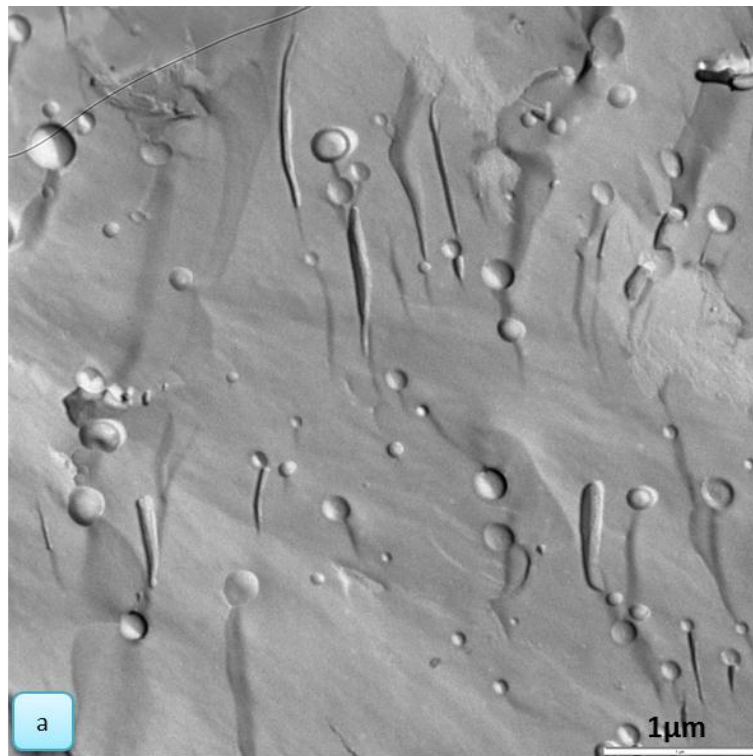


Figure 3.13. FFEM of NIVs prepared with 150 μ mol lipid concentration and hydrated with 0.5mg/ml cisplatin (a) and freeze-dried empty NIVs prepared with 150 μ mol lipid concentration and rehydrated with 0.5mg/ml cisplatin (b).

3.2.2.2. Non-processed NIVs hydrated with 6mg/ml cisplatin

NIVs were prepared as described (Section 2.2.1). The FFEM images show a wide distribution in vesicle size. Different vesicle sizes were observed and it appears that different types of vesicles are also present such as MLVs (Figure 3.14.a). There also appears to be very large vesicles approximately 3 μ m in diameter, which encapsulate smaller vesicles (Figure 3.14.b) as will be discussed later. This wide distribution is in accordance with the high PDI values observed with the non-processed NIVs.

3.2.2.3. Processed NIVs hydrated with 6mg/ml cisplatin

These NIVs were prepared (Section 2.2.1) and processed (Section 2.2.3) as described. Images obtained by FFEM shows even a greater vesicle density in comparison to non-processed NIVs (Figure 3.15). A wide size distribution is observed with some vesicles around 100nm and others around 2 μ m in diameter, suggesting different vesicle types.

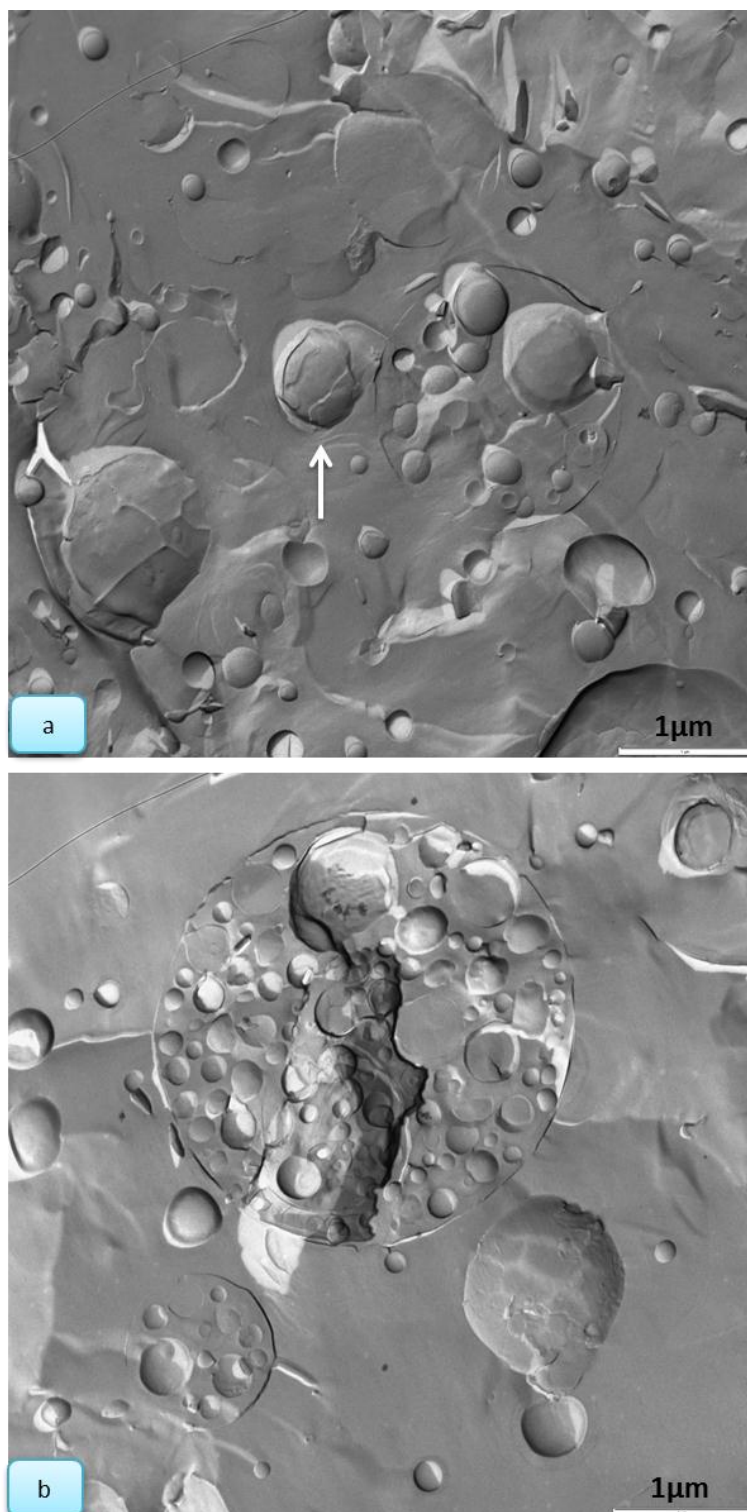


Figure 3.14. FFEM of NIVs hydrated with 6mg/ml without diafiltration showing possible MLVs as indicated by white arrow (a) and multi-vesicular niosomes akin to multi-vesicular liposomes (b) – see Figures 3.16 and 3.17.

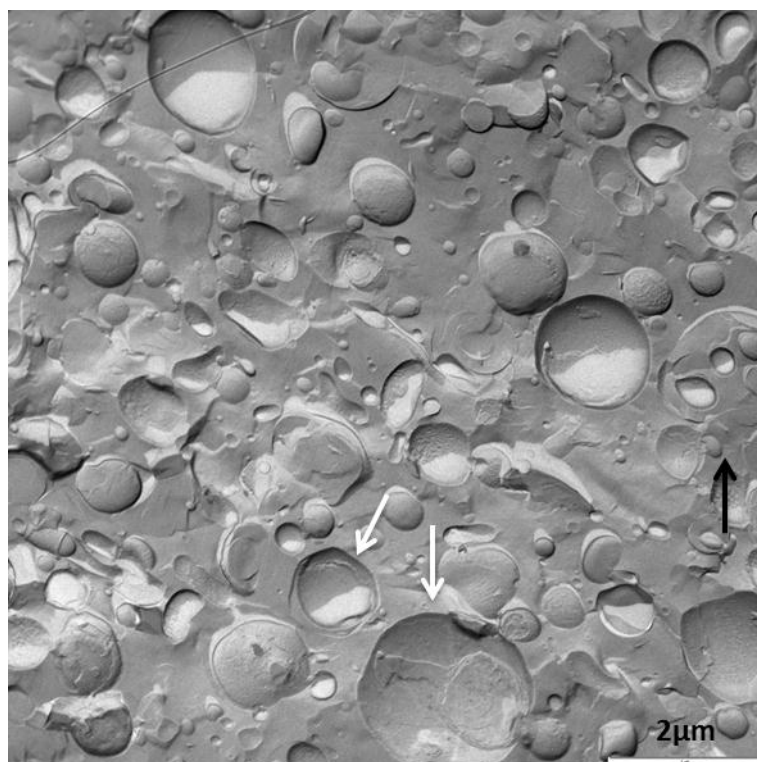


Figure 3.15. FFEM of processed NIVs hydrated with 6mg/ml cisplatin suggesting presence of MLVs as indicated by white arrows and possible multi-vesicular vesicle as indicated by black arrow.

3.3. Discussion

The effectiveness of a vesicular delivery system is manifested in the sufficient and sustainable entrapment efficiency up until required drug release *in vivo* (Kisak *et al.*, 2004). Preparation method can influence entrapment efficiency depending on the technique of drug loading, hydration temperature, drug solubility, cholesterol content and the resulting vesicle size obtained after preparation (Uchegbu and Florence, 1995). However, the preparation method regarding drug loading technique, hydration temperature, cholesterol content have already been optimised for the NIVs as drug carriers in the present study (Mullen *et al.*, 2000) and these NIVs have successfully been used as vehicles in the delivery of sodium stibogluconate (Mullen *et al.*, 1998) and amphotericin B (Mullen *et al.*, 1997). The influence of cisplatin solubility and

vesicle size resulting from cisplatin encapsulation remain to influence the entrapment efficiency.

Obtaining vesicles with high entrapment efficiency can be challenging especially if the vesicles were small in size (Lasic *et al.*, 1995). One strategy to improve entrapment is the preparation of vesicles using high concentrations of lipid and drug (Lasic, 1998). This can be a problem for drugs with low water solubility like cisplatin, thereby limiting the entrapment efficiency (Newman *et al.*, 1999; Velinova *et al.*, 2004). However, the solubility of cisplatin which ranges from 1-2mg/ml at room temperature can be enhanced by heating up to 8-10mg/ml at 60°C (Arčon *et al.*, 2004). More specifically, Woo *et al.* (2008) reported that the maximum solubility (\pm SD) of a saline solution of cisplatin at room temperature was 1.49 ± 0.21 mg/ml and increased to 10.20 ± 0.36 mg/ml when heated to 70°C. This meant that vesicles could be prepared at 70°C using a high cisplatin concentration and after cooling down vesicles entrapping a non-crystallised supersaturated solution of cisplatin could be obtained provided that it does not leak out. This was attributed to the insolubility of cisplatin in the lipid interior of the bilayer which would prevent cisplatin leakage and precipitation (Peleg-Shulman *et al.*, 2001). It was also suggested that the large surface area/volume ratio of the aqueous core would be energetically unfavourable in the formation of cisplatin crystals (Barenholz, 2001). This was confirmed by nuclear magnetic resonance (Peleg-Shulman *et al.*, 2001) and extended X-ray absorption fine structure (Arčon *et al.*, 2004) who both conducted a study on stealth liposomes hydrated with 8mg/ml cisplatin, and by cryo-transmission electron microscopy (Woo *et al.*, 2008) using thermosensitive liposomes hydrated with 10mg/ml cisplatin.

NIVs in the present study were hydrated at 70°C with a cisplatin concentration of 6mg/ml. For subsequent use it was necessary to dilute them to prevent precipitation of untrapped cisplatin. As this could compromise the delivered number of vesicles/ml, the NIVs were processed by diafiltration to prevent dilutorious process effect. This way diluted NIVs were returned back to their starting volume whilst maintaining an untrapped cisplatin concentration of 0.5mg/ml.

The characteristics of the processed NIVs in comparison to non-processed NIVs showed lower entrapment efficiency, smaller size and lower ZP (Figures 3.5 to 3.7).

The use of mechanical homogenisation adds a size reduction step to the resulting vesicles during formulation which is directly related to the homogenised volume at a fixed homogenisation time and speed (Mullen *et al.*, 2000). At first it was thought that the greater size of non-processed NIVs was due to the larger volume prepared by the same method. However when one batch was prepared and half of it was processed, the same results were obtained where processed NIVs still showed lower entrapment efficiency, smaller size and lower ZP (Figures 3.8 to 3.10).

Therefore, it was concluded that the diafiltration process was also a major contributing factor in further reducing vesicle size of the niosomal formulation. The possible mechanism that could explain the size reduction of the vesicles by diafiltration is kinetic collision. The process of diafiltration also managed to reduce the degree of heterogeneity in comparison to non-processed NIVs as indicated by their corresponding PDI values (Tables 3.1 and 3.2)

Furthermore, size reduction of vesicles via diafiltration had a direct effect on the entrapment efficiency of processed NIVs in comparison to non-processed NIVs. Many studies have supported the direct relation of entrapment efficiency with vesicular size (Fresta *et al.*, 1993; Lasic, 1998; Arunothayanun *et al.*, 2000; Jahn *et al.*, 2007).

Over time an overall stability in size was observed although inter-day variations were noted. In a study by Ramachandran *et al.* (2006), cisplatin was reported to form heterogeneous particles of varying size and shape in solution form. It was found that cisplatin particles ranging in diameter between 10-100nm were formed in a 1mg/ml solution using atomic force microscopy. The study indicated that the observed heterogeneity directly influenced liposomal size and entrapment efficiency (Ramachandran *et al.*, 2006). However, it is unknown whether the degree of cisplatin heterogeneity would increase with increased cisplatin concentration. Nonetheless, this could reasonably explain the variations in size and the great size distribution of cisplatin NIVs obtained in the present study from size and PDI results. FFEM images can further endorse the influence of entrapped cisplatin in obtaining NIVs of variable sizes (Figures 3.13 to 3.15). Moreover, this could explain the

interday variations in entrapment efficiency of cisplatin NIVs as well despite the overall stability observed, not to mention batch to batch variations.

The entrapment efficiency of the different processed NIVs batches over one week ranged between approximately 15-24% (Figure 3.5), 14-21% (Figure 3.8) and 21-38% (Table 3.3). On the day of preparation entrapment efficiency of these NIVs in the same order were $21.0 \pm 2.73\%$, $17.8 \pm 1.19\%$ and $37.8 \pm 2.87\%$. However, as will be discussed later (Chapter 4), the HPLC method used in the quantification of entrapped cisplatin is not exclusive to native cisplatin and is capable of detecting any platinum species present in unbound form. Therefore the variations in entrapment efficiency could also be a result of the analytical method used.

Nonetheless, it is anticipated that entrapped cisplatin whether intact or transformed will be released from the NIVs and capable of exerting an effective anti-cancer effect through *in vivo* studies. The success of a vesicular delivery system not only relies on its entrapment efficiency but also on its ability to release entrapped drug *in vivo* when required and in quantities sufficient to produce therapeutic outcomes (Lasic, 1998). For instance, SPI-077 cisplatin liposomes were designed with a high entrapment efficiency of more than 90% and 110nm size to elude the MPS and target the tumour vasculature (Vail *et al.*, 2002). However, clinical studies demonstrated failure of the vesicular structure to release cisplatin efficiently and exert a therapeutic effect (Harrington *et al.*, 2001; Kim *et al.*, 2001; Meerum Terwogt *et al.*, 2002; White *et al.*, 2006). This was further endorsed by the low Pt-GG DNA adducts formed in comparison to cisplatin solution extracted from B16 tumours. When C57BL/6 mice were administered a single intravenous injection of either formulation in a 10mg/kg dose, tumours contained higher levels of cisplatin but lower adduct numbers with SPI-077 in comparison with cisplatin solution (Zamboni *et al.*, 2004).

Another effect observed with decreased vesicle size in the present study was a corresponding increase in negativity. It was observed that the surface charge of smaller processed NIVs showed greater negativity than larger non-processed NIVs (Figures 3.7 and 3.10). In a study by Roy *et al.* (1998), phosphatidylserine containing liposomes were found to increase in negativity with increased size and lamellarity. This is somewhat contradictory to what was observed in the present study. In the

present study, both processed and non-processed NIVs contain the same amount of added charge, same lipid composition and same drug concentration. The only difference was size reduction of processed NIVs following ultrafiltration. During diafiltration, larger vesicles were broken down to smaller vesicles. As a result, the vesicle curvature is increased with decreased size leading to greater proportion of the negatively charged lipid on the exterior (Roy *et al.*, 1997). Michaelson *et al.* (1973) indicated that asymmetric distribution of lipids in cosonicated vesicles is related to small radius of curvature where the head groups in the inner bilayer are packed more tightly than in the outer bilayer. As a result the electrostatic repulsion between negatively charged lipids in the outer bilayer is less allowing more lipids to organise in the outer layer thereby contributing to increased charge. Israelachvili (1973) also showed increased surface charge density on the outer membranes with increased curvature.

It appeared that diafiltration managed to standardise the vesicle size and the ZP regardless of drug concentration used to prepare them, where processed NIVs prepared with 0.5 and 6mg/ml cisplatin did not differ in size or ZP (Tables 3.7 and 3.9).

However, one effect observed with reduced cisplatin concentration used in NIVs hydration was the inability to separate entrapped from unentrapped drug by ultracentrifugation. A possible explanation could be viscosity differences between niosomes with lower cisplatin concentrations. Ultracentrifugation of processed 0.5mg/ml and 1mg/ml NIVs at 4°C initially formed a pellet which was lost upon minor mechanical agitation experienced during normal handling or upon standing of the pellet, whilst in solution, at room temperature. Placement of tubes in ice after ultracentrifugation did not solve the problem as slight perturbation of the material during removal of the supernatant disrupted the pellet. Another attempt at ultracentrifugation of the niosomal suspension alone (without addition of 0.9% w/v NaCl) also failed. Arunothayanun and Florence (2000) have reported the ability of saline to reduce the viscosity of Span 60 niosomes significantly in comparison to water. However, all NIVs in the present study were prepared with 0.9% w/v NaCl and produced in a similar size distribution with the only variable being the

concentration of cisplatin used to hydrate the vesicles. Even when processed NIVs suspension prepared with 6mg/ml cisplatin was added to either 0.9% w/v NaCl, 0.5mg/ml or 1mg/ml cisplatin solutions, it was possible to pellet the NIVs, indicating that the initial concentration of cisplatin used to hydrate the NIVs plays a role in controlling the viscosity.

Over the course of time, lipid vesicles are prone to leak their entrapped material (Jahn *et al.*, 2007). Presence of concentration gradients across lipid membranes enhances drug leakage which can be minimised by using macromolecular or hydrophobic drugs (Uchegbu and Vyas, 1998) as well as charged forms of drugs (Cullis *et al.*, 1997) that have lower membrane permeabilities. However, the consequence of drug leakage as a result of concentration gradient could eventually result in lower drug efficacy. This was demonstrated when sodium stibogluconate NIVs were separated from untrapped drug and re-suspended in phosphate buffered solution (Williams *et al.*, 1995). The ability of cisplatin to enter cells by passive diffusion (Krieger *et al.*, 2010), could correlate with free passage through lipid vesicle membranes. However as mentioned previously, the limited solubility of cisplatin necessitated diafiltration of NIVs thereby creating a concentration gradient.

The concentration gradients, and therefore the resultant cisplatin payload differed between the different processed NIVs batches. Processed NIVs (Section 3.2.1.1.1; Figure 3.5) maintained stable entrapment efficiency over one week indicating absence of leakage. Processed NIVs (Section 3.2.1.1.2; Figure 3.8) maintained stable entrapment efficiency up to day 3 post-preparation and then started to leak. Processed NIVs (Section 3.2.1.2; Table 3.3) leaked from day 0 to 1 post-preparation and stability was maintained afterwards up to day 32 post-preparation.

Furthermore, changing the concentration gradient by re-suspension of processed NIVs (Section 3.2.1.2) on day 1 post-preparation in different concentrations of cisplatin solutions and 0.9% w/v NaCl did not alter the leakage rate. It was expected that leakage rate of NIVs re-suspended in 0.9% w/v NaCl would be the greatest and in 1mg/ml cisplatin the least. Nonetheless, all formulations maintained considerably stable entrapment until significant leakage was observed day on 32 post-preparation (Table 3.6) even though parent processed NIVs maintained stable entrapment

simultaneously. It is difficult to interpret these observations but as mentioned previously the analytical method used in quantification could be responsible for these variabilities or the heterogeneity of cisplatin solute itself when in solution.

Further visualisation of the vesicles with FFEM provided further insight into the characteristics of cisplatin NIVs. By reducing the lipid concentration smaller and less vesicle numbers were formed (Figure 3.13.a). Mullen *et al.* (2000) demonstrated the effect of lipid concentration on the vesicle size where higher lipid concentrations, subjected to a constant time and speed of homogenisation as lower lipid concentrations, resulted in larger vesicles. However by reconstituting a freeze-dried empty NIVs formulation of the same lipid concentration and with the same drug concentration vesicles of larger size were obtained with no signs of aggregation (Figure 3.13.b). Santos Giuberti *et al.* (2011) also demonstrated the significant increase in liposomal size of SpHL-cisplatin when subjected to freeze drying. This was suggested to be a result of mechanical stress due to ice formation which damages the membrane structure leading to fusion of vesicles into larger ones (Mohammed *et al.*, 2006; Santos Giuberti *et al.*, 2011). The difference in physical properties between liquid and freeze-dried NIVs will be further reported (Chapter 5) as well as the effect of cisplatin on vesicle properties in comparison to empty ones.

Non-processed NIVs were seen as very large vesicle structures with apparent encapsulation of vesicles (Figure 3.14.b). These structures resembled two types of previously reported vesicular structures, vesosomes and multivesicular liposomes (MVLs). However both types were reported to be produced through specific procedures and not formed spontaneously as seen with non-processed NIVs.

Non-processed NIVs had a greater similarity to the so called vesosomes (Figure 3.16), which have been described and shown by FFEM in many studies (Walker *et al.*, 1997b; Kisak *et al.*, 2002; Kisak *et al.*, 2004; Boyer and Zasadzinski, 2007). Vesosomes are defined as vesicles containing distinct bilayer compartments separated from the external membrane with an average diameter of approximately 1 μ m (Boyer and Zasadzinski, 2007). However, these structures were described as difficult to produce by conventional self-assembly of vesicles and involve facilitation of irreversible phase transition of open bilayer sheets hydrated with vesicle

suspension to closed shells encapsulating the vesicles (Kisak *et al.*, 2002; Kisak *et al.*, 2004).

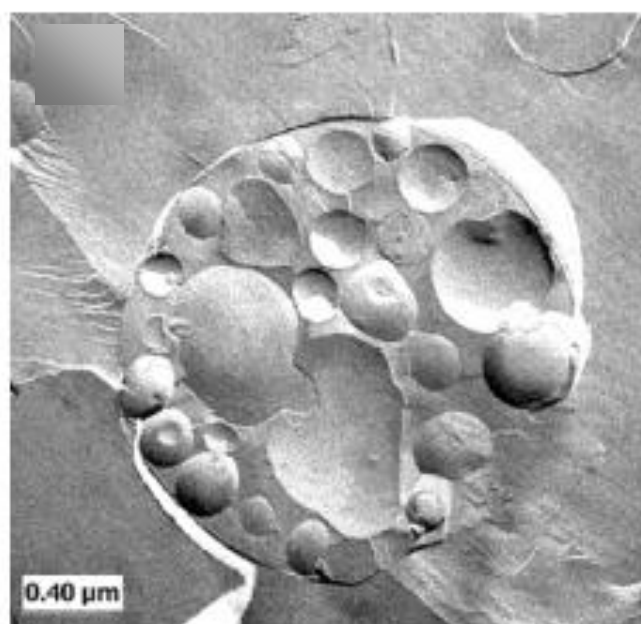
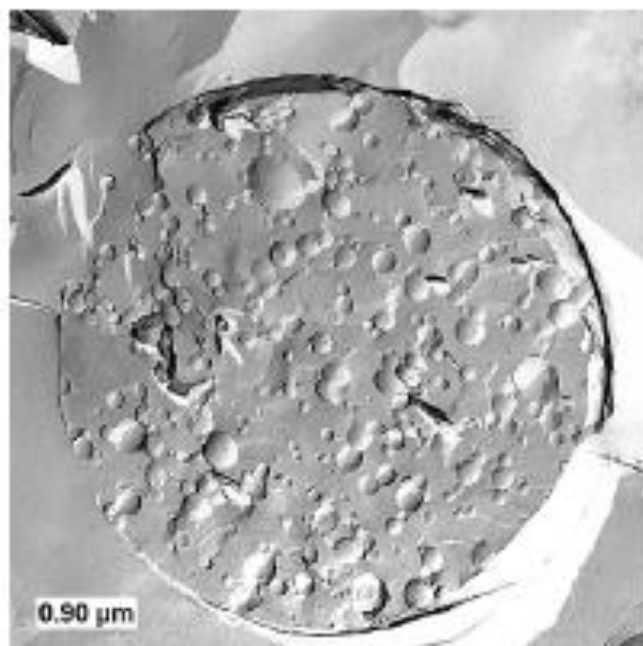


Figure 3.16. FFEM images of vesosomes which is a class of multivesicular vesicle showing similarity to multivesicular niosomes shown in Figure 3.15b. Images adapted from Kisak *et al.* (2004).

The other vesicular structure which showed less similarity to non-processed NIVs was the MVLs (Figure 3.17). The production of this type of vesicles is based on DepoFoam[®] technology resulting in a sustained release depot (Mantripragada *et al.*, 2002). The technology is based on the preparation of the MVLs through a double emulsification process to produce a w/o/w emulsion and the necessary presence of a neutral lipid such as triglycerides in the lipid phase (Zhong *et al.* 2005). MVLs contain multiple non-concentric internal aqueous chambers which are closely packed and separated by a network of lipid membranes (Mantripragada *et al.*, 2002) and range in size from 1-100 μ m (Chen *et al.*, 2010a). Drug products that have been produced based on this technology and approved for clinical use include the anti-cancer drug cytarabine (DepoCyt[®]) and morphine (DepoDur[®]; Zhong *et al.*, 2005). FFEM of MVLs indicated that the closely packed compartments showed different polyhedral shapes and sizes and exhibited a tetrahedral coordination similar to a gas-liquid foam that persists to the bilayer level (Spector *et al.*, 1996).

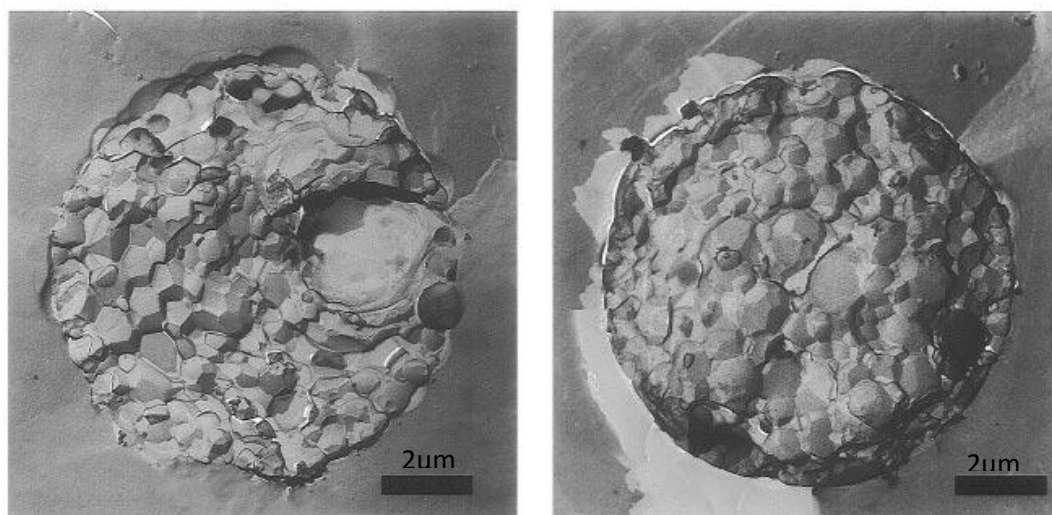


Figure 3.17. FFEM images of multivesicular vesicles prepared using DepoFoam[®] technology. Images are adapted from Spector *et al.* (1996).

The influence of diafiltration on reducing the vesicle size and size distribution of processed NIVs in comparison to non-processed NIVs (Figures 3.6 and 3.9) were in agreement with the FFEM images (Figure 3.15). It appeared that diafiltration led to

vesicle size reduction by the possible rupture of the multivesicular structures and the release of encapsulated vesicles or their reduction to smaller multivesicular structures. In comparison with other studies it is suggested that processed NIVs are mostly multilamellar (Pereira-Lachataignerais *et al.*, 2006; Braun *et al.*, 2007), with the presence of smaller vesicles which most likely are unilamellar. Perhaps it would be worthwhile if other imaging techniques are used in combination with FFEM that can support and further clarify lamellarity of the vesicular structures such as cryo-electron microscopy or confocal laser scanning microscopy.

The processed NIVs appeared to be multilamellar and this, together with their smaller size compared to non-processed NIVs would explain their limited entrapment efficiency. MLVs contain small aqueous cores (Szoka and Papahadjopoulos, 1978) where cisplatin would likely be entrapped in. The encapsulating volumes of SUVs, LUVs and MLVs have been reported to be about 0.5, 11 and 4 μ l/mg lipid, respectively (Gray and Morgan, 1991). Multilamellarity of processed NIVs could also explain the reasonable stable entrapment efficiency observed as well as the slow leakage rate when concentration gradients were changed as there are more barriers to leakage. Entrapped solutes have been reported to leak out of MLVs much less than LUVs due to the increased number of membranes they have to permeate (Fresta *et al.*, 1993).

Characterisation studies are fundamental in predicting the *in vivo* fate of vesicular delivery systems. The aim of the present study is to exploit the MPS to deliver cisplatin NIVs preferentially in the lungs. The negative surface charge and large size of cisplatin NIVs can facilitate opsonisation by plasma proteins and sequential uptake by the MPS (Lian and Ho, 2001). Uptake of large particles following intravenous administration is more likely to occur in the lungs as the pulmonary circulation is the primary site for particle clearance (Washington *et al.*, 2001b). Evading large particles are taken up by the MPS in the liver and spleen whereas particles less than 100nm will evade MPS and circulate for longer times. Accordingly MLVs and LUVs are taken up quicker than SUVs (Ranade *et al.*, 1989). Moreover, the negative surface charge can prevent undesirable aggregation through sufficient repulsion and thereby maintain a stable system. However, prediction of *in*

vivo fate following inhalation will depend on factors other than vesicle characterisation which will be discussed in greater detail (Chapter 7).

However, an issue arising from the current research is the variable entrapment efficiency from NIVs batch to batch. If size variability is the main reason behind the different entrapment efficiency, perhaps it would be better to unify vesicle size and narrow the size distribution range between batches. Many studies have emphasised the importance of unifying vesicle size and size distribution (Lasic, 1995; Wagner *et al.*, 2002) in standardising dosage based on entrapment efficiency (Jahn *et al.*, 2007) and batch to batch reproducibility (Sharma and Sharma, 1997). Methods to reduce vesicle size include sonication, extrusion or microfluidisation (Sharma and Sharma, 1997).

3.4. Conclusion

From the present characterisation study it can be concluded that NIVs can be prepared using high cisplatin concentrations. However, the limited solubility of cisplatin at room temperature necessitates downstream diafiltration in preference over dilution of NIVs products post-manufacture to prevent precipitation of unentrapped cisplatin when hydrated at concentrations higher than 1mg/ml. The size and surface charge of NIVs can play a role in targeting the MPS.

Over the short term, NIVs maintained a stable size and offered a stable delivery system that could resist aggregation problems associated with colloidal systems through the inclusion of a negative charge. Although inter-day fluctuations in entrapment efficiency were observed, overall stability could be maintained throughout the time period. Variability in measurements could be due to fluctuations in the state of cisplatin solution, which in turn could affect size and entrapment efficiency correspondingly (Ramachandran *et al.*, 2006). Additional stability studies will be necessary to confirm NIVs suitability.

Chapter 4. Development of HPLC methods for platinum and lipid quantification

4.1. Introduction

HPLC has been described as the analytical technique that continues to be most widely used in the assessment of pharmaceutical compounds (Gilpin and Gilpin, 2009) in terms of purity, quality control and assurance of final drug product (Ahuja, 2005). HPLC is an analytical technique widely used in the quantitative analysis of biomolecules, polymers and other organic compounds (Ornaph and Dong, 2005).

The basic theory of HPLC is that compounds are separated and eluted based on their different affinities between stationary and mobile phases (McMaster, 2007a). The three major steps in HPLC are injection, separation and then elution (Bidleymeyer, 1992a). In HPLC, the sample is injected using an automated injector onto the column containing the stationary phase while fresh solvent is pumped down the column at high pressure using a pump. As the liquid sample moves down the column the components are separated and elute in turn based on their relative affinity for stationary or mobile phase. The higher the affinity to the stationary phase relative to the mobile phase the slower the elution (Bidleymeyer, 1992a). The column eluent typically passes through an online detector and the resultant electrical signal is converted to a chromatogram corresponding to the concentration of analyte detected (Ornaph and Dong, 2005).

Samples can be separated by using HPLC in different modes. Major modes of separation include normal phase (NP), reverse phase (RP), ion-exchange, size-exclusion, chiral separation and affinity liquid chromatography (Eksteen, 1996; Hanai, 1999). NP-HPLC and RP-HPLC are based on the partition coefficients of sample components between mobile phase and polar or non-polar stationary phases, respectively. In NP-HPLC, the polarity of the stationary phase is typically greater than the mobile phase and thereby the order of elution is non-polar analytes, then components of increasing polarity. In RP-HPLC, which is the most widely used, the order of elution is reversed compared to NP-HPLC with the stationary phase typically less polar than the mobile phase (Dong, 2006a).

During HPLC analysis, it is common for the mobile phase composition to remain unchanged throughout the run. This is known as isocratic elution. However, in some cases analytes within a sample may have wide polarity ranges or wide molecular weight ranges and are generally poorly separated using an isocratic mobile phase (Scott, 1996). In these cases, gradient elution is employed where the mobile phase composition changes throughout the run with the mobile phase solvent composition increasing in concentration or polarity over time (Bidingmeyer, 1992b). The more the polarities of the mobile and stationary phases are similar, the quicker the elution of analytes strongly attracted to the stationary phase (McMaster, 2007a).

A variety of detectors can be used with HPLC such as UV/Vis, fluorescence, refractive index, evaporative light scattering, mass spectroscopy and nuclear magnetic resonance (Dong, 2006b).

4.1.1. Quantification of platinum by HPLC

Analytical methods for the detection of platinum are necessary whether for detecting platinum levels *in vivo* or for determining the amount entrapped in drug formulations. The various analytical methods adapted in the detection of platinum in biological samples were discussed previously (Section 1.5). Similar analytical methods have also been reported to determine entrapment efficiency with flameless atomic absorption spectroscopy and HPLC being the most widely used.

Flameless atomic absorption spectroscopy was used to evaluate the entrapment efficiency of liposomal formulation SPI-77 (Zamboni *et al.*, 2004), other cisplatin liposomes (Hwang *et al.*, 2007; Hirai *et al.*, 2010) and nanoparticles (Burger *et al.*, 2002; Velinova *et al.*, 2004). On the other hand, HPLC has been employed in evaluating the entrapment efficiency of SLIT cisplatin liposomes (Wittgen *et al.*, 2007), SpHL cisplatin (Júnior *et al.*, 2007a; Leite *et al.*, 2009; Santos Giuberti *et al.*, 2011) and other liposomal cisplatin formulations (Arçon *et al.*, 2004).

In the present research, HPLC-UV was chosen for platinum analysis in biological samples and in the determination of platinum content in NIVs. The choice was prompted by its availability, feasibility, simplicity, sensitivity and selectivity.

UV detection is the most widely used detector because of its sensitivity, which is of the order around 10^{-8} g/ml. It also relatively inexpensive, can be used with gradient elution and is temperature insensitive (Christian, 1994). However, the use of UV detection is limited to substances that absorb light in the UV wavelength range (Christian, 1994).

4.1.2. Quantification of lipids by HPLC

In addition to analysing platinum content of the NIVs, analysis of lipid content is equally important. Lipid content analysis is important in evaluating the chemical stability of the vesicle forming lipids, as changes in their chemical properties may affect NIVs stability and impact on biological safety and efficacy.

Chromatographic methods have become superior to chemical and enzymatic assays for analysing lipids, being in that they are less complicated and they can simultaneously separate and quantify at the same time (Edwards and Baeumner, 2006). Among the suitable chromatographic methods for lipid quantification, HPLC is considered as the method of choice for most researchers. This arises from the inaccurate quantification and unsuitability of thin layer chromatography for all purposes and the inability of gas chromatography to analyse many of the lipids due to their lack of volatility (Hammond, 1993).

The use of UV detection with HPLC in the analysis of lipids is unsuitable because most of them lack suitable chromophores (Hvattum *et al.*, 2006). Lipids that do exhibit absorption properties typically absorb in the range of 200 to 210nm which limits the solvent choice to minimise spectral interference (Hvattum *et al.*, 2006). The use of refractive index detectors is also limited in lipid quantification because they are sensitive to slight changes in ambient temperature, flow rate and pressure which indicate sensitivity to gradient elution separation techniques leading to inaccurate results (Hammond, 1993).

Evaporative light scattering detection (ELSD), in contrast, has been reported to be the most suitable detector in combination with HPLC for the quantification of lipids (Zhong *et al.*, 2010). Although both NP-HPLC-ELSD (Sas *et al.*, 1999; Rabinovich-Guilatt *et al.*, 2005; Hvattum *et al.*, 2006) and RP-HPLC-ELSD (Zhong *et al.*, 2010)

have been utilised in lipid quantification, NP-HPLC-ELSD has been regarded as the method of choice in lipid analysis (Deschamps *et al.*, 2001a)

ELSD is a universal detector capable of detecting any compound as long as it is less volatile than the mobile phase. It has useful sensitivity and is compatible with most solvents and separation techniques employing gradient elution (Rabinovich-Guilatt *et al.*, 2005).

The operation of ELSD is based on the passage of eluent into the detector where it is transformed into droplets by a nebuliser. As these droplets pass through the heated drift tube the volatile mobile phase evaporates leaving solute particles. When the particles pass through a laser beam, light scattering results which is proportional to mass, and this is converted into an electronic signal (Deschamps *et al.*, 2001b).

In the present research, NP-HPLC-ELSD was adapted as the method of choice for lipid analysis.

4.2. Results

4.2.1. Quantification of platinum by HPLC

The chromatographic conditions used in the analysis of platinum have been described (Section 2.2.5)

4.2.1.1. Method I

Platinum analysis, as described (Section 2.2.5.2) was adapted prior to use in the present research. It had been reported to have been validated and showed good separation of the analytes where retention times were in the order of approximately 6, 8 and 10min for DDTC, Pt(DDTC)₂ then Ni(DDTC)₂, respectively (Figure 4.1).

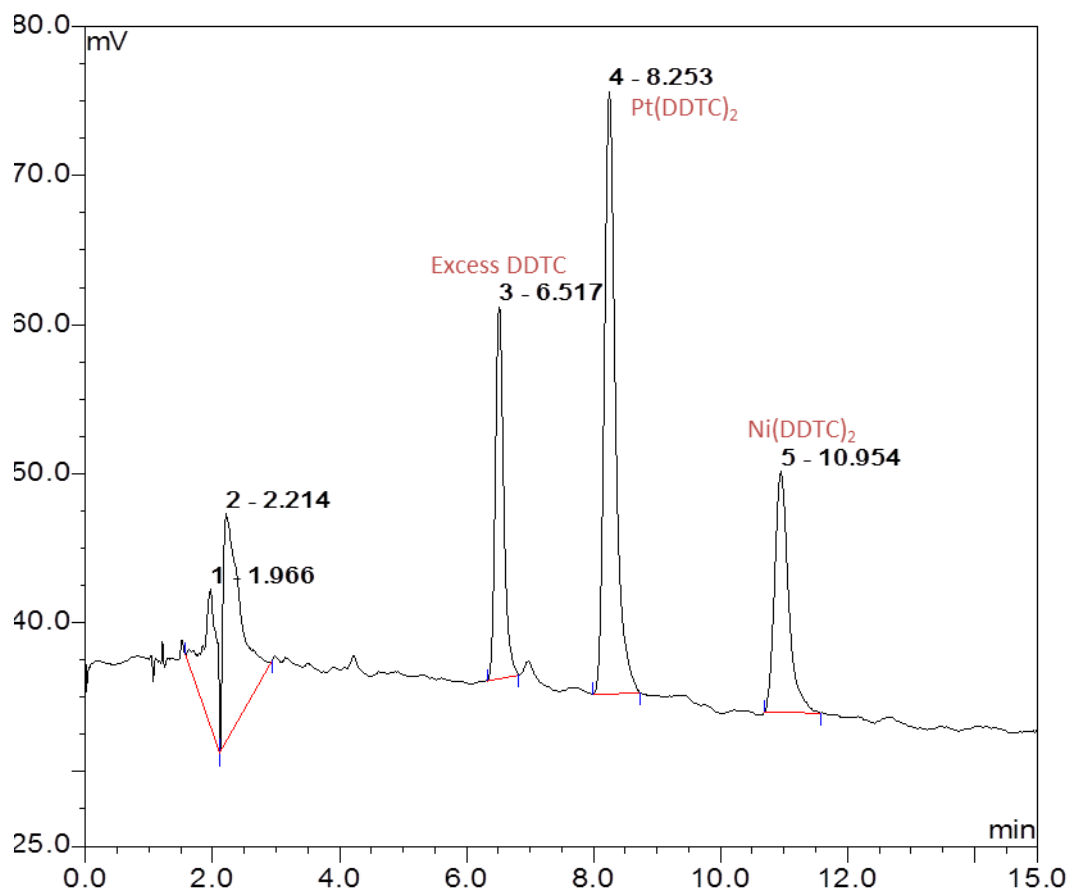


Figure 4.1. A chromatogram illustrating the separation and elution of excess DDTC, Pt(DDTC)₂ and Ni(DDTC)₂ at 6, 8 and 10min, respectively, using method I. The sample was prepared from a 0.9% w/v NaCl solution containing 5µg/ml cisplatin.

The concentration range used showed good linearity with $R^2=0.999$ (Figure 4.2)

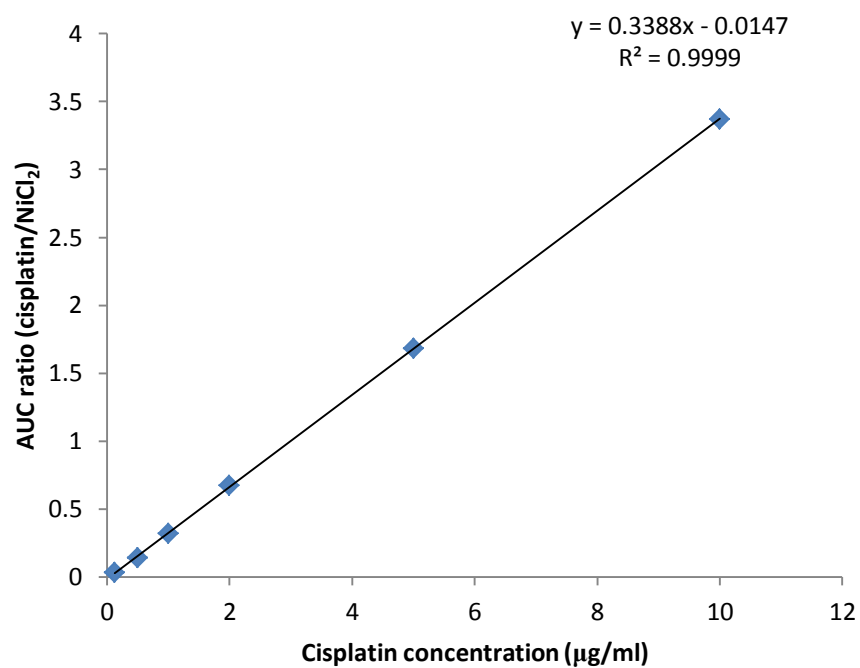


Figure 4.2. A typical calibration curve obtained using method I for the quantification of platinum. Concentrations used to establish the calibration curve were 0, 0.125, 0.5, 1, 2, 5 and 10µg/ml in 0.9% w/v NaCl (n=1).

However, over the course of study the eluted peaks occasionally were split, making quantification impossible (Figure 4.3). This led to the development and modification of the existing method.

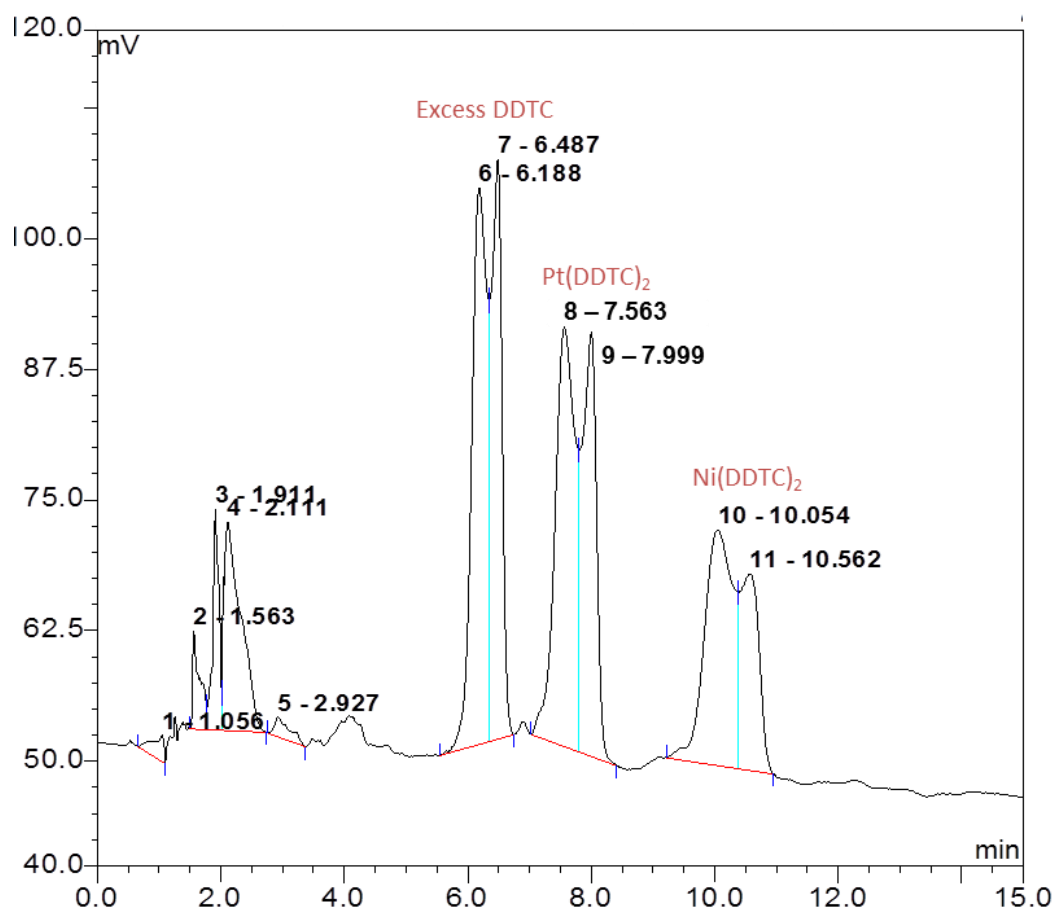


Figure 4.3. A chromatogram illustrating the separation and elution of excess DDTC, Pt(DDTC)₂ and Ni(DDTC)₂ using method I. The sample was prepared from a 0.9% w/v NaCl solution containing 5µg/ml cisplatin.

As will be discussed later, two possible technical solutions to the problem were studied. The first approach was to reduce the injection volume of the chloroform layer. The second approach was to evaporate the chloroform layer and reconstitute the dried sample in a suitable solvent. Reducing the injection volume of the chloroform layer to 10 μ l or evaporating the chloroform layer and reconstituting the sample in 75% v/v acetonitrile in water solved this issue. However, favourable peak properties were obtained with the second approach in comparison to the first (Table 4.1). Evaporation and reconstitution with 75% v/v acetonitrile in water produced very sharp peaks of high efficiency with greater AUCs and heights unlike peaks resulting from reducing the injection volume.

Table 4.1. Comparison of peak properties obtained by direct injection of chloroform layer in a 10 μ l volume (A) and 20 μ l injection of a sample reconstituted in 75% v/v acetonitrile in water following evaporation of the chloroform layer (B). The sample was prepared from a 0.9% w/v NaCl solution containing 5 μ g/ml cisplatin.

Method	Peak of interest	Retention time (min)	AUC (mV* min)	Height (mV)	Asymmetry	Efficiency
A	Pt(DDTC) ₂	7.36	3.83	16.3	1.24	6503
B	Pt(DDTC) ₂	6.52	14.49	97.9	1.07	12590
A	Ni(DDTC) ₂	9.79	4.28	13.5	1.22	6189
B	Ni(DDTC) ₂	8.68	9.14	49.3	1.08	13851

4.2.1.2. Method II

This method (Section 2.2.5.3), was adapted based on the preferential peak qualities obtained (Table 4.1). Chromatogram of a blank sample containing only DDTC and NiCl₂ showed good separation with excess DDTC and Ni(DDTC)₂ eluting at approximately 5 and 9min, respectively (Figure 4.4). The peaks were sharper with greater efficiency.

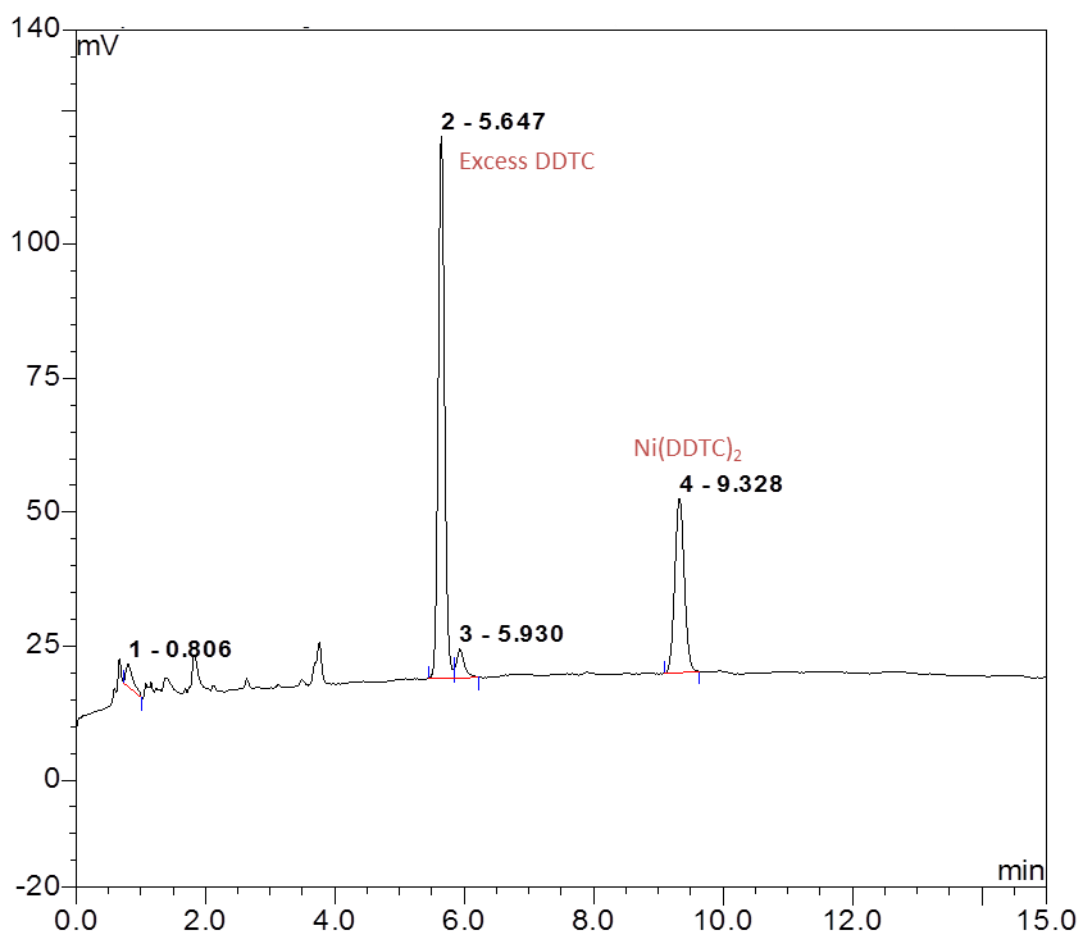


Figure 4.4. A chromatogram illustrating the separation and elution of excess DDTC, and Ni(DDTC)₂ at 5 and 9min, respectively, using method II. Chloroform layer was evaporated and the sample was reconstituted in 75% v/v acetonitrile in water. The sample was a blank sample containing no cisplatin.

The chromatogram of a sample containing cisplatin in a concentration of 5 $\mu\text{g}/\text{ml}$ with added DDTC and NiCl_2 showed good separation with excess DDTC, $\text{Pt}(\text{DDTC})_2$ and $\text{Ni}(\text{DDTC})_2$ eluting at approximately 5, 7 and 9min, respectively (Figure 4.5).

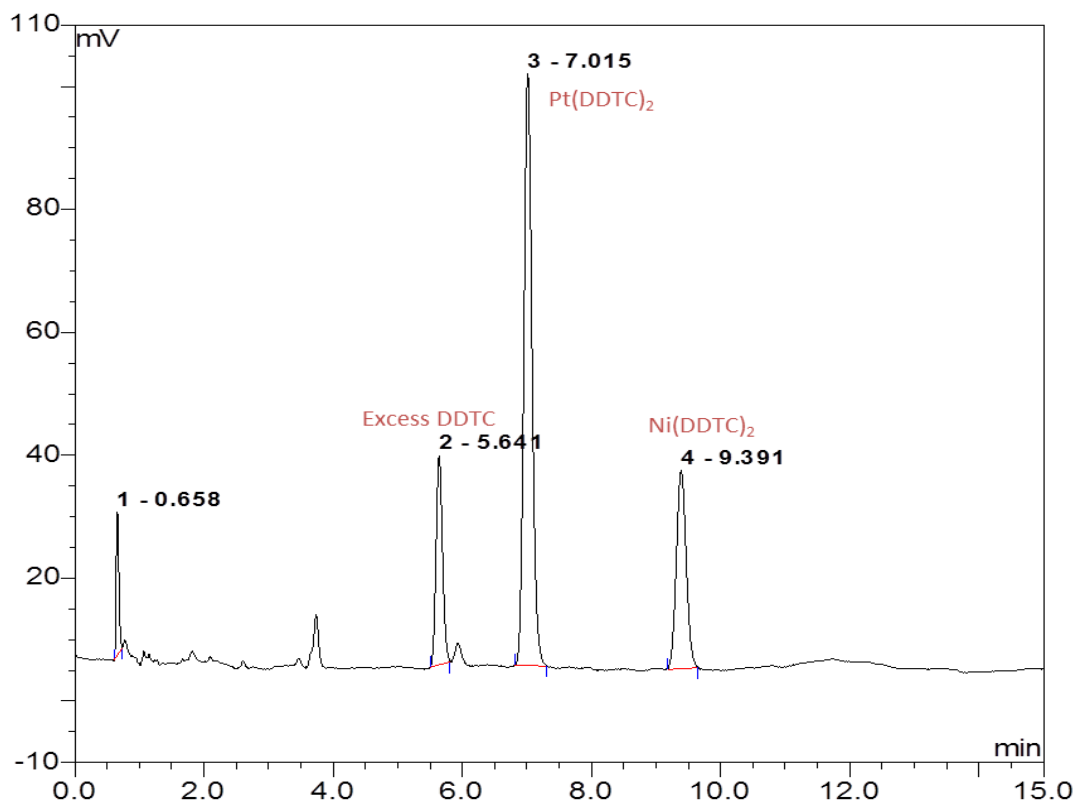


Figure 4.5. A chromatogram illustrating the separation and elution of excess DDTC, $\text{Pt}(\text{DDTC})_2$ and $\text{Ni}(\text{DDTC})_2$ at 5, 7 and 9min, respectively, using method II. Chloroform layer was evaporated and the sample was reconstituted in 75% v/v acetonitrile in water. The sample was prepared from a 0.9% w/v NaCl solution containing 5 $\mu\text{g}/\text{ml}$ cisplatin.

The concentration range used showed good linearity with $R^2=0.999$ (Fig 4.6).

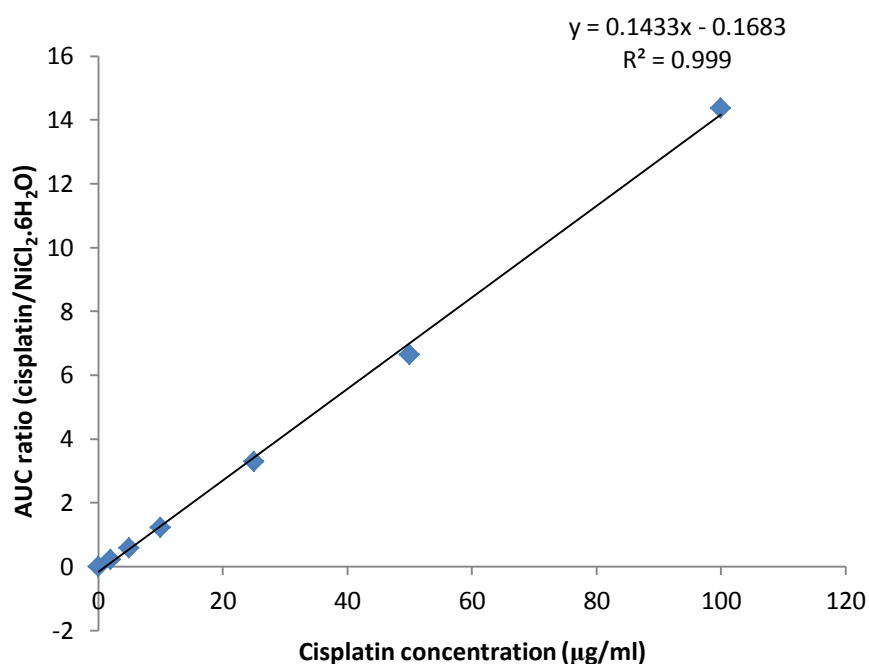


Figure 4.6. A typical calibration curve obtained using method II for the quantification of platinum. Concentrations used to establish the calibration curve were 0, 2, 5, 10, 25, 50 and 100µg/ml in 0.9% w/v NaCl (n=1).

This method was employed in the determination of the cisplatin content of NIVs used in the first and second stability study (Chapter 5) with the exception of NIVs on day 469 post-preparation from the first stability study. However the method had not been validated prior to its adaptation. Over the course of the study, inconsistent results were obtained which necessitated additional modification of the analytical method. These will be discussed later. This was proven when the method was validated for intra-day and inter-day precision (Table 4.2). Results showed high relative standard deviation (%RSD) values obtained especially after inter-day analysis. The accuracy obtained when 50 and 5µg/ml were analysed in duplicates was 105.8 and 79.6%, respectively. The retention time precision for the peaks of

interest were 2.8% for Pt(DDTC)₂ and 3.1% for Ni(DDTC)₂. The results showed the requirement for further method development.

Table 4.2. The intra-day and inter-day precision of method II as represented by %RSD values. Two sets of standards were analysed in triplicates for intra-day precision and three sets of standards were analysed in triplicates for inter-day precision.

Concentration (µg/ml)	Intra-day precision (%RSD) (n=2)	Inter-day precision (%RSD) (n=3)
100	22.0	22.8
50	4.2	21.7
25	5.7	16.4
10	2.5	26.1
5	16.1	20.2
2	3.2	2.8

4.2.1.3. Method III

In this method the starting adapted method was restored. Chloroform layer was injected directly but injection volume was reduced to 10 μ l instead of 20 μ l (Figure 4.7).

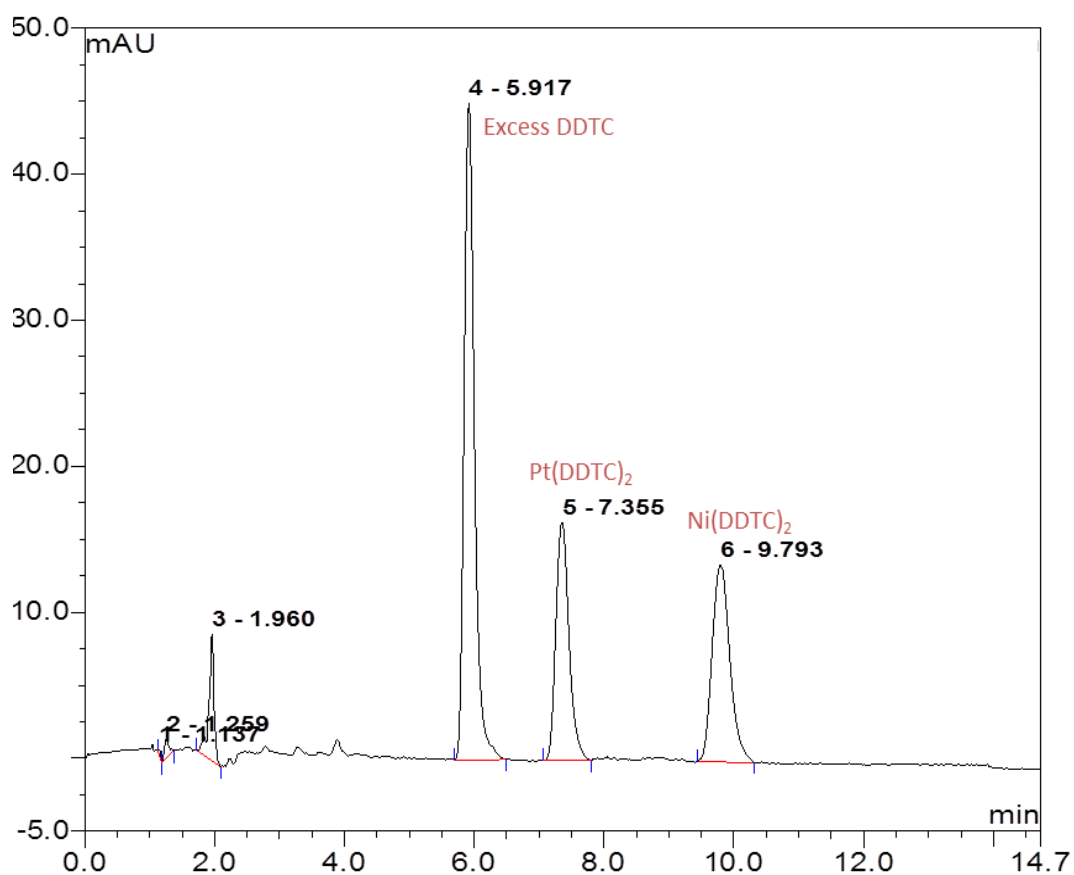


Figure 4.7. A chromatogram illustrating the separation and elution of excess DDTC, Pt(DDTC)₂ and Ni(DDTC)₂ at 5, 7 and 9min, respectively. Chloroform layer was injected directly but the injection volume was reduced to 10 μ l. The sample was prepared from a 0.9% w/v NaCl solution containing 5 μ g/ml cisplatin.

Further development of the method included additional column heating, as will be discussed later. Peak characteristics at 40°C were studied where an inverse relationship between flow rate and elution time of the analytes was observed (Table 4.3). In order to maintain the same retention times of the analytes with increasing temperature, flow rate had to be reduced to 1.2ml/min at 40°C. Furthermore the column back-pressure at this condition was 200 bars. However, the optimum temperature shown to maintain typical retention times as the starting method without having to reduce flow rate was 30°C. Furthermore, the method involved two calibration ranges as described (Section 2.2.5.4).

Table 4.3. Peak characteristics of DDTC, Pt(DDTC)₂ and Ni(DDTC)₂ when elution was carried out at 40°C at different flow rates.

Peak of interest	Flow rate at 40°C	Retention time (min)	AUC (mV*min)	Height (mV)	Asymmetry	Efficiency
DDTC	0.9ml/min	8.86	16.69	59.30	1.13	6018
	1.2ml/min	6.68	12.67	50.16	1.01	4162
	1.6ml/min	5.07	9.29	44.92	1.14	3590
Pt(DDTC) ₂	0.9ml/min	10.43	76.53	231.47	1.14	5786
	1.2ml/min	7.87	58.80	190.92	1.01	3785
	1.6ml/min	5.99	42.31	167.41	1.10	3255
Ni(DDTC) ₂	0.9ml/min	13.55	26.78	62.67	1.14	5801
	1.2ml/min	10.23	21.56	52.08	1.01	3610
	1.6ml/min	7.81	15.45	45.95	1.06	3175

Chromatogram of a blank sample containing only DDTC and NiCl₂ showed excess DDTC and Ni(DDTC)₂ eluting at approximately 5 and 8min, respectively (Figure 4.8).

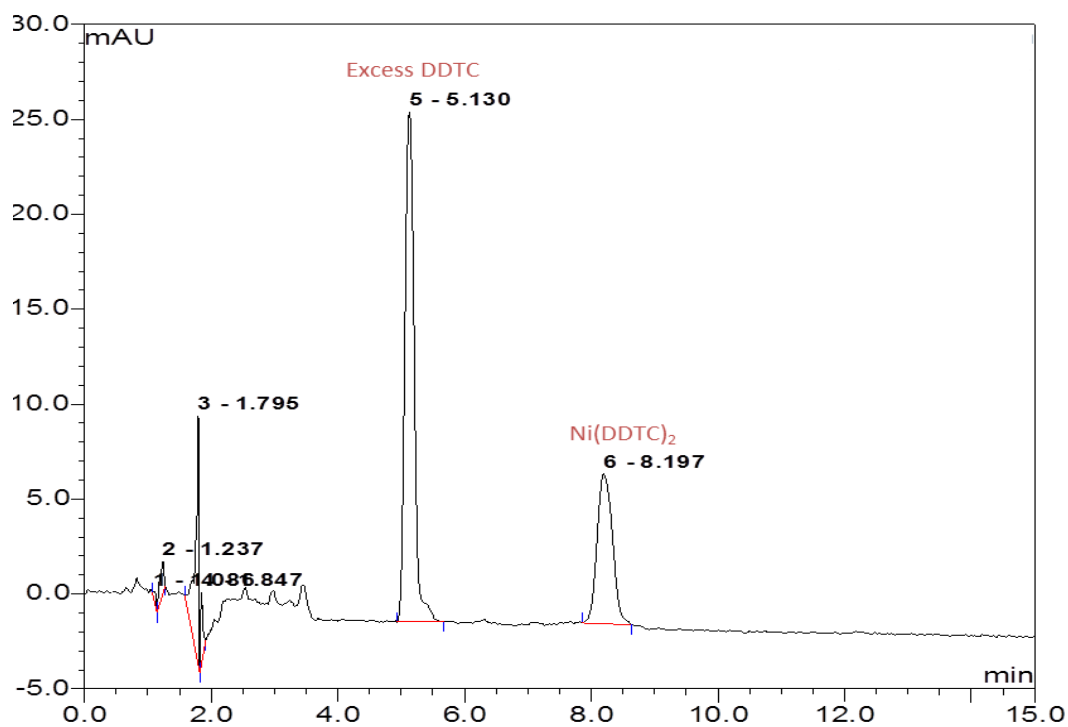


Figure 4.8. A chromatogram illustrating the separation and elution of excess DDTC and Ni(DDTC)₂ at 5 and 8min, respectively, using method III. Chloroform layer was injected directly but the injection volume was reduced to 10 μ l and column was heated to 30°C. The sample was a blank sample containing no cisplatin.

The chromatogram of a sample containing cisplatin in a concentration of 5 $\mu\text{g}/\text{ml}$ with added DDTC and NiCl_2 showed good separation with excess DDTC, $\text{Pt}(\text{DDTC})_2$ and $\text{Ni}(\text{DDTC})_2$ eluting at approximately 5, 6 and 8min, respectively (Figure 4.9).

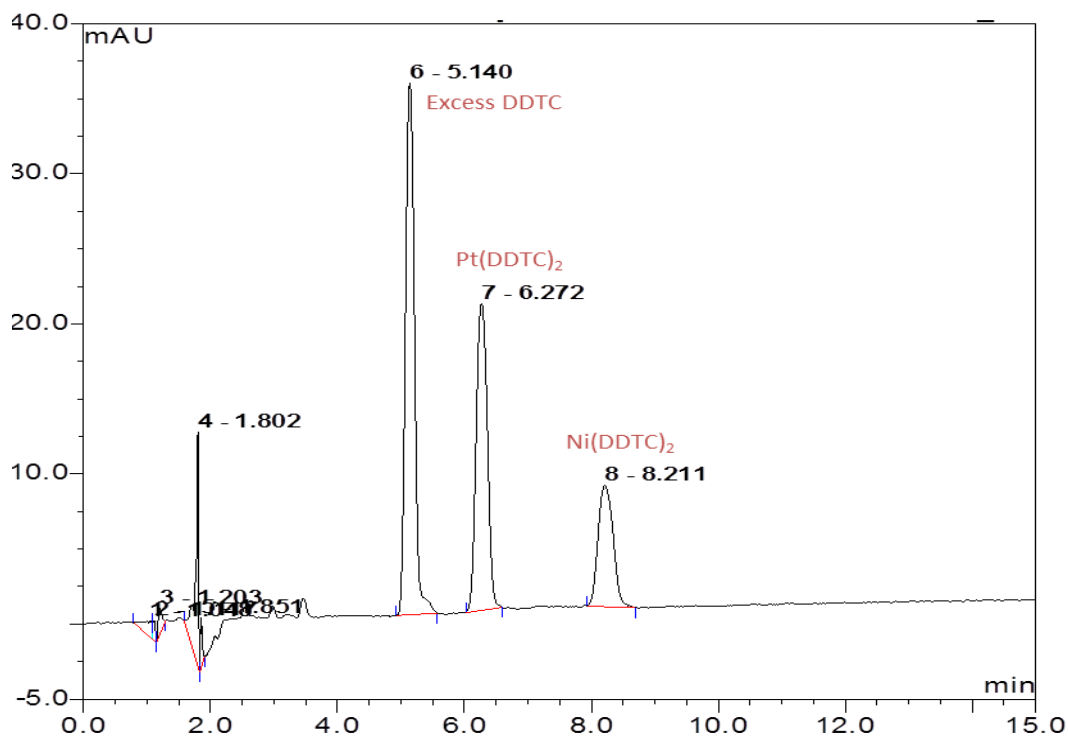


Figure 4.9. A chromatogram illustrating the separation and elution of excess DDTC, $\text{Pt}(\text{DDTC})_2$ and $\text{Ni}(\text{DDTC})_2$ at 5, 6 and 8min, respectively, using method III. Chloroform layer was injected directly but the injection volume was reduced to 10 μl and column was heated to 30°C. The sample was prepared from a 0.9% w/v NaCl solution containing 5 $\mu\text{g}/\text{ml}$ cisplatin.

Validation was performed on two calibration ranges. The first calibration ranged from 0 to 10 $\mu\text{g/ml}$ and used 5 μl of internal standard. The second calibration standard ranged from 0 to 100 $\mu\text{g/ml}$ and used 10 μl of internal standard.

Validation of the low calibration range showed good linearity with $R^2=0.9994$ (Figure 4.10). The precision of retention times for the peaks of interest were 0.4 and 0.7% for $\text{Pt}(\text{DDTC})_2$ and $\text{Ni}(\text{DDTC})_2$, respectively.

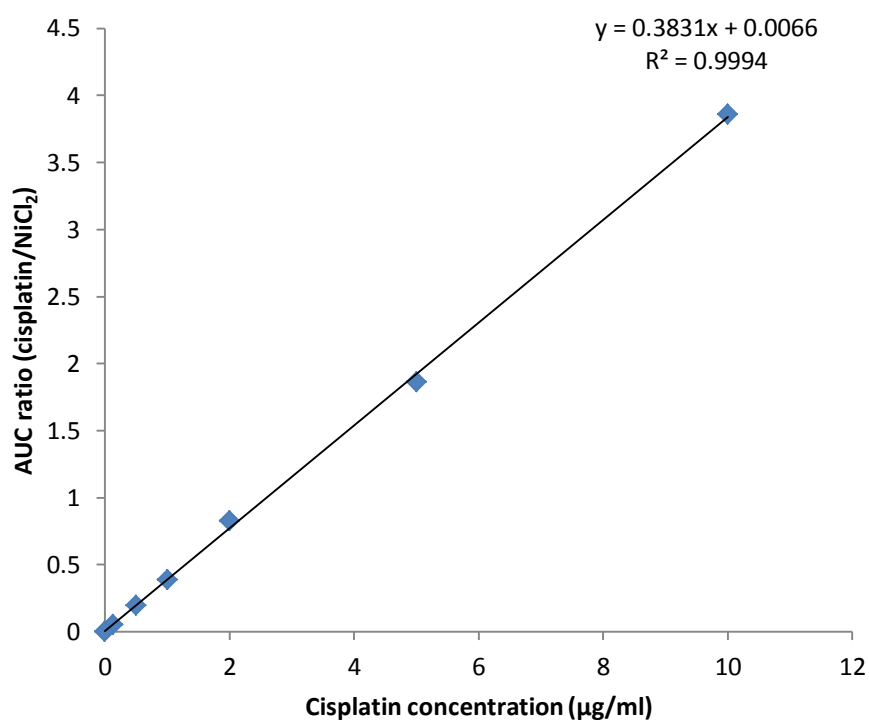


Figure 4.10. A typical calibration curve obtained using method III for the quantification of platinum. Concentrations used to establish the calibration curve were 0, 0.125, 0.5, 1, 2, 5 and 10 $\mu\text{g/ml}$ in 0.9% w/v NaCl (n=1).

The intra-day and inter-day precision were greatly improved with %RSD for almost all the concentrations < 5% (Table 4.4).

The accuracy of three concentrations in the calibration range were detected (Table 4.5) and showed % recovery between 95 and 109%.

Table 4.4. The intra-day and inter-day precision of method III in the analysis of cisplatin standard concentrations in 0.9% w/v NaCl. Values are representative of %RSD. Two sets of standards were analysed in triplicates for intra-day precision and three sets of standards were analysed in triplicates for inter-day precision.

Concentration (µg/ml)	Intra-day precision (%RSD) (n=2)	Inter-day precision (%RSD) (n=3)
10	3.5	4.9
5	3.8	3.1
2	1.4	14.8
1	2.8	2.4
0.5	4.1	4.5
0.125	16.5	20.6

Table 4.5. Accuracy of method III in the detection of platinum using three concentrations prepared in 0.9% w/v NaCl and analysed in triplicates.

Concentration (µg/ml)	Mean %recovery ± SD (n=1)	Precision (%RSD)
3.5	108.6 ± 0.62	0.6
5.0	95.0 ± 1.42	1.4
6.5	100.7 ± 1.02	1.0

Validation of the high calibration range showed good linearity with $R^2=0.99$ (Figure 4.11). The precision of retention times for the peaks of interest were 0.4 and 0.5% for $\text{Pt}(\text{DDTC})_2$ and $\text{Ni}(\text{DDTC})_2$, respectively.

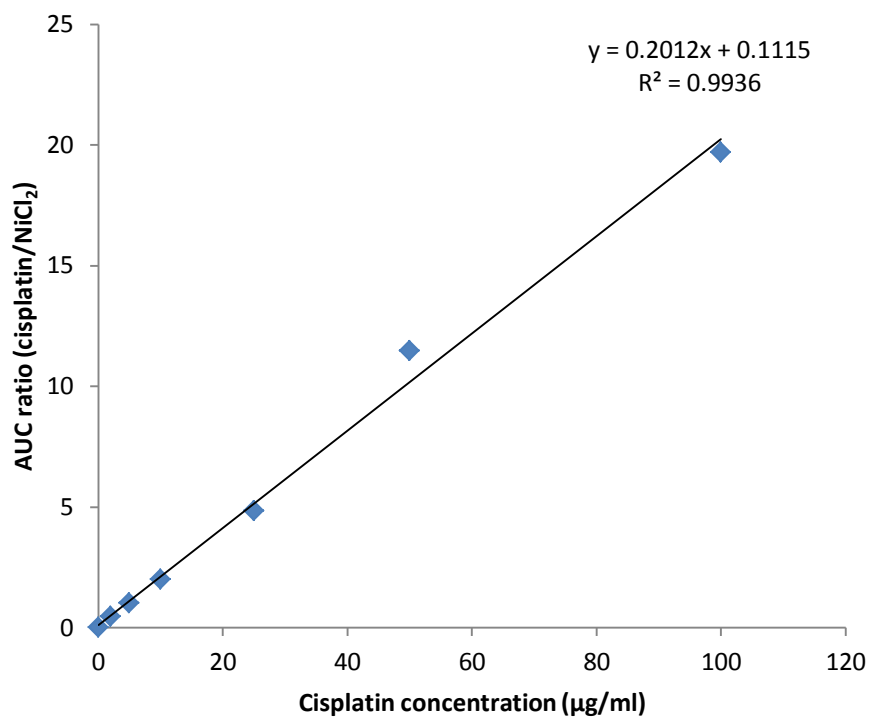


Figure 4.11. A typical calibration curve obtained using method III for the quantification of platinum. Concentrations used to establish the calibration curve were 0, 2, 5, 10, 25, 50 and 100µg/ml in 0.9% w/v NaCl (n=1).

The intra-day and inter-day precision for all concentrations showed %RSD values <5%, with the exception of 50 and 2 µg/ml (Table 4.6).

The accuracy of three concentrations in the calibration range were detected (Table 4.7) and showed % recovery between 92 and 96%.

Table 4.6. The intra-day and inter-day precision of method III in the analysis of cisplatin standard concentrations in 0.9% w/v NaCl. Values are representative of %RSD. Two sets of standards were analysed in triplicates for intra-day precision and three sets of standards were analysed in triplicates for inter-day precision.

Concentration (µg/ml)	Intraday precision (%RSD) (n=6)	Interday precision (%RSD) (n=9)
100	1.9	4.2
50	6.6	7.5
25	1.3	3.7
10	3.5	3.2
5	4.6	3.7
2	14.3	13.4

Table 4.7. Accuracy of method III in the detection of platinum using three concentrations prepared in 0.9% w/v NaCl and analysed in triplicates.

Concentration (µg/ml)	Mean %recovery ± SD (n=1)	Precision (%RSD)
17.5	96.1 ± 0.91	0.9
25.0	92.2 ± 0.92	0.9
32.5	93.3 ± 0.65	0.7

This method was used only in the detection of cisplatin content of NIVs on day 469 post-preparation from the first stability study (Chapter 5).

4.2.3. Quantification of lipids by HPLC

The method used in the quantification of lipid content was described (Section 2.2.6). This method was developed and modified from an unpublished method (personal communication, Prof Alex Mullen, University of Strathclyde)

In the unpublished method, the ternary gradient elution consisted of the same mobile phase composition described (Section 2.2.6) with a 22min run and a gradient flow rate from 0.5ml/min to 1ml/min as shown (Table 4.8).

Table 4.8. The ternary gradient elution sequence used in the analysis of lipid ingredients as indicated from the unpublished method. Solvent channels consisted of 100% isohexane (A), 100% ethyl acetate (B) and a mixture of 60% propan-2-ol, 30% acetonitrile and 10% methanol, 142 μ l/100ml glacial acetic acid and 378 μ l/100ml triethylamine (C).

Time (min)	Flow rate (ml/min)	Solvent channel		
		A	B	C
0	0.50	100	-	-
4	1.00	90	10	-
5	1.00	80	20	-
6	1.00	72	25	3
7	1.00	64	30	6
8	1.00	56	35	9
9	1.00	48	40	12
10	1.00	40	45	15
11	1.00	40	45	15
13	1.00	30	70	-
18	1.00	100	-	-
22	0.50	100	-	-

The chromatogram of the lipids showed the separation of the lipid ingredients in the order of cholesterol, surfactant VIII and then DCP at approximately 7, 9 and 14min, respectively (Figure 4.12). The order of lipids separated was confirmed by injecting each lipid individually.

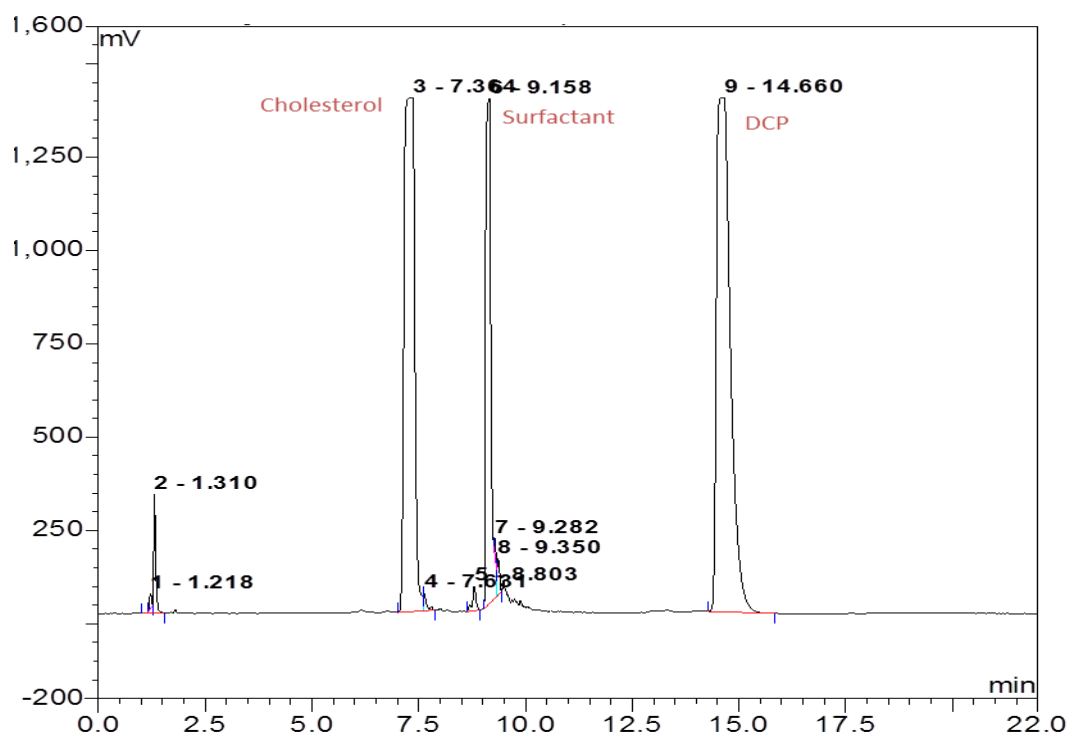


Figure 4.12. A chromatogram illustrating the separation and elution of cholesterol, surfactant and DCP at 7, 9 and 14min, respectively. Separation was achieved using the ternary gradient elution described (Table 4.8).

In the adapted method (Section 2.2.6), the sequence of the gradient elution was modified by starting with a mixture of solvent A and solvent B (80:20) to allow a further reduction in the elution time of the ingredients. Also the flow rate was kept stable at 1ml/min and the run time was reduced to 15min (Table 4.9).

Table 4.9. Gradient elution sequence used in lipid analysis using 100% isohexane (A), 100% ethyl acetate (B) and a mixture of 60% propan-2-ol, 30% acetonitrile and 10% methanol, 142 μ l/100ml glacial acetic acid and 378 μ l/100ml triethylamine (C).

Time (min)	Solvent channel		
	A	B	C
0	80	20	-
2	72	25	3
3	64	30	6
4	56	35	9
5	48	40	12
6	35	45	20
7	35	45	20
8	35	45	20
9	72	25	3
10	80	20	-
15	80	20	-

The chromatogram obtained showed the significant reduction in the elution time of cholesterol, surfactant VIII and DCP at 1, 4, and 9min, respectively (Figure 4.13). A slight rise in the baseline was observed between 6 and 8min, which corresponded to the increase of propan-2-ol in the mobile phase. Therefore, a significant improvement in this method in comparison to the original method was observed where separation was achieved at a shorter analysis time.

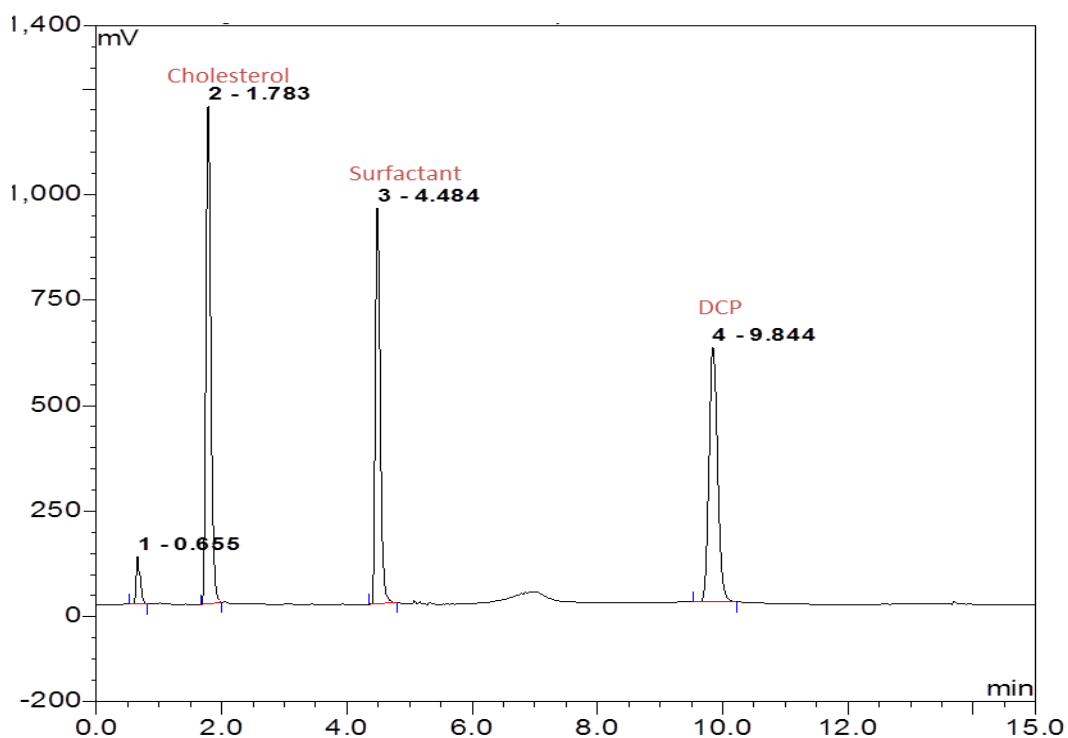


Figure 4.13. A chromatogram illustrating the separation and elution of cholesterol, surfactant and DCP at 1, 4 and 9min, respectively. Separation was achieved using the modified ternary gradient elution (Table 4.9).

Prednisolone was used as internal standard and when injected alone as a blank sample showed elution time of 6min (Figure 4.14). No other peaks were observed to interfere with peaks of interest.

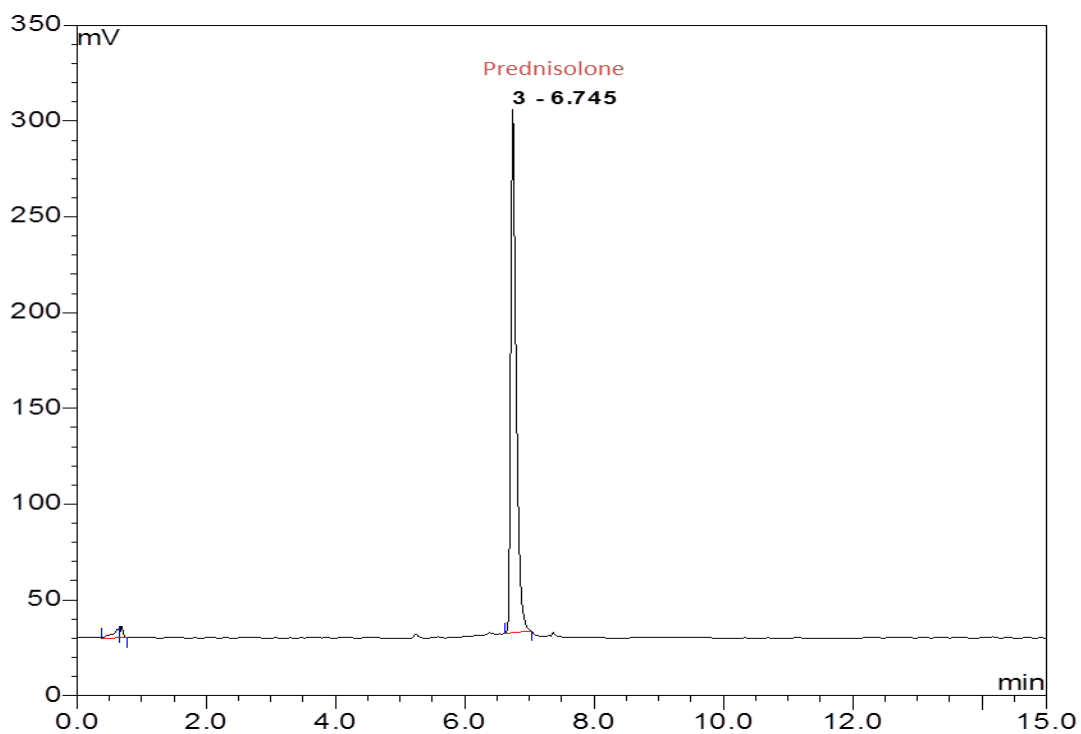


Figure 4.14. A chromatogram illustrating the separation and elution of prednisolone as an internal standard at 6min. The sample was prepared as a blank sample containing no cholesterol, surfactant and DCP.

The injection of all lipids with internal standard showed cholesterol, surfactant, prednisolone and DCP eluting at approximately 1, 4, 6 and 9min, respectively (Figure 4.15). The peaks obtained showed good separation and efficiency. The retention time precision for each peak of interest was 0.4, 0.4, 0.3 and 0.3% for cholesterol, surfactant VIII, prednisolone and DCP, respectively.

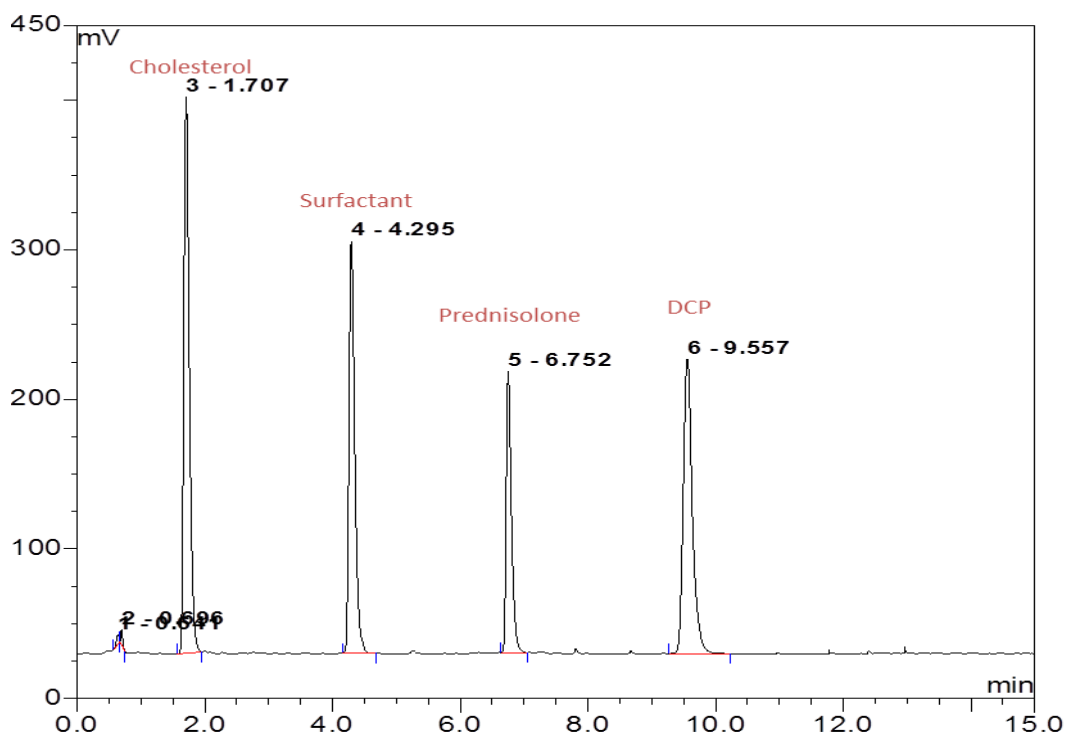


Figure 4.15. Separation and elution of cholesterol, surfactant, prednisolone and DCP at 1, 4, 6 and 9min, respectively, as illustrated in the chromatogram. Separation was achieved using the modified ternary gradient elution (Table 4.9).

This method was adapted in the analysis of lipid content of NIVs as part of the stability study (Chapter 5). As will be discussed further (Chapter 5), typical chromatograms as illustrated (Figure 4.15) were obtained containing only peaks corresponding to the analytes of interest.

Cholesterol showed good linearity where $R^2 > 0.99$ (Figure 4.16). The intra-day and inter-day precision for cholesterol did not exceed 5% except for the lowest concentration at 0.025mg/ml (Table 4.10).

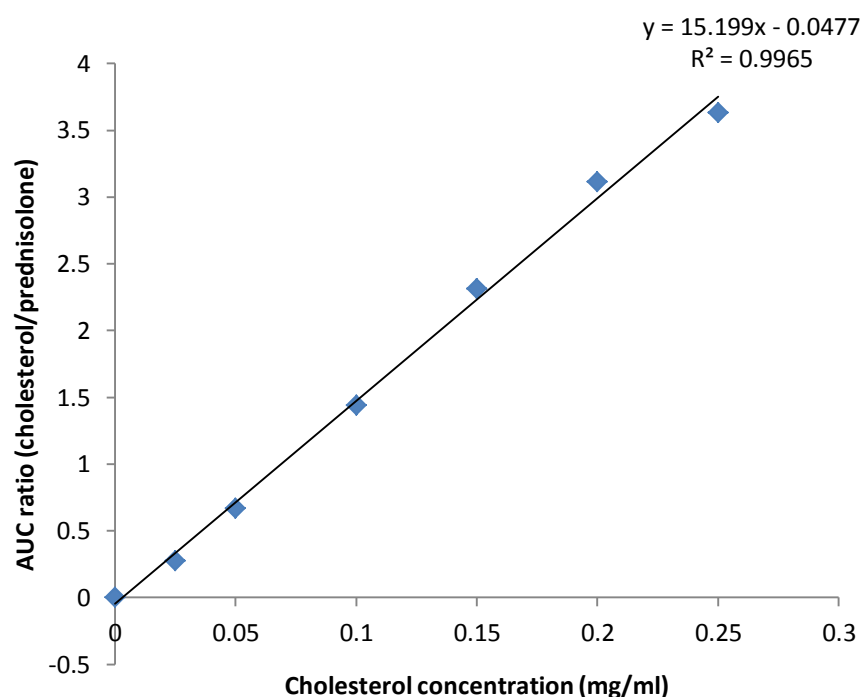


Figure 4.16. A typical calibration curve of cholesterol obtained using the developed method for lipid analysis. Concentrations used to establish the calibration curve were 0, 0.025, 0.05, 0.10, 0.15, 0.20 and 0.25mg/ml (n=1).

Table 4.10. The intra-day and inter-day precision of the developed method in the analysis of cholesterol standard concentrations. Values are representative of %RSD. Two sets of standards were analysed in triplicates for intra-day precision and three sets of standards were analysed in triplicates for inter-day precision.

Concentration (mg/ml)	Intra-day precision (%RSD) (n=2)	Inter-day precision (%RSD) (n=3)
0.25	3.8	5.3
0.20	4.4	3.6
0.15	5.3	4.3
0.10	2.3	2.1
0.05	4.0	5.7
0.025	7.3	14.0

The calibration range of surfactant VIII was linear with $R^2 > 0.99$ (Figure 4.17). The intra-day and inter-day precision for surfactant VIII overall did not exceed 10% (Table 4.11).

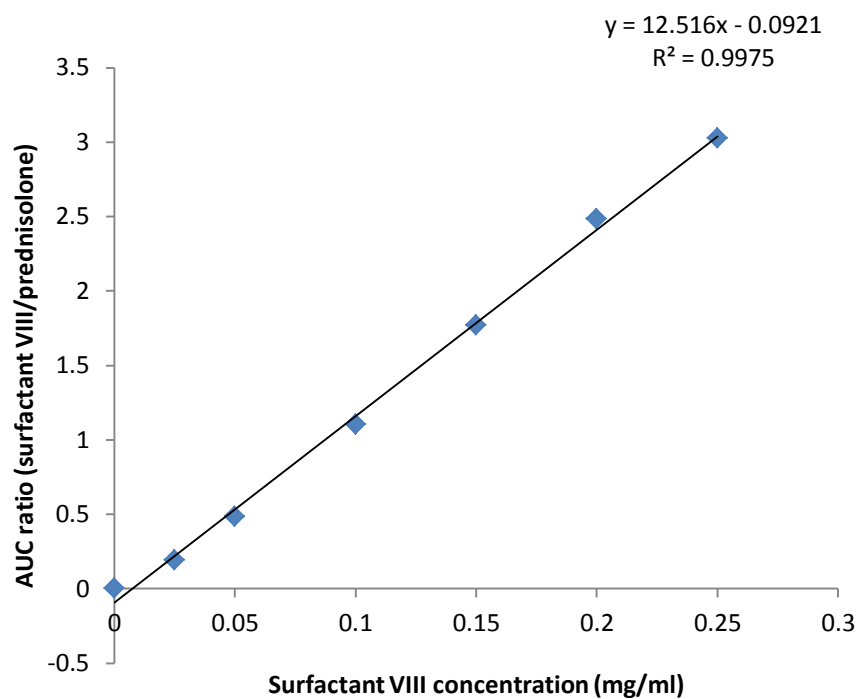


Figure 4.17. A typical calibration curve of surfactant VIII obtained using the developed method for lipid analysis. Concentrations used to establish the calibration curve were 0, 0.025, 0.05, 0.10, 0.15, 0.20 and 0.25mg/ml (n=1).

Table 4.11. The intra-day and inter-day precision of the developed method in the analysis of surfactant VIII standard concentrations. Values are representative of %RSD. Two sets of standards were analysed in triplicates for intra-day precision and three sets of standards were analysed in triplicates for inter-day precision.

Concentration (mg/ml)	Intra-day precision (%RSD) (n=2)	Inter-day precision (%RSD) (n=3)
0.25	3.8	11.9
0.20	6.2	7.9
0.15	6.4	7.0
0.10	2.8	4.8
0.05	3.3	3.9
0.025	10.3	14.8

The calibration range of DCP was linear with $R^2 > 0.99$ (Figure 4.18). The intra-day and inter-day precision for DCP did not exceed 5% for all concentrations (Table 4.12).

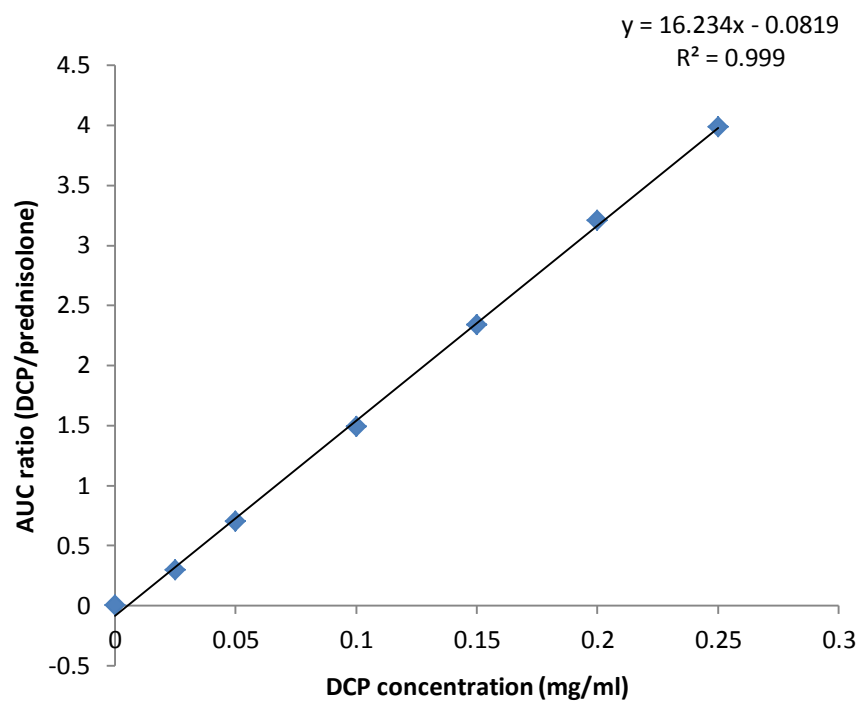


Figure 4.18. A typical calibration curve of DCP obtained using the developed method for lipid analysis. Concentrations used to establish the calibration curve were 0, 0.025, 0.05, 0.10, 0.15, 0.20 and 0.25mg/ml (n=1).

Table 4.12. The intra-day and inter-day precision of the developed method in the analysis of DCP standard concentrations. Values are representative of %RSD. Two sets of standards were analysed in triplicates for intra-day precision and three sets of standards were analysed in triplicates for inter-day precision.

Concentration (mg/ml)	Intra-day precision (%RSD) (n=2)	Inter-day precision (%RSD) (n=3)
0.25	2.9	2.7
0.20	3.0	2.6
0.15	3.0	2.6
0.10	1.5	1.9
0.05	3.4	3.4
0.025	5.6	5.3

4.3. Discussion

The HPLC method adapted for the quantification of platinum in the present study was first described by Bannister *et al.* (1979). In this study, cisplatin was derivatised with DDTC to form a complex with strong absorption properties. Cisplatin itself absorbs weakly in the UV region and cannot readily be detected. In the reaction, 2 moles of DDTC chelates with 1 mole of cisplatin as shown in the equation below.



The Pt(DDTC)₂ complex formed showed maximum absorption at 254nm. However an extraction step was required as the complex was freely soluble in chloroform and nearly insoluble in water. Drummer *et al.* (1984) improved the method by using

NiCl₂ as an internal standard in order to compensate for any errors and allow for the correction of the matrix effects. Andrews *et al.* (1984) then modified the method by using reverse phase HPLC instead of normal phase HPLC as used in the first two studies. Lopez-Flores *et al.* (2006) further developed the method from Andrews *et al.* (1984). The mobile phase consisted of acetonitrile, water and methanol in a ratio of 29:31:40 v/v, respectively, instead of water and methanol in a ratio of 20:80 v/v, respectively. The flow rate was increased slightly from 1.5 to 1.6ml/min.

However, from all these reported methods it should be stressed that chelation to DDTC is not exclusive to native cisplatin. Cisplatin species capable of losing their ligands such as transplatin and hydrated forms of cisplatin were found to chelate with DDTC and elute at the same time as native cisplatin (Drummer *et al.*, 1984). Bannister *et al.* (1979) indicated that native cisplatin and biodegradation products of cisplatin in the plasma chelated with DDTC to the same extent. Furthermore, DDTC is incapable of chelating with cisplatin in bound form such as to plasma proteins and sulphur containing compounds. Andrews *et al.* (1984) reported that the reactivity of cisplatin with DDTC was reduced when cisplatin forms complexes with glutathione and cysteine. All these studies concluded that the exact species of cisplatin detected by derivatisation with DDTC are unknown as well as their relative potency and cytotoxicity. However, they considered their methods selective to unbound cisplatin unlike the bound forms which are considered inactive from the onset (Bannister *et al.*, 1979; Andrews *et al.*, 1984, Goel *et al.*, 1990).

In the present study, an existing HPLC method (method I) used in the lab was adapted from Lopez-Flores *et al.* (2006). The method was reported to have been validated prior to the launch of the present project. It was successfully used in the characterisation of cisplatin NIVs (Chapter 3) and the determination of tissue levels *in vivo* (Chapter 7). However over the course of study, occasional peak splitting was observed in the resulting chromatograms (Figure 4.3). This problem arose from chloroform being a stronger solvent than the mobile phase and when injected onto the column in large volumes it can cause peak distortions (Dolan, 1986).

Two solutions to alleviate the peak splitting problem were attempted according to the troubleshooting guidance provided by Dolan (1992). The first was to reduce the

injection volume of the chloroform layer. The second was to evaporate the chloroform layer and reconstitute the sample in the mobile phase or with another solvent of weaker polarity. A series of studies were carried out adjusting the injection volume of chloroform or using different solvents for reconstituting the extracted and dried sample. By reducing the injection volume it was found that an injection volume of 10µl was optimal in preventing peak splitting. By evaporating the chloroform layer it was found that using 75% v/v acetonitrile in water was optimal for reconstituting the dried sample.

When the injection volume was reduced the peak heights and AUCs decreased correspondingly. This was feared to be disadvantageous in the detection of very low concentrations of platinum. Furthermore, the peaks produced by lowering the injection volume were less efficient and less sharp than the peaks produced by reconstituting the sample in 75% v/v acetonitrile in water (Table 4.1).

Therefore, method II was adapted in the analysis of platinum where the chloroform layer containing the extracted sample was evaporated to completion and reconstituted in 75% v/v acetonitrile in water. However, due to time constraints method validation was not performed immediately but calibration standards were analysed prior to every analysis. Over the course of the research discrepancies in the standard calibration concentrations were observed for method II. These discrepancies had a direct effect on the calculated concentrations in the unknown samples. Cisplatin NIVs from the first and second stability study (Chapter 5) were characterised by this method except for NIVs on day 469 post-preparation from the first study. As will be seen further in the related chapter, it was observed that inter-day results were inconsistent where sometimes unusually high entrapment results were observed or the entrapment efficiency would increase significantly over time.

Method validation showed that the concentration range was linear with R^2 values above 0.99 and the retention times of the peaks of interest were precise. Nonetheless, %RSD of the concentrations analysed was in the 20% range which was considered very high and unacceptable (Table 4.2). It was thereby concluded that further method development was required.

Despite the occasional peak splitting observed using method I, the results from the standard concentrations showed better consistency than method II. Therefore, it seemed that reducing the injection volume of the chloroform layer would be a better choice. Thereby the precision could be improved but it would be on the expense of lower efficiency (Table 4.1).

With both methods I and II, the starting back-pressure was approximately 270 bars which then increased to 310 bars with column usage. With the improvement of column packing from the supplier itself, a new column of the same specifications would already have a high back-pressure at 300 bars. However, it is not recommended to operate a silica based column above 4000psi, which is about 276 bars (McMaster, 2007b). Operating at high pressures can also result in mechanical wear of the HPLC system (Dolan, 2004).

As a result, injection volume of the chloroform layer was reduced to 10 μ l and a column oven was installed to develop method III. The column oven was operated at 30°C to reduce the viscosity of the mobile phase and thereby reduce column back-pressure. The column oven temperature was optimised in a way that does not affect the retention times of the peaks. The higher the temperature the less viscous the mobile phase and the earlier the peaks elute (McMaster, 2007c).

In general, validation of method III was improved in comparison to method II, especially in terms of precision (Tables 4.4 and 4.6). Therefore, this method can be considered to provide a fast and reliable method for the analysis of platinum.

It would be interesting if the final method was employed in the determination of platinum in biological samples. With research time constraints, it was not possible to retrospectively analyse biological samples from previous studies. The suitability of the method can be initially validated using serum samples to determine the range, linearity, precision and accuracy.

However, further modifications to the method can also be applied and validated. If the same column was employed then the column temperature can be further raised. As mentioned previously increasing the column temperature reduces mobile phase viscosity. This can result in lower column back-pressure and faster elution of the

analytes. Consequently, the flow rate can be reduced so that elution is kept the same which results in further back-pressure reduction. Increasing temperature and reducing flow rate can also result in sharper peaks with enhanced efficiency. Indeed, in the present study such an effect was briefly studied. When the column was heated to 40°C, it was found that as the flow rate was reduced the efficiency of the eluted peaks was enhanced and their elution times were increased (Table 4.3). If the same elution times of the analytes of interest as in method I were to be maintained at 40°C it was found that the flow rate had to be reduced to 1.2ml/min. The back-pressure recorded at these conditions was approximately 200 bars, which is considered acceptable. Therefore, the advantage of reducing column back-pressure and reducing mechanical wear of the HPLC pump can be achieved, as well as reducing the solvent flow rate which could have economic benefits in the long run. However time constraints had unfortunately limited further adjustments and subsequent evaluation of applied improvements.

The HPLC method adapted for the analysis of the lipid content of the vesicles was developed by unpublished method of Mullen. Method modification only involved alterations in the ternary gradient sequence. The method was modified to reduce the analysis time of the three analytes.

In this method, a NP-HPLC separation was used in the analysis of the lipid contents. The column used in the separation contained an YMC polyvinyl alcohol (PVA) bonded to silica. This bonded phase allows shortening of reconditioning time and maintains the same properties of silica but overcomes its disadvantage of irreversible adsorption of solutes. Also the bonded phase eliminates the presence of residual silanols which contribute to poor peak shapes as observed with diol phase columns (Deschamps *et al.*, 2001b; Rabinovich-Guilatt *et al.*, 2005).

The ELSD detector used is known to provide good quantification provided that it is carefully adjusted for optimum nebulizer function and evaporator temperature (Hammond, 1993). ELSD was optimised prior to any lipid analysis studies in the present study.

Furthermore, to minimise baseline noise and prevent the appearance of ghost peaks co-eluting with less polar lipids, chloroform that was stabilised with ethanol instead of amylene was used (Deschamps *et al.*, 2001b). However, in the present study tiny peaks were present in both blank (Figure 4.14) and lipid (Figure 4.15) samples although chloroform stabilised with ethanol was used. It is unlikely that these tiny peaks would be a result of lipid degradation as firstly the samples containing lipids were freshly prepared and secondly these peaks also appeared when a blank sample containing no lipids was analysed. This could mostly be related to natural contaminants in the lipids or during sample preparation despite the extreme care taken in handling the samples to avoid such contamination.

In the present study, modification of the original unpublished method reduced the elution times of the lipids and thereby reduced the run time from 22min (Figure 4.12) to 15min (Figure 4.13). This can be advantageous in reducing the time required in sample analysis and thereby increasing the number of samples that can be analysed. Also, reducing analysis time can be economic in reducing solvent consumption.

Using the present method, it was also possible to obtain a linear response with the concentration range measured (0.025-0.2mg/ml) (Figures 4.16 to 4.18). It has been reported that non-linear responses is a major drawback of ELSD (Deschamps *et al.*, 2002). In particular, Zhong *et al.*, (2010) measured cholesterol in a similar concentration range (0.02-0.20mg/ml) but obtained a non-linear response and subsequently used a logarithmic plot for quantification.

In general, from the validation results (Tables 4.10 to 4.12) the present method seems to provide a simple and reliable method in the determination of the lipid content. This method was employed in the analysis of the lipid content of NIVs from both stability studies (Chapter 5), as will be represented in the related chapter.

Further studies can be performed to demonstrate the suitability of this method in the analysis other lipids, such as phospholipids, as well as their degradation products.

4.4. Conclusion

From the present study, modification of the HPLC-UV method was shown to improve its reliability in the determination of platinum levels. This was achieved by reducing the injection volume of the chloroform layer and performing elution at 30°C. However with additional work, further modifications can be applied to further improve the method and optimise peak properties as well as obtain a valid and reliable method. The suitability of the method with biological samples will also need to be verified. Time constraints have limited further improvements to the developed method which can be used in the quantification of platinum in both formulations and biological samples.

The use of HPLC-ELSD proved to be sensitive, simple, rapid and reliable in the quantification of lipid contents of NIVs composed of cholesterol, surfactant VIII and DCP. Consequently, this method was used in the analysis of the lipid content of NIVs as part of the stability study. Further studies can be performed to demonstrate the potential of this method to be used in the analysis of different classes of lipids.

Chapter 5. Stability studies of NIVs produced in a pilot scale

5.1. Introduction

One of the prerequisites for the acceptance of a vesicular delivery system as a pharmaceutical product is the demonstration of long term stability (Glavas-Dodov *et al.*, 2005). This is crucial for the vesicular delivery system in sustaining a safe and effective product (Heurtault *et al.*, 2003). The reported time period a vesicle system should remain stable has differed from 12 months (Lasic, 1998) to between 18 and 24 months (Watwe and Bellare, 1995) and this appears to reflect the shelf life of the marketed vesicle systems presently available. However, there is consensus that stability is evaluated through the physical and chemical properties of vesicles over time (Ozer and Talsma, 1989). Physical properties associated with stable vesicles include uniform size distribution, sufficient surface charge and minimal leakage whereas chemical stability involves minimal degradation of lipid ingredients (Lasic, 1998; Uchegbu and Vyas, 1998).

The physical stability of a vesicular delivery system is affected by its chemical stability. Lipid degradation can result in alterations of the vesicular delivery system and consequently affecting entrapment efficiency and the release mechanisms of the system. Bilayer changes due to lipid degradation will also affect vesicle size and size distribution (Mohammed *et al.*, 2006). Changes in entrapment efficiency as a result of drug leakage or precipitation, will accordingly affect the amount of drug actually delivered and will make it difficult to determine the optimal dose intended for administration (Heurtault *et al.*, 2003). The drug itself may directly react with membrane components and affect stability (Ozer and Talsma, 1989). Changes in size distribution could be a result of aggregation or fusion, which can affect the intended properties of the vesicles. For instance, vesicle fusion can result in an irreversible formation of new colloidal structures (Crommelin and Schreier, 1994).

It is generally anticipated to maintain long term stability of lipid vesicles by optimising the formulation process. For instance, conferring a charge to the formulation can maintain sufficient repulsion between the vesicles and avoid aggregation or fusion (Jadon *et al.*, 2009). Addition of cholesterol can reduce

membrane permeability (Junyaprasert *et al.*, 2008). The choice of non-ionic surfactants over phospholipids is also considered to provide better chemical stability and a reason why niosomes are suggested as a better alternative to liposomes whose phospholipids are subject to oxidation and hydrolysis (Cortesi *et al.*, 2007).

However, the storage conditions are also an additional factor that should be taken into account regarding vesicle stability (Mohammed *et al.*, 2006). Many studies have recommended the storage of lipid vesicles at 4°C. In one study, liposomes of different compositions and lamellarities showed physical signs of instability when stored at 25°C in comparison to 4°C over 6 months (du Plessis *et al.*, 1996). The study also indicated that LUVs offered greater stability than MLVs in terms of size stability, which was explained as a result of multimembrane fusion into one larger vesicle. Di Marzio *et al.* (2011) performed stability studies on Tween 21 niosomes at 4°C, 25°C and 40°C over 90 days and indicated that only samples stored at 4°C were stable. Niosomes prepared with Span 20, 40 and 60 in different molar ratios with cholesterol and DCP also demonstrated greater stability at 4°C in comparison to 25°C when stored for 30 days (Jadon *et al.*, 2009).

Studies concerning stability of liposomal cisplatin have also been reported. Multi-vesicular vesicles (MVLs) loaded with cisplatin were reported to be more stable in terms of entrapment efficiency at 6°C in comparison to 25°C after a 3 month storage period (Xiao *et al.*, 2004). They also reported a significant 2-fold decrease in entrapment efficiency within 15 days when these MVLs were stored at 40°C. In contrast, another study demonstrated that stealth pH-sensitive cisplatin liposomes (spHL-CDDP) stored at 4°C after 153 days showed a significant decrease in entrapment efficiency by 2-fold with no change in vesicle size (Santos Giuberti *et al.*, 2011).

However, none of these mentioned studies were concerned with evaluating the chemical stability. Although many methods have been developed to determine lipid stability (Sas *et al.*, 1999; Rabinovich-Guillatt *et al.* 2005; Hvattum *et al.*, 2006; Zhong *et al.*, 2010), few researchers have reported performing these studies (Barbeau *et al.*, 2011).

In the present study, the aim was to monitor the physical and chemical stability of empty and cisplatin NIVs over a one year period. Three storage conditions were selected for the stability study at 4°C, 25°C/60% RH and 40°C/75% RH. The physical studies involved evaluation of entrapment efficiency, size distribution and surface charge. Chemical studies involved analysis of the lipid contents of the vesicles for any signs of degradation.

5.2. Results

5.2.1. Comparison between empty NIVs and cisplatin NIVs – Stability study I

Two large scale batches of empty and cisplatin NIVs were prepared, processed, aliquoted into vials and stored as described (Section 2.2.7.1). Lyophilised NIVs were prepared from the empty NIVs as described (Section 2.2.2). At specific time points (days 1, 28, 189, 266 and 469 post-preparation) the vials were taken from storage and analysed for cisplatin content (cisplatin NIVs only), lipid content, size and ZP. The freeze-dried samples taken from the empty NIVs batch were used as a reference for the samples.

5.2.1.1. Physical appearance of cisplatin NIVs

By the time the NIVs were sampled into vials, labelled and placed in the required storage conditions, 3 days had past. During this time all the NIVs were refrigerated at 4°C, which led to obvious precipitation of cisplatin. On day 469 post-preparation (Figure 5.1), other than signs of cisplatin precipitation, it was noticed that cisplatin NIVs stored at 40°C/75% RH had turned a light brownish colour. However no signs of flocculation or sedimentation were observed in any of the NIVs that could indicate gross colloidal instability.

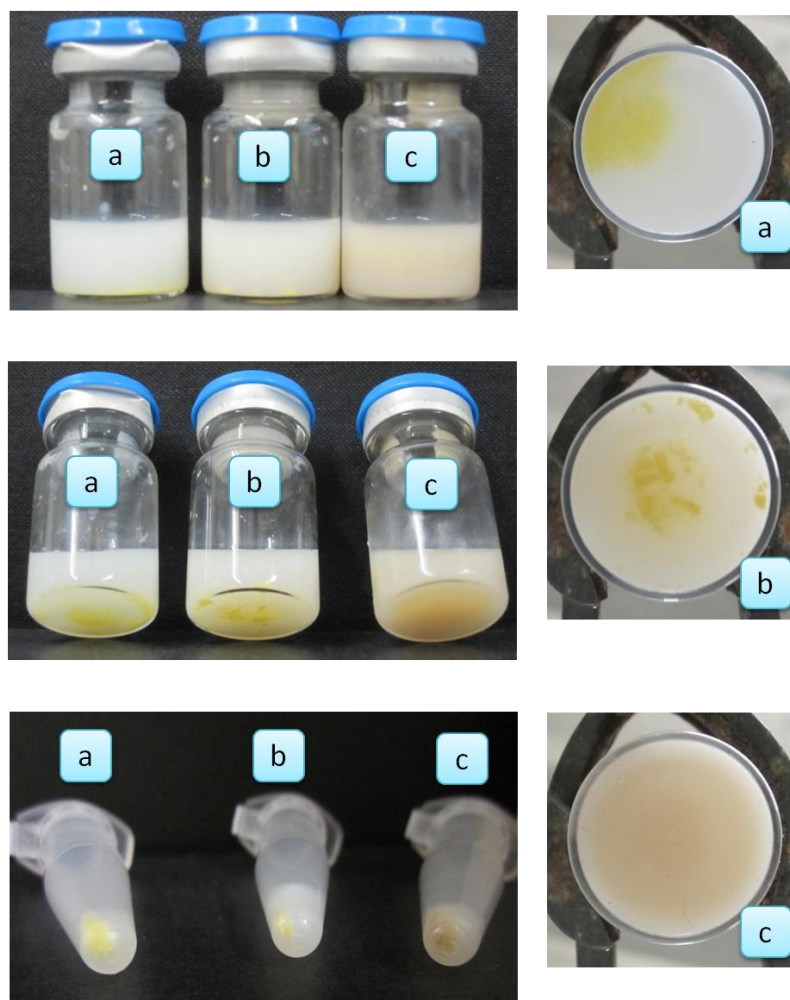


Figure 5.1. The physical appearance of processed cisplatin NIVs 469 days post-preparation when stored at 4°C (a), 25°C/60% RH (b) and 40°C/75% RH (c) showing clear precipitation of cisplatin. Bottom picture on the left shows precipitated cisplatin pellet after the NIVs had been centrifuged at 13000rpm for 5min.

5.2.1.2. Cisplatin content in NIVs (entrapment efficiency, supernatant and total)

Cisplatin content (entrapped, unentrapped and total) from days 1 to 266 post-preparation was determined by HPLC method II (Section 2.2.5.3) and then for day 469 by HPLC method III (Section 2.2.5.4). The results for day 1 post-preparation for all conditions are the same, since the NIVs had not been divided yet. Prior to analysis NIVs were separated from precipitated cisplatin as described (Section 2.2.7.1) and prepared for analysis as described (Section 2.2.4.1).

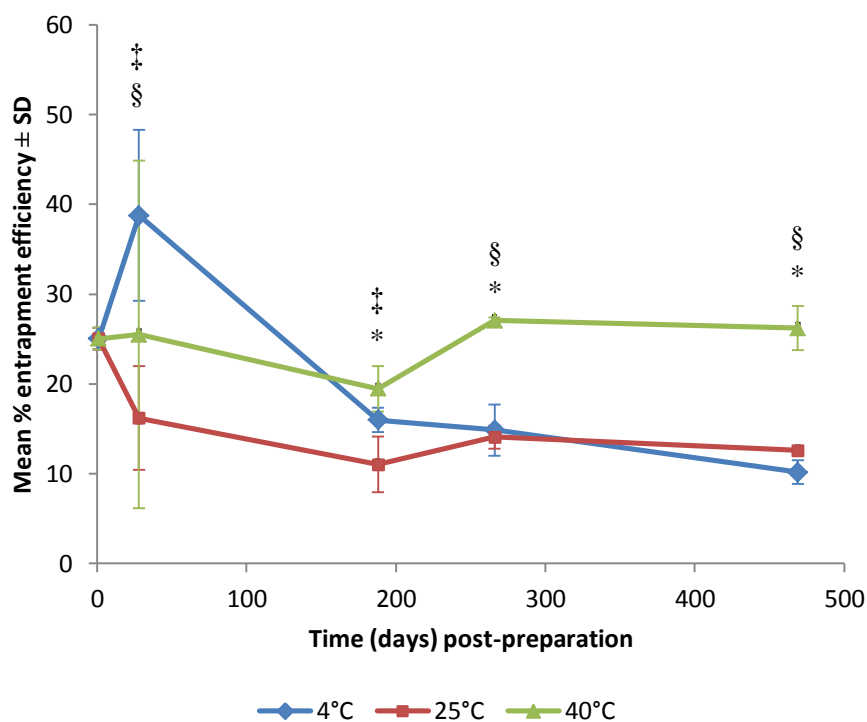


Figure 5.2. The entrapment efficiency of processed cisplatin NIVs stored at 4°C, 25°C/60% RH and 40°C/75% RH determined over time at 1, 28, 189, 266 and 469 days post-preparation (n=3). ‡ indicates significant difference between 4°C and 25°C/60% RH. § indicates significant difference between 4°C and 40°C/75% RH. * indicates significant difference between 25°C/60% RH and 40°C/75% RH ($p \leq 0.05$).

The entrapment efficiency of cisplatin processed NIVs stored at 4°C, 25°C/60% RH and 40°C/75% RH over time were compared (Figure 5.2). Cisplatin NIVs stored at 4°C showed stable entrapment on days 1, 189 and 266 post-preparation where then the entrapment fell significantly on day 469 post-preparation ($p=0.000$). Cisplatin NIVs stored at 25°C/60% RH showed a significant fall in the entrapment efficiency from day 1 to 28 post-preparation ($p=0.002$), which remained stable afterwards. Cisplatin NIVs stored at 40°C/75% RH were stable throughout the time period with day 189 post-preparation the only outlier ($p=0.005$). Comparison of entrapment efficiency between the different storage conditions at each time point (Figure 5.2) showed significant differences from the other storage conditions on days 28 post-

preparation for NIVs at 4°C (p=0.016), 189 post-preparation for NIVs at 25°C/60% RH (p=0.015) and 266 and 469 post-preparation for NIVs at 40°C/75% (p=0.000).

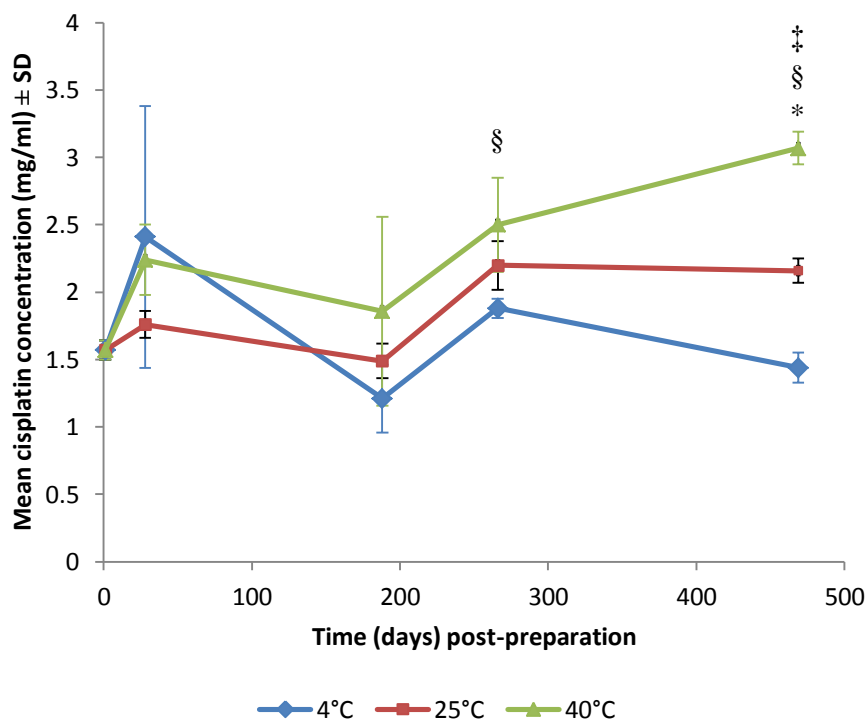


Figure 5.3. The concentration of total cisplatin (entrapped and unentrapped) in processed NIVs stored at 4°C, 25°C/60% RH and 40°C/75% RH determined over time at 1, 28, 189, 266 and 469 days post-preparation (n=3). ‡ indicates significant difference between 4°C and 25°C/60% RH. § indicates significant difference between 4°C and 40°C/75% RH. * indicates significant difference between 25°C/60% RH and 40°C/75% RH (p≤0.05).

Assay of total cisplatin concentration (entrapped and unentrapped) in NIVs (Figure 5.3), showed no change over time at 4°C. However, at 25°C/60% RH a significant increase in total concentration was observed on day 266 post-preparation and onwards (p=0.000). At 40°C/75% RH, total cisplatin concentration remained stable over time until it increased significantly on day 469 post-preparation (p=0.005). Total cisplatin concentration was similar between the storage conditions from day 1 to 189 post-preparation where then 4°C and 40°C/75% RH differed significantly

($p=0.046$) on day 266 and then all differed significantly ($p=0.000$) on day 469 post-preparation (Figure 5.3).

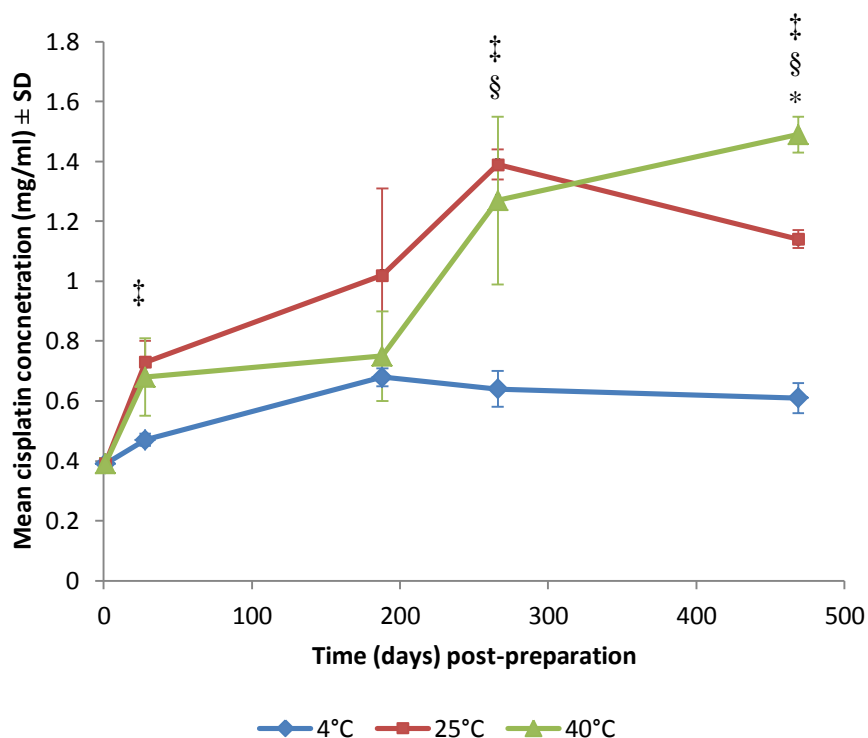


Figure 5.4. The concentration of untrapped cisplatin present in the supernatant of processed NIVs stored at 4°C, 25°C/60% RH and 40°C/75% RH determined over time at 1, 28, 189, 266 and 469 days post-preparation ($n=3$). ‡ indicates significant difference between 4°C and 25°C/60% RH. § indicates significant difference between 4°C and 40°C/75% RH. * indicates significant difference between 25°C/60% RH and 40°C/75% RH ($p\leq 0.05$).

Analysis of supernatant (Figure 5.4) showed an increase in cisplatin concentration over time. At 4°C and 25°C/60% RH, cisplatin content increased significantly ($p=0.000$) from day 1 to day 189 post-preparation and then remained stable onwards. At 40°C/75% RH, cisplatin content increased significantly ($p=0.000$) on day 28 post-preparation and then again on day 266 post-preparation. Cisplatin content in supernatant (Figure 5.4) at 4°C differed significantly ($p=0.019$) from 25°C/60% RH

on day 28 post-preparation and on day 266 post-preparation differed ($p=0.003$) from both conditions. On day 469 post-preparation the cisplatin content was different ($p=0.000$) between all storage conditions.

5.2.1.3. Lipid content – cholesterol, surfactant VIII and dicetyl phosphate (DCP)

Lipid content was determined by the HPLC method described (Section 2.2.6). The actual lipid weights to prepare the empty and cisplatin NIVs are indicated (Table 2.2) and the actual concentration of each lipid ingredient (mg/ml) in the formulation is also indicated (Table 2.3). Empty NIVs stored at 25°C/60% RH and 40°C/75% RH were not found to perform analysis for days 266 and 469 post-preparation. Lipid content for day 1 post-preparation was the same at all storage conditions for each ingredient individually.

5.2.1.3.1. Cholesterol content

In processed empty NIVs (Table 5.1), cholesterol content showed significant difference only on day 189 post-preparation ($p\leq 0.050$) in comparison to other days for all storage conditions. No significant differences between the different storage conditions were observed at each time point.

Table 5.1. The concentration of cholesterol in processed empty NIVs stored at 4°C, 25°C/60% RH and 40°C/75% RH determined over time at 1, 28, 189, 266 and 469 days post-preparation with samples stored at 25°C/60% RH and 40°C/75% RH not available on days 266 and 469 post-preparation ($n=3$). * indicates $n=2$ due to sample spoilage.

Storage condition (°C/%RH)	Mean concentration (mg/ml) \pm SD over time (days) post-preparation				
	1	28	189	266	469
4	23.9 \pm 2.9	25.1 \pm 0.9	17.1 \pm 2.4	*20.3 \pm 0.0	22.3 \pm 2.3
25/60		24.7 \pm 0.5	16.1 \pm 0.6	ND	ND
40/75		24.1 \pm 0.8	*16.9 \pm 0.0	ND	ND

As discussed (Section 2.2.7.1), high viscosity in the empty NIVs formulations led to non-uniform filling of vials. As a consequence the lipid composition ratio at each time point was determined and compared to the actual lipid composition ratio used in the preparation of processed empty NIVs and processed cisplatin NIVs to facilitate comparison.

The cholesterol/DCP ratio over time (Table 5.2) for empty processed NIVs stored at 4°C did not differ from the actual starting ratio used to formulate the samples. Significant differences between cholesterol/DCP ratios to the starting actual ratio were found over time at 25°C/60% RH and 40°C/75% RH ($p \leq 0.050$). Over time, cholesterol/DCP ratio showed stability for empty processed NIVs stored at 4°C and 25°C/60% RH, whereas the ratio on day 28 post-preparation was the outlier ($p = 0.028$) for NIVs stored at 40°C/75% RH. The cholesterol/DCP ratios between the different storage conditions at each time point did not differ from each other.

Table 5.2. The ratio between cholesterol and DCP weights in processed empty NIVs stored at 4°C, 25°C/60% RH and 40°C/75% RH determined over time at 1, 28, 189, 266 and 469 days post-preparation with samples stored at 25°C/60% RH and 40°C/75% RH not available on days 266 and 469 post-preparation (n=3). * indicates n=2 due to sample spoilage.

Storage condition (°C/%RH)	Actual ratio	Mean ratio (cholesterol/DCP) ± SD over time (days) post-preparation				
		1	28	189	266	469
4	2.1	2.4 ± 0.1	2.3 ± 0.1	2.3 ± 0.4	*1.9 ± 0.0	2.2 ± 0.2
25/60			2.3 ± 0.0	2.4 ± 0.1	ND	ND
40/75			2.3 ± 0.1	*2.5 ± 0.0	ND	ND

In processed cisplatin NIVs (Table 5.3), cholesterol content showed significant changes over time ($p \leq 0.050$) with days 1 and 189 post-preparation and days 28 and 469 post-preparation similar. Cholesterol content at each time point did not differ significantly between the different storage conditions.

Table 5.3. The concentration of cholesterol in processed cisplatin NIVs stored at 4°C, 25°C/60% RH and 40°C/75% RH determined over time at 1, 28, 189, 266 and 469 days post-preparation (n=3).

Storage condition (°C/%RH)	Mean concentration (mg/ml) ± SD over time (days) post-preparation				
	1	28	189	266	469
4	16.5 ± 1.7	20.1 ± 0.3	15.5 ± 0.4	18.0 ± 0.4	19.9 ± 0.3
25/60		19.9 ± 0.6	15.2 ± 1.4	17.8 ± 1.2	20.5 ± 0.7
40/75		20.7 ± 0.9	15.1 ± 0.7	18.1 ± 0.2	20.0 ± 0.9

The cholesterol/DCP ratios over time were compared to the actual cholesterol/DCP ratios of weights used in the preparation of processed cisplatin NIVs (Table 5.4). The actual cholesterol/DCP ratio differed significantly ($p \leq 0.050$) from the cholesterol/DCP ratios determined over time for processed cisplatin NIVs at all storage conditions. The cholesterol/DCP ratio over time showed ratio stability for NIVs stored at 4°C and 25°C/60% RH and significant changes ($p=0.000$) over time for processed cisplatin NIVs stored at 40°C/75% RH. The cholesterol/DCP ratio between the different storage conditions were similar at each time point up to day 189 post-preparation where NIVs stored at 40°C/75% RH differed significantly from the other storage conditions on days 266 and 469 post-preparation ($p=0.015$ and 0.002, respectively).

Table 5.4. The ratio between cholesterol and DCP weights in processed cisplatin NIVs stored at 4°C, 25°C/60% RH and 40°C/75% RH determined over time at 1, 28, 189, 266 and 469 days post-preparation (n=3). § indicates significant difference between 4°C and 40°C/75% RH. * indicates significant difference between 25°C/60% RH and 40°C/70% RH ($p \leq 0.05$).

Storage condition (°C/%RH)	Actual ratio	Mean ratio (cholesterol/DCP) ± SD over time (days) post-preparation				
		1	28	189	266	469
4	2.1	2.5 ± 0.2	2.6 ± 0.1	2.6 ± 0.1	2.5 ± 0.1	2.7 ± 0.0
25/60			2.6 ± 0.0	2.5 ± 0.2	2.7 ± 0.3	2.8 ± 0.1
40/75			2.6 ± 0.0	2.4 ± 0.2	3.2 ± 0.2	3.3 ± 0.2
				§*	§*	

A comparison between empty processed, cisplatin processed and lyophilised NIVs in terms of ratios between cholesterol and DCP at different storage conditions was studied (Figures 5.5 to 5.7).

At 4°C (Figure 5.5), cholesterol/DCP ratios for empty processed NIVs differed significantly ($p=0.003$) from the other formulations on day 28 post-preparation. Cholesterol/DCP ratio for processed cisplatin NIVs differed significantly ($p=0.009$) from the other formulations on day 469 post-preparation.

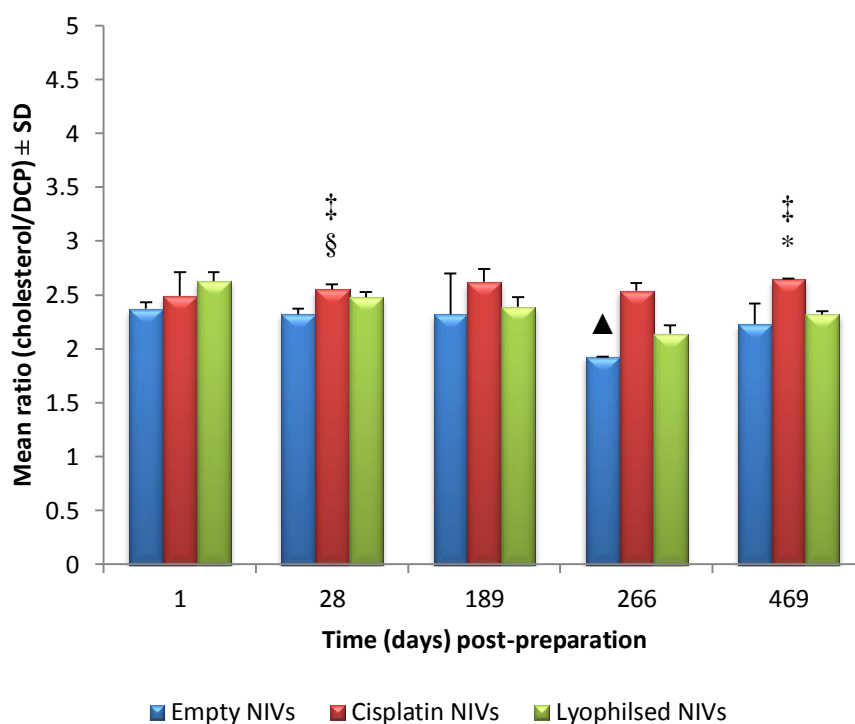


Figure 5.5. The ratio between cholesterol and DCP weights in processed empty NIVs and processed cisplatin NIVs stored at 4°C in comparison to lyophilised processed NIVs prepared from empty NIVs over time at 1, 28, 189, 266 and 469 days post-preparation ($n=3$). ▲ indicates $n=2$ due to sample spoilage. ‡ indicates significant difference between empty and cisplatin NIVs. § indicates significant difference between empty and lyophilised NIVs. * indicates significant difference between cisplatin and lyophilised NIVs ($p\leq 0.05$).

At 25°C/60% RH (Figure 5.6.), cholesterol/DCP ratio of empty processed NIVs differed significantly ($p=0.001$) from the other formulations on day 28 post-preparation. Cholesterol/DCP ratio of cisplatin processed NIVs differed significantly ($p=0.029$) from lyophilised NIVs on day 469 post-preparation.

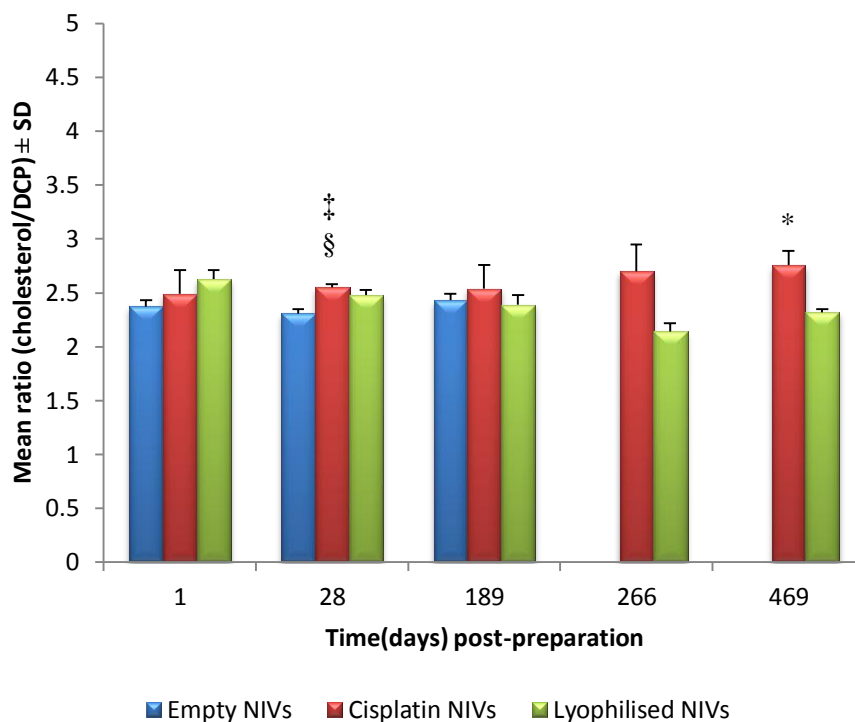


Figure 5.6. The ratio between cholesterol and DCP weights in processed empty NIVs and processed cisplatin NIVs stored at 25°C/60% RH in comparison to lyophilised processed NIVs prepared from empty NIVs over time at 1, 28, 189, 266 and 469 days post-preparation with empty NIVs not available on days 266 and 469 post-preparation ($n=3$). ‡ indicates significant difference between empty and cisplatin NIVs. § indicates significant difference between empty and lyophilised NIVs. * indicates significant difference between cisplatin and lyophilised NIVs ($p\leq 0.05$).

At 40°C/75% RH (Figure 5.7), cholesterol/DCP ratio of processed empty NIVs differed significantly ($p=0.001$) from the other formulations on day 28 post-preparation. The cholesterol/DCP ratio of processed cisplatin NIVs differed significantly from lyophilised NIVs on days 266 ($p=0.017$) and 469 ($p=0.012$) post-preparation.

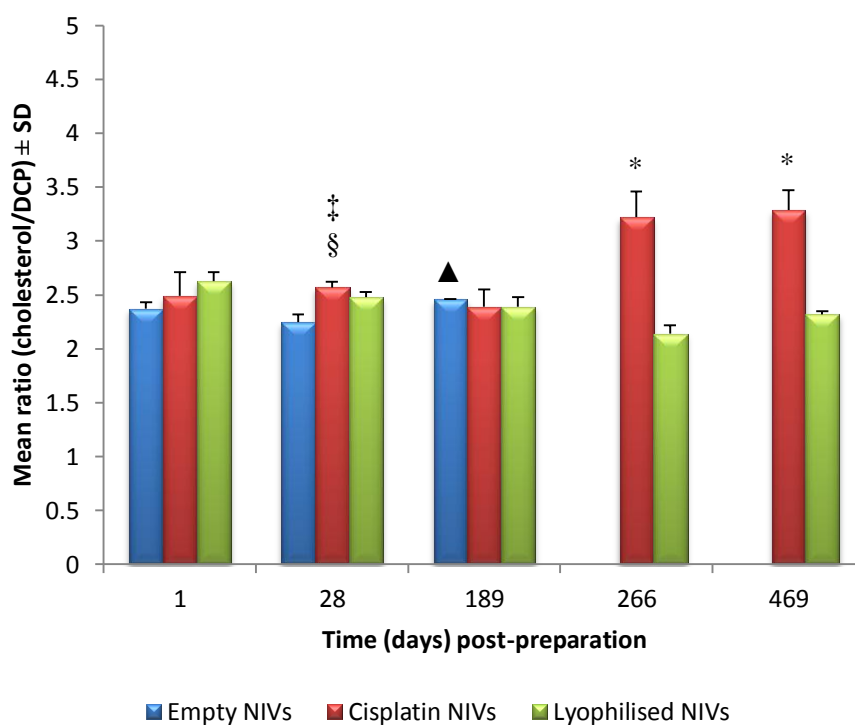


Figure 5.7. The ratio between cholesterol and DCP weights in processed empty NIVs and processed cisplatin NIVs stored at 40°C/75% RH in comparison to lyophilised processed NIVs prepared from empty NIVs over time at 1, 28, 189, 266 and 469 days post-preparation with empty NIVs not available on days 266 and 469 post-preparation ($n=3$). ▲ indicates $n=2$ due to sample spoilage. ‡ indicates significant difference between empty and cisplatin NIVs. § indicates significant difference between empty and lyophilised NIVs. * indicates significant difference between cisplatin and lyophilised NIVs ($p\leq 0.05$).

5.2.1.3.2. Surfactant VIII content

In processed empty NIVs (Table 5.5), surfactant VIII content showed no significant difference between the different storage conditions at each time point. At 4°C, surfactant VIII content showed stability over time with only days 28 and 189 post-preparation significantly different (p=0.044). At 25°C/60% RH, surfactant VIII content decreased significantly from day 1 to 189 post-preparation (p=0.034). At 40°C/75% RH, no significant changes were shown.

Table 5.5. The concentration of surfactant VIII in processed empty NIVs stored at 4°C, 25°C/60% RH and 40°C/75% RH determined over time at 1, 28, 189, 266 and 469 days post-preparation with samples stored at 25°C/60% RH and 40°C/75% RH not available on days 266 and 469 post-preparation (n=3). * indicates n=2 due to sample spoilage.

Storage condition (°C/%RH)	Mean concentration (mg/ml) ± SD over time (days) post-preparation				
	1	28	189	266	469
4	24.5 ± 3.8	24.0 ± 0.6	18.4 ± 1.5	*22.5 ± 0.0	24.0 ± 2.1
25/60		23.6 ± 0.4	18.6 ± 0.2	ND	ND
40/75		23.8 ± 0.3	*18.8 ± 0.0	ND	ND

The surfactant VIII/DCP ratios over time in comparison to the actual surfactant VIII/DCP ratios of weights used in the preparation of processed empty NIVs (Table 5.6) showed no significant difference at 4°C. At 25°C/60% RH and 40°C/75% RH, the surfactant VIII/DCP ratios were similar to the actual ratio over time with only day 189 post-preparation significantly different (p=0.000 and p=0.001, respectively). The surfactant VIII/DCP ratio over time showed stability for NIVs stored at 4°C. At 25°C/60% RH and 40°C/75% RH, day 189 post-preparation was significantly different from the other days (p=0.001 and 0.006, respectively). No significant difference between the different storage conditions at each time point was observed.

Table 5.6. The ratio between surfactant VIII and DCP weights in processed empty NIVs stored at 4°C, 25°C/60% RH and 40°C/75% RH determined over time at 1, 28, 189, 266 and 469 days post-preparation with samples stored at 25°C/60% RH and 40°C/75% RH not available on days 266 and 469 post-preparation (n=3). * indicates n=2 due to sample spoilage.

Storage condition (°C/%RH)	Actual ratio	Mean ratio (surfactant VIII/DCP) ± SD over time (days) post-preparation				
		1	28	189	266	469
4	2.3	2.4 ± 0.1	2.2 ± 0.0	2.5 ± 0.4	*2.1 ± 0.0	2.4 ± 0.2
25/60			2.2 ± 0.1	2.8 ± 0.1	ND	ND
40/75			2.2 ± 0.1	*2.8 ± 0.0	ND	ND

In processed cisplatin NIVs (Table 5.7), surfactant VIII content did not show significant difference between the different storage conditions at each time point. A similar trend in surfactant VIII content for all three conditions over time was observed where days 1 and 469 differed significantly ($p \leq 0.050$).

Table 5.7. The concentration of surfactant VIII in processed cisplatin NIVs stored at 4°C, 25°C/60% RH and 40°C/75% RH determined over time at 1, 28, 189, 266 and 469 days post-preparation (n=3).

Storage condition (°C/%RH)	Mean concentration (mg/ml) ± SD over time (days) post-preparation				
	1	28	189	266	469
4	17.8 ± 2.7	18.7 ± 0.5	17.4 ± 0.6	20.1 ± 0.2	22.2 ± 0.4
25/60		18.7 ± 0.5	17.3 ± 0.9	20.1 ± 1.4	22.0 ± 0.5
40/75		19.6 ± 0.9	16.1 ± 0.6	20.2 ± 0.8	21.6 ± 0.7

The surfactant VIII/DCP ratios over time increased in comparison to the actual surfactant VIII/DCP weight ratio used in the formulation for processed cisplatin NIVs (Table 5.8). At 4°C and 25°C/60% RH, surfactant VIII/DCP ratios on day 28 were similar to the starting formulation weight ratio. At 40°C/75% RH, surfactant VIII/DCP ratios from days 1 to 189 post-preparation were similar to starting formulation weight ratio. Surfactant VIII/DCP ratio over time showed significant changes on days 1 and 28 post-preparation (p=0.000) for NIVs stored at 4°C. At 25°C/60% RH, ratio stability was shown throughout with only day 28 post-preparation significantly different (p=0.003). At 40°C/75% RH, ratio stability was shown up to day 189 post-preparation where a significant change (p=0.000) was shown afterwards. Similarity between processed cisplatin NIVs stored at 4°C and 25°C/60% RH was shown at each time point whereas NIVs stored at 40°C/75% differed significantly (p≤0.050) from the other storage conditions at each time point except on day 28 post-preparation.

Table 5.8. The ratio between surfactant VIII and DCP weights in processed cisplatin NIVs stored at 4°C, 25°C/60% RH and 40°C/75% RH determined over time at 1, 28, 189, 266 and 469 days post-preparation (n=3). § indicates significant difference between 4°C and 40°C/75% RH. * indicates significant difference between 25°C/60% RH and 40°C/75% RH (p≤0.05).

Storage condition (°C/%RH)	Actual ratio	Mean ratio (surfactant VIII/DCP) ± SD over time (days) post-preparation				
		1	28	189	266	469
4	2.3	2.7 ± 0.12	2.4 ± 0.1	2.9 ± 0.1	2.8 ± 0.1	3.0 ± 0.1
25/60			2.4 ± 0.1	2.9 ± 0.1	3.0 ± 0.3	3.0 ± 0.1
40/75			2.4 ± 0.1	2.6 ± 0.1	3.6 ± 0.3	3.5 ± 0.2
				§*	§*	§*

A comparison between empty processed, cisplatin processed and lyophilised NIVs in terms of ratios between surfactant VIII and DCP at different storage conditions was studied (Figures 5.8 to 5.10).

At 4°C (Figure 5.8), similar surfactant VIII/DCP ratios between the formulations were observed over time with only the ratio of cisplatin processed NIVs significantly different ($p=0.002$) from the other formulations on day 469 post-preparation.

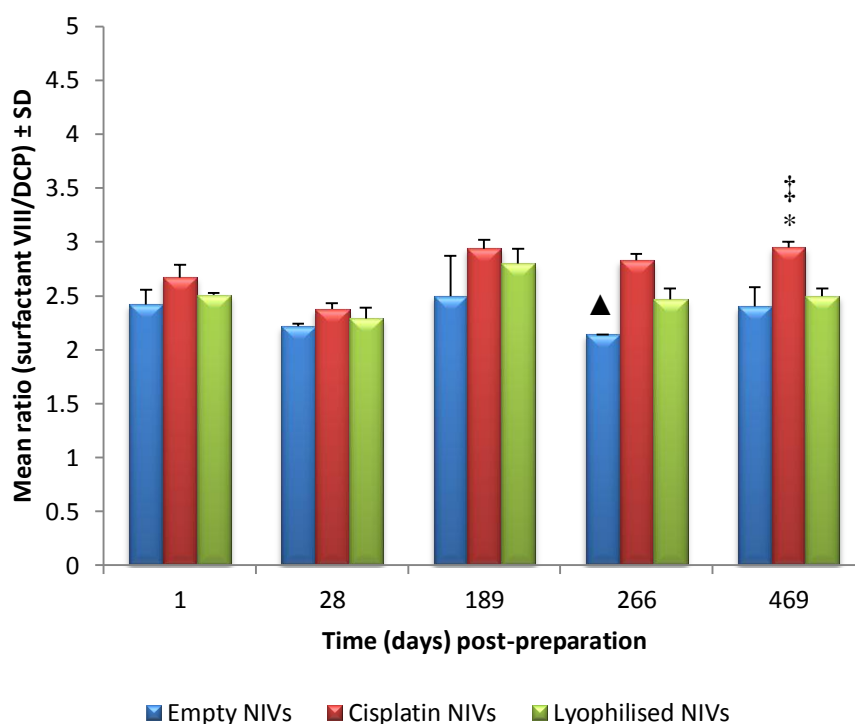


Figure 5.8. The ratio between surfactant VIII and DCP weights in processed empty NIVs and processed cisplatin NIVs stored at 4°C in comparison to lyophilised processed NIVs prepared from empty NIVs over time at 1, 28, 189, 266 and 469 days post-preparation ($n=3$). ▲ indicates $n=2$ due to sample spoilage. ‡ indicates significant difference between empty and cisplatin NIVs. * indicates significant difference between cisplatin and lyophilised NIVs ($p \leq 0.05$).

At 25°C/60% RH (Figure 5.9), similar surfactant VIII/DCP ratios between the formulations was observed over time with only the ratio of cisplatin processed NIVs significantly different ($p=0.007$) from that of lyophilised NIVs on day 469 post-preparation.

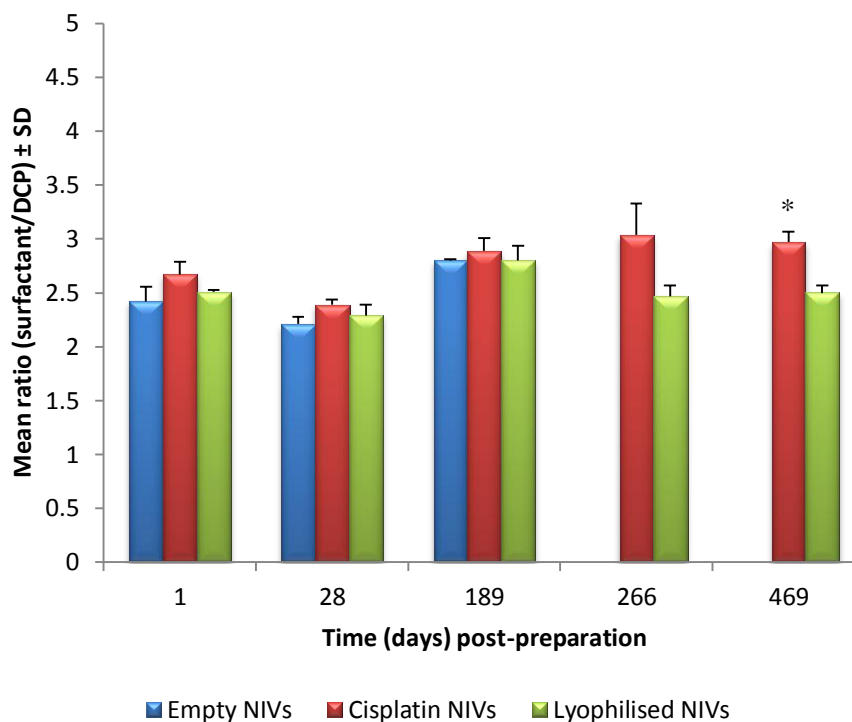


Figure 5.9. The ratio between surfactant VIII and DCP weights in processed empty NIVs and processed cisplatin NIVs stored at 25°C/60% RH in comparison to lyophilised processed NIVs prepared from empty NIVs over time at 1, 28, 189, 266 and 469 days post-preparation with samples stored at 25°C/60% RH and 40°C/75% RH not available on days 266 and 469 post-preparation (n=3). * indicates significant difference between cisplatin and lyophilised NIVs ($p\leq 0.05$).

At 40°C/75% RH (Figure 5.10), surfactant VIII/DCP ratios was similar between empty and lyophilised NIVs over time, whereas significant difference between empty NIVs and cisplatin NIVs was observed on day 28 post-preparation (p=0.042). The surfactant VIII/DCP ratio of cisplatin NIVs differed significantly from that of lyophilised NIVs on days 266 and 469 post-preparation (p=0.030 and 0.009, respectively).

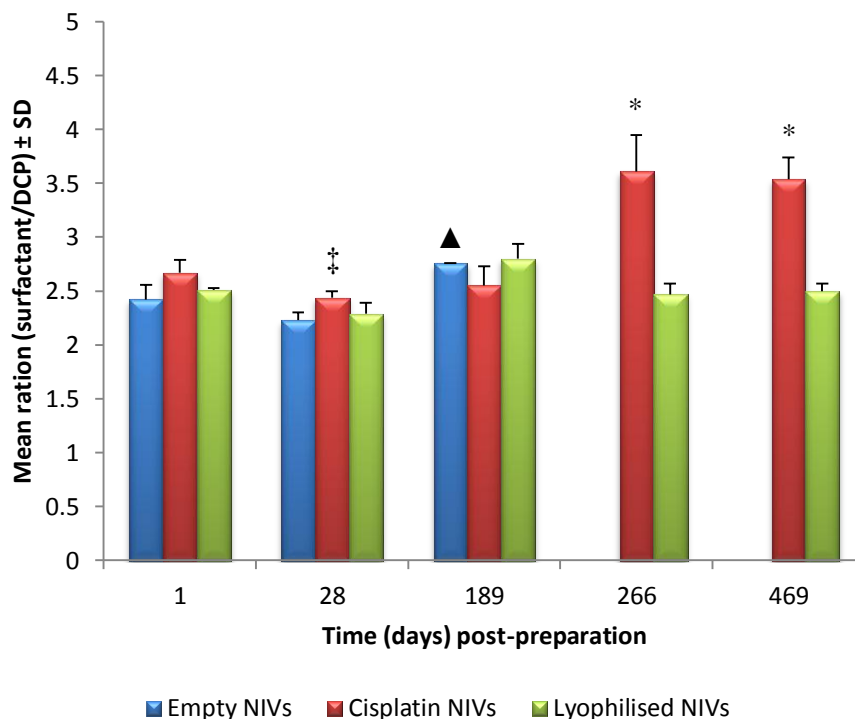


Figure 5.10. The ratio between surfactant VIII and DCP weights in processed empty NIVs and processed cisplatin NIVs stored at 40°C/75% RH in comparison to lyophilised processed NIVs prepared from empty NIVs over time at 1, 28, 189, 266 and 469 days post-preparation with empty NIVs not available on days 266 and 469 post-preparation (n=3). ▲ indicates n=2 due to sample spoilage. ‡ indicates significant difference between empty and cisplatin NIVs. * indicates significant difference between cisplatin and lyophilised NIVs (p≤0.05).

5.2.1.3.3. DCP content

In processed empty NIVs (Table 5.9), DCP content at 4°C showed stability over time with only the content on day 189 post-preparation significantly different (p=0.023). At 25°C/60% RH and 40°C/75% RH, DCP content also fell significantly on day 189 post-preparation (p=0.000 and 0.003, respectively). The DCP content of the NIVs stored at different conditions at each time point did not differ significantly from each other (Table 5.9).

Table 5.9. The concentration of dicetyl phosphate in processed empty NIVs stored at 4°C, 25°C/60% RH and 40°C/75% RH determined over time at 1, 28, 189, 266 and 469 days post-preparation with samples stored at 25°C/60% RH and 40°C/75% RH not available on days 266 and 469 post-preparation (n=3). * indicates n=2 due to sample spoilage.

Storage condition (°C/%RH)	Mean concentration (mg/ml) ± SD over time (days) post-preparation				
	1	28	189	266	469
4	10.1 ± 1.0	10.8 ± 0.2	7.4 ± 1.2	*10.7 ± 0.0	10.0 ± 0.2
25/60		10.7 ± 0.4	6.6 ± 0.1	ND	ND
40/75		10.7 ± 0.0	*6.8 ± 0.0	ND	ND

To investigate the trend in DCP content with respect to time, DCP concentrations at specific time points were used as a denominator with the starting actual concentration of DCP in the formulation used as the numerator. This was calculated to allow ease of comparison across different formulation types. It was anticipated that the ratio could give a more sensitive indication of DCP stability. At all storage conditions (Table 5.10), stability appeared maintained for processed empty NIVs with the exception for day 189 post-preparation which differed significantly ($p \leq 0.050$). The results for day 189 appear to be inconsistent with the general trend but no obvious reason could account for the measurements. The DCP weight ratio at each time point did not differ between the different storage conditions.

Table 5.10. The dicetyl phosphate weight ratios in processed empty NIVs stored at 4°C, 25°C/60% RH and 40°C/75% RH determined over time at 1, 28, 189, 266 and 469 days post-preparation with samples stored at 25°C/60% RH and 40°C/75% RH not available on days 266 and 469 post-preparation (n=3). * indicates n=2 due to sample spoilage.

Storage condition (°C/%RH)	Actual ratio	Mean ratio (actual DCP/measured DCP) ± SD over time (days) post-preparation				
		1	28	189	266	469
4	1.0	1.2 ± 0.10	1.1 ± 0.0	1.6 ± 0.2	*1.1 ± 0.0	1.2 ± 0.0
25/60			1.1 ± 0.0	1.8 ± 0.0	ND	ND
40/75			1.1 ± 0.0	*1.7 ± 0.0	ND	ND

In processed cisplatin NIVs (Table 5.11), DCP content at different storage conditions were similar from day 1 to 189 post-preparation. For the later time points (days 266 and 469 post-preparation) DCP content at 40°C/75% RH differed significantly from the other storage conditions ($p \leq 0.050$). Over time, DCP content showed stability with only days 28 and 189 post-preparation significantly different from each other ($p=0.040$) at 25°C/60% RH. At 4°C, samples from day 189 post-preparation were significantly different ($p=0.028$). At 40°C/75% RH, samples from day 28 post-preparation were significantly different ($p=0.013$).

Table 5.11. The concentration of dicetyl phosphate in processed cisplatin NIVs stored at 4°C, 25°C/60% RH and 40°C/75% RH determined over time at 1, 28, 189, 266 and 469 days post-preparation (n=3). § indicates significant difference between 4°C and 40°C/75% RH. * indicates significant difference between 25°C/60% RH and 40°C/75% RH ($p \leq 0.05$).

Storage condition (°C/%RH)	Mean concentration (mg/ml) ± SD over time (days) post-preparation				
	1	28	189	266	469
4	6.7 ± 1.4	7.9 ± 0.1	5.9 ± 0.4	7.1 ± 0.1	7.5 ± 0.1
25/60		7.8 ± 0.2	6.0 ± 0.2	6.6 ± 0.3	7.4 ± 0.3
40/75		8.0 ± 0.5	6.3 ± 0.2	5.6 ± 0.1	6.1 ± 0.3
				§*	§*

The weight ratio for DCP in processed cisplatin NIVs varied with respect to time (Table 5.12). Significant differences between ratios at all storage conditions and time points were observed compared to the starting ratio ($p \leq 0.050$). This would suggest that the loss of DCP within the formulation appears to occur immediately. However on subsequent storage, DCP loss stabilised with significant differences only observed for day 189 samples stored at 4°C and 25°C/60% RH ($p=0.027$ and 0.031 , respectively). A significant difference was observed at samples stored at 40°C/75% RH on day 28 ($p=0.012$). At each time point the DCP weight ratios were similar for all storage conditions up to day 189 post-preparation. On days 266 and 469 post-preparation the DCP weight ratios at 40°C/75% RH were significantly different from the other storage conditions ($p=0.002$ and 0.001 , respectively).

Table 5.12. The dicetyl phosphate weight ratios in processed cisplatin NIVs stored at 4°C, 25°C/60% RH and 40°C/75% RH determined over time at 1, 28, 189, 266 and 469 days post-preparation (n=3). § indicates significant difference between 4° and 40°C/75% RH. * indicates significant difference between 25°C/60% RH and 40°C/75% RH ($p \leq 0.05$).

Storage condition (°C/%RH)	Actual ratio	Mean ratio (actual DCP/measured DCP) ± SD over time (days) post-preparation				
		1	28	189	266	469
4	1.0	1.8 ± 0.3	1.5 ± 0.0	2.0 ± 0.1	1.7 ± 0.0	1.6 ± 0.0
25/60			1.5 ± 0.1	2.0 ± 0.1	1.8 ± 0.1	1.6 ± 0.1
40/75			1.5 ± 0.1	1.9 ± 0.1	2.1 ± 0.1	1.9 ± 0.1
				§*	§*	

A comparison between empty processed, cisplatin processed and lyophilised NIVs in terms of DCP weight ratios at different storage conditions was studied (Figures 5.11 to 5.13).

At 4°C (Figure 5.11), similar DCP weight ratios were observed for processed empty NIVs and lyophilised NIVs. Processed cisplatin NIVs was significantly different from the other formulations at each time point ($p \leq 0.050$) except on day 189 post-preparation where the ratio was similar for processed cisplatin NIVs and lyophilised NIVs.

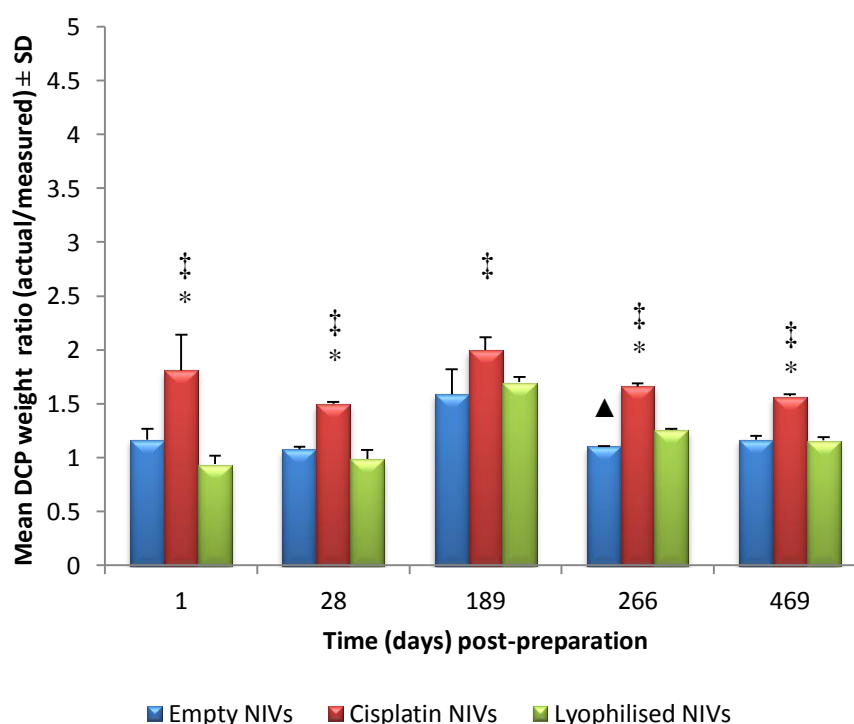


Figure 5.11. The dicetyl phosphate weight ratios in processed empty NIVs and processed cisplatin NIVs stored at 4°C in comparison to lyophilised processed NIVs prepared from empty NIVs over time at 1, 28, 189, 266 and 469 days post-preparation (n=3). ▲ indicates n=2 due to sample spoilage. ‡ indicates significant difference between empty and cisplatin NIVs. * indicates significant difference between cisplatin and lyophilised NIVs ($p \leq 0.05$).

At 25°C/60% RH (Fig. 5.12), the DCP weight ratio was similar for processed empty NIVs and lyophilised NIVs at each time point. The ratio for cisplatin NIVs differed significantly from the other formulations at each time point ($p \leq 0.050$).

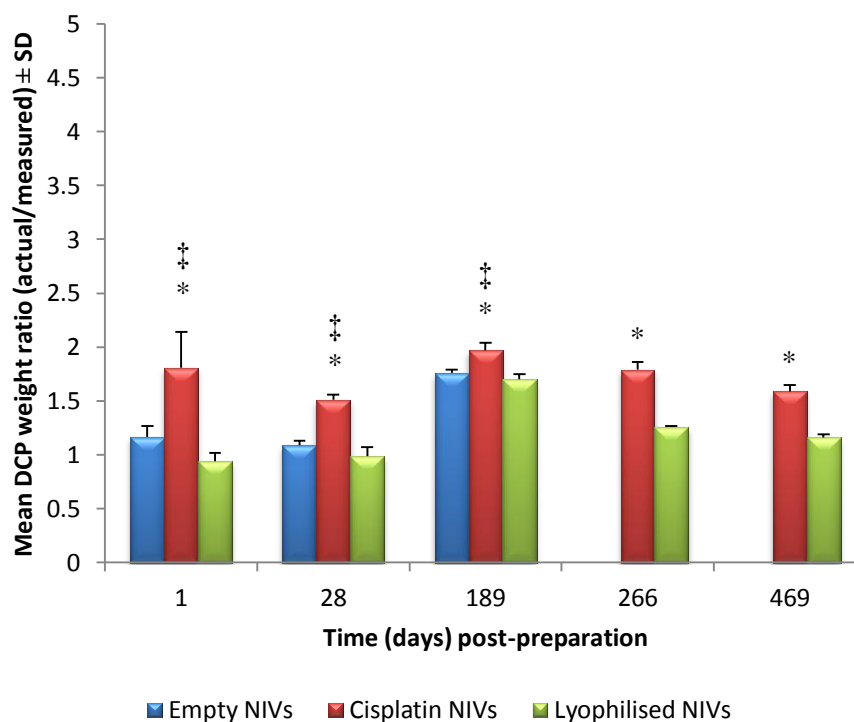


Figure 5.12. The dicetyl phosphate weight ratios in processed empty NIVs and processed cisplatin NIVs stored at 25°C/60% RH in comparison to lyophilised processed NIVs prepared from empty NIVs over time at 1, 28, 189, 266 and 469 days post-preparation with empty NIVs not available on days 266 and 469 post-preparation (n=3). ‡ indicates significant difference between empty and cisplatin NIVs. * indicates significant difference between cisplatin and lyophilised NIVs ($p \leq 0.05$).

At 40°C/75% RH (Fig 5.13), the DCP weight ratio was similar for processed empty NIVs and lyophilised NIVs at each time point. The DCP weight ratio for processed cisplatin NIVs was significantly different from the other formulations at each time point ($p \leq 0.050$).

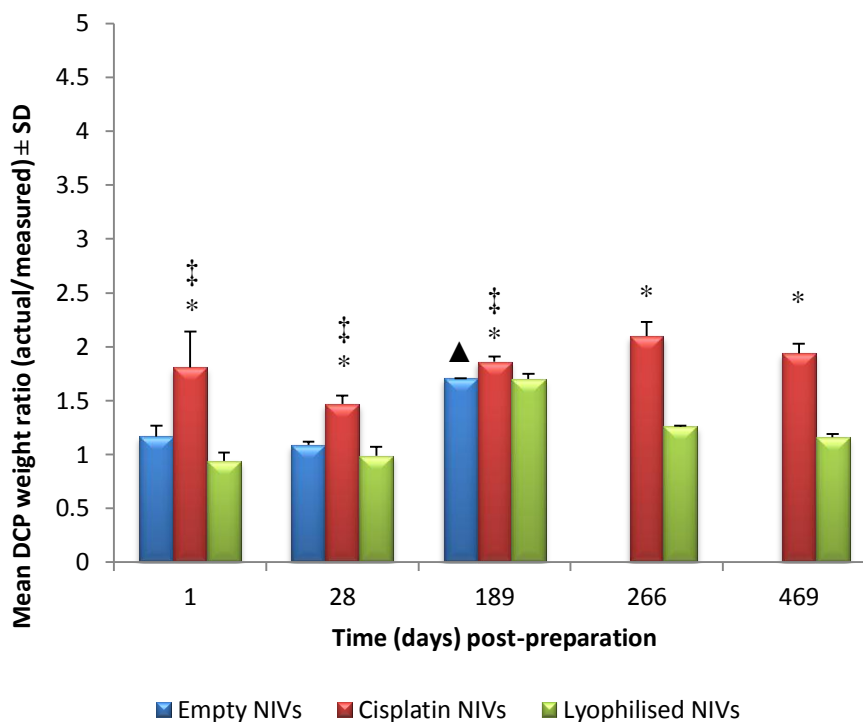


Figure 5.13. The dicetyl phosphate weight ratios in processed empty NIVs and processed cisplatin NIVs stored at 40°C/75% RH in comparison to lyophilised processed NIVs prepared from empty NIVs over time at 1, 28, 189, 266 and 469 days post-preparation with empty NIVs not available on days 266 and 469 post-preparation ($n=3$). ▲ indicates $n=2$, due to sample spoilage. ‡ indicates significant difference between empty and cisplatin NIVs. * indicates significant difference between cisplatin and lyophilised NIVs ($p \leq 0.05$).

5.2.1.4. Size and zeta potential (ZP) of empty and cisplatin NIVs

The measurement of size and ZP were performed as described (Section 2.2.4.2). Empty NIVs stored at 25°C/60% RH and 40°C/75% were not available for size and ZP measurements on days 266 and 469 post-preparation. Results for day 1 post-preparation were the same for empty NIVs at all storage conditions, as samples had not been divided yet. The same applied to cisplatin NIVs.

5.2.1.4.1. Size results

In processed empty NIVs (Figure 5.14), vesicle size at all storage conditions ranged between 270 and 370nm. At 4°C and 40°C/75% RH, vesicle size did not differ significantly. At 25°C/75% RH, vesicle size differed between days 28 and 189 only ($p=0.017$). A comparison of vesicle size between the different storage conditions showed no significant difference at each time point except on day 189 post-preparation where vesicle size at 25°C/60% RH was significantly higher ($p=0.025$) than the other conditions.

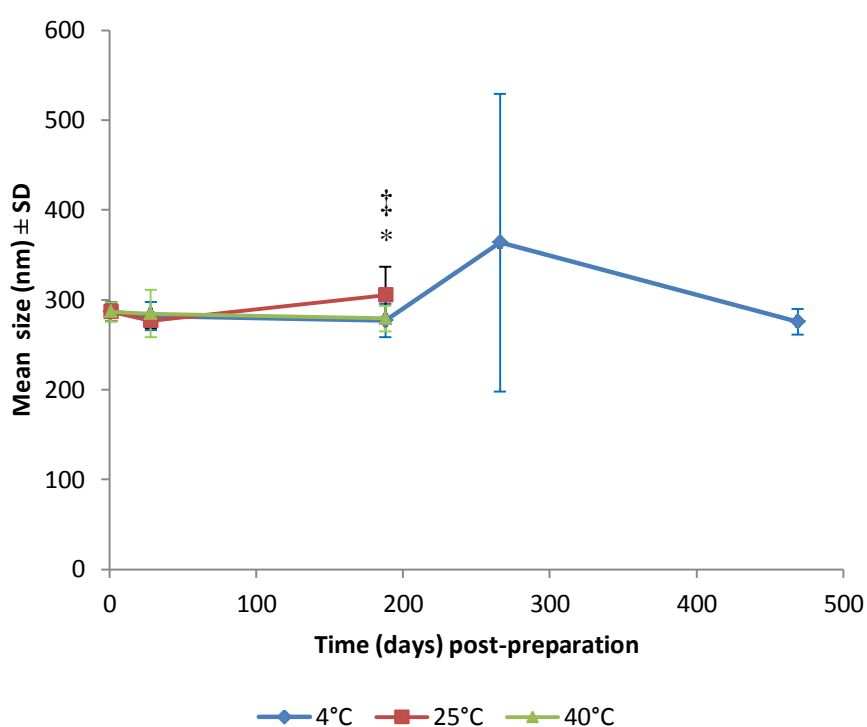


Figure 5.14. The size of empty processed NIVs stored at 4°C, 25°C/60% RH and 40°C/75% RH determined over time at 1, 28, 189, 266 and 469 days post-preparation with samples stored at 25°C/60% RH and 40°C/75% RH not available on days 266 and 469 post-preparation ($n=3$ except for day 1 post-preparation where $n=1$). ‡ indicates significant difference between 4°C and 25°C/60% RH. * indicates significant difference between 25°C/60% RH and 40°C/75% RH ($p\leq 0.05$).

In processed cisplatin NIVs (Figure 5.15), vesicle size at all storage conditions ranged between 660 and 1140nm. At 4°C, an overall stability in size was shown with only days 189 and 266 post-preparation being significantly different from each other (p=0.040). At 25°C/60% RH, vesicle size remained stable up to day 469 post-preparation where it then increased significantly (p=0.000). At 40°C/75% RH, vesicle size remained stable up to day 469 post-preparation where it then increased significantly (p=0.000). Vesicle size between the different storage conditions was only similar on day 266 post-preparation, where on days 28 and 189 post-preparation 40°C/75% RH was the outlier (p=0.001 and 0.000, respectively) and on day 469 post-preparation 4°C was the outlier (p=0.000).

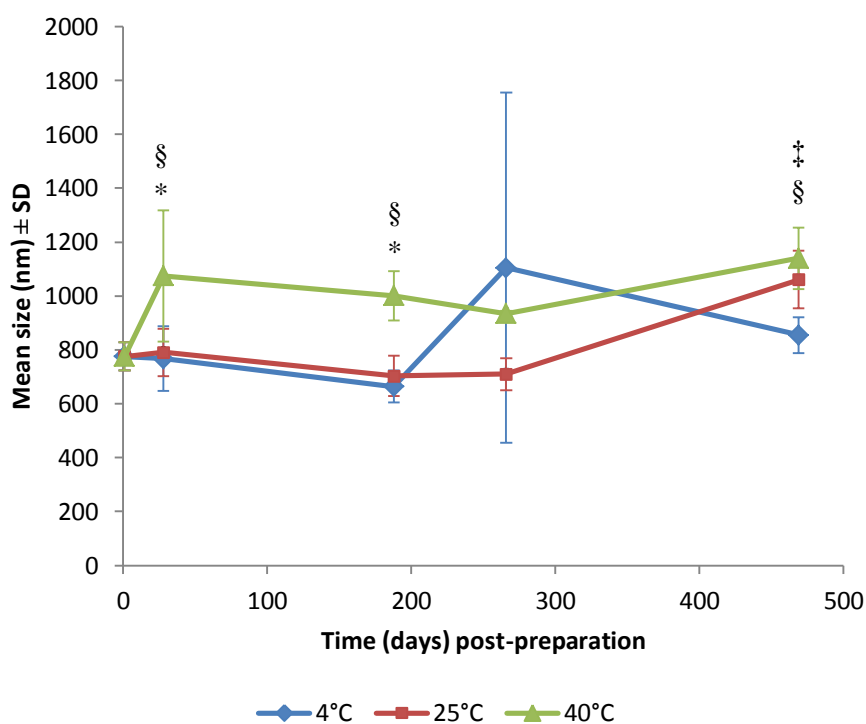


Figure 5.15. The size of processed cisplatin NIVs stored at 4°C, 25°C/60% RH and 40°C/75% RH determined over time at 1, 28, 189, 266 and 469 days post-preparation (n=3 except for day 1 post-preparation where n=1). ‡ indicates significant difference between 4°C and 25°C/60% RH. § indicates significant difference between 4°C and 40°C/75% RH. * indicates significant difference between 25°C/60% RH and 40°C/75% RH (p≤0.05).

A comparison of vesicle size between processed empty NIVs, processed cisplatin NIVs and lyophilised NIVs was studied (Figures 5.16 to 5.18). The vesicle size of lyophilised NIVs ranged between 1280 and 1440 nm.

At 4°C (Figure 5.16), the vesicle size of empty NIVs was always significantly smaller than lyophilised NIVs as well as cisplatin NIVs ($p \leq 0.050$). Cisplatin NIVs were also significantly smaller in size than lyophilised NIVs, with the exception of day 266 post-preparation where the size of cisplatin and lyophilised NIVs were not significantly different.

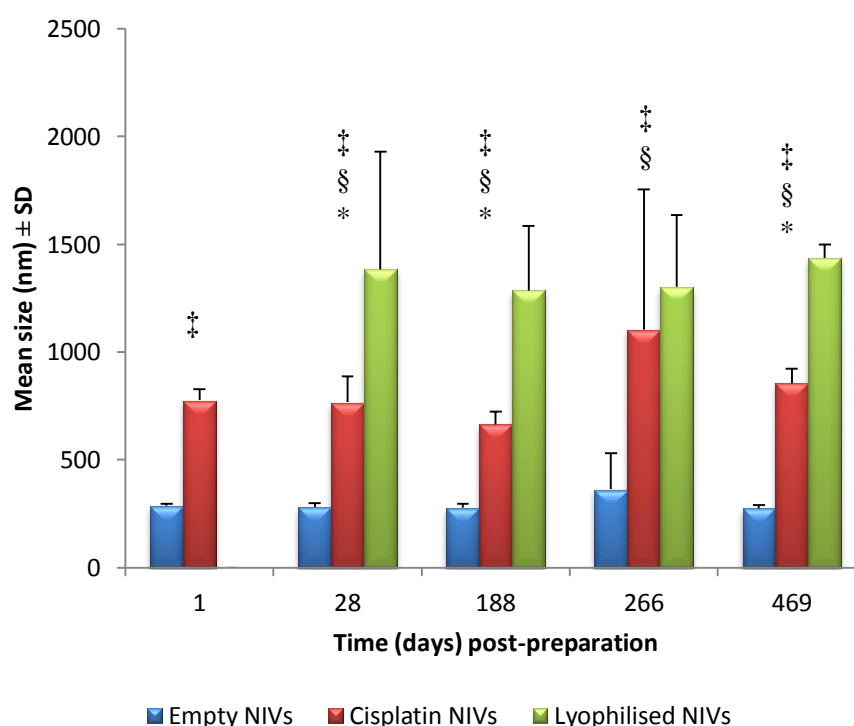


Figure 5.16. The size of processed empty NIVs and processed cisplatin NIVs stored at 4°C in comparison to lyophilised NIVs prepared from empty NIVs over time at 1, 28, 161, 235 and 534 days post-preparation ($n=3$ except for day 1 post-preparation where $n=1$). ‡ indicates significant difference between empty and cisplatin NIVs. § indicates significant difference between empty and lyophilised NIVs. * indicates significant difference between cisplatin and lyophilised NIVs ($p \leq 0.05$).

At 25°C/60% RH (Figure 5.17), empty NIVs showed significantly smaller size than cisplatin NIVs stored in the same conditions and lyophilised NIVs on the available time points. Cisplatin NIVs were also significantly smaller than the lyophilised NIVs at the all measured time points ($p \leq 0.050$).

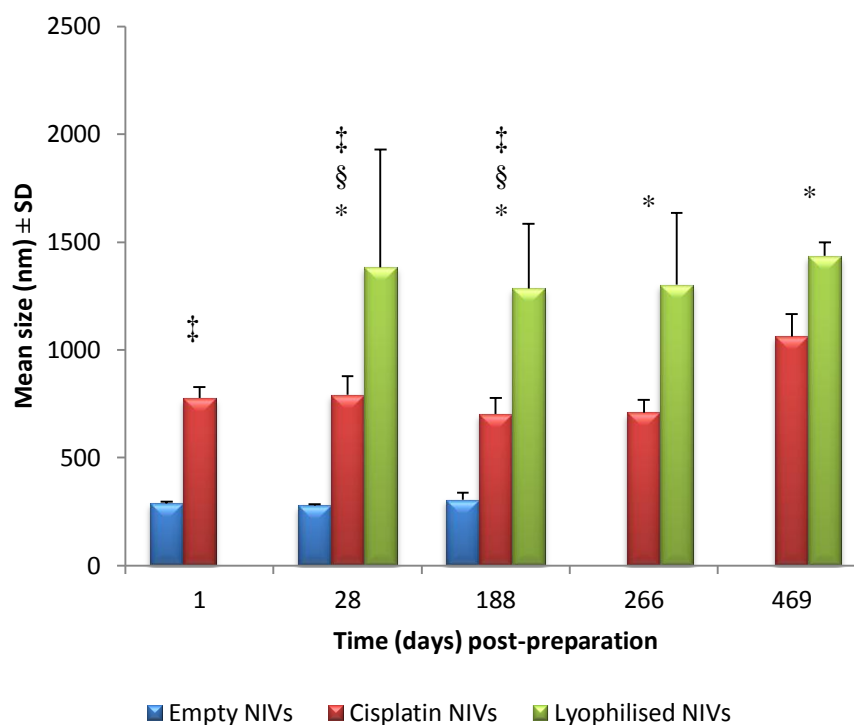


Figure 5.17. The size of processed empty NIVs and processed cisplatin NIVs stored at 25°C/60% RH in comparison to lyophilised NIVs prepared from empty NIVs over time at 1, 28, 189, 266 and 469 days post-preparation with empty NIVs not available on days 266 and 469 post-preparation ($n=3$ except for day 1 post-preparation where $n=1$). ‡ indicates significant difference between empty and cisplatin NIVs. § indicates significant difference between empty and lyophilised NIVs. * indicates significant difference between cisplatin and lyophilised NIVs ($p \leq 0.05$).

At 40°C/75% RH (Figure 5.18), empty NIVs maintained a significantly smaller size than cisplatin NIVs stored at the same conditions and lyophilised NIVs up to the time point they were available. The size of cisplatin NIVs were also significantly smaller than lyophilised NIVs ($p \leq 0.050$) except day 28 post-preparation.

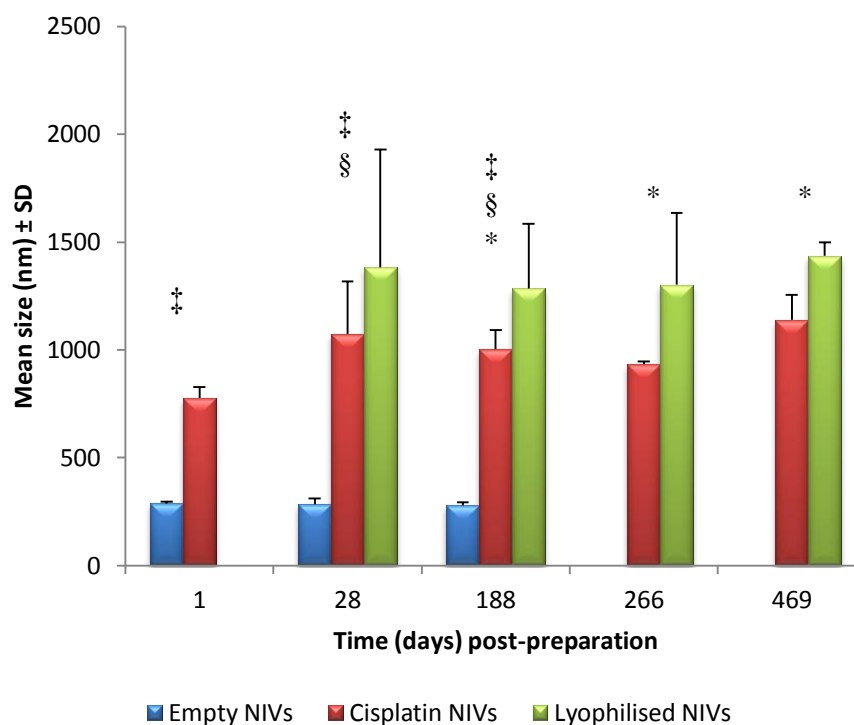


Figure 5.18. The size of processed empty NIVs and processed cisplatin NIVs stored at 40°C/75% RH in comparison to lyophilised NIVs prepared from empty NIVs over time at 1, 28, 189, 266 and 469 days post-preparation with empty NIVs not available on days 266 and 469 post-preparation ($n=3$ except for day 1 post-preparation where $n=1$). ‡ indicates significant difference between empty and cisplatin NIVs. § indicates significant difference between empty and lyophilised NIVs. * indicates significant difference between cisplatin and lyophilised NIVs ($p \leq 0.05$).

5.2.1.4.2. ZP results

In processed empty NIVs (Figure 5.19), ZP at all storage conditions ranged between -63 and -76mV. At 4°C, ZP showed significant changes over time ($p=0.000$) with only days 28, 266 and 469 post-preparation similar (Figure 5.25). At 25°C/60% RH and 40°C/75% RH, stable ZP was maintained at all available time points. A comparison between ZP at different storage conditions showed no significant differences at each time point.

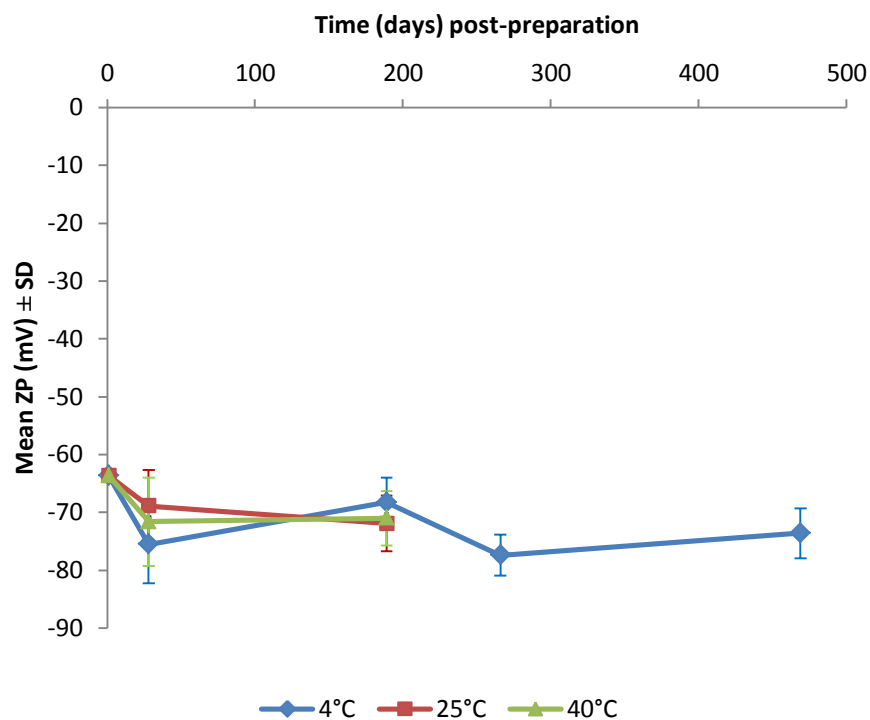


Figure 5.19. The ZP of processed empty NIVs stored at 4°C, 25°C/60% RH and 40°C/75% RH determined over time at 1, 28, 189, 266 and 469 days post-preparation with samples stored at 25°C/60% RH and 40°C/75% RH not available on days 266 and 469 post-preparation ($n=3$ except for day 1 post-preparation where $n=1$).

In processed cisplatin NIVs (Figure 5.20), ZP at all storage condition ranged between -73 and -90mV. At 4°C, ZP demonstrated an overall stability over time with only day 189 post-preparation significantly different (p=0.043). At 25°C/60% RH, similar ZP results were shown only between days 1, 28 and 469 post-preparation. At 40°C/75% RH, ZP decreased significantly (p=0.000) between days 1 and 469 post-preparation, particularly on day 189 post-preparation. The ZP was similar between the different storage conditions up to day 189 post-preparation where afterwards ZP at 40°C/75% RH differed significantly on day 266 post-preparation (p=0.006) from 4°C and was an outlier (p=0.000) on day 469 post-preparation.

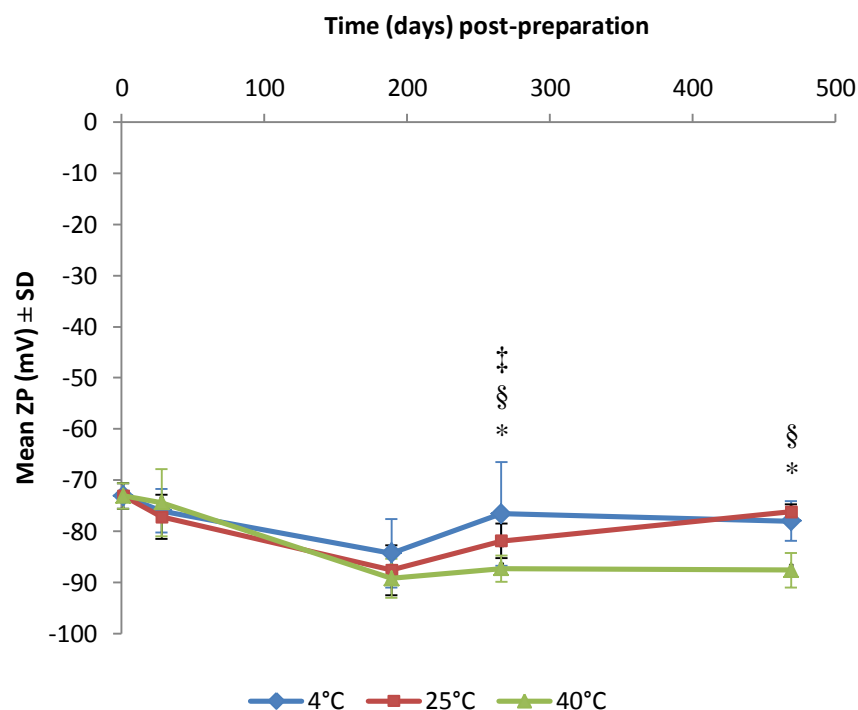


Figure 5.20. The ZP of processed cisplatin NIVs stored at 4°C, 25°C/60% RH and 40°C/75% RH determined over time at 1, 28, 189, 266 and 469 days post-preparation (n=3 except for day 1 post-preparation where n=1). ‡ indicates significant difference between 4°C and 25°C/60% RH. § indicates significant difference between 4°C and 40°C/75% RH. * indicates significant difference between 25°C/60% RH and 40°C/75% RH (p≤0.050).

A comparison between the surface charge of processed empty NIVs, processed cisplatin NIVs and lyophilised NIVs were studied (Figures 5.21 to 5.23). The ZP of lyophilised NIVs ranged between -55 and -70mV.

At 4°C (Figure 5.21), lyophilised NIVs demonstrated significantly higher ZP ($p \leq 0.050$) than both empty and cisplatin NIVs. Cisplatin and empty NIVs showed similar ZP values on days 28, 266 and 469 post-preparation.

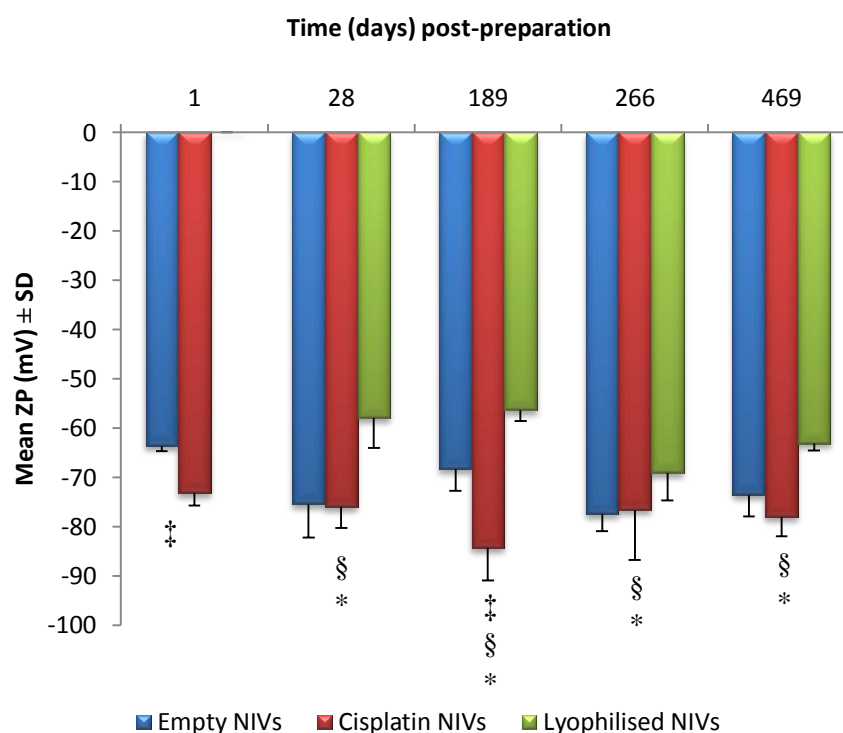


Figure 5.21. The ZP of processed empty NIVs and processed cisplatin NIVs stored at 4°C in comparison to lyophilised NIVs prepared from empty NIVs over time at 1, 28, 189, 266 and 469 days post-preparation (n=3 except for day 1 post-preparation where n=1). ‡ indicates significant difference between empty and cisplatin NIVs. § indicates significant difference between empty and lyophilised NIVs. * indicates significant difference between cisplatin and lyophilised NIVs ($p \leq 0.05$).

At 25°C/60% RH (Figure 5.22), the ZP between all three formulations was significantly different at each time point ($p \leq 0.050$).

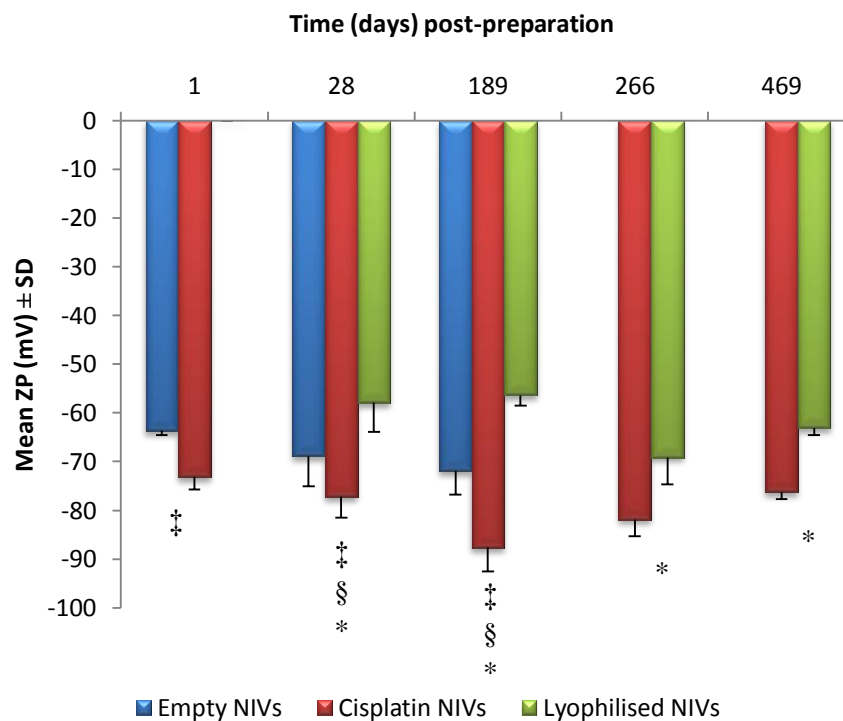


Figure 5.22. The ZP of processed empty NIVs and processed cisplatin NIVs stored at 25°C/60% RH in comparison to lyophilised NIVs prepared from empty NIVs over time at 1, 28, 189, 266 and 469 days post-preparation with empty NIVs not available on days 266 and 469 post-preparation ($n=3$ except for day 1 post preparation where $n=1$). ‡ indicates significant difference between empty and cisplatin NIVs. § indicates significant difference between empty and lyophilised NIVs. * indicates significant difference between cisplatin and lyophilised NIVs ($p \leq 0.05$).

At 40°C/75% RH (Figure 5.23), significant differences in ZP between lyophilised NIVs in comparison to empty and cisplatin NIVs were observed over the course of time. Cisplatin and empty NIVs also differed significantly in ZP ($p \leq 0.050$) with the exception of day 28 post-preparation.

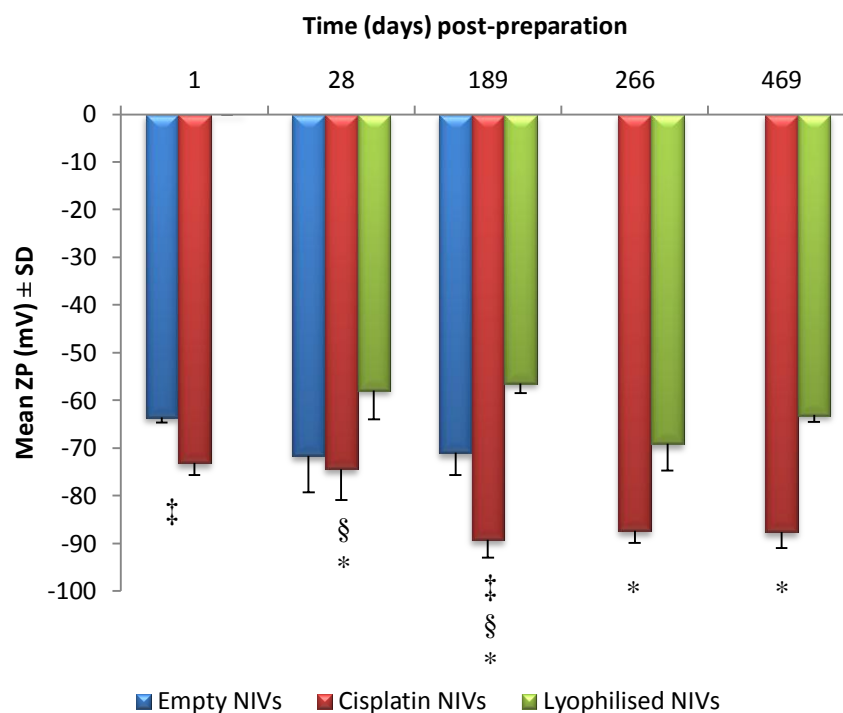


Figure 5.23. The ZP of processed empty NIVs and processed cisplatin NIVs stored at 40°C/75% RH in comparison to lyophilised NIVs prepared from empty NIVs over time at 1, 28, 189, 266 and 469 days post-preparation with empty NIVs not available on days 266 and 469 post-preparation ($n=3$ except for day 1 post-preparation where $n=1$). ‡ indicates significant difference between empty and cisplatin NIVs. § indicates significant difference between empty and lyophilised NIVs. * indicates significant difference between cisplatin and lyophilised NIVs ($p \leq 0.05$).

5.2.2. Comparison between NIVs of different cisplatin concentrations – stability study II

Three batches of NIVs using 1, 3 and 6mg/ml cisplatin were prepared, processed, aliquoted into vials and stored as described (Section 2.2.7.2). At specific time points (days 97 and 168 post-preparation) samples were analysed for cisplatin content, lipid content (day 3 post-preparation also assayed), size and ZP.

5.2.2.1. Physical appearance of NIVs prepared with different cisplatin concentrations

NIVs hydrated with 3 and 6mg/ml cisplatin showed obvious signs of cisplatin precipitation, whereas NIVs hydrated with 1mg/ml cisplatin did not. However no signs of flocculation or sedimentation were noticed in any of the NIVs. Photographs of NIVs hydrated with different cisplatin concentrations and stored at 4°C were taken on day 97 post-preparation to show how cisplatin had precipitated (Figure 5.24). NIVs stored at 25°C/60% RH and 40°C/75% RH showed similar characteristics.

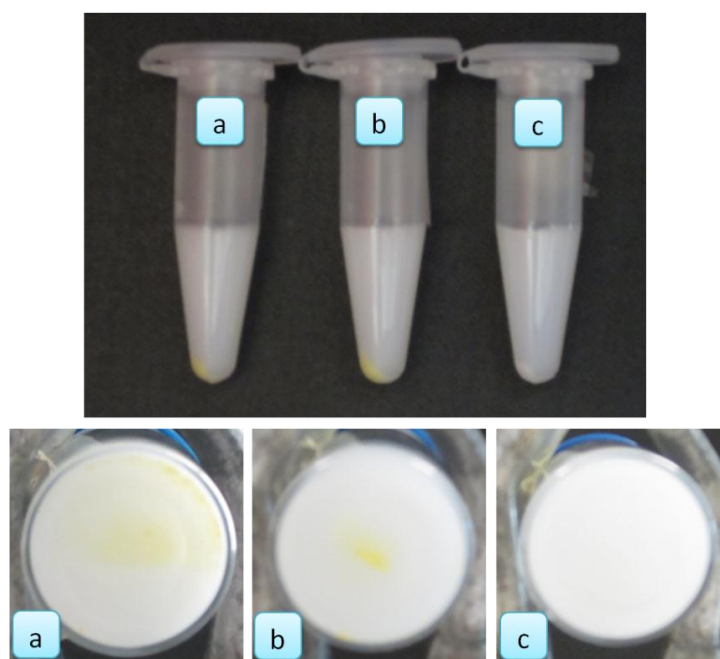


Figure 5.24. The physical appearance of NIVs hydrated with 6mg/ml (a), 3mg/ml (b) and 1mg/ml (c) cisplatin 97 days post-preparation and stored at 4°C showing signs of precipitation in a and b.

5.2.2.2. Cisplatin content in NIVs (entrapment efficiency, supernatant and total)

Cisplatin content (entrapped, unentrapped and total) on days 97 and 168 post-preparation was determined by HPLC (Section 2.2.5) using method II (Section 2.2.5.3). Only NIVs hydrated with 3 and 6mg/ml cisplatin were analysed for entrapment efficiency and cisplatin concentration in the supernatant.

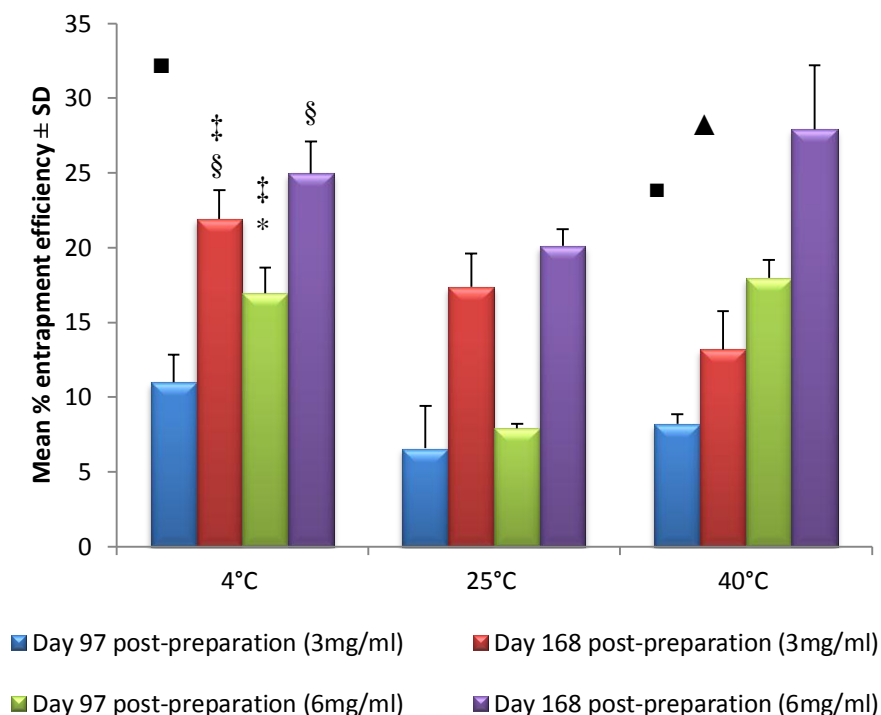


Figure 5.25. The entrapment efficiency of NIVs, hydrated with 3 and 6mg/ml cisplatin, stored at 4°C, 25°C/60% RH and 40°C/75% RH determined at 97 and 168 post-preparation (n=3). ‡ indicates significant difference between 4°C and 25°C/60% RH of the same group. § indicates significant difference between 4°C and 40°C/75% RH of the same group. * indicates significant difference between 25°C/60% RH and 40°C/75% RH of the same group. ■ indicates significant difference between 3 and 6mg/ml on day 97 post-preparation of the same storage condition. ▲ indicates significant difference between 3 and 6mg/ml on day 168 post-preparation of the same storage condition (p≤0.05).

The entrapment efficiency of NIVs hydrated with 6mg/ml cisplatin (Figure 5.25) was significantly higher than the formulations hydrated with 3mg/ml cisplatin on day 97 post-preparation when stored at 4°C (p=0.026) and on both time points when stored at 40°C/75% RH (day 97, p=0.001 and day 168, p=0.014).

NIVs hydrated with 3mg/ml cisplatin (Figure 5.25) and stored at 4°C showed significantly different entrapment efficiency between both time points (p=0.032). However, at 25°C/60% RH and 40°C/75% RH no significant difference in entrapment efficiency was observed between both time points. On day 97 post-preparation the entrapment efficiency of NIVs hydrated with 3mg/ml cisplatin did not differ whether the NIVs were stored at 4°C, 25°C/60% RH or 40°C/75% RH. However the entrapment efficiency on day 168 post-preparation for NIVs hydrated with 3mg/ml cisplatin was significantly higher when stored at 4°C than the other two conditions (p=0.009).

NIVs hydrated with 6mg/ml cisplatin and stored at 25°C/60% RH showed significant difference (p=0.001) in entrapment efficiency between days 97 and 168 post-preparation (Figure 5.25), whereas the other two conditions did not show any significant difference in entrapment efficiency between both days. The entrapment efficiency of NIVs hydrated with 6mg/ml cisplatin and stored at 25°C/60% RH was significantly lower than the other two conditions on day 97 post-preparation (p=0.000), and was only different from the same NIVs stored at 40°C/75% RH on day 168 post-preparation (p=0.040).

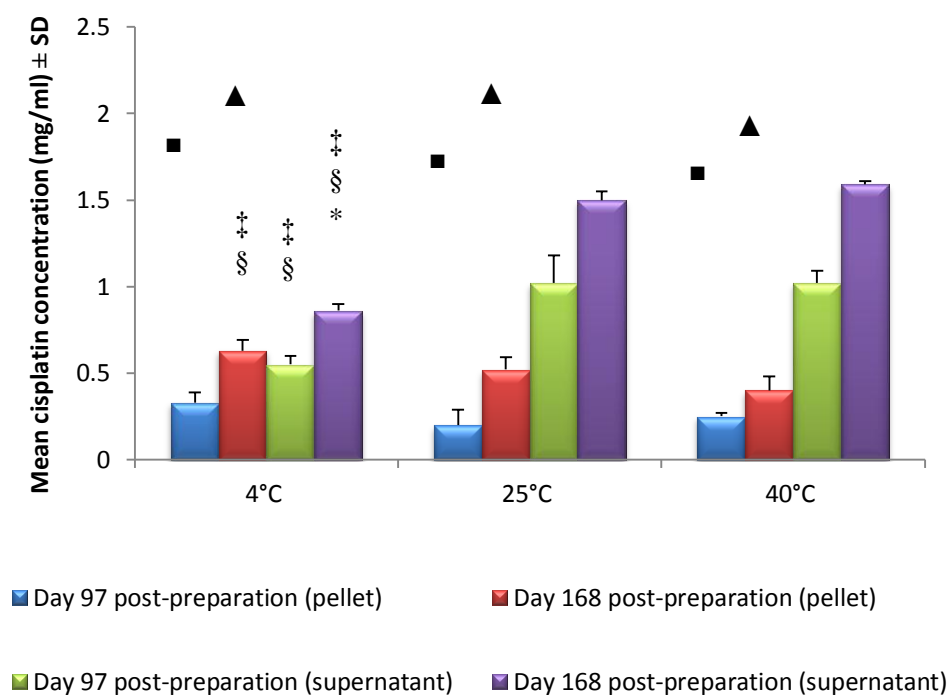


Figure 5.26. The concentration of untrapped and entrapped cisplatin in NIVs hydrated with 3mg/ml cisplatin and stored at 4°C, 25°C/60% and 40°C/75% RH determined at 97 and 168 post-preparation (n=3). ‡ indicates significant difference between 4°C and 25°C/60% RH of the same group. § indicates significant difference between 4°C and 40°C/75% RH of the same group. * indicates significant difference between 25°C/60% RH and 40°C/75% RH of the same group. ■ indicates significant difference between pellet and supernatant on day 97 post-preparation of the same storage condition ▲ indicates significant difference between pellet and supernatant on day 168 post-preparation of the same storage condition ($p \leq 0.05$).

NIVs hydrated with 3mg/ml cisplatin (Figure 5.26) showed significant difference in cisplatin concentration of supernatant between days 97 and 168 post-preparation at 4°C and 40°C/75% RH ($p=0.021$ and 0.006 , respectively), whereas at 25°C/60% the difference was just non-significant ($p=0.059$). A comparison between the storage conditions showed significantly lower concentration in the supernatant at 4°C on day 97 post-preparation than the other storage conditions ($p=0.002$) and significant difference between all storage conditions on day 168 post-preparation ($p=0.000$).

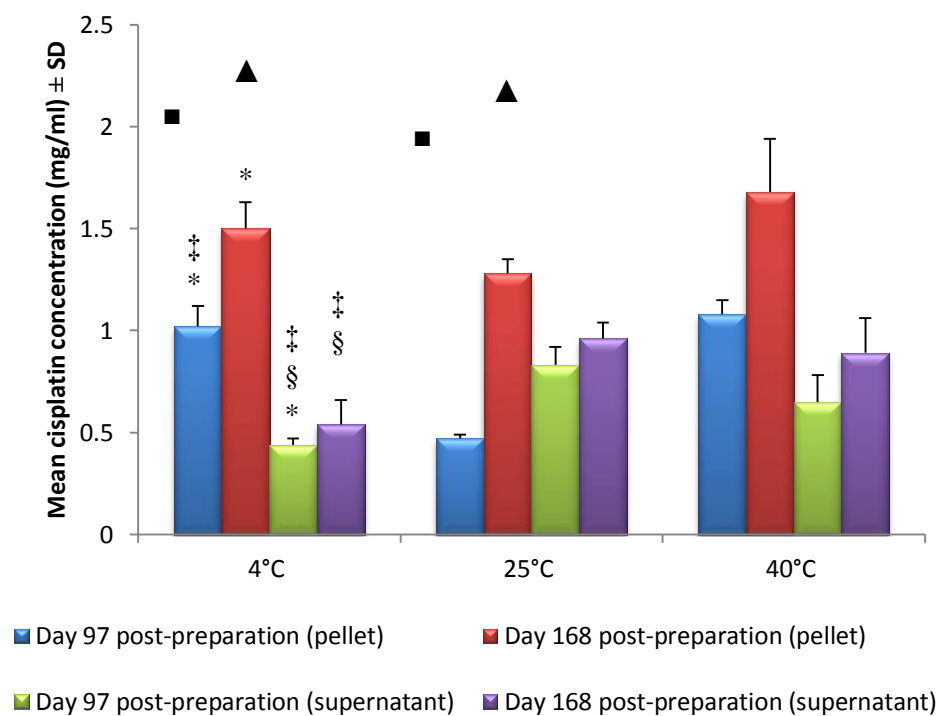


Figure 5.27. The concentration of untrapped and entrapped cisplatin in NIVs hydrated with 6mg/ml cisplatin and stored at 4°C, 25°C/60% and 40°C/75% RH determined at 97 and 168 post-preparation (n=3). ‡ indicates significant difference between 4°C and 25°C/60% RH of the same group. § indicates significant difference between 4°C and 40°C/75% RH of the same group. * indicates significant difference between 25°C/60% RH and 40°C/75% RH of the same group. ■ indicates significant difference between pellet and supernatant on day 97 post-preparation of the same storage condition. ▲ indicates significant difference between pellet and supernatant on day 168 post-preparation of the same storage condition ($p \leq 0.050$).

NIVs hydrated with 6mg/ml cisplatin (Figure 5.27), showed no significant difference in cisplatin concentration in the supernatant from day 97 to day 168 post-preparation at all storage conditions. A comparison between the storage conditions showed significant differences between all storage conditions on day 97 post-preparation ($p=0.006$) and significantly lower concentration in the supernatant at 4°C on day 168 post-preparation than the other storage conditions ($p=0.014$).

A comparison between untrapped and entrapped cisplatin showed that the amount of cisplatin entrapped was lower than in the supernatant for NIVs hydrated with 3mg/ml cisplatin (Figure 3.26) and vice versa for NIVs hydrated with 6mg/ml cisplatin (Figure 3.27).

In the assessment of total NIVs concentration, the total (entrapped and untrapped) cisplatin concentration of NIVs hydrated with 1, 3 and 6mg/ml were determined on days 97 and 168 post-preparation as represented (Tables 5.13 to 5.15).

NIVs hydrated with 1mg/ml cisplatin (Table 5.13) showed significant differences in total cisplatin concentration between days 97 and 168 post-preparation when stored at 4°C, 25°C/60% RH and 40°C/75% RH (p=0.008, 0.017 and 0.001, respectively). At each time point no significant difference in the cisplatin concentration between the different storage conditions was observed.

Table 5.13. The concentration of total cisplatin (entrapped and untrapped) in NIVs hydrated with 1mg/ml cisplatin and stored at 4°C, 25°C/60% and 40°C/75% RH determined on days 97 and 168 days post-preparation (n=3).

Storage condition	Mean concentration (mg/ml) ± SD over time	
	97 days post-preparation	168 days post-preparation
4°C	0.48 ± 0.02	0.76 ± 0.03
25°C/60% RH	0.45 ± 0.07	0.72 ± 0.02
40°C/75% RH	0.42 ± 0.02	0.71 ± 0.02

NIVs hydrated with 3mg/ml cisplatin (Table 5.14) showed significant differences between days 97 and 168 post-preparation when stored at 4°C, 25°C/60% RH and 40°C/75% RH (p=0.002, 0.001 and 0.046, respectively). On day 97 post-preparation the cisplatin concentration did not differ significantly between the different storage conditions. However, on day 168 post-preparation the concentration of cisplatin at 4°C was significantly lower than the other storage conditions (p=0.000).

Table 5.14. The concentration of total cisplatin (entrapped and unentrapped) in NIVs hydrated with 3mg/ml cisplatin and stored at 4°C, 25°C/60% and 40°C/75% RH determined on days 97 and 168 post-preparation (n=3). ‡ indicates significant difference between 4°C and 25°C/60% RH. § indicates significant difference between 4°C and 40°C/75% RH (p≤0.05).

Storage condition	Mean concentration (mg/ml) ± SD over time	
	97 days post-preparation	168 days post-preparation
4°C	1.0 ± 0.0	1.6 ± 0.1 ‡§
25°C/60% RH	1.3 ± 0.0	2.0 ± 0.1
40°C/75% RH	1.1 ± 0.3	2.0 ± 0.1

Table 5.15. The concentration of total cisplatin (entrapped and unentrapped) in NIVs hydrated with 6mg/ml cisplatin and stored at 4°C, 25°C/60% and 40°C/75% RH determined on days 97 and 168 post-preparation (n=3). § indicates significant difference between 4°C and 40°C/75% RH. * indicates significant difference between 25°C/60% RH and 40°C/75% RH (p≤0.05).

Storage condition	Mean concentration (mg/ml) ± SD over time	
	97 days post-preparation	168 days post-preparation
4°C	2.1 ± 0.2	2.4 ± 0.1
25°C/60% RH	1.4 ± 0.4	2.2 ± 0.1
40°C/75% RH	1.8 ± 0.4	3.6 ± 0.3 §*

NIVs hydrated with 6mg/ml cisplatin (Table 5.15) showed significant difference in total cisplatin concentration between days 97 and 168 post-preparation only at 40°C/75% RH (p=0.048). On day 97 post-preparation, cisplatin concentration did not change significantly between the different storage conditions. However on day 168 post-preparation, the total cisplatin concentration at 40°C/75% RH was significantly higher than the other storage conditions (p=0.000).

5.2.2.3. Vesicle size and ZP of NIVs hydrated with different concentrations of cisplatin

The size and ZP of the NIVs hydrated with 1, 3 and 6mg/ml was determined by method described (Section 2.2.4.2).

5.2.2.3.1. Vesicle size results

NIVs hydrated with 1mg/ml cisplatin (Table 5.16) showed no significant difference between days 97 and 168 post-preparation at 4°C and 40°C/75% RH. At 25°C/60% RH, a significant difference in vesicle size between both time points was observed (p=0.032). On days 97 and 168 post-preparation, no significant differences in vesicle size between the different storage conditions were observed.

Table 5.16. The size of processed NIVs hydrated with 1mg/ml cisplatin and stored at 4°C, 25°C/60% RH and 40°C/75% RH determined on days 97 and 168 post-preparation (n=3).

Storage condition (°C/%RH)	Mean size (nm) ± SD over time	
	97 days post-preparation	168 days post-preparation
4	590.5 ± 68.1	530.1 ± 108.4
25/60	568.1 ± 53.6	514.5 ± 46.5
40/75	575.4 ± 34.5	566.4 ± 43.9

Table 5.17. The size of processed NIVs hydrated with 3mg/ml cisplatin and stored at 4°C, 25°C/60% RH and 40°C/75% RH determined on days 97 and 168 post-preparation (n=3). § indicates significant difference between 4°C and 40°C/75% RH. * indicates significant difference between 25°C/60% RH and 40°C/75% RH (p≤0.05).

Storage condition (°C/%RH)	Mean size (nm) ± SD over time	
	97 days post-preparation	168 days post-preparation
4	531.7 ± 42.2	493.7 ± 60.9
25/60	511.5 ± 37.7	502.7 ± 48.6
40/75	547.1 ± 35.5	585.8 ± 58.1 §*

NIVs hydrated with 3mg/ml cisplatin (Table 5.17) maintained a stable size between days 97 and 168 post-preparation at all storage conditions. Vesicle size was similar between the different storage conditions on day 97 post-preparation but showed significantly larger vesicle size (p=0.003) at 40°C/75% RH on day 168 post-preparation than the other storage conditions.

Table 5.18. The size of processed NIVs hydrated with 6mg/ml cisplatin and stored at 4°C, 25°C/60% RH and 40°C/75% RH determined on days 97 and 168 post-preparation (n=3). * indicates significant difference between 25°C/60% RH and 40°C/75% RH (p≤0.05).

Storage condition (°C/%RH)	Mean size (nm) ± SD over time	
	97 days post-preparation	168 days post-preparation
4	618.7 ± 45.4	647.9 ± 57.0
25/60	585.6 ± 48.7 *	594.6 ± 45.0
40/75	652.4 ± 21.6	648.8 ± 80.7

NIVs hydrated with 6mg/ml cisplatin (Table 5.18) showed no significant differences in vesicle size between days 97 and 168 post-preparation at all storage conditions. On day 97 post-preparation, NIVs stored at 25°C/60% RH were significantly smaller

in size than those stored at 40°C/75% RH (p=0.007). However, no significant difference in vesicle size between the different storage conditions was observed on day 168 post-preparation.

A comparison of vesicle size between NIVs hydrated with 1, 3 and 6mg/ml cisplatin at different storage conditions was studied (Tables 5.19 to 5.21).

At 4°C (Table 5.19), NIVs hydrated with 3mg/ml cisplatin differed significantly (p=0.006) from the other formulations on day 97 post-preparation. NIVs hydrated with 6mg/ml cisplatin differed significantly (p=0.001) from the other formulations on day 168 post-preparation.

Table 5.19. The size of processed NIVs hydrated with 1, 3 and 6mg/ml cisplatin and stored at 4° determined on days 97 and 168 post-preparation (n=3). ‡ indicates significant difference between 1 and 3mg/ml. § indicates significant difference between 1 and 6mg/ml. * indicates significant difference between 3 and 6mg/ml (p≤0.05).

Concentration of cisplatin (mg/ml)	Mean size (nm) ± SD over time	
	97 days post-preparation	168 days post-preparation
1	590.5 ± 68.1	530.1 ± 108.4
3	531.7 ± 42.2 ‡*	493.7 ± 60.9
6	618.7 ± 45.4	647.9 ± 57.0 §*

At 25°C/60% RH (Table 5.20), the size of NIVs hydrated with 3mg/ml cisplatin was significantly different from the other NIVs on day 97 post-preparation (p=0.007). The size of NIVs hydrated with 6mg/ml cisplatin on day 168 post-preparation was the significantly different from the other NIVs (p=0.001).

Table 5.20. The size of processed NIVs hydrated with 1, 3 and 6mg/ml cisplatin and stored at 25°C/60% RH determined on days 97 and 168 post-preparation (n=3). ‡ indicates significant difference between 1 and 3mg/ml. § indicates significant difference between 1 and 6mg/ml. * indicates significant difference between 3 and 6mg/ml (p≤0.05).

Concentration of cisplatin (mg/ml)	Mean size (nm) ± SD over time	
	97 days post-preparation	168 days post-preparation
1	568.1 ± 53.6	514.6 ± 46.5
3	511.5 ± 37.7 ‡*	502.7 ± 48.6
6	585.6 ± 48.7	594.6 ± 45.0 §*

A comparison of vesicle size between the different NIVs at the studied time points when stored at 40°C/75% RH showed that NIVs hydrated with 6mg/ml cisplatin were significantly different from those prepared with 1 and 3mg/ml cisplatin at both days 97 (p=0.000) and 168 (p=0.026) post-preparation (Table 5.21).

Table 5.21. The size of processed NIVs hydrated with 1, 3 and 6mg/ml cisplatin and stored at 40°C/75% RH determined on days 97 and 168 post-preparation (n=3). § indicates significant difference between 1 and 6mg/ml. * indicates significant difference between 3 and 6mg/ml (p≤0.05).

Concentration of cisplatin (mg/ml)	Mean size (nm) ± SD over time	
	97 days post-preparation	168 days post-preparation
1	575.4 ± 34.5	566.4 ± 43.9
3	547.1 ± 35.5	585.8 ± 58.1
6	652.4 ± 21.6 §*	648.8 ± 80.7 §*

5.2.2.3.2. ZP results

NIVs hydrated with 1mg/ml cisplatin (Table 5.22), showed no significant difference in ZP from day 97 to 168 post-preparation at all storage conditions. The different storage conditions showed no significant effect on the ZP of NIVs hydrated with 1mg/ml on each time point.

Table 5.22. The ZP of processed NIVs hydrated with 1mg/ml cisplatin and stored at 4°C, 25°C/60% RH and 40°C/75% RH determined on days 97 and 168 post-preparation (n=3).

Storage condition (°C/%RH)	Mean ZP (mV) ± SD over time	
	97 days post-preparation	168 days post-preparation
4	-76.5 ± 2.2	-77.5 ± 2.0
25/60	-79.1 ± 4.8	-78.0 ± 2.1
40/75	-77.4 ± 2.3	-76.9 ± 3.1

Table 5.23. The ZP of processed NIVs hydrated with 3mg/ml cisplatin and stored at 4°C, 25°C/60% RH and 40°C/75% RH determined on days 97 and 168 post-preparation (n=3). * indicates significant difference between 25°C/60% RH and 40°C/75% RH (p≤0.05).

Storage condition (°C/%RH)	Mean ZP (mV) ± SD over time	
	97 days post-preparation	168 days post-preparation
4	-87.1 ± 2.6	-85.8 ± 1.5
25/60	-83.0 ± 4.9 *	-87.5 ± 3.1
40/75	-86.0 ± 1.9	-83.7 ± 4.5

NIVs hydrated with 3mg/ml cisplatin (Table 5.23) showed no significant differences in ZP between days 97 and 168 post-preparation with the exception of those stored at 25°C/60% RH (p=0.006). On day 97 post-preparation, only NIVs stored at 25°C/60%RH and 40°C/75% RH showed a significant difference in ZP (p=0.042).

No significant changes in the ZP between the different storage conditions of NIVs hydrated with 3mg/ml cisplatin were observed on day 168 post-preparation.

Table 5.24. The ZP of processed NIVs hydrated with 6mg/ml cisplatin and stored at 4°C, 25°C/60% RH and 40°C/75% RH determined on days 97 and 168 post-preparation (n=3). ‡ indicates significant difference between 4°C and 25°C/60% RH. § indicates significant difference between 4°C and 40°C/75% RH. * indicates significant difference between 25°C/60% RH and 40°C/75% RH (p≤0.05).

Storage condition (°C/%RH)	Mean ZP (mV) ± SD over time	
	97 days post-preparation	168 days post-preparation
4	-88.8 ± 2.3	-83.0 ± 2.3
25/60	-87.5 ± 4.1	-86.1 ± 1.7
40/75	-88.1 ± 3.7	-89.7 ± 1.8 ‡§*

At 4°C (Table 5.24), the ZP of NIVs hydrated with 6mg/ml cisplatin differed significantly between days 97 and 168 post-preparation (p=0.008). The other two storage conditions however, showed no significant difference in ZP between days 97 and 168 post-preparation. A comparison of the ZP between the different storage conditions of NIVs hydrated with 6mg/ml cisplatin did not show any significant difference on day 97 post-preparation. However, on day 168 post-preparation the ZP of the NIVs differed significantly between each other.

A comparison of the ZP between the NIVs hydrated with different concentrations of cisplatin and stored at 4°C showed a significantly lower negativity of NIVs hydrated with 1mg/ml cisplatin as opposed to those hydrated with 3 and 6mg/ml cisplatin (p=0.000) on day 97 post-preparation (Table 5.25). On day 168 post-preparation, the ZP differed significantly between all the NIVs (p=0.000).

Table 5.25. The ZP of processed NIVs hydrated 1, 3 and 6mg/ml cisplatin and stored at 4°C determined on days 97 and 168 post-preparation (n=3). ‡ indicates significant difference between 1 and 3mg/ml of the same day post-preparation. § indicates significant difference between 1 and 6mg/ml. * indicates significant difference between 3 and 6mg/ml (p≤0.05).

Concentration of cisplatin (mg/ml)	Mean ZP (mV) ± SD over time	
	97 days post-preparation	168 days post-preparation
1	-76.5 ± 2.2 ‡§	-77.5 ± 2.0
3	-87.1 ± 2.6	-85.8 ± 1.5
6	-88.8 ± 2.3	-83.0 ± 2.3 ‡§*

Table 5.26. The ZP of processed NIVs hydrated with 1, 3 and 6mg/ml cisplatin and stored at 25°C/60% RH determined on days 97 and 168 post-preparation (n=3). ‡ indicates significant difference between 1 and 3mg/ml. § indicates significant difference between 1 and 6mg/ml. * indicates significant difference between 3 and 6mg/ml (p≤0.05).

Concentration of cisplatin (mg/ml)	Mean ZP (mV) ± SD over time	
	97 days post-preparation	168 days post-preparation
1	-79.1 ± 4.9	-78.0 ± 2.1 ‡§
3	-83.0 ± 4.9	-87.5 ± 3.1
6	-87.5 ± 4.1 §*	-86.1 ± 1.7

At 25°C/60% RH (Table 5.26), the ZP of NIVs hydrated with 6mg/ml cisplatin differed significantly from NIVs of other cisplatin concentrations (p=0.003) on day 97 post-preparation. On the other hand, NIVs hydrated with 1mg/ml cisplatin differed significantly in terms of ZP in comparison to NIVs of other concentrations on day 168 post-preparation (p=0.000).

Table 5.27. The ZP of processed NIVs hydrated with 1, 3 and 6mg/ml cisplatin and stored at 40°C/75% RH determined on days 97 and 168 days post-preparation (n=3). ‡ indicates significant difference between 1 and 3mg/ml. § indicates significant difference between 1 and 6mg/ml. * indicates significant difference between 3 and 6mg/ml (p≤0.05).

Concentration of cisplatin (mg/ml)	Mean ZP (mV) ± SD over time	
	79 days post-preparation	168 days post-preparation
1	-77.4 ± 2.3 ‡§	-76.9 ± 3.1
3	-86.0 ± 1.9	-83.7 ± 4.5
6	-88.1 ± 3.7	-89.7 ± 1.8 ‡§*

On day 97 post-preparation, the ZP of NIVs hydrated with 1mg/ml cisplatin was significantly different (p=0.000) from those hydrated with 3 and 6mg/ml cisplatin when stored at 40°C/75% RH (Table 5.27). On day 168 post-preparation, the ZP became significantly different between NIVs of all cisplatin concentrations (p=0.000).

5.2.2.4. Lipid content

The lipid content of NIVs was determined as described (Section 2.2.4.4) using HPLC as described (Section 2.2.6). Lipid content of each NIVs formulation was determined on days 3, 97 and 168 post-preparation. As each NIVs formulation had not yet been divided into different storage conditions on day 3 post-preparation, the results obtained for this time point were used in all the storage conditions.

5.2.2.4.1. Cholesterol content

The cholesterol content of NIVs hydrated with 1mg/ml cisplatin (Figure 5.28) maintained a stable concentration over time at 4°C, whereas increased significantly from day 3 to 97 post-preparation and remained stable onwards at 25°C/60% RH (p=0.002). The cholesterol content of the same NIVs stored at 40°C/75% RH showed

a significant difference between each time point ($p=0.000$). The cholesterol content each time point, 97 and 168 post-preparation, did not differ significantly between the different storage conditions. Comparison of the cholesterol/DCP ratio over time also showed considerable stability over time with only day 3 significantly different from the other time points at 4°C ($p=0.032$) and 25°C/60% RH ($p=0.048$). The cholesterol/DCP ratio was similar between the different storage conditions at each time point.

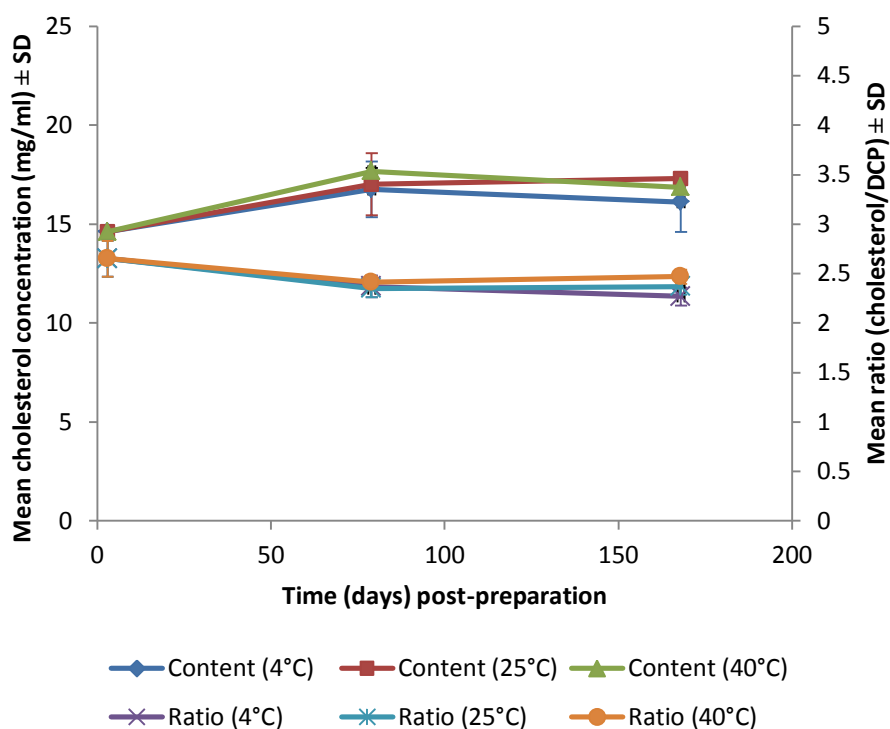


Figure 5.28. The concentration of cholesterol and ratio between cholesterol and DCP weights in processed NIVs hydrated with 1mg/ml cisplatin and stored at 4°C, 25°C/60% RH and 40°C/75% RH determined on days 3, 97 and 168 post-preparation (n=3).

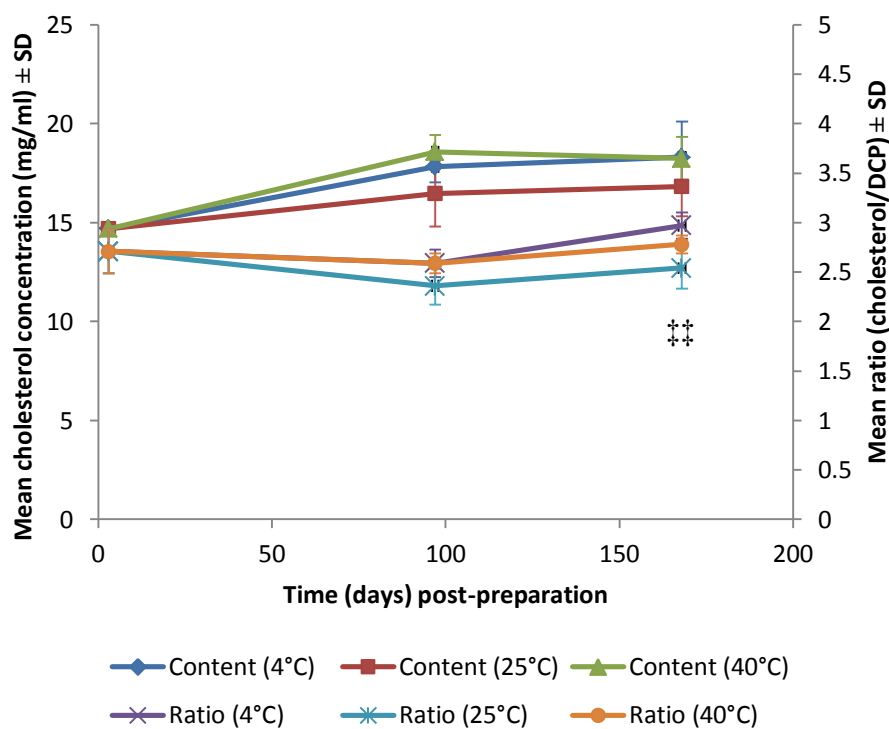


Figure 5.29. The concentration of cholesterol and ratio between cholesterol and DCP weights in processed NIVs hydrated with 3mg/ml cisplatin and stored at 4°C, 25°C/60% RH and 40°C/75% RH determined on days 3, 97 and 168 post-preparation (n=3). ‡‡ indicates significant difference in ratio between 4°C and 25°C/60% RH ($p \leq 0.05$).

The cholesterol content of NIVs hydrated with 3mg/ml cisplatin and stored at 4°C and 40°C/75% RH followed a similar trend over time where the concentration increased significantly from day 3 to 97 post-preparation ($p=0.016$ and 0.002 , respectively) and remained stable onwards (Figure 5.29). However at 25°C/60% RH, the cholesterol content of the same NIVs remained stable over time. When the cholesterol content at each time point was compared between the different storage conditions, no significant difference was observed at both 97 and 168 days post-preparation. The cholesterol/DCP ratio showed stability over time at all storage conditions. Day 97 post-preparation showed no significant difference between the different storage conditions whereas day 168 post-preparation showed significant difference between 4°C and 25°C/60% RH ($p=0.039$).

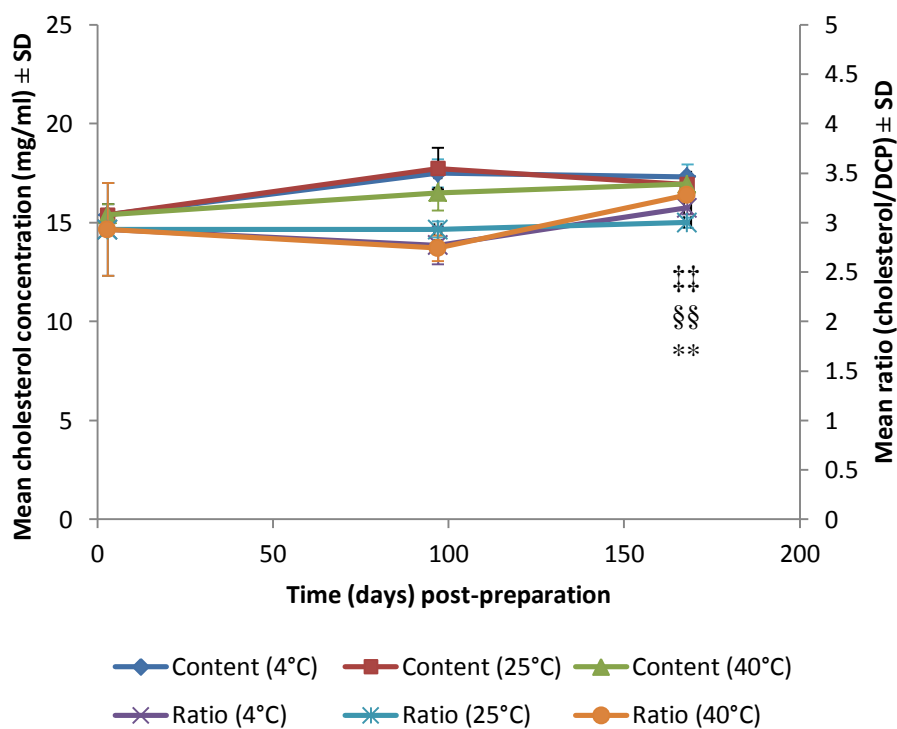


Figure 5.30. The concentration of cholesterol and ratio between cholesterol and DCP weights in processed NIVs hydrated with 6mg/ml cisplatin and stored at 4°C, 25°C/60% RH and 40°C/75% RH determined on days 3, 97 and 168 post-preparation (n=3). ‡‡ indicates significant difference in ratio between 4°C and 25°C/60% RH. §§ indicates significant difference in ratio between 4°C and 40°C/75% RH. ** indicates significant difference in ratio between 25°C/60% RH and 40°C/75% RH (p≤0.050).

Over time, the cholesterol content of NIVs hydrated with 6mg/ml cisplatin and stored at 4°C and 25°C/60% RH increased significantly from day 3 to day 97 post-preparation (p=0.011 and 0.008, respectively), whereas a stable cholesterol content was maintained at 40°C/75% RH (Figure 5.30). No significant difference between the different storage conditions was observed on day 97 or day 168 post-preparation. The cholesterol/DCP ratio showed stability over time for all storage conditions. Cholesterol/DCP ratio showed no significant difference between the different storage conditions on day 97 post-preparation, whereas on day 168 post-preparation significant difference was shown between all storage conditions (p=0.002).

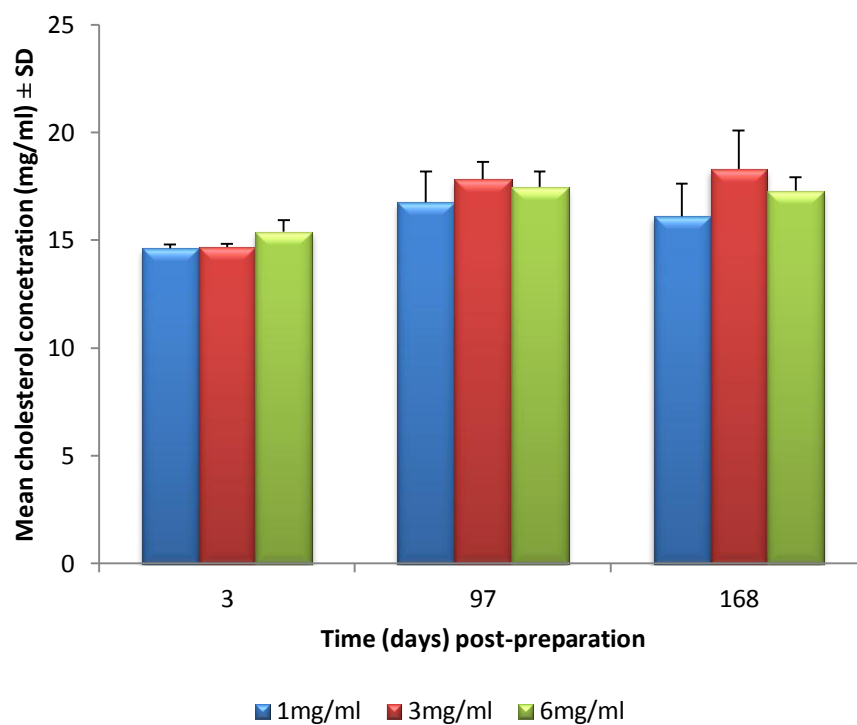


Figure 5.31. The concentration of cholesterol in processed NIVs hydrated with different cisplatin concentrations of 1, 3 and 6mg/ml and stored at 4°C determined on days 3, 97 and 168 post-preparation (n=3).

The cholesterol content of the different cisplatin NIVs was compared over time at 4°C (Figure 5.31). Over time, no significant difference in cholesterol content was observed in NIVs whether they were hydrated with 1, 3 or 6mg/ml cisplatin.

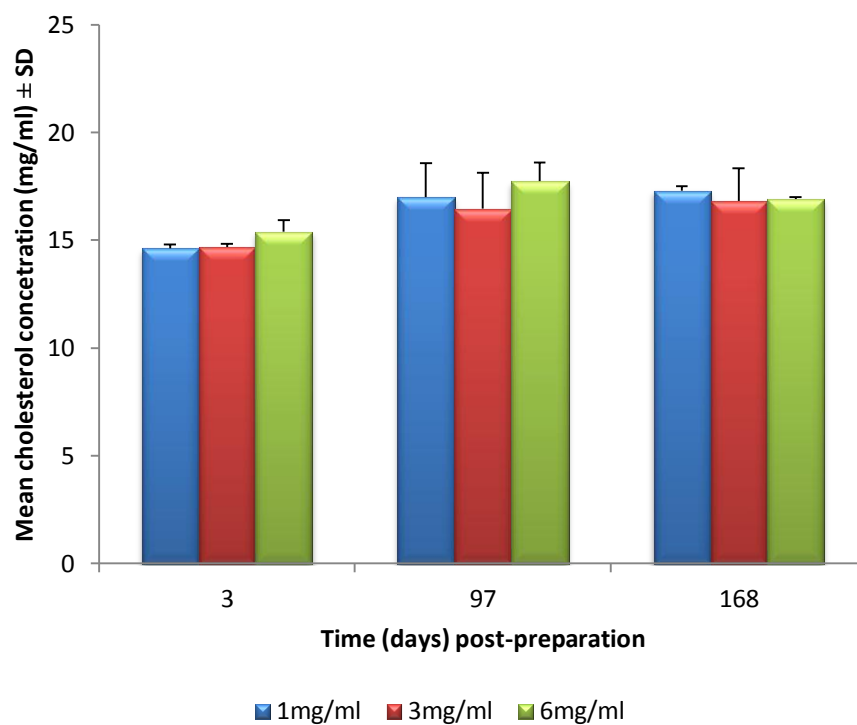


Figure 5.32. The concentration of cholesterol in processed NIVs hydrated with different cisplatin concentrations of 1, 3 and 6mg/ml and stored at 25°C/60% RH determined on days 3, 97 and 168 post-preparation (n=3).

At 25°C/60% RH, the cholesterol content of NIVs hydrated with 1, 3 and 6mg/ml cisplatin was similar at the different time points studied (Figure 5.32).

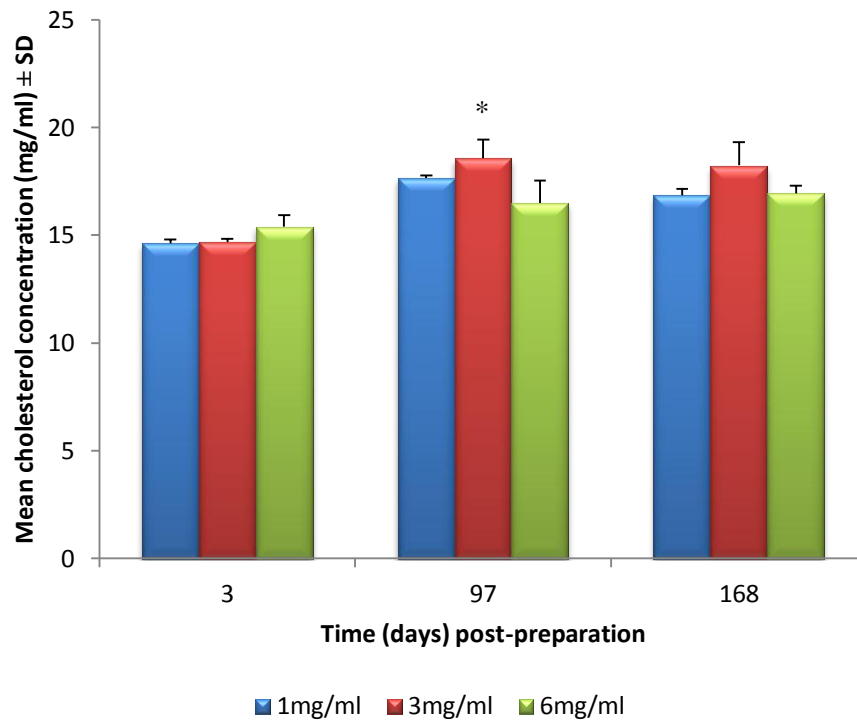


Figure 5.33. The concentration of cholesterol in processed NIVs hydrated with different cisplatin concentrations of 1, 3 and 6mg/ml and stored at 40°C/75% RH determined on days 3, 97 and 168 post-preparation (n=3). * indicates significant difference between 3 and 6mg/ml ($p \leq 0.05$).

The cholesterol content of NIVs hydrated with 1, 3 and 6mg/ml cisplatin and stored at 40°C/75% RH (Figure 5.33) showed no significant differences in the concentration over time with the exception of day 97 post-preparation where the content between NIVs hydrated with 3 and 6mg/ml cisplatin were just significantly different ($p=0.050$).

5.2.2.4.2. Surfactant VIII content

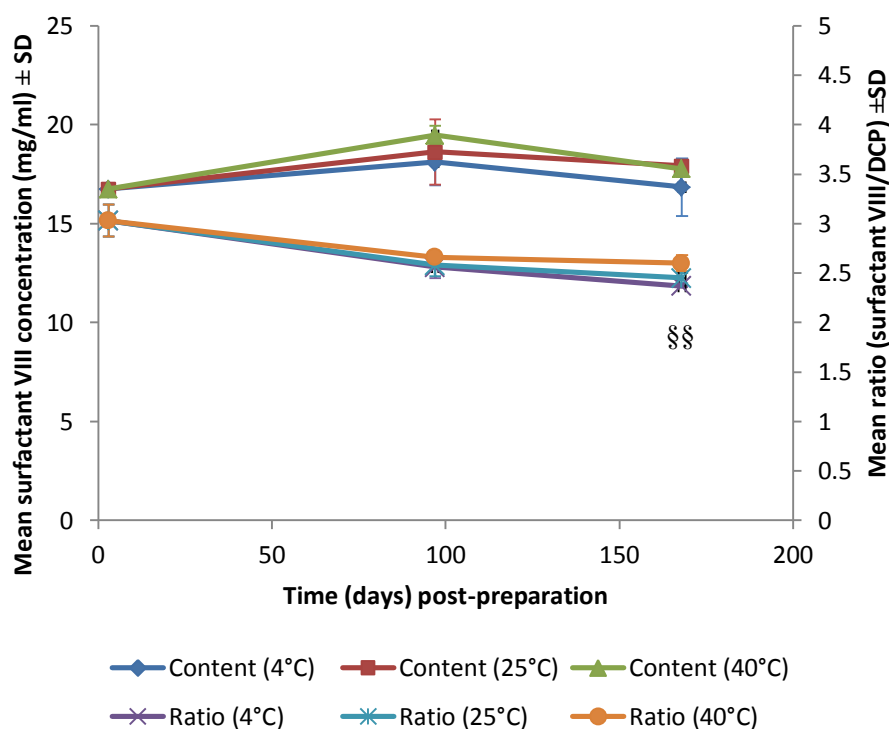


Figure 5.34. The concentration of surfactant VIII and ratio between surfactant VIII and DCP weights in processed NIVs hydrated with 1mg/ml cisplatin and stored at 4°C, 25°C/60% RH and 40°C/75% RH determined on days 3, 97 and 168 post-preparation (n=3). §§ indicates significant difference in ratio between 4°C and 40°C/75% RH ($p \leq 0.05$).

The surfactant VIII content of NIVs hydrated with 1mg/ml cisplatin did not change significantly over time when stored at 4°C and 25°C/60% RH unlike 40°C/75% RH, where a significant difference ($p=0.000$) between the different time points was observed (Figure 5.34). No significant difference in surfactant VIII content was shown on days 97 and 168 post-preparation between the different storage conditions. The surfactant VIII/DCP ratio over time showed day 3 post-preparation to be significantly different from other time points for all storage conditions ($p \leq 0.050$). Surfactant VIII/DCP ratio showed no significant difference between the different

storage conditions on day 97 post-preparation, whereas a significant difference ($p=0.018$) between 4°C and 40°C/60% was shown on day 168 post-preparation.

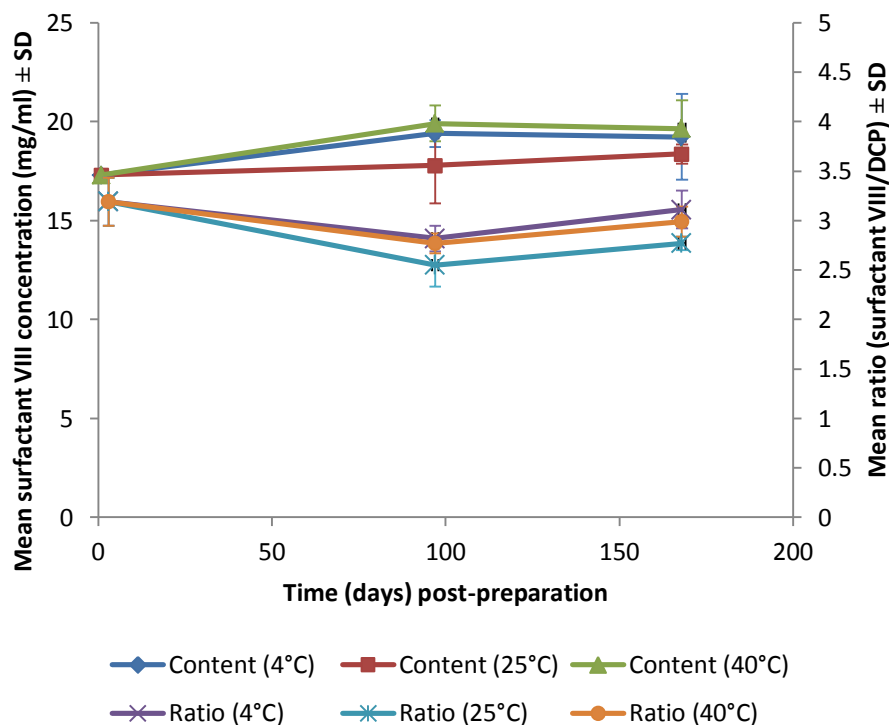


Figure 5.35. The concentration of surfactant VIII and ratio between surfactant VIII and DCP weights in processed NIVs hydrated with 3mg/ml cisplatin and stored at 4°C, 25°C/60% RH and 40°C/75% RH determined on days 3, 97 and 168 post-preparation (n=3).

The content of surfactant VIII in NIVs hydrated with 3mg/ml cisplatin did not differ significantly over time when stored at 4°C and 25°C/60% RH (Figure 5.35). However, a significant change in surfactant VIII content between days 3 and 97 post-preparation was observed for the same NIVs when stored at 40°C/75% RH ($p=0.033$). No significant difference in surfactant VIII content was observed between the different conditions at each time point. Surfactant VIII/DCP ratio showed stability over time at 4°C and 40°C/75% RH and only day 3 post-preparation significantly different ($p=0.017$) from the other time points at 25°C/60% RH.

Surfactant VIII/DCP ratio between the different storage conditions did not differ significantly at each time point.

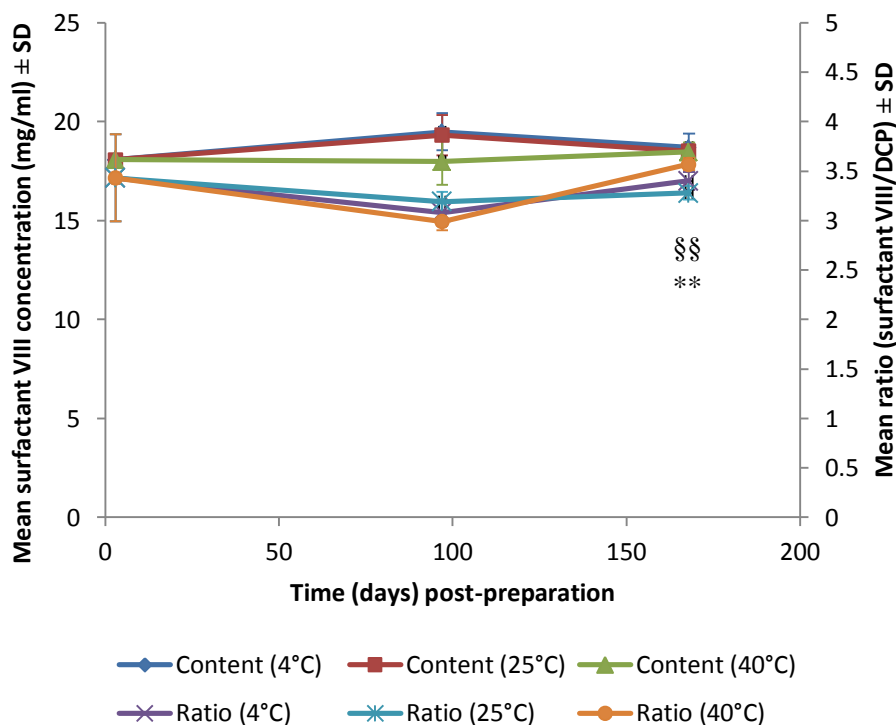


Figure 5.36. The concentration of surfactant VIII and ratio between surfactant VIII and DCP weights in processed NIVs hydrated with 6mg/ml cisplatin and stored at 4°C, 25°C/60% RH and 40°C/75% RH determined on days 3, 97 and 168 post-preparation (n=3). §§ indicates significant difference in ratio between 4°C and 40°C/75% RH. ** indicates significant difference in ratio between 25°C/60% RH and 40°C/75% RH ($p \leq 0.05$).

Over time, NIVs hydrated with 6mg/ml cisplatin maintained stable content of surfactant VIII at all storage conditions (Figure 5.36). A comparison of the surfactant VIII content between the different storage conditions at 97 and 168 post-preparation also revealed no significant difference. The surfactant VIII/DCP ratio demonstrated no significant difference over time for all storage conditions. Surfactant VIII/DCP ratio was similar between the different storage conditions on day 97 post-preparation,

whereas on day 168 post-preparation NIVs at 40°C/75% RH was significantly different from the other storage conditions.

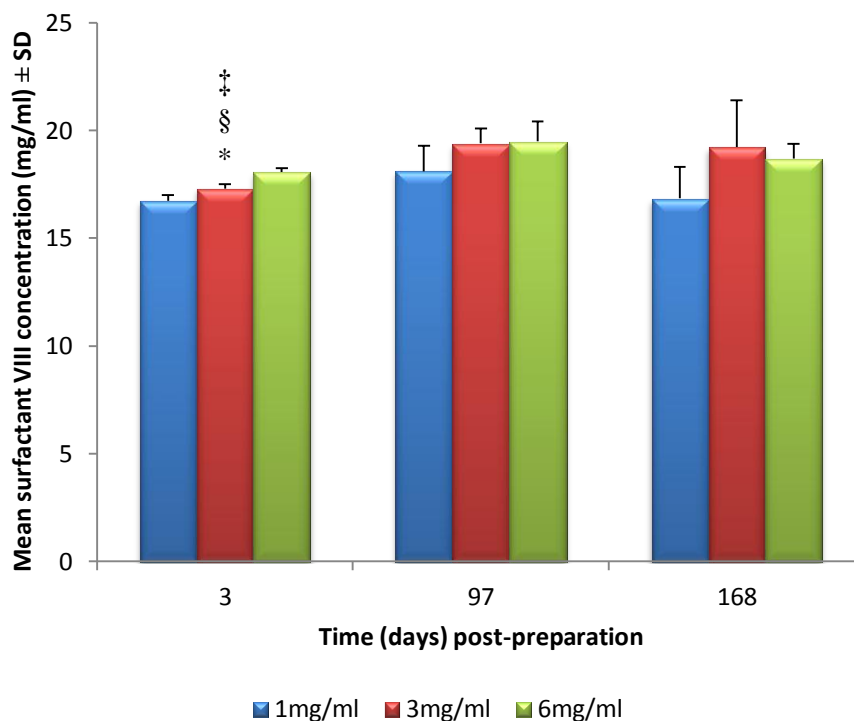


Figure 5.37. The concentration of surfactant VIII in processed NIVs hydrated with different cisplatin concentrations of 1, 3 and 6mg/ml and stored at 4°C determined on days 3, 97 and 168 post-preparation (n=3). ‡ indicates significant difference between 1 and 3mg/ml. § indicates significant difference between 1 and 6mg/ml. * indicates significant difference between 3 and 6mg/ml (p≤0.05).

A comparison of surfactant VIII content between NIVs hydrated with 1, 3 and 6mg/ml and stored at 4°C demonstrated similar content on days 97 and 168 post-preparation regardless of the concentration of cisplatin used to hydrate the NIVs (Figure 5.37).

Similarly, no significant difference in surfactant VIII content was observed between the NIVs hydrated with different cisplatin concentrations when stored at 25°C/60% RH (Figure 5.38) and at 40°C/75% RH (Figure 5.39) on days 97 and 168 post-preparation.

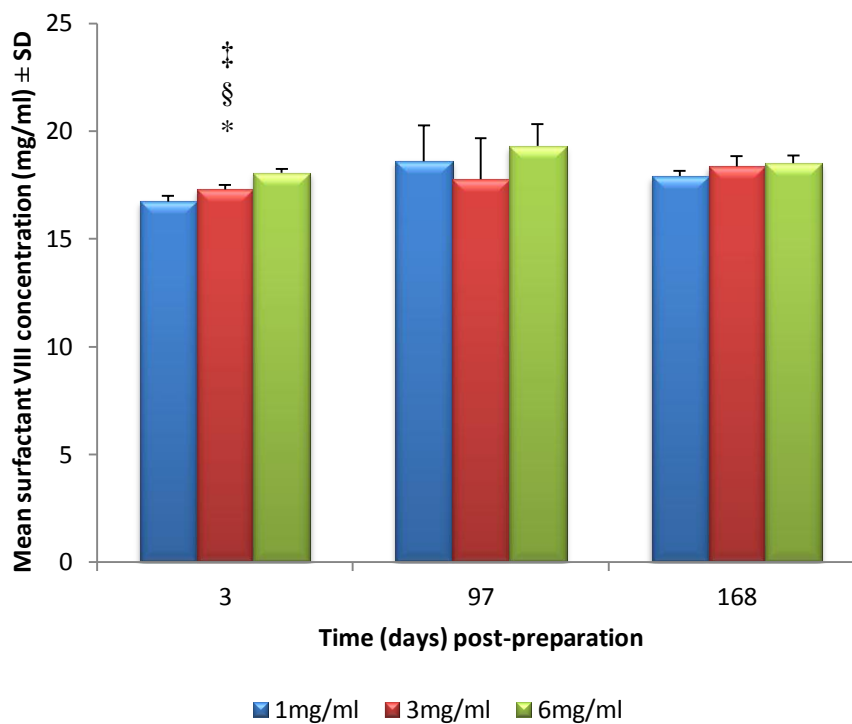


Figure 5.38. The concentration of surfactant VIII in processed NIVs hydrated with different cisplatin concentrations of 1, 3 and 6mg/ml and stored at 25°C/60% RH determined on days 3, 97 and 168 post-preparation (n=3). ‡ indicates significant difference between 1 and 3mg/ml. § indicates significant difference between 1 and 6mg/ml. * indicates significant difference between 3 and 6mg/ml ($p \leq 0.05$).

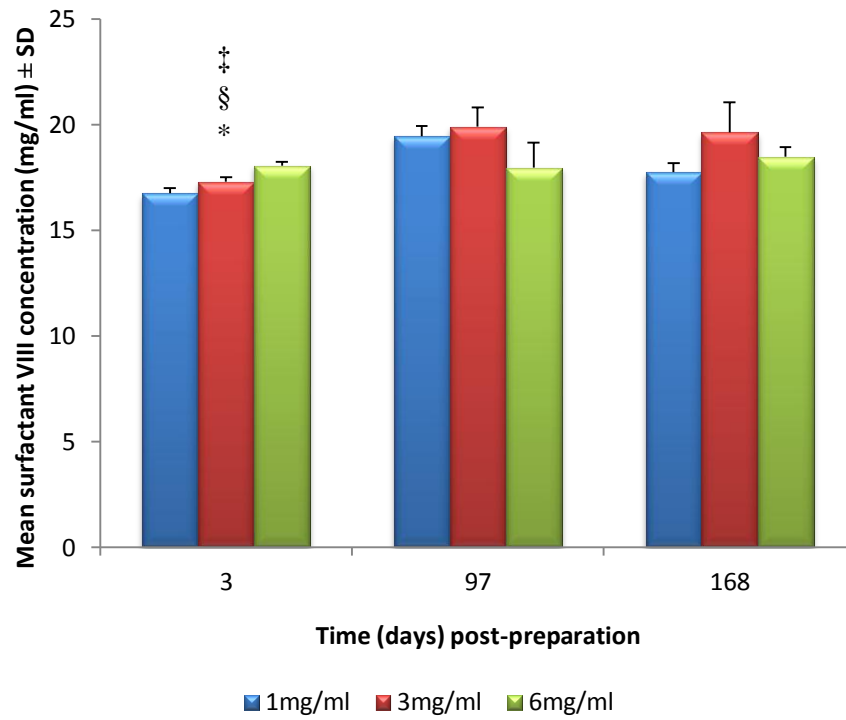


Figure 5.39. The concentration of surfactant VIII in processed NIVs hydrated with different cisplatin concentrations of 1, 3 and 6mg/ml and stored at 40°C/75% RH determined on days 3, 97 and 168 post-preparation (n=3). ‡ indicates significant difference between 1 and 3mg/ml. § indicates significant difference between 1 and 6mg/ml. * indicates significant difference between 3 and 6mg/ml (p≤0.05).

5.2.2.4.3. DCP content

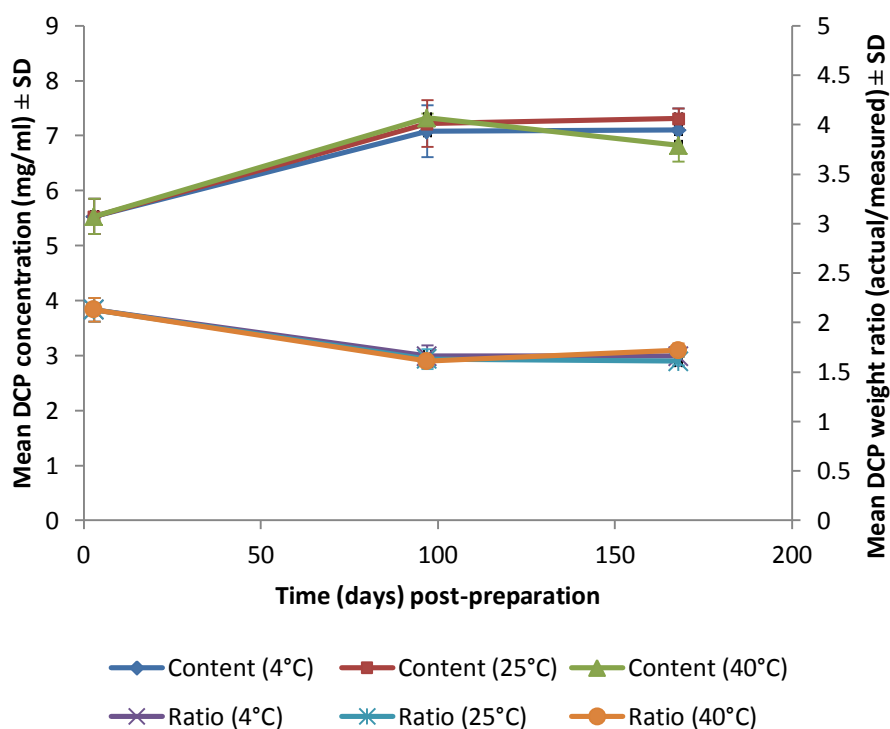


Figure 5.40. The concentration of dicetyl phosphate and dicetyl phosphate weight ratios in processed NIVs hydrated with 1mg/ml cisplatin and stored at 4°C, 25°C/60% RH and 40°C/75% RH determined on days 3, 97 and 168 post-preparation (n=3).

The content of DCP in NIVs hydrated with 1mg/ml cisplatin at 4°C, 25°C/60% RH and 40°C/75% RH followed the same trend over time, where a significant increase in the DCP content was observed from day 3 to 97 post-preparation ($p=0.004$, 0.001 and 0.000 , respectively) which remained stable afterwards (Figure 5.40). No significant differences in DCP content was observed between the different storage conditions at each time point. Similarly (Section 5.2.1.3.3), the DCP weight ratios were determined for further comparison. DCP weight ratio was only significantly different ($p\leq 0.050$) on day 3 post-preparation for all storage conditions. DCP weight

ratios between the different storage conditions did not differ from each other at each time point.

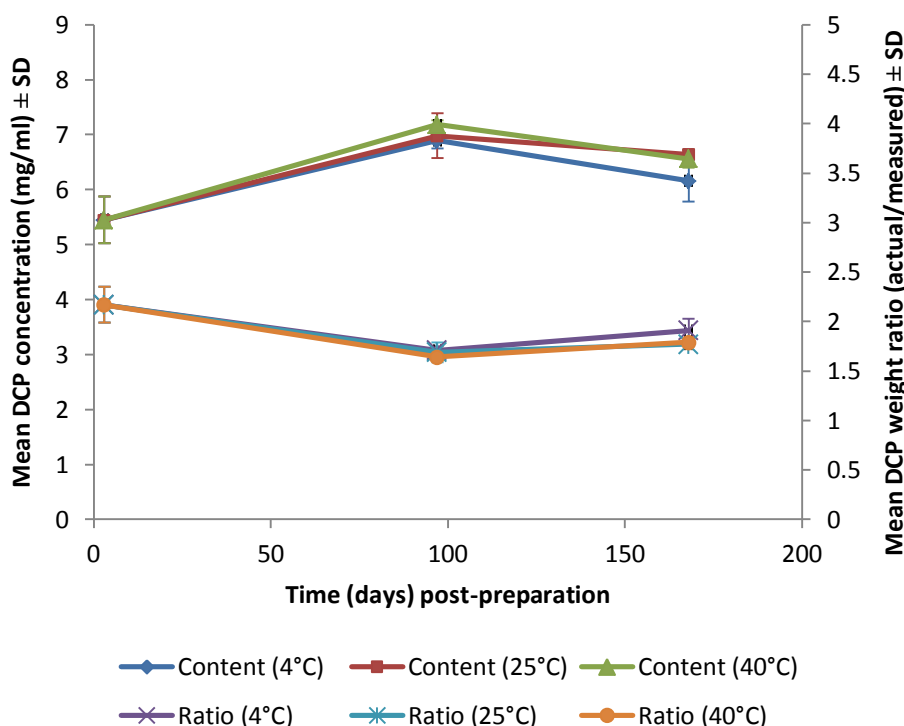


Figure 5.41. The concentration of dicetyl phosphate and dicetyl phosphate weight ratios in processed NIVs hydrated with 3mg/ml cisplatin and stored at 4°C, 25°C/60% RH and 40°C/75% RH determined on days 3, 97 and 168 post-preparation (n=3).

NIVs hydrated with 3mg/ml cisplatin and stored at 4°C and 40°C/75% RH showed significant changes in the DCP content over time ($p=0.006$ and 0.001 , respectively), whereas the same NIVs stored at 25°C/60% RH only showed a significant increase ($p=0.004$) from day 3 to 97 post-preparation which did not change onwards (Figure 5.41). On days 97 and 168 post-preparation, the DCP content did not differ significantly between the different conditions. The DCP weight ratio was only significantly different ($p\leq 0.050$) on day 3 post-preparation for all storage conditions. The DCP weight ratio showed no significant difference between the different storage conditions at each time point.

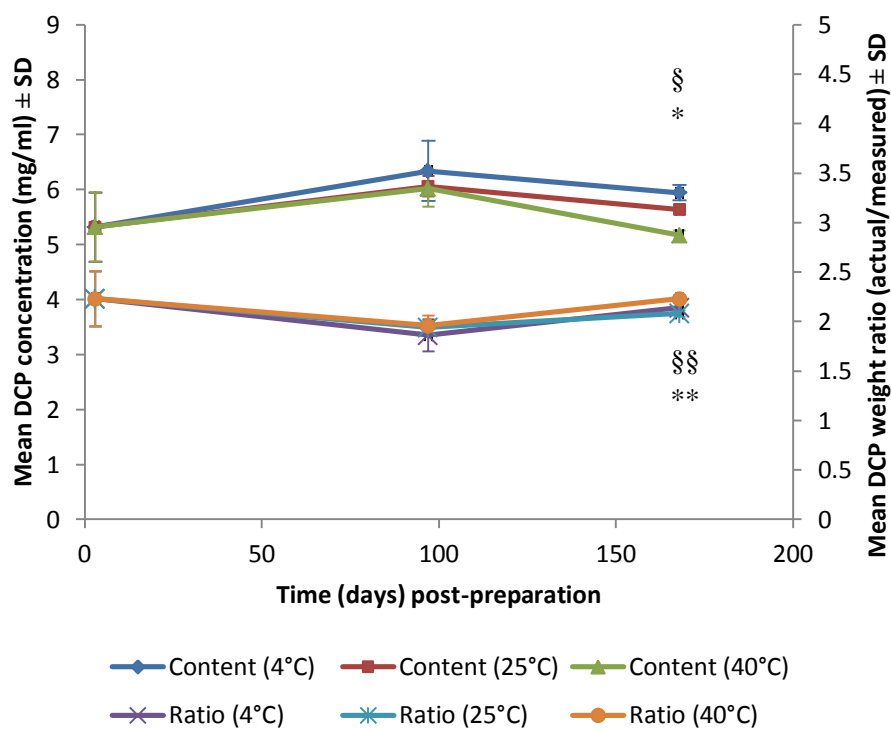


Figure 5.42. The concentration of dicetyl phosphate and dicetyl phosphate weight ratios in processed NIVs hydrated with 6mg/ml cisplatin and stored at 4°C, 25°C/60% RH and 40°C/75% RH determined on days 3, 97 and 168 post-preparation (n=3). § indicates significant difference in content between 4°C and 40°C/75% RH. * indicates significant difference in content between 25°C/60% RH and 40°C/75% RH. §§ indicates significant difference in ratio between 4°C and 40°C/75% RH. ** indicates significant difference in ratio between 25°C/60% RH and 40°C/75% RH (p≤0.05).

The DCP content of NIVs hydrated with 6mg/ml cisplatin maintained a stable DCP concentration over time at all storage conditions (Figure 5.42). DCP concentration on day 97 post-preparation was similar between the different storage conditions. However, the DCP content of the same NIVs stored at 40°C/75% differed significantly from those stored at the other conditions on day 168 post-preparation (p=0.005). The DCP weight ratios showed stability over time for all storage conditions. The DCP weight ratios were similar on day 97 post-preparation between

the different storage conditions, whereas differed significantly on day 168 post-preparation at 40°C/75% RH in comparison to the other storage conditions.

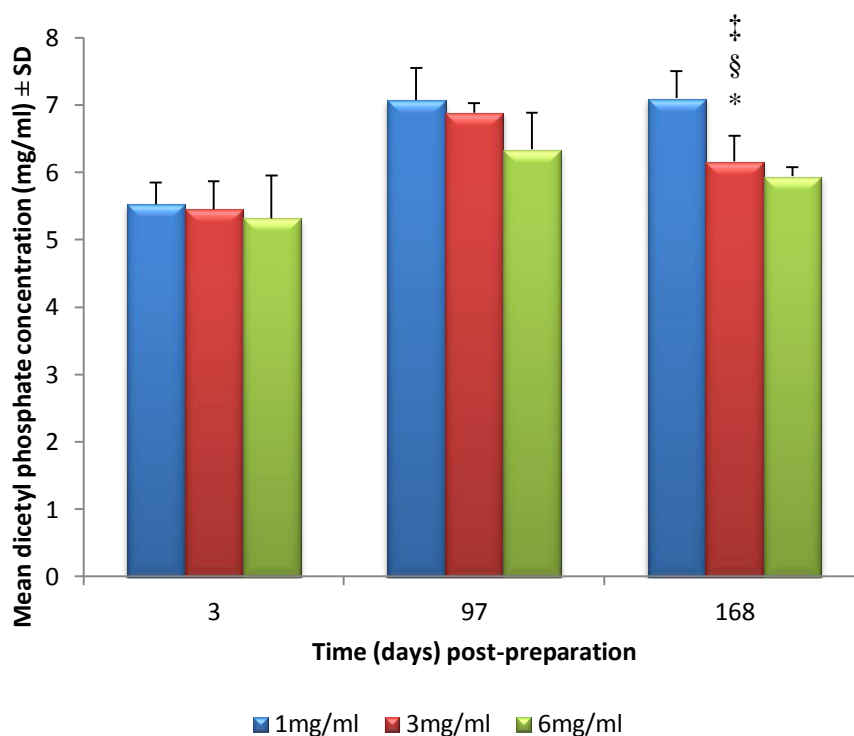


Figure 5.43. The concentration of dicetyl phosphate in processed NIVs hydrated with different cisplatin concentrations of 1, 3 and 6mg/ml and stored at 4°C determined on days 3, 97 and 168 post-preparation (n=3). ‡ indicates significant difference between 1 and 3mg/ml. § indicates significant difference between 1 and 6mg/ml. * indicates significant difference between 3 and 6mg/ml ($p \leq 0.050$).

A comparison of DCP content between NIVs hydrated with 1, 3 and 6mg/ml cisplatin and stored at 4°C showed no significant difference except for day 168 post-preparation, where the DCP content was significantly different ($p=0.003$) between the NIVs of all three types (Figure 5.43).

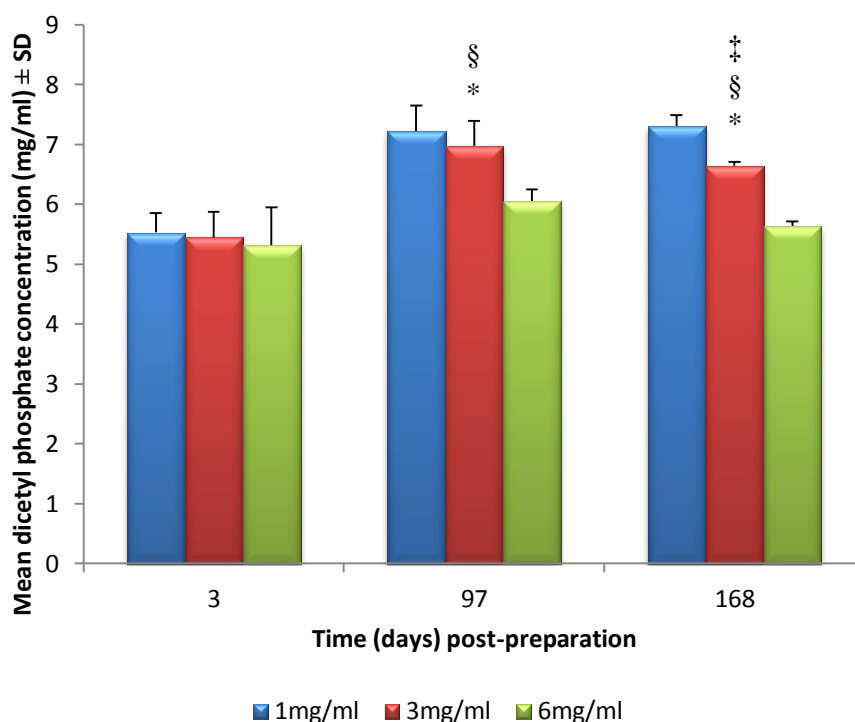


Figure 5.44. The concentration of dicetyl phosphate in processed NIVs hydrated with different cisplatin concentrations of 1, 3 and 6mg/ml and stored at 25°C/60% RH determined on days 3, 97 and 168 post-preparation (n=3). ‡ indicates significant difference between 1 and 6mg/ml. § indicates significant difference between 1 and 6mg/ml. * indicates significant difference between 3 and 6mg/ml ($p \leq 0.050$).

NIVs prepared with different cisplatin concentrations and stored at 25°C/60% RH showed significantly lower DCP content ($p=0.017$) in NIVs hydrated with 6mg/ml cisplatin as compared to the other two types of NIVs on day 97 post-preparation (Figure 5.44). Then on day 168 post-preparation the DCP content in all three types of NIVs were significantly different from each other ($p=0.000$).

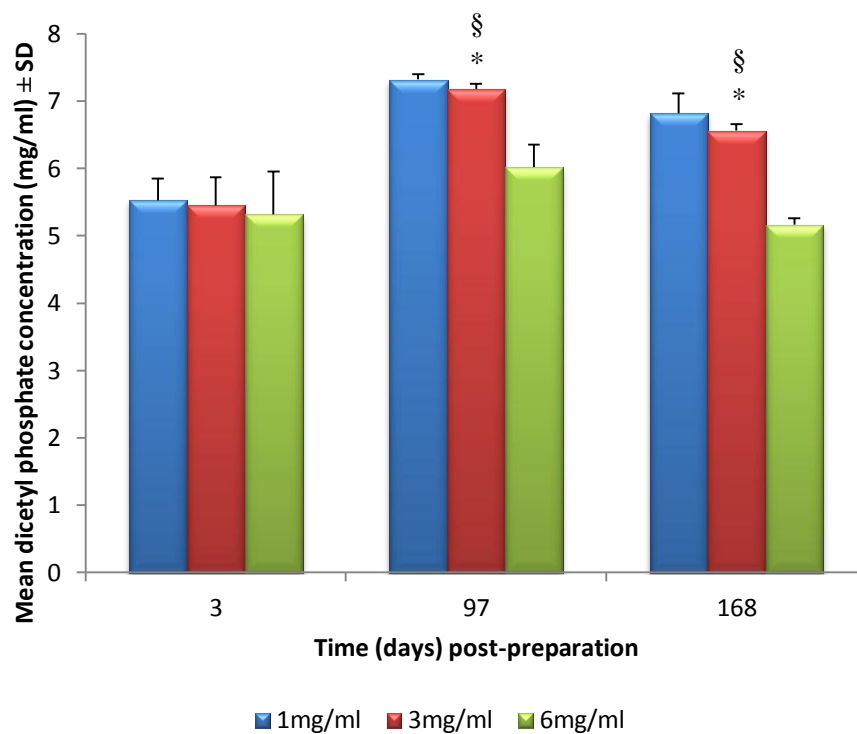


Figure 5.45. The concentration of dicetyl phosphate in processed NIVs hydrated with different cisplatin concentrations of 1, 3 and 6mg/ml and stored at 40°C/75% RH determined on days 3, 97 and 168 post-preparation (n=3). § indicates significant difference between 1 and 6mg/ml. * indicates significant difference between 3 and 6mg/ml ($p \leq 0.050$).

At 40°C/60% RH, the DCP content in NIVs hydrated with 6mg/ml cisplatin differed significantly from both NIVs hydrated with 1 and 3mg/ml on both days 97 ($p=0.000$) and 168 ($p=0.000$) post-preparation (Figure 5.45).

5.3. Discussion

In the first stability study empty and cisplatin NIVs were prepared, processed and aliquoted into glass vials under aseptic conditions. When the batches were aliquoted into the vials, it was observed that it was difficult to accurately measure empty NIVs into the vials, due to their increased viscosity, as compared to cisplatin NIVs which

could be easily measured due to their lower viscosities. Saline has been reported to reduce the viscosity of niosomes prepared with Span 60 in comparison to water (Arunothayanun and Florence, 2000). This explains the greater viscosity of the empty NIVs as water was used in hydrating the lipid components unlike the saline solution used in the preparation of the cisplatin NIVs. However, the inability to measure an accurate volume of empty NIVs could impede accurate assessment of lipid content in these NIVs per unit volume. Therefore, lipid content in empty NIVs was based on unit weight of lyophilised cake prior to lipid analysis as described (Section 2.2.7.1).

On day 1 post-preparation aliquoted NIVs formulations had not yet been allocated to final storage conditions and no signs of drug precipitation were obvious. As day 2 and 3 post-preparation fell on a weekend, all vials were stored at 4°C and subsequently transferred to final storage conditions on day 4 post-preparation. It was observed that after refrigeration of the samples over the weekend, cisplatin had precipitated out in vials containing cisplatin NIVs. Day 1 samples taken for analysis were not refrigerated and therefore no precipitation was observed. The low initial storage temperature could have accelerated the precipitation of cisplatin by lowering its solubility limit below 1mg/ml at 4°C, especially from the observation that the cisplatin concentration in the supernatant of cisplatin NIVs stored at 4°C did not exceed 0.5mg/ml (day 1 to 28 post-preparation) or 0.7mg/ml at later time periods. Marketed cisplatin solutions listed in the electronic Medicines Compendium indicated special storage precautions restricting the refrigeration of cisplatin solutions as it may lead to cisplatin precipitation (eMC, 2011). Furthermore, all processed cisplatin NIVs hydrated with 6mg/ml cisplatin and studied in Chapter 3 did not exhibit any signs of cisplatin precipitation throughout the course of their short-term study. Nonetheless, these NIVs were always kept at room temperature, with no refrigeration.

Over time, no apparent changes in the physical appearance of empty NIVs were observed that could indicate colloidal system instability such as sedimentation and flocculation (Junyaprasert *et al.*, 2009). Other than the precipitation of cisplatin, no signs of colloidal system instability were observed as well with cisplatin NIVs over

time. One observation however, was the slight discolouration of cisplatin NIVs, stored at 40°C/75% RH on day 469 post-preparation, with the suspension developing a noticeable light brownish yellow colour (Figure 5.1). As only the cisplatin NIVs stored at 40°C/75% RH temperature showed colour change, it would appear that elevated temperatures accelerate this process. It has been observed that cisplatin solutions, prepared for separate experiments since 2008/2009, and left at room temperature, had turned into a darker brown-yellow colour. The lighter colour shade observed in the NIVs from the stability study in comparison to the mentioned cisplatin solutions could be attributable to dilution of colour intensity by the NIVs suspension. This may indicate transformation of cisplatin. However if cisplatin was intended to be stored at lower temperatures then such instability may not be an issue over shorter time periods.

Between days 1 and 469 post-preparation, a significant fall in the entrapment efficiency of 60% and 50%, respectively, for processed cisplatin NIVs stored at 4°C and 25°C/60% RH was observed (Figure 5.2). This indicated cisplatin leakage from the lipid vesicles over time which corresponded with a significant increase in cisplatin supernatant concentration in the samples (Figure 5.4). Overall, it was observed that the concentration of cisplatin in the supernatant of NIVs decreased as the storage temperature decreased, possibly indicating lower cisplatin solubility. While the solubility of cisplatin did not exceed 0.7mg/ml at 4°C, an increase in solubility up to 1.4mg/ml was observed at 25°C. This agreed with the reported solubility of a saline solution of cisplatin (\pm SD) at room temperature, which reached 1.49 ± 0.21 mg/ml (Woo *et al.*, 2008). Accordingly, as cisplatin leaks out of the vesicles the concentration of cisplatin correspondingly increases in the supernatant within the solubility limit at the given conditions until beyond that limit released cisplatin starts to precipitate. This would mean that as the temperature decreases more cisplatin would be expected to precipitate.

At higher storage temperature (40°C/75% RH) increased aqueous solubility of cisplatin is anticipated and this is reflected in increased NIVs entrapment efficiency and cisplatin concentration in the supernatant compared to the two lower storage conditions (Figures 5.2 and 5.4). Although the entrapment efficiency was

considerably stable over time, a continuous and significant rise in untrapped cisplatin was observed from day 1 to 266 post-preparation at 40°C/75% RH (Figure 5.4). This could indicate that cisplatin that precipitated from day 4 post-preparation when NIVs were stored at 4°C prior to transfer at elevated temperatures, had started to slowly solubilise leading to increased concentration in supernatant. However, the observed change in colour of cisplatin NIVs stored at 40°C/75% RH (Figure 5.1) could indicate that whatever platinum species that was quantified was not actually cisplatin but another species. Brière *et al.* (1996) indicated that cisplatin in a saline solution was stable for at least 2 months and should not be kept for longer than 5 months at room temperature and protected from light. They studied the chemical properties of cisplatin solution over time using ¹⁹⁵Pt NMR and observed a reduced signal intensity for native cisplatin indicating degradation into other platinum species. As previously mentioned (Chapter 4), the adapted HPLC method in the present study is intended to measure only unbound forms of cisplatin but is not exclusive to native cisplatin itself. That means any platinum-containing species that are unbound can be detected with this method, as they will be available to chelate with DDTC and elute at the same retention time. Furthermore, these studies indicated that it is unknown whether these other detectable species are cytotoxic or not (Drummer *et al.*, 1984; Bannister *et al.*, 1979; Andrews *et al.*, 1984; Goel *et al.*, 1990).

However, the current analytical method used to determine entrapment efficiency may have contributed to the fluctuation in entrapment results, especially the unusual rise in entrapment on day 28 post-production for NIVs stored at 4°C. The HPLC method for analysing the NIVs on days 1, 28, 189 and 266 post-preparation was subsequently modified and differed from the modified analytical method used on day 469 post-preparation. The HPLC method used at the beginning of the stability study was not validated prior to it being adapted due to time constraints. Prior to every analysis, standards would be analysed to establish the calibration curve. It was noticed the inconsistency in the ratios were obtained in every calibration curve and that would influence the calculated amount in the NIVs. When the method was finally validated inconsistent results were obtained, which confirmed the unreliability of the original

analytical method which necessitated further development until a final HPLC method was reached.

The study of lipid content in empty and cisplatin NIVs at all storage conditions showed a similar pattern over time (Tables 5.1, 5.3, 5.5, 5.7, 5.9 and 5.11). Overall, variability in lipid content was observed over time, especially on day 189 post-preparation which generally showed a significant drop in lipid content particularly DCP. A possible reason could be lipid degradation. One of the main problems of liposomes with long-term stability in aqueous form is oxidation and hydrolysis of phospholipids (Grit and Crommelin, 1993).

This is one of the main reasons that niosomes are considered to be advantageous over liposomes. It is anticipated that non-ionic surfactants will be less susceptible to chemical degradation, thereby rendering niosomes more stable than liposomes. However, the surfactant used in the present study, $C_{16}H_{33}O(CH_2CH_2O)_4H$, belongs to the ethoxylated surfactant group that has been reported to be easily oxidised by atmospheric oxygen (Bodin *et al.*, 2003). In a study on a similar surfactant from the same group with the chemical structure $C_{12}H_{25}O(CH_2CH_2O)_5H$, the surfactant was kept at room temperature without light protection for 6 months. Following GC analysis in comparison to a fresh surfactant sample, it was found that surfactant oxidation resulted in multiple oxidation products including 5 aldehydes (Bergh *et al.*, 1998). Cholesterol as an unsaturated fatty acid may also be subjected to oxidation yielding oxidation products, with 7-keto-cholesterol the major and most stable product (Chang *et al.*, 1997). However, it has been reported that even under stressed conditions the oxidation rate is relatively low (Schnitzer *et al.*, 2007). Several studies have indicated the stability of cholesterol in liposomal formulations in comparison to phospholipids (Grit and Crommelin, 1993, Zhong *et al.*, 2010).

Nonetheless, any degradation product(s) would be evidenced by additional chromatographic peak(s) during analysis. Furthermore, if lipids had degraded by day 189 post-preparation, it would be expected that lipid degradation would also be observed in the later time points. Nonetheless, lipid content on days 266 and 469 post-preparation were relatively consistent with days 1 and 28 post-preparation. Therefore, the fall in lipid content on day 189 post-preparation could just be a

reflection of discrepancies in the instrumental quantification of the ingredients. To rule out the likelihood of lipid degradation, the mean lipid composition ratio (surfactant VIII: cholesterol: DCP) was determined for every time point (Tables 5.2, 5.4, 5.6 and 5.8) and compared over time and to the actual lipid ratio used in the preparation of the NIVs. Although some statistical significance was observed due to the very small values and small sample size, the general trend of the lipid ratios was considerably stable, especially day 189 post-preparation which was far more consistent with the other time points. Processed empty NIVs showed reasonable stability of cholesterol/DCP (Table 5.2) and surfactant VIII/DCP (Table 5.6) ratios over time and overall comparability to the actual ratios of cholesterol/DCP and surfactant VIII/DCP used to prepare the NIVs. Processed cisplatin NIVs showed reasonable stability of cholesterol/DCP (Table 5.4) and surfactant VIII (Table 5.8) ratios over time when stored at 4°C and 25°C/60% RH. However an increase in cholesterol/DCP and surfactant VIII/DCP ratios from day 266 post-preparation was observed at 40°C/75% RH. Furthermore, comparability to actual ratios was absent for cholesterol/DCP ratios and maintainable up to 28 days post-preparation for surfactant VIII/DCP ratios. The increase in lipid ratios of processed cisplatin NIVs especially at 40°C/75%RH was a reflection of decreased DCP values in the denominator. This will be further discussed below.

The lipid ratio between processed empty NIVs and lyophilised NIVs at each time point were comparable at all storage conditions (Figures 5.5 to 5.7 and 5.8 to 5.10). The lipid ratio of processed cisplatin NIVs, although apparently higher, were comparable to that of lyophilised NIVs although at prolonged time points a significant increase in the ratio was observed (Figures 5.5 to 5.7 and 5.8 to 5.10). Cisplatin NIVs stored at 4°C and 25°C/60% RH showed a significant increase in cholesterol/DCP and surfactant VIII/DCP ratios on day 469 post-preparation whereas NIVs stored at 40°C/75% RH increased significantly from day 266 post-preparation onwards. The fact that processed empty NIVs maintained similar lipid ratios as lyophilised NIVs, when subjected to the same storage conditions as processed cisplatin NIVs, seem to validate the low chances of lipid degradation during storage. However, with the increasing lipid ratios of processed cisplatin NIVs, in comparison

to lyophilised NIVs over time, and with increasing temperature, could indicate interaction of cisplatin with the lipid components, particularly DCP.

To further study this possibility, the actual DCP weights used in preparing empty and cisplatin NIVs were divided by DCP weights at each time point including starting amount. The DCP weight ratio was considerably stable over time and comparable to the starting actual time point (Table 5.10) for processed empty NIVs at all storage conditions. The DCP weight ratios over time for processed empty NIVs were also comparable to that of lyophilised NIVs (Figures 5.11 to 5.13).

In sharp contrast, the ratios of actual DCP/measured DCP were significantly higher than the actual starting time point for NIVs hydrated with 6mg/ml cisplatin (Table 5.12). The values observed in Table 5.12 would appear to confirm that there is a chemical interaction with cisplatin that is causing loss of dicetyl phosphate and that this is more noticeable at higher temperatures and prolonged time points.

The DCP weight ratios for NIVs hydrated with 6mg/ml cisplatin and then subsequently processed were also significantly higher than lyophilised NIVs over time and at each storage condition (Figures 5.11 to 5.13) strengthening the link between cisplatin interaction with DCP.

Several studies have reported the interaction of cisplatin with the phospholipid ingredients of cells and liposomes. Nonetheless, future studies comparing the recovery of DCP in the presence and absence of cisplatin would be beneficial in characterising what the mechanism of interaction is. In one study, the interaction between cisplatin and phosphatidylserine present in erythrocyte membrane was observed in damaged cells (Burger *et al.*, 1999). This was attributed to the loss of protective antioxidants such as glutathione. In another study, the reaction of cisplatin with the serine moiety of phosphatidylserine was proven by NMR and indicated that this reaction was likely to occur with the hydrated state (aquated species) of cisplatin (Jensen and Nerdal, 2008). The hydrated form of cisplatin was found to interact to a greater extent than cisplatin itself with negatively charged phospholipids, where no interaction was seen with zwitterionic lipids (Speelmans *et al.*, 1996). Differential scanning calorimetry (DSC) in this study, showed a change in transition temperature

of the phospholipid when hydrated cisplatin was used in comparison to cisplatin. In fact this property was exploited in the preparation of lipid coated aggregates of cisplatin formed by binding of hydrolysed cisplatin with a negatively charged phospholipid (Burger *et al.*, 2002; Velinova *et al.*, 2004).

Furthermore, hydrated forms of cisplatin have been reported to exhibit great reactivity towards phosphate which can readily displace coordinated water (Berners-Price and Appleton, 2000).

Therefore, in the present study the phosphate moiety of DCP seems to provide an attractive site for cisplatin interaction. The coordinate structure of cisplatin contains two nitrogen donor amine ligands (Sherman and Lippard, 1987; Haxton and Burt, 2009), rendering them strong hydrogen bond donors. As a result, the amines could possibly act as strong hydrogen bond donors with the hydrogen bond acceptors present on the lipids. Nonetheless, although cisplatin in the present study was prepared in 0.9% w/v NaCl in order to minimise hydrolysis, it has been estimated that cisplatin at physiological pH and in a solution containing chloride equivalent to extracellular chloride *in vivo* would produce an equilibrium involving native cisplatin (68%), $\text{PtCl}(\text{NH}_3)_2\text{H}_2\text{O}$ (7%) and $\text{PtCl}(\text{NH}_3)_2\text{OH}$ (24%) in about 6h (Berners-Price and Appleton, 2000).

However, the possible cisplatin–DCP interaction observed in the current studies does not appear to be significant enough to jeopardise the colloidal stability of the NIVs as observed by maintenance of an appreciable negative zeta potential. Speelmans *et al.* (1996) reported a reduced negativity of liposomal cisplatin as a result of cisplatin binding to the phospholipids. The binding of cisplatin to negatively charged phospholipids to form lipid coated aggregates also showed reduced negativity (Burger *et al.*, 2002). Shielding of vesicle surface charge can have serious effects on vesicle stability where unwanted vesicle aggregation can be induced. This has been observed with other drugs such as primaquine (Stensrud *et al.*, 2000) and doxorubicin (Fonseca *et al.*, 1997) where binding of the drug to the negatively charged phospholipids of their carrier liposomes resulted in charge shielding hence vesicle aggregation. Therefore in the present study, if the cisplatin–DCP interaction was significant it would be expected to see a lower charge in comparison to the other

NIVs. Nonetheless, the ZP of cisplatin NIVs in comparison to empty and lyophilised NIVs exhibited the highest negativity (Figures 5.21 to 5.23).

In the present research, vesicle size of cisplatin NIVs appeared to increase with increasing storage temperature (Figure 5.15). A likely explanation for the increased size is vesicle fusion or aggregation. Temperature can indirectly affect bilayer properties and induce vesicle fusion (Cevc and Richardsen, 1999). However, if temperature had an effect on vesicle size, an increased size of empty NIVs would also be expected. The size of empty NIVs was observed to remain stable regardless of the storage conditions (Figure 5.14). Unfortunately, the unavailability of size and ZP data for empty NIVs stored at 25°C/60% RH and 40°C/75% RH on days 266 and 469 post-preparation prevented a complete comparison. But from the available data it can be seen that cisplatin NIVs stored at 40°C/75% increased in size from day 28 post-preparation, whereas empty NIVs remained stable in size throughout the time period analysed at the same conditions, i.e. up to 189 post-preparation (Figure 5.18).

However some caution should be applied in interpreting the results. Statistically significant changes in the size results could simply be instrumental, although dynamic light scattering (DLS) is considered the preferred method of size characterisation. DLS is very sensitive to any other scattering particles such as dust particles (Cevc and Richardsen, 1999). In the case of cisplatin NIVs, precipitated cisplatin particles could affect the size measurement, although extreme care was taken in separating precipitated cisplatin by centrifugation there may have been some residual particulate contamination that varied between specific time points and impacted on the absolute values measured. Another issue with DLS is that the software presents size as a mean value of individual readings, meaning that an outlier value may significantly skew results. As size measurements are taken using replicates of the same sample, the results can be misleading where these results represent variations in the sample itself and not the whole population (Gaumet *et al.*, 2008). This is particularly more so when considering the possibility of contamination with dense cisplatin precipitates that may sediment to the bottom of the measuring cell during repeated measurements thereby altering the dynamic size range measured. As an example of the instrumental effects on size results, the size results for both

empty and cisplatin NIVs on day 266 post-preparation were found to show great variability with high SD values. On additional investigation it was discovered that one of the cuvettes used for the size measurement was faulty and resulted in unusually higher size measurements.

Significant changes in vesicle size, if due to aggregation and fusion, could be a result of bilayer defects induced by chemical degradation of lipid ingredients (Mohammed *et al.*, 2006). However, in the present study the only change in lipid content observed in cisplatin NIVs in comparison to lyophilised and empty NIVs was with DCP content, possibly due to chemical interaction with cisplatin. As mentioned previously, this interaction was not significant enough to reduce the vesicle charge. Furthermore, if the observed lower DCP content was a precursor for vesicle aggregation and fusion, an increase in vesicle size of cisplatin NIVs stored at 4°C would also have been expected. However, vesicle size at 4°C remained stable even though the DCP weight ratios were significantly high similarly to the other storage conditions (Figure 5.11 to 5.13).

Moreover, vesicle aggregation results from insufficient repulsion and causes the suspension to collapse into a dry lipid crystal (Cevc and Richardsen, 1999). In the present study, if cisplatin NIVs had undergone aggregation or fusion that would mean that they had managed to overcome the potential barrier. However, with the ZP of cisplatin NIVs reasonably stable over time, and always less than -30mV this would be deemed sufficient repulsion to prevent fusion and aggregation (Malvern, 2004). In addition, flocculation and sedimentation are reversible and irreversible physical forms of vesicle aggregation, respectively. However these were not observed.

Furthermore, with the possibility of vesicle aggregation and fusion seemingly unlikely, the significant variations in vesicle size of processed cisplatin NIVs between 660 and 1140nm are not likely to have a severe impact on clinical outcomes. Whether vesicle size was 660nm or 1140nm, both are expected to be easily and rapidly taken up by the mononuclear phagocytic system, which is the aim of the present study. Crommelin *et al.* (2001) indicated that all particles in the size range of 0.1 to 7µm are subjected to clearance by the MPS. An early study by Pratten and

Lloyd (1986) indicated that particle clearance increases with increasing size where particles with 1100nm diameters were cleared 10 and 60 times more than particles with 100nm and 30nm diameters, respectively. They also reported that clearance rate of 1100nm particles was about 2 times greater than 600nm particles, which further supports rapid uptake of particles in the size range between 660nm and 1140nm measured in the present research.

The comparison of empty and cisplatin NIVs to lyophilised NIVs in terms of vesicle size demonstrated significantly larger size of lyophilised NIVs than both empty and cisplatin NIVs (Figures 5.16 to 5.18). This was observed even though the lyophilised NIVs were prepared from the same batch of empty NIVs. It has been reported that the lyophilisation of lipid vesicles would cause vesicles to fuse and increase significantly in size and probably even form vesicles of a different type (Zhang *et al.*, 1997). During lyophilisation the sample is first subjected to freezing then sublimation, which is a primary drying step, then finally a secondary drying step (Fransen *et al.*, 1986). The damage to the vesicles can start from the freezing process where external medium freezes before the interior leading to an osmotic gradient across the lipid membrane (Izutsu *et al.*, 2011). This causes the salt concentration in the exterior to increase leading to osmotic stress and causing the vesicles to shrink (Fransen *et al.*, 1986). In absence of salts or osmotic gradient, the vesicle can also be ruptured as a result of the mechanical stress inflicted on the vesicle membranes caused by the growth of ice crystals (Zhang *et al.*, 1997). The ice crystals in-between the head groups of the vesicle membrane when dried leave spaces. During the rehydration process and due to the defective membranes, any entrapped material would leak and vesicles would fuse and increase in size (Chen *et al.*, 2010).

In general the size of cisplatin NIVs were larger in size than empty NIVs (Figures 5.16 to 5.18). Cisplatin liposomes have been reported to be larger than empty liposomes and with a polydisperse size distribution using atomic force microscopy (Ramachandran *et al.*, 2006). This was attributed as reported previously to the heterogeneous size and shape of cisplatin particles in solution form, which in turn affects liposomal size and entrapment efficiency. This could possibly explain the

fluctuated size and entrapment efficiency results of cisplatin NIVs in addition to the previously explained instrumental variations.

Another possible explanation of increased vesicle size of cisplatin NIVs comes from the previously reported instability of cisplatin itself beyond 5 months (Brière *et al.*, 1996). If cisplatin had changed into other chemical species, their size of the chemical species in solution form could be different, thereby changing vesicle size in return. The reaction of cisplatin with phosphate could also produce different platinum structures as suggested by Berners-Price and Appleton (2000).

Overall, although size results of cisplatin NIVs stored at 25°C/60% RH and 40°C/75% RH may refer to vesicle aggregation and fusion, the other properties do not support such a hypothesis. Visualisation of the NIVs could perhaps explain the discrepancies in the size of cisplatin NIVs. Visualisation could also be used to compare the morphological changes between empty, cisplatin and lyophilised NIVs at least at the launch and end of the stability study.

In the ZP study, lyophilised NIVs were found always to have higher ZP values (less negative) than both empty and cisplatin NIVs (Figures 5.21 to 5.23). This agrees with the results obtained previously in Chapter 3 where the influence of diafiltration on vesicle size reduction resulted in greater negativity of the same NIVs formulation. Therefore lyophilised NIVs although prepared from processed empty NIVs, were lower in charge because of the larger size than empty NIVs.

However an interesting observation was the equal or sometimes less negative charge of processed empty NIVs in comparison to processed cisplatin NIVs, although the latter were significantly larger in size (Figures 5.21 to 5.23). This somehow contradicts the previously observed trend of increased negativity with decreased vesicle size. However in this case there is a difference in the entrapped substance between empty and cisplatin NIVs. This could be related to bulkiness of cisplatin molecules in solution form in comparison to water molecules, which would result in cisplatin molecules occupying a larger interior space than water. This could result in greater electrostatic repulsion between the bilayers of cisplatin NIVs thereby increasing negativity. The larger size and greater negativity of sodium stibogluconate

NIVs in comparison to same NIVs hydrated with PBS was attributed to this explanation (Mullen *et al.*, 2000). The similar charge of empty and cisplatin NIVs despite the size difference, in some instances, could indicate the charge limit that DCP can confer regardless of size differences.

The second stability study was aimed at comparing NIVs hydrated with different concentrations of cisplatin at 1, 3 and 6mg/ml. In the first study, the problem with cisplatin NIVs was the undesirable precipitation of cisplatin. Therefore it was thought to lower the concentration of cisplatin used to hydrate the NIVs and compare their characteristics with NIVs hydrated with 6mg/ml cisplatin. Furthermore, it was thought to dilute all the NIVs to 0.5mg/ml with 0.9% w/v NaCl and allow 24h for the vesicles to adjust themselves to the concentration gradient in order to minimise leakage. As the NIVs hydrated with 6mg/ml would require greater dilution, diafiltration was performed on these NIVs first and time required for processing was recorded. The other preparations were processed until they had reached their original volumes and then recycled through the diafiltration membranes for the same amount of time as the NIVs hydrated with 6mg/ml cisplatin. This was to unify the processing time for all the NIVs formulations.

It was intended to carry out analysis over a one year period and at specific time points as planned with the first study. However due to time constraints and technical difficulties only 2 or 3 time points were analysed.

The physical appearance of the NIVs on day 97 post-preparation showed that cisplatin had precipitated from the NIVs hydrated with 6 and 3mg/ml. It was also noticed that precipitated cisplatin was greater with increased cisplatin concentration and was greater as storage temperature decreased. NIVs hydrated with 1mg/ml cisplatin on the other hand showed no signs of drug precipitation (Figure 5.24).

As observed and discussed previously (Chapter 3), it was not possible to measure the entrapment efficiency of NIVs hydrated with 1mg/ml cisplatin. Therefore, NIVs hydrated with 3 and 6mg/ml cisplatin only were analysed for entrapment efficiency. It appeared that the concentration of cisplatin used to hydrate the NIVs had an effect on the entrapment efficiency where the higher the concentration the greater the

entrapment efficiency (Figure 5.25). Only NIVs stored at 25°C/60% RH showed similar entrapment efficiency between 3 and 6mg/ml cisplatin. However, it could be observed that at this storage condition, the entrapment efficiency of NIVs hydrated with 6mg/ml cisplatin was significantly lower than the other two conditions on both time points analysed. This could explain why the entrapment efficiencies between NIVs hydrated with 3 and 6mg/ml cisplatin were similar at 25°C/60% RH.

Another observation was the unusual increase in cisplatin concentration in all NIVs from day 97 to day 168 post-preparation whether as entrapped, unentrapped or as total (Figures 5.25 to 5.27, Tables 5.13 to 5.15). This could further demonstrate the unreliability of the HPLC method used to analyse the cisplatin content, which was the same method used at the beginning of the first stability study.

However when the concentration of cisplatin entrapped inside the NIVs was compared to unentrapped cisplatin concentration on the same days, a different trend in entrapped cisplatin between NIVs hydrated with 3 and 6mg/ml cisplatin was observed. NIVs hydrated with 3mg/ml cisplatin were not as efficient as 6mg/ml cisplatin in entrapping cisplatin. The concentration of unentrapped cisplatin was greater than entrapped cisplatin when a 3mg/ml concentration was used (Figure 5.26), whereas the concentration of unentrapped cisplatin was lower than entrapped cisplatin when a 6mg/ml concentration was used (Figure 5.27). The increased entrapment efficiency with increasing drug concentration agrees with what has been suggested (Lasic, 1998).

Overall, the vesicle size of each NIVs preparation separately was considerably stable from day 97 to day 168 post-preparation (Tables 5.16 to 5.18). However, the vesicle size of NIVs hydrated with 6mg/ml cisplatin in comparison to 3mg/ml cisplatin was found to be significantly larger (Tables 5.19 to Table 5.21). This could further support the fact that increased entrapment correlates to increased vesicle size. However, this relationship was not observed when NIVs were hydrated with 1mg/ml cisplatin. Hypothetically, although the entrapment of NIVs hydrated with 1mg/ml cisplatin could not be determined, it would be expected that the entrapment efficiency would be less than hydrating with 3 and 6mg/ml cisplatin. Accordingly, if vesicle size were to decrease with decreased entrapment then NIVs hydrated with

1mg/ml cisplatin would be smaller in size. However, the size of NIVs hydrated with 1mg/ml cisplatin did not differ significantly from those hydrated 6mg/ml cisplatin on day 97 post-preparation and from those hydrated with 3mg/ml cisplatin on day 168 post-preparation (Tables 5.19 to 5.21). In Chapter 3, when the vesicle size of NIVs hydrated with 0.5 and 6mg/ml cisplatin were compared also no significant difference was observed. However, as discussed previously, just because vesicles differed significantly in size does not mean that their *in vivo* uptake will be proportionally compromised. A vesicle size range between 600 and 800nm will still be taken up efficiently by mononuclear phagocytic system.

Therefore it appears that entrapment efficiency is affected by vesicle size and drug concentration, where entrapment increases with increased vesicle size (processed and non-processed NIVs) and increased drug concentration. On the other hand vesicle size does not seem to be affected by entrapment efficiency when different concentrations of the same drug are used, but is affected by the type of material entrapped, for instance if water or cisplatin were used.

Overall, the ZP was also considerably stable for each NIVs preparation from day 97 to 168 post-preparation (Tables 5.22 to 5.24). The negativity between the different NIVs did not follow any pattern where in some instances ZP was different between all the NIVs and in other instances NIVs hydrated with 6mg/ml exhibited greater negativity or NIVs hydrated with 1mg/ml exhibited lower negativity than the other two NIVs (Tables 5.25 to 5.27). Most importantly, the ZP of all the NIVs never increased above -30mV.

The lipid content in each of the NIVs in general was relatively stable over time and did not differ from one storage condition to another (Figures 5.28 to 5.30, 5.34 to 5.36 and 5.40 to 5.42). Lipid ratio results also agreed with lipid content results indicating relative stability (Figures 5.28 to 5.30, 5.34 to 5.36 and 5.40 to 5.42). A comparison between the different NIVs showed that cholesterol and surfactant VIII content were similar whether NIVs were hydrated with 1, 3 or 6mg/ml cisplatin (Figures 5.31 to 5.33, 5.43 to 5.45). However it was noticed that NIVs hydrated with 6mg/ml cisplatin reasonably had a significantly lower DCP content than when hydrated with 1 and 3mg/ml (Figures 5.37 to 5.39).

In the first stability study, the lipid content and in particular DCP content was found to be less in NIVs hydrated with 6mg/ml cisplatin than empty NIVs. In the second stability study, NIVs hydrated with 6mg/ml cisplatin also showed lower DCP content than NIVs hydrated with the other lower cisplatin concentrations. This could suggest that the possible interaction between cisplatin and DCP could be directly related to the concentration of cisplatin used. Furthermore, increased temperature could further enhance such possible interaction.

From the agreement between size, ZP and lipid content results in both stability studies it seems that NIVs have the potential as a successful delivery system where they managed to overcome aggregation problems through sufficient repulsion and maintain the integrity of bilayer membrane structure where stable lipid content was maintained. According to the British Pharmacopeia, the recommended storage condition of cisplatin is at 25°C protected from light, and NIVs at this temperature were stable. However the use of NIVs as cisplatin carriers, a major limitation lies in their inability to maintain stable entrapment efficiency thereby resulting in drug precipitation outside the vesicles. Therefore it appears that entrapment of cisplatin in NIVs needs to be optimised. One mechanism suggested to maintain vesicle stability over long periods of time is lyophilisation, but with the use of a lyoprotectant to minimise vesicle aggregation and drug leakage (Izutsu *et al.*, 2011; Zhang *et al.*, 2008). However, the effect of lyophilisation and rehydration on cisplatin itself, especially in a high concentration of 6mg/ml, will need to be studied in additional detail.

Another suggestion would be to prepare NIVs with a lower cisplatin concentration such as 1mg/ml. This concentration did not show any signs of precipitation when studied in the second pilot production. Of course this would contradict the hypothesis of increasing drug concentration to enhance entrapment, thereby NIVs with low entrapment efficiency would be obtained. But a high entrapment was required because the vesicles would be separated from untrapped drug. However, it is intended in this case to administer NIVs without separation of untrapped drug. Therefore the required concentration would be administered as entrapped and free form. Another issue is how to determine the entrapped amount if low cisplatin

concentrations decreases the NIVs viscosity and prevents separating entrapped and unentrapped drug by ultracentrifugation. Although NIVs would be used without separation of free drug, but still determining the entrapment efficiency is crucial to assess the stability of the NIVs and whether stable entrapment is maintained. Entrapment efficiency determination can play a role in interpreting any related *in vivo* data. For instance, this can assist to determine if NIVs do actually deliver most of the drug or if the uptake of the unentrapped majority is facilitated by NIVs and if a prolonged effect would be obtained. Therefore, different separation techniques other than ultra-centrifugation should be considered.

The lyophilisation of NIVs may still be a necessary step even with the use of low cisplatin concentrations, since the transformation of cisplatin is probably inevitable. Accompanying *in vitro* and *in vivo* studies may provide the means to evaluate any changes in cytotoxic activity.

To assist the optimisation of cisplatin entrapment in NIVs and determine their stability, a few points should be taken into consideration.

As the HPLC method used to analyse the NIVs for the majority of the first stability study and all of the second study turned out to be unreliable, it should be confirmed that any analytical method used prior to commencing any stability is completely reliable through validation. It might also be appropriate to use other methods for platinum detection if HPLC is not reliable e.g. ICP-MS.

Supporting vesicle size results using DLS with suitable imaging techniques e.g. freeze fracture electron microscopy, can provide detailed insight into any morphological differences.

5.4. Conclusion

From the stability studies performed it can be concluded that NIVs prepared with surfactant VIII, cholesterol and DCP have proven to provide stable vesicular structures in the absence of cisplatin. Stable vesicle size with sufficient repulsion and chemical stability was obtained with no physical signs of sedimentation or flocculation at 4°, 25°C/60% RH and 40°/75% RH. However, the utilisation of these NIVs as delivery vehicles for cisplatin, despite maintaining stable size, charge and chemical stability, did not meet one of the generally regarded standards for vesicular systems. Using a high cisplatin concentration to enhance entrapment efficiency can be achieved but long-term stability could not be maintained, with cisplatin precipitation observed. Lowering the cisplatin concentration may solve the problem of drug precipitation, but alternative ways to separate entrapped from free drug are required to assess entrapment efficiency. The possibility of cisplatin interacting with DCP would be interesting to study to assess its impact on long-term colloidal stability of cisplatin NIVs. With the required storage temperature of cisplatin at 25°C, it would be logical to perform long-term stability studies for niosomal cisplatin suspensions at that temperature, as the use of higher temperatures may not be a true representation of performance over time. Another alternative worth pursuing in greater detail would be the storage of niosomal cisplatin in lyophilised form to overcome some of the limitations of systems stored in an aqueous form.

Chapter 6. *In vitro* evaluation of cisplatin NIVs – a preliminary study

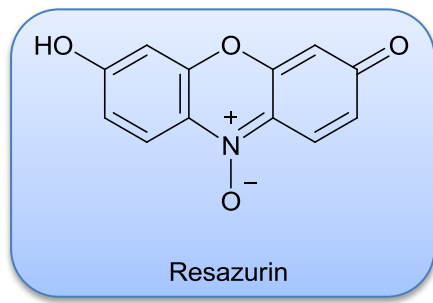
6.1. Introduction

Cytotoxicity studies are a necessity prior to the clinical use of any drug, whether it is to prove the ability of a particular drug to kill cancer cells or to establish a drug's safety against normal cells. Cytotoxicity studies that start off with *in vitro* assays and then progress to *in vivo* assays are highly recommended as they can provide an initial drug profile estimate that can be adapted for the later *in vivo* studies. This way the number of animal experiments can be minimised, which is of great ethical and economical importance. Therefore, the use of *in vitro* studies when possible are encouraged because they can provide a cheaper, easier to perform and reproducible alternative to *in vivo* studies (Wilson, 1992; Freshney, 1994a).

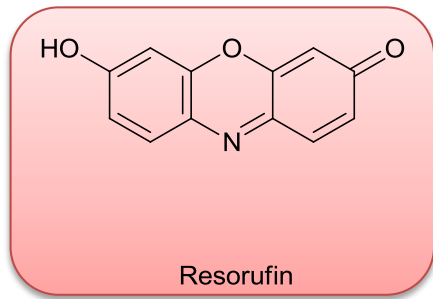
In vitro cytotoxicity studies may be achieved by measuring the effect of the drug under study on the membrane integrity or the metabolic events of a particular cell line that can be directly or indirectly related to cell death (Wilson, 1992). Alamar Blue (AB) is considered to be a safe, simple and cheap method that allows rapid assessment of cell proliferation and is non-toxic to cells thereby allowing further studies on the cells unlike the 3-(4,5-dimethylthiazol-2-yl)-2,5-diphenyl-tetrazolium bromide (MTT) test in which the cells die at the end and need to be discarded (Ahmed *et al.*, 1994).

AB was first developed to detect bacterial and yeast contamination of milk and the quality of semen (O'Brien *et al.*, 2000). It has shown success in both proliferation and cytotoxicity studies in bacteria (Sarker *et al.*, 2007) and mammalian cells whether they were normal (Ahmed *et al.*, 1994; Slaughter *et al.*, 1999) or cancerous (Hamid *et al.*, 2004; Anoopkumar-Dukie *et al.*, 2005).

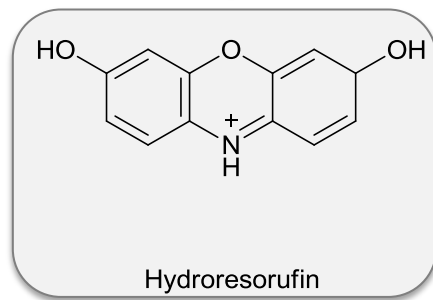
AB contains resazurin as the active ingredient responsible for the results obtained by the assay. Due to the metabolic activity of proliferating cells, oxygen consumption leads to the reduction of resazurin from the oxidised blue colour to a reduced red compound called resorufin (O'Brien *et al.*, 2000) through the irreversible loss of the oxygen attached to the nitrogen of phenoxazine (Guerin *et al.*, 2001). This reaction is illustrated in the equation below.



Reduction by
proliferating
cells



Extensive
reduction by
proliferating
cells



It is suggested that AB enters the cytoplasm of cells and as a result of mitochondrial enzyme activity, resazurin accepts electrons from NADH (reduced nicotinamide adenine dinucleotide), NADPH (reduced nicotinamide adenine dinucleotide phosphate), FADH (reduced flavin adenine dinucleotide) or FMNH (reduced flavin mononucleotide) and the cytochrome resulting in its reduction to resorufin which can be detected spectrophotometrically and spectrofluorometrically (Al-Nasiry *et al.*, 2007).

However, resorufin can be further reduced to a colourless and non-fluorescent compound called hydroresorufin due to excessive reduction by proliferating cells, which can lead to unreliable results where spectrophotometric analysis would indicate cell death that does not exist (O'Brien *et al.*, 2000). Also, because the reduction of resazurin to resorufin is irreversible, dying cells could change the colour at the beginning thus giving an overestimation of cell viability (Ahmed *et al.*, 1994). Therefore, optimisation of AB assay conditions is crucial for its reliability. Such conditions, which vary from one cell line to another due to their different metabolic properties, include concentration of AB used; exposure time and cell density and viability (Nakayama *et al.*, 1997).

Once a cell line has been chosen, it is important that the cells are in an active proliferative state for performing cytotoxicity assays. The proliferation of cells goes through three stages of what is known as the growth cycle. The first phase is known as the lag phase and it is the phase where cells are accommodating to their new environment and not growing much. Afterwards, the cells enter into the second phase known as the log phase or the exponential phase. In this phase an exponential increase in cell numbers occurs until confluence is achieved. That is when the cells enter the third phase known as the stationary phase or the plateau phase where cell growth is minimised or even seized and sometimes the cells might start to die. It is the exponential phase where cells are highly viable and the optimal time where cells should be chosen for sampling (Freshney, 1994b).

The range of cell numbers in the exponential phase can then be used to optimise the concentration of AB and duration of exposure. Many studies have indicated the use of AB at a 10% (v/v) concentration as instructed by its manufacturer (Ahmed *et al.*,

1994; Hamid *et al.*, 2004). However a range between 5-25% (v/v) has been reported as well (Gloeckner *et al.*, 2001) and even as low as 1% was reported (McMillian *et al.*, 2002). Because cells lines can differ in their metabolic rates, incubation time with AB can range from 2-72h depending on how fast cells are proliferating (Gloeckner *et al.*, 2001). Once the AB concentration and exposure time have been optimised, it is important that the cell density chosen for cytotoxicity studies is within the range where a linear relationship between AB reduction and cell number exists. A cell density above that range even if it is in the log phase could lead to excessive reduction of AB, hence unreliable results.

In this research, the use of 5% AB for a 24h incubation period was used to optimise the cell density in the log phase that can be used in cytotoxicity studies based on the proliferation assay. Accordingly, the first cytotoxicity study investigated the efficacy of cisplatin solution on the proliferation of murine B16-F0 melanoma cells. Then a comparison between entrapped and free cisplatin on cell proliferation was conducted. The toxicity of the NIV vehicle was also evaluated.

6.2. Results

B16-F0 cells used in the *in vitro* studies were harvested and passaged as described (Section 2.2.8.1).

6.2.1. *In vitro* proliferation studies

As described (Section 2.2.8.2), AB was used to study the proliferation of B16-F0 cells. By plotting the % growth of the cells against their corresponding density, a proliferation curve was obtained (Figure 6.1). As can be observed, the growth of cells increased as their numbers increased up to 3.125×10^5 cells/ml where maximum growth (\pm SEM) was reached at $83 \pm 0.9\%$. Afterwards the proliferation of cells had ceased and no further proliferation beyond this point, as measured by AB reduction, even as the number of the cells increased up to 1.25×10^6 cells/ml, where the % cell growth started to decline. After a 24h incubation period, a direct linear relationship between AB reduction and cell density was observed in the range

between 39062 and 312500 cells/ml where the correlation coefficient was 0.934. A cell density of 1.88×10^5 cells/ml was chosen from the linear range as the optimum cell density used in the cytotoxicity assays.

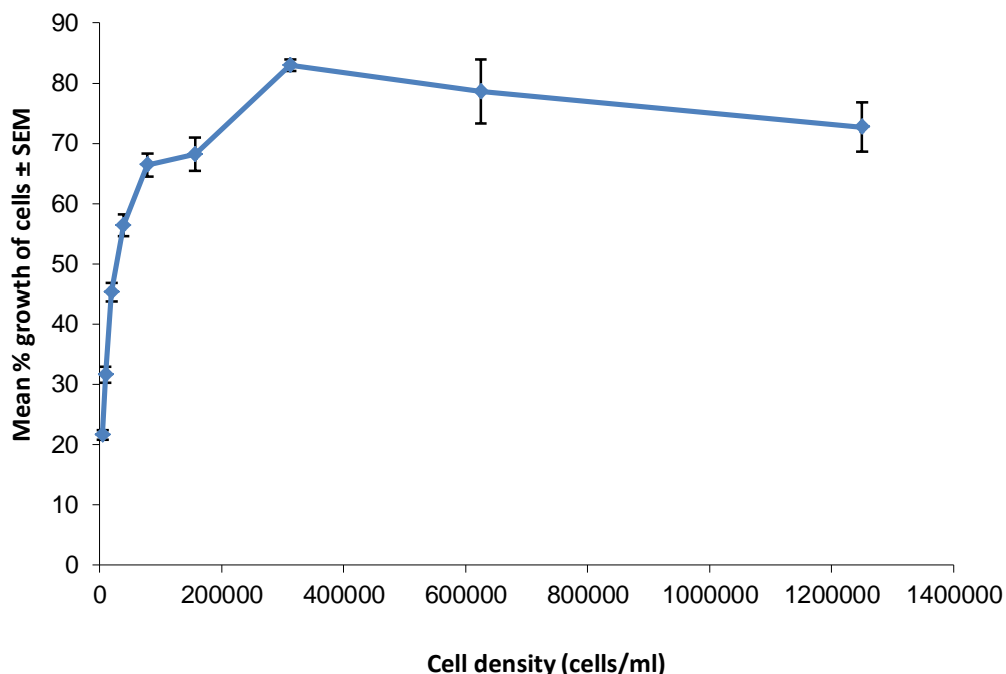


Figure 6.1. The proliferation of B16-F0 using AB after a 24h incubation period with a starting seeding density of 1.25×10^6 cells/ml serially diluted down to 4882 cells/ml (n=6).

6.2.2. *In vitro* cytotoxicity studies

As described (Section 2.2.8.3), the cytotoxic effect of cisplatin solution on the proliferation of B16-F0 was investigated in the first part of the study. The results obtained by AB showed a direct relationship between the concentration of cisplatin and inhibition of cell growth was observed. Fewer cells were dying at lower cisplatin concentrations as indicated by the change of AB to a red colour whereas increasing cisplatin concentration resulted in cell death as recognised by the blue colour of AB remaining unchanged. By representing the the results through fitting the data in a

sigmoidal dose-response curve (Figure 6.2), the growth inhibitory concentration of cisplatin solution for 50% of the cell population (IC_{50}) was 0.4006mM

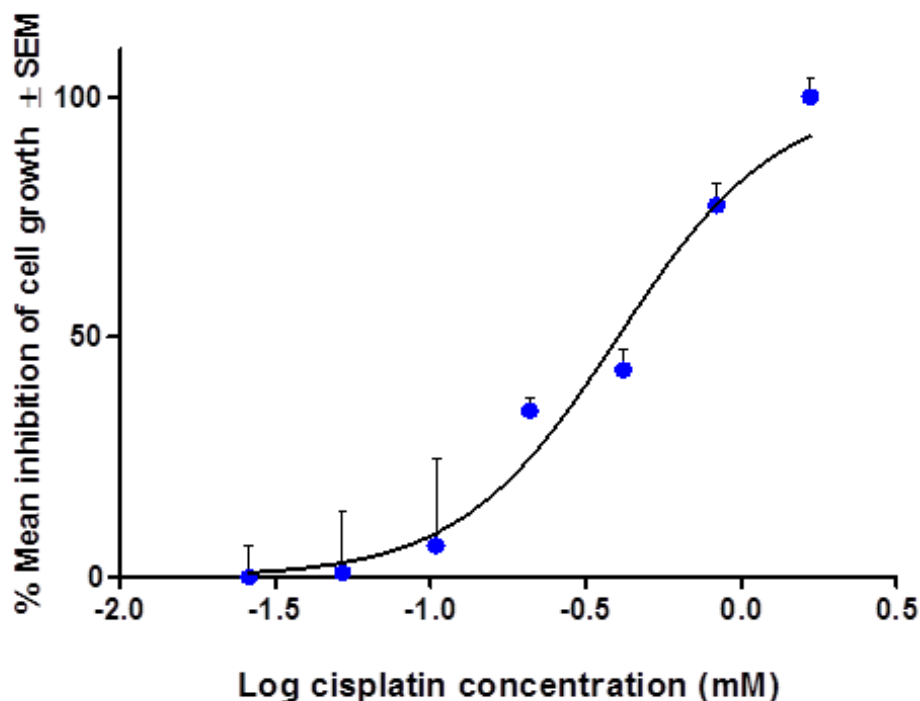


Figure 6.2. The effect of cisplatin solution with a starting concentration of 1.667mM serially diluted down to 0.026mM on the proliferation of B16-F0 seeded at a density of 1.88×10^5 cells/ml incubated for 24h with AB as represented by a sigmoidal dose-response curve (experiment performed once with $n=6$ for each concentration level).

In the second part of the cytotoxicity studies, the cytotoxic effect of cisplatin NIVs in comparison to cisplatin solution on the proliferation of B16-F0 cells was studied. An empty NIV formulation was also investigated for the safety of its ingredients towards cellular activity (Figure 6.3). The results revealed an improved cytotoxicity profile of cisplatin NIVs in comparison to cisplatin solution through the enhanced inhibitory effect on the cells. Although at the starting concentration of 1.667mM cisplatin NIVs, solution and empty NIVs exhibited the same level of toxicity; different

toxicity profiles were achieved when the formulations were diluted. At 0.833mM, cisplatin NIVs significantly inhibited the proliferation of B16-F0 cells (\pm SEM) by $42.6 \pm 2.1\%$, in comparison to cisplatin solution which inhibited cellular proliferation by $27.6\% \pm 4.9$ ($p \leq 0.05$). Significant cytotoxicity of cisplatin NIVs over cisplatin solution was observed down to 0.417mM. At lower concentrations cisplatin NIVs were ineffective. The effect of empty NIVs on the proliferation of B16-F0 changed significantly ($p \leq 0.05$) from being cytotoxic at 1.667mM to non-toxic at 0.833mM and lower, indicating the lack of toxicity from NIV components at these concentrations and the exclusive toxic affect arising from cisplatin itself without any synergistic effect.

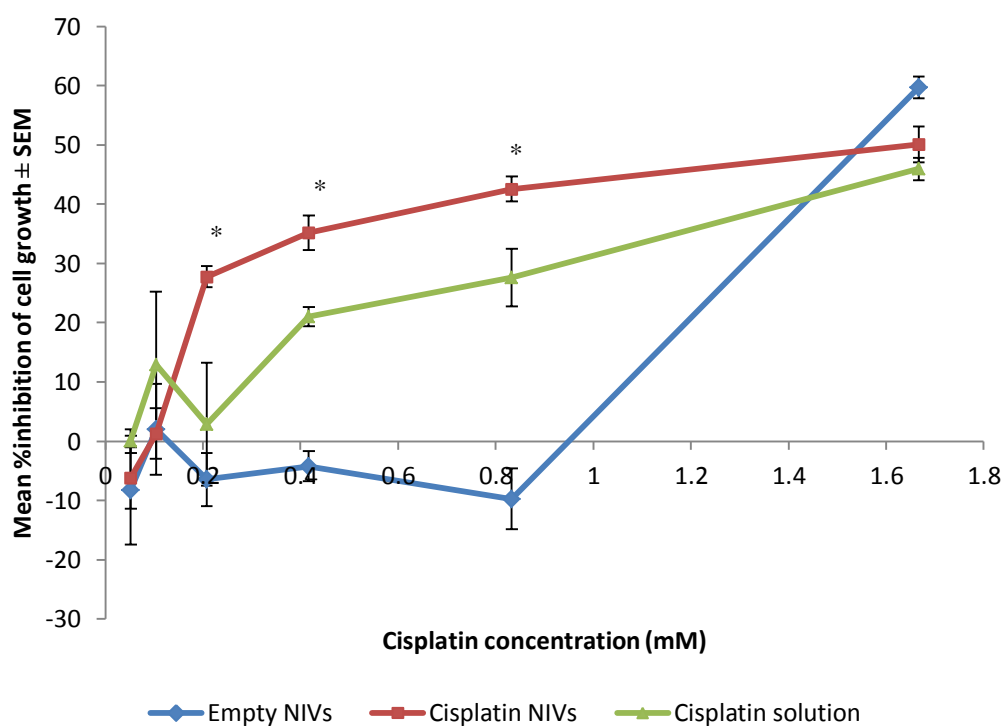


Figure 6.3. Comparison between the effect of cisplatin NIVs, cisplatin solution and empty NIVs at a starting concentration of 1.667mM and serially diluted down to 0.052mM on the proliferation of B16-F0 seeded at a density of 1.88×10^5 cells/ml and incubated for 24h with AB (n=6). * indicates a significant difference between cisplatin NIVs and solution ($p \leq 0.05$).

Fitting the data into a sigmoidal dose-response curve (Figure 6.4) showed that IC_{50} for each treatment group was significantly different ($p < 0.0001$) from the other. This indicated that cisplatin NIVs had a greater cytotoxic effect being approximately 2 times and 4 times more cytotoxic than cisplatin solution and empty NIVs, respectively. The IC_{50} values for cisplatin NIVs, cisplatin solution and empty NIVs were 0.33, 0.63 and 1.18mM, respectively.

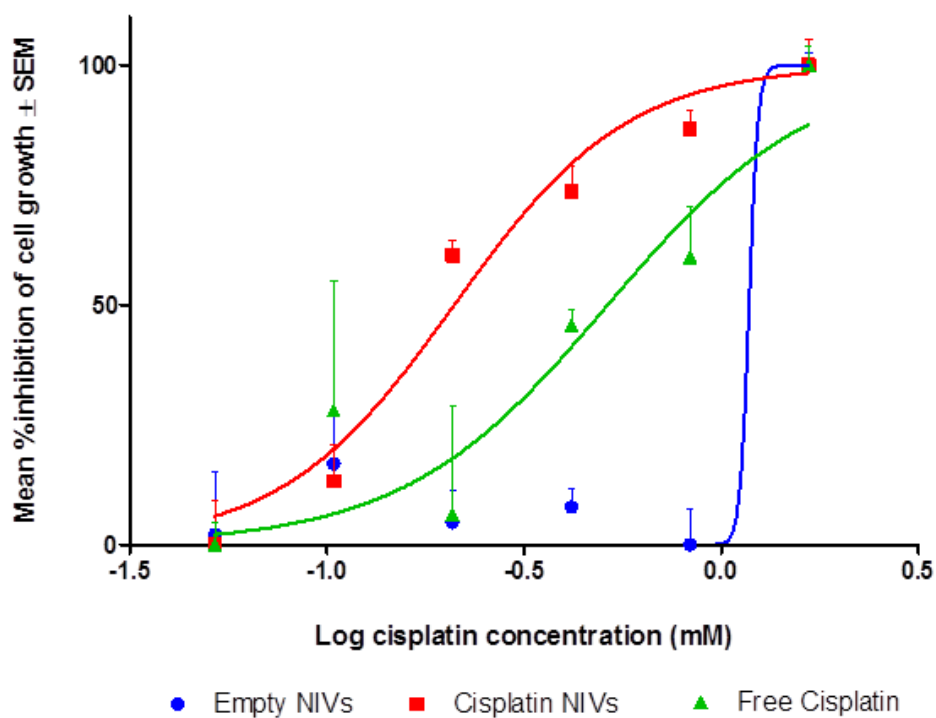


Figure 6.4. The effect of cisplatin NIVs, cisplatin solution and empty NIVs at a starting concentration of 1.667mM and serially diluted down to 0.052mM on the proliferation of B16-F0 seeded at a density of 1.88×10^5 cells/ml and incubated for 24h with AB represented by a sigmoidal dose-response curve (experiment performed once with $n=6$ for each concentration level).

6.3. Discussion

The reduction of AB from the oxidized blue colour to the reduced red colour is a reflection of cellular metabolic activity where the amount of AB reduced is proportional to the number of proliferating cells. This colour change is accompanied by a structural change in AB that could be measured colorimetrically or fluorometrically (Nikolaychik *et al.*, 1996; Gazzano-Santoro *et al.*, 1997). In the *in vitro* proliferation study on B16-F0, a growth evaluation of the cells was performed in relation to cell density. The obtained growth curve facilitated the determination of the optimum cell density that lies in the linear range between AB reduction and cell number that can be used for cytotoxicity assays. This method was described by Alley *et al.* (1988) where the relation between cell density and absorbance using microculture tetrazolium assay (MTA) and microculture cellular protein assay (MPCA) was used to establish a growth curve and detect the density range that shows linearity with the resulting absorbance. From the different cell lines that were tested with these assays, correlation coefficients of 0.89-0.98 for MTA and 0.94-0.99 for MPCA were reported and considered to be excellent. With AB, correlation coefficients were reported at 0.99-0.995 (Nikolaychik *et al.*, 1996) and 0.997 (Gazzano-Santoro *et al.*, 1997).

As expected with an approved drug for treating cancer, cisplatin solution showed an inhibitory effect on the growth of B16-F0 cells in a concentration dependent manner (Figure 6.2). However, the use of NIVs as a delivery system (Figure 6.3) enhanced the uptake of cisplatin by B16-F0 cells as demonstrated by the significantly higher cytotoxic effect of cisplatin NIVs, in terms of IC_{50} (Figure 6.4), over the free drug on their proliferation using AB even though the cell line is not recognised as being phagocytic. A similar study using negatively charged phosphatidylethanolamine liposomes containing cisplatin also demonstrated significant cytotoxic effect of liposomal cisplatin against the solution form on the B16-F0 cell line using MTT (Hwang *et al.*, 2007). The improved cytotoxic effect was attributed the enhanced uptake of cisplatin using liposomes, which was suggested to occur either by endocytosis of the liposomes or by fusion of the lipid bilayer with the cell membrane (Hwang *et al.*, 2007). Ranade (1989) suggested that negatively charged vesicles are

more likely to fuse with cell membranes thereby releasing their contents into the cytoplasm of cells. Therefore, the negatively charged NIVs may also enhance cisplatin delivery to the cells through fusion of the NIVs bilayer with the cellular membrane. Enhanced cytotoxic effect of cisplatin NIVs in comparison to cisplatin solution could reflect enhanced accumulation of cisplatin in cancer cells by NIVs. Low accumulation of cisplatin in cancer cells is one of the precursors for chemoresistance which is a disadvantage in conventional cisplatin chemotherapy (Kelland, 2007).

However, the results obtained by the present *in vitro* study may not necessarily correlate with the actual fate of cisplatin NIVs *in vivo* and whether a significant effect in comparison to cisplatin solution is obtained *in vivo* as well or not. *In vitro* studies may be inadequate for a complete evaluation of the potential of the delivery system as it does not take into account the different physiological barriers present *in vivo*. For instance, when the effect of sPHL-DDP was compared to cisplatin solution on the growth of baby hamster kidney cells by MTT as an indication of renal toxicity, similar cytotoxic effects from both formulations were observed (Júnior *et al.*, 2007b). But *in vivo* assessment of both formulations showed lower renal accumulation of cisplatin following liposomal administration thereby contradicting the *in vitro* investigation (Júnior *et al.*, 2007a). Contradictory results were also observed from a different *in vitro* assay based on studying the retention of cisplatin in liposomes. In that study, thermosensitive liposomes designed to release cisplatin at temperatures higher than 37°C were able to retain entrapped cisplatin at 37°C for an hour *in vitro*. But when these liposomes were injected into mice, whose core body temperatures were maintained at 37°C, 50% of the entrapped cisplatin was released in the plasma between 1-1.5h from the liposomes as a result of other critical factors that determine *in vivo* fate (Woo *et al.*, 2008). A review by Shabbits *et al.* (2002) supported the fact that *in vitro* retention of any drug by liposomes may be jeopardised *in vivo* due to a different environment where drugs can distribute into the large membrane pool offered by the blood cells and tissues. This indicates the requirement of further studies to support the possibility of NIVs in enhancing cisplatin delivery *in vivo*.

An unusual observation from the *in vitro* results was the sudden change in the toxic effect of empty NIVs just by a 1:2 dilution (Figure 6.3). This impacted the resultant IC_{50} of empty NIVs (Figure 6.4), which although was significantly lower than that of cisplatin NIVs and solution, could have been even greater than 1.18mM. A simple explanation could just be an indication that the lipid components were toxic at that concentration, but if there was an effect from the lipid components then a combination of toxicity from entrapped cisplatin and lipids would be seen. So if at 0.833mM the % suppression by cisplatin NIVs is 42.6% and empty NIVs was less than zero, that would mean that at 1.667mM if empty NIVs killed about 60% of the cells it would be logical that cisplatin NIVs would have a significantly higher toxic effect, which was not obtained. A possible explanation would be that at 1.667mM because 100 μ l of the formulation at its starting concentration was added and finished with 100 μ l of complete medium containing cells and dye, those wells would contain less medium compared to the other wells which contain 100 μ l of drug that was serially diluted with medium to half the concentration, therefore the other wells would contain 50 μ l more medium. This could indicate that the cells are dying because of insufficient nutrients rather than a toxic effect exhibited by the formulation. Historically, when empty NIVs have been intravenously injected into mice by the supervisors, no toxicity of any type was observed, thereby emphasising the importance of performing *in vivo* studies without an over-reliance on *in vitro* studies alone.

6.4. Conclusion

In vitro studies are a useful means of providing insight into the toxicity profile of a particular drug and screening its activity alone or in combination with a delivery vehicle. But with an established anti-cancer drug as cisplatin with renowned effectiveness towards cancer, the *in vitro* studies were used to investigate the impact of NIVs as a delivery system on the activity of cisplatin. From the studies it was shown that the NIVs not only were able to deliver cisplatin to exert its anti-cancer effect, but also to enhance its toxicity against cancer cells. However, in clinical use cisplatin NIVs will not be administered directly to the cancer cells and will have to

bypass physiological barriers related to the route of administration, combined with the physicochemical properties of the formulation that will govern the nature of these interactions. These factors can control the amount of drug that reaches the tumour cells. Therefore, although the NIVs showed favourable results *in vitro*, further *in vivo* studies are required to demonstrate the superiority of NIVs as a delivery system in enhancing anti-cancer effect of cisplatin and endorse the *in vitro* findings.

Chapter 7. *In vivo* evaluation of cisplatin NIVs – a preliminary study

7.1. Introduction

The process for the regulatory approval of any therapeutic agent needs to be endorsed by preclinical studies (Arentsen *et al.*, 2009). Although *in vitro* studies can prove successful whilst taking into consideration humane and economical aspects (Freshney, 1994a), they have not reached the stage to completely replace *in vivo* studies (Welch *et al.*, 1997). Therefore, the necessity of *in vivo* studies to endorse *in vitro* results is important, and is regarded as critical in the process of drug approval (Becker *et al.*, 2010).

Preclinical studies require the novel drug or drug formulation to demonstrate enhanced safety and/or efficacy in comparison to conventional therapeutics in animal models (Talmadge *et al.*, 2007). Therefore, it is critical to select a clinically relevant animal and tumour model to study tumour biology and drug activity (Heindryckx *et al.*, 2010). Rodent models have been considered as the most suitable for preclinical efficacy studies, where they have played a historical role in establishing the activity and the ultimate clinical approval of more than 100 anticancer drugs (Hollingshead, 2008). The use of such models for toxicological studies have also played a reliable role in identifying safe initial doses for phase I human studies (Talmadge *et al.*, 2007). Nevertheless, there are cases where rodent models can provide an overestimation of drug activity and the drug subsequently fails to establish effectiveness during human trials (Hollingshead, 2008). Despite that, the mouse has proven an excellent platform for cancer modelling (Carver and Pandolfi, 2006). The value of mouse models in cancer research owes to the genetic and physiologic similarity to humans, where the mouse genome has been found to be sequenced and annotated to a high standard, second only to that of humans (Mattison *et al.*, 2009). Also, mice can breed well in captivity and have a rapid rate of reproduction and can be maintained in limited space in large numbers because of their small size (Mattison *et al.*, 2009).

Therefore, in the present study mouse model was used to evaluate the therapeutic effectiveness of NIVs in enhancing cisplatin uptake and anti-tumour activity by

exploiting the mononuclear phagocytic system (MPS). Single doses of cisplatin NIVs or solution administered by intravenous or pulmonary routes were compared against a metastatic lung cancer model of B16-F0 melanoma. Intravenous administration was chosen as cisplatin is conventionally administered as an intravenous infusion (O'Dwyer *et al.*, 2000). Inhalation therapy was chosen as a non-invasive localised route of treatment to target lung cancer. This offers the advantage of providing rapid action and minimising systemic exposure thereby delivering higher concentrations to the lungs and subsequently may allow reduction of the dose normally administered systemically (Labiris and Dolovich, 2003a).

Furthermore, the mouse has been used as a preclinical model in the evaluation of many liposomal cisplatin formulations such as SPI-077 either alone (Newman *et al.*, 1999; Zamboni *et al.*, 2004) or in combination with other drugs such as doxorubicin (Harrington *et al.*, 2000b), pH sensitive liposomes (Júnior *et al.*, 2007a, Leite *et al.*, 2009) and other liposomal formulations (Hwang *et al.*, 2007; Woo *et al.*, 2008; Schroeder *et al.*, 2009; Hirai *et al.*, 2010).

The rat has also been used as a model in evaluating liposomal cisplatin (Devarajan *et al.*, 2004). In the present study, the rat model was used in a preliminary evaluation of pharmacokinetic profile of cisplatin NIVs in comparison with drug solution. This was primarily due to the larger blood volume that can be collected for pharmacokinetic studies in comparison with mice.

7.1.1. Theory of vibrating plate technology in inhalation therapy

Inhalation therapy was performed using vibrating plate technology. In this technology an aperture plate or mesh vibrates to produce a liquid aerosol with high fine-particle fraction (Siekmeier and Scheuch, 2008). The nebuliser used in the present chapter, Aeroneb[®] Lab nebuliser system, was supplied by Aerogen Inc. This system utilises the patented OnQ[™] aerosol generator utilising micropump technology. With its unique wafer-thin dome-shaped aperture plate with more than 1000 holes, this structure acts as a micopump where it vibrates over a 100000 times per second when energy is applied to the surrounding vibrational element. OnQ produces a fine liquid mist, between 1-5 μ m in particle size, designed for pulmonary

therapy and is capable of delivering a broad range of drugs in solution or suspension form. The advantage of this technology lies in its ability to aerosolise a complete dose without leaving any residue, preserve drug stability as it does not generate heat or require propellant and efficiently produce consistently sized high quality respirable aerosols to target deep lung delivery and avoid deposition in the nasopharynx area thereby rapidly delivering a predictable and reproducible dose (Aerogen, 2010).

7.1.2. Theory of inductively coupled plasma mass spectroscopy (ICP-MS)

ICP-MS was employed in detecting the platinum levels in rats for the pharmacokinetic study, instead of HPLC-UV method employed in the detection of platinum levels in mice.

The basis of ICP-MS involves reducing a sample to ions by the ICP then separating the ions of interest by a magnetic field to be measured by a mass detector. Reducing a sample or generating ions from a sample occurs through a series of steps involving aerosolisation, drying, decomposition, vaporisation, atomisation and then finally ionisation (Montaser *et al.*, 1998).

When a sample is introduced into the system, the sample is mixed with argon gas to form an aerosol. The nebulised aerosol is passed into the plasma torch consisting of three concentric quartz tubes, where aerosol is passed in the central tube. As the aerosol reaches the end of the torch, an induction or load coil wrapped around the torch end conducts a high power and high frequency electrical current. This electrical current creates an intense magnetic field leading to collision-induced ionisation. The very high temperature of the plasma, between 7500 and 10000K, accelerates the ionisation process where the sample is aerosolised, dried, decomposed, atomised and ionised to positively charged ions in a matter of milliseconds (Montaser *et al.*, 1998; Brouwers *et al.*, 2008a).

In the Agilent 7500 bench top ICP-MS used in the present study, ions are then passed into a high vacuum region through a sampling orifice and a skimmer cone. Then an off-axis electrostatic lens focuses the ion beam whilst separating unwanted neutral species and photons to ensure low background noise. The system features a unique

Octopole Reaction System (ORS) technology used to remove polyatomic spectral interferences from the entering ion beam. The ORS consists of an octopole ion guide contained within a pressurised reaction cell. The high pressure allows greater collision of the helium atoms with the larger polyatomic interference thereby slowing them down and allowing only analyte ions to pass into the mass spectrometer. The mass spectrometer then separates the ions of interest based on their mass to charge ratio (m/z) using a quadrupole. Ions exiting the quadrupole then enter an electron multiplier detector, which counts and stores the total signal for each mass resulting in a mass spectrum directly relating the intensity of the peak of a given mass to the concentration of the isotope at that mass (Agilent, 2011).

In the case of platinum there are three naturally occurring isotopes ^{194}Pt , ^{195}Pt and ^{196}Pt and the natural abundance of these isotopes is 32.9%, 33.8% and 25.2%, respectively, and ICP-MS is very sensitive in detecting trace levels reaching 0.001-0.01ng/ml (Horlick and Shao, 1992). The studies involved in platinum analysis by ICP-MS have either detected the ^{194}Pt isotope (Hann *et al.*, 2005; Brouwers *et al.*, 2008b; Brouwers *et al.*, 2008c), the ^{195}Pt isotope (Heudi *et al.*, 1997; Falter and Wilken, 1999; Falta *et al.*, 2011) or both isotopes (Bell *et al.*, 2006; Esteban-Fernández *et al.*, 2007; Hemström *et al.*, 2008).

However, before the introduction of biological samples into the ICP-MS for elemental analysis care must be taken to prevent matrix effects from interfering with the results and damaging the instrument itself. Briefly, this can be prevented in two ways; the first is by sample pre-treatment and the second is by calibration to avoid and compensate for matrix effects. Sample pre-treatment of biological fluids usually involves dilution, whereas for tissue samples digestion with subsequent dilution is most commonly used. Method calibration usually involves the use of an internal standard where it can normalise analyte signal and thereby correct for matrix effects and instrumental signal drifts. To achieve this it is generally preferred to use an internal standard with a mass number close to that of the analyte. In case of platinum, iridium ^{191}Ir and ^{193}Ir are the most commonly used internal standard isotopes (Brouwers *et al.*, 2008a).

7.2. Results

7.2.1. *In vivo* anti-tumour activity

Mice were inoculated with a specific number of B16-F0 cells to induce metastatic cancer. After 7 days mice were treated by inhalation and sacrificed 14 or 21 days post-inoculation for lungs and livers to be dissected, weighed and examined histologically for tumour burdens as described (Section 2.2.9.2).

7.2.1.1. Comparison between control (0.9% w/v NaCl) solution, cisplatin solution and non-processed cisplatin NIVs

Male BALB/c mice were inoculated with 2.7×10^5 B16-F0 cells. On day 7 post-inoculation mice were administered 0.5ml by inhalation of either a control (0.9% w/v NaCl) solution, 0.5mg/ml cisplatin solution or a cisplatin NIVs formulation hydrated with 6 mg/ml and diluted to 0.5mg/ml. The amount of cisplatin administered in each formulation is indicated (Table 7.1). Mice were sacrificed 14 days post-inoculation.

Table 7.1. Amount of cisplatin contained in a 0.5ml dose of cisplatin solution or non-processed NIVs administered by inhalation.

Formulation composition	Concentration of cisplatin	
	In formulation	In 0.5ml dose
Cisplatin solution	0.5mg/ml	0.25mg
Non-processed NIVs hydrated with 6mg/ml cisplatin and diluted by factor of 12	2.93mg/ml (entrapped) diluted by factor of 12 = 0.24mg/ml	0.12mg

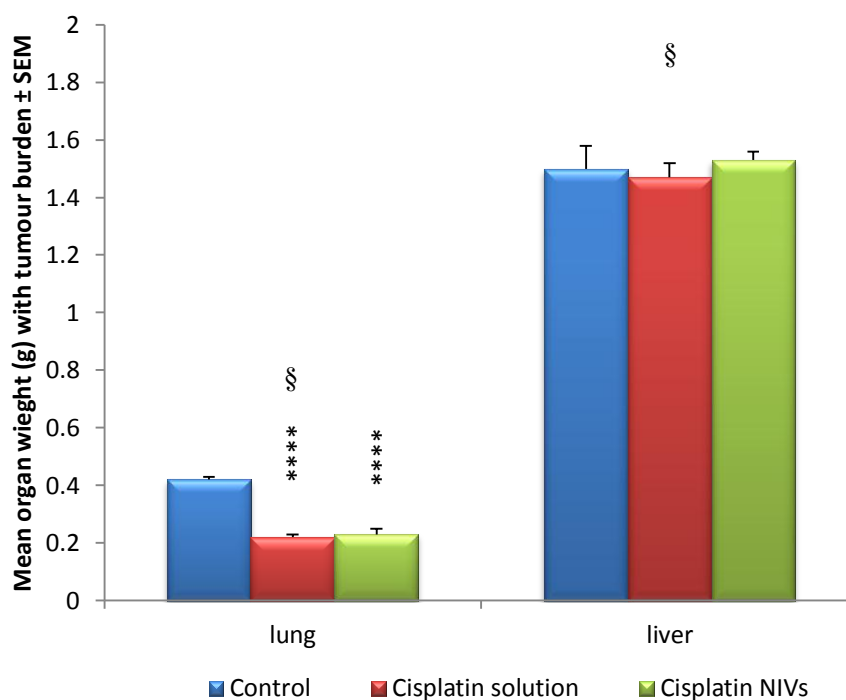


Figure 7.1. Tumour burdens in lungs and livers of BALB/c mice inoculated with 2.7×10^5 B16-F0 cells and administered 7 days post-inoculation by inhalation a single dose of control (0.9% w/v NaCl) solution, cisplatin solution or non-processed cisplatin NIVs hydrated with 6mg/ml and diluted to 0.5mg/ml (n=8). Doses of solution and NIVs administered contained 0.25mg and 0.12mg cisplatin, respectively. Mice were sacrificed 14 days post-inoculation. § indicates n=7 where an animal died during the study before reaching the end point. **** indicates significant differences in comparison to the control group in reducing tumour burdens ($p \leq 0.00005$).

As shown from the results (Figure 7.1), cisplatin solution and NIVs reduced the tumour burdens significantly ($p=0.000$) in the lungs as compared to a control (0.9% w/v NaCl) solution. Lung weights (\pm SEM) decreased from 0.42 ± 0.01 g in the control group to 0.22 ± 0.01 g and 0.23 ± 0.02 g in the solution and non-processed NIVs treated groups, respectively. However this significant reduction in tumour burdens was not observed in the livers from either formulation where liver weights in

the control, solution and non-processed NIVs treated groups were $1.50 \pm 0.08\text{g}$, $1.47 \pm 0.05\text{g}$ and $1.53 \pm 0.03\text{g}$, respectively.

7.2.1.2. Comparison between control (0.9% w/v NaCl) solution, cisplatin solution and processed cisplatin NIVs over one time-point

Male BALB/c mice were inoculated with 3.33×10^5 B16-F0 cells. On day 7 post-inoculation mice were divided into three groups of five and administered with 0.5ml by inhalation either a control (0.9% w/v NaCl) solution, 1mg/ml cisplatin solution or processed cisplatin NIVs. The amount of cisplatin administered in each formulation is indicated (Table 7.2). Mice were sacrificed 21 days post-inoculation.

Table 7.2. Amount of cisplatin contained in a 0.5ml dose of cisplatin solution or processed NIVs administered by inhalation.

Formulation composition	Concentration of cisplatin	
	In formulation	In 0.5ml dose
Cisplatin solution	0.5mg/ml	0.5mg
Processed NIVs hydrated with 6mg/ml cisplatin	0.67mg/ml (entrapped)	0.34mg

From the results (Figure 7.2) it can be seen that there is no significant effect from the processed cisplatin NIVs in reducing tumour burdens in comparison with the control and cisplatin solution, although the weights were lower. The tumour numbers and dimensions were not significantly lower for the NIVs treated group (Tables 7.3 and 7.4)

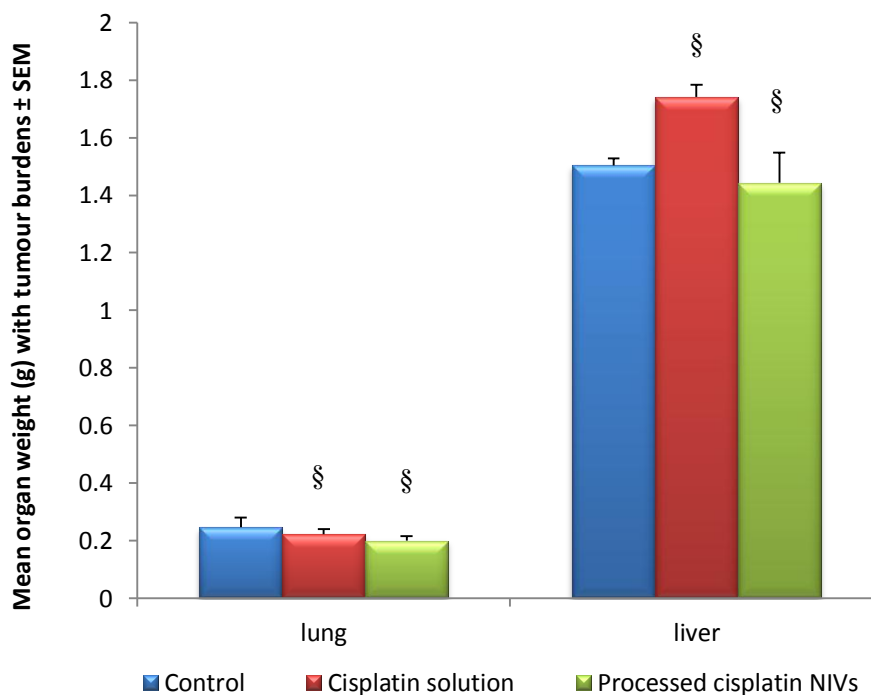


Figure 7.2. Tumour burdens in lungs and livers of BALB/c mice inoculated with 3.33×10^5 B16-F0 cells and administered 7 days post-inoculation by inhalation a single dose of control (0.9% w/v NaCl) solution, cisplatin solution or processed cisplatin NIVs (n=5). Doses of solution and NIVs administered contained 0.5mg and 0.34mg cisplatin, respectively. Mice were sacrificed 21 days post-inoculation. § indicates n=4 where an animal died during the study before reaching the end point. No significant difference was observed between treatments.

Table 7.3. Incidence of tumour metastasis in lungs of BALB/c mice inoculated with 3.33×10^5 B16-F0 cells and administered 7 days post-inoculation by inhalation a single dose of saline control (0.9% w/v NaCl) solution, cisplatin solution or processed cisplatin NIVs (n=5). Doses of solution and NIVs administered contained 0.5mg and 0.34mg cisplatin, respectively. Mice were sacrificed 21 days post-inoculation. No significant difference was observed between treatments. § indicates n=4 where an animal died during the study before reaching the endpoint.

Endpoint criteria		Treatment		
		Control	Solution (§)	Processed NIVs (§)
Incidence of tiny tumours in treatment group		100%	60%	40%
Number of tumours by grade ± SEM	Small	6.4 ± 2.1	7.8 ± 1.1	6.5 ± 1.3
	Medium	Nil	0.5 ± 0.3	Nil
	Large	0.4 ± 0.2	Nil	Nil
Largest tumour dimensions (mm x mm) ± SEM		$2.2 \pm 0.6 \times$ 1.7 ± 0.0	$1.5 \pm 0.1 \times$ 1.1 ± 0.2	$1.2 \pm 0.1 \times$ 1.0 ± 0.2

Table 7.4. Incidence of tumour metastasis in livers of BALB/c mice inoculated with 3.33×10^5 B16-F0 cells and administered 7 days post-inoculation by inhalation a single dose of control (0.9% w/v NaCl) solution, cisplatin solution or processed cisplatin NIVs (n=5). Doses of solution and NIVs administered contained 0.5mg and 0.34mg cisplatin, respectively. Mice were sacrificed 21 days post-inoculation. No significant difference was observed between treatments. § indicates n=4 where an animal died during the study before reaching the endpoint.

Endpoint criteria		Treatment		
		Control	Solution (§)	Processed NIVs (§)
Incidence of tiny tumours in treatment group		Nil	Nil	25%
Number of tumours by grade \pm SEM	Small	9.5 ± 2.1	3.5 ± 1.3	3.4 ± 3.7
	Medium	3.2 ± 2.3	2.0 ± 1.4	0.8 ± 0.8
	Large	2.2 ± 0.7	2.5 ± 1.5	1.0 ± 1.0
Largest tumour dimensions (mm \times mm) \pm SEM		$3.1 \pm 0.1 \times$ 3.0 ± 0.0	$2.6 \pm 0.7 \times$ 2.3 ± 0.7	$2.6 \pm 1.0 \times$ 1.8 ± 0.7

7.2.1.3. Comparison between control (0.9% w/v NaCl) solution and processed cisplatin NIVs over two time-points

Male BALB/c mice were inoculated with 1×10^5 B16-F0 cells. On day 7 post-inoculation, mice were divided into two groups of twelve and each group received 0.5ml control (0.9% w/v NaCl) solution or 0.5ml of processed cisplatin NIVs by inhalation. The amount of cisplatin administered in processed NIVs is indicated (Table 7.5). On day 14 post-inoculation half the mice from each group were sacrificed and the other halves were sacrificed on day 21 post-inoculation.

Table 7.5. Amount of cisplatin contained in 0.5ml dose of processed cisplatin NIVs administered by inhalation.

Formulation composition	Concentration of cisplatin	
	In formulation	In 0.5ml dose
Processed NIVs hydrated with 6mg/ml cisplatin	1.62mg/ml (entrapped)	0.81mg

Results showed that mice that were sacrificed on day 14 post-inoculation, showed significantly reduced tumour burdens in both the lungs (Figure 7.3.) and livers (Figure 7.4.) for the treated group in contrast to the control group ($p=0.001$ and 0.030 , respectively). Lung weights (\pm SEM) decreased from 0.34 ± 0.02 g in the control group to 0.18 ± 0.01 g in the treated group ($p=0.001$). Liver weights decreased from 1.47 ± 0.05 g in the control group to 1.28 ± 0.06 g ($p=0.03$). However, mice sacrificed 21 days post-inoculation had no significant difference in lung (Figure 7.3.) and liver (Figure 7.4) weights between the control and treated groups.

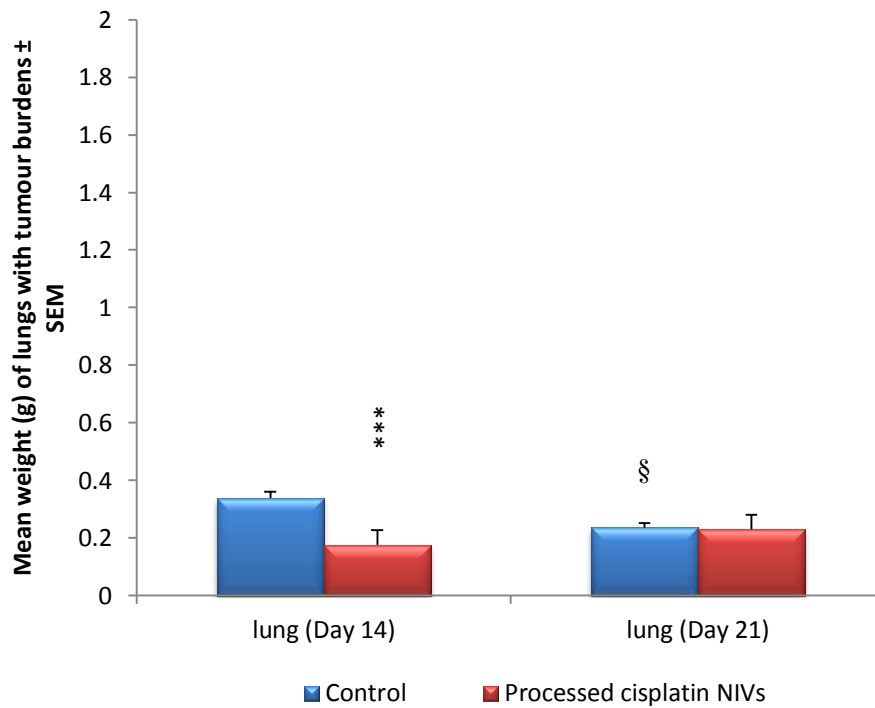


Figure 7.3. Tumour burdens in lungs of BALB/c mice inoculated with 1×10^5 B16-F0 cells and administered 7 days post-inoculation by inhalation a single dose of control (0.9% w/v NaCl) solution or processed cisplatin NIVs (n=6). Dose of administered NIVs contained 0.81mg cisplatin. Mice were sacrificed 14 and 21 days-post inoculation. § indicates n=5 where an animal died during the study before reaching the end point. *** indicates significant differences in comparison to the control group in reducing tumour burdens ($p \leq 0.001$).

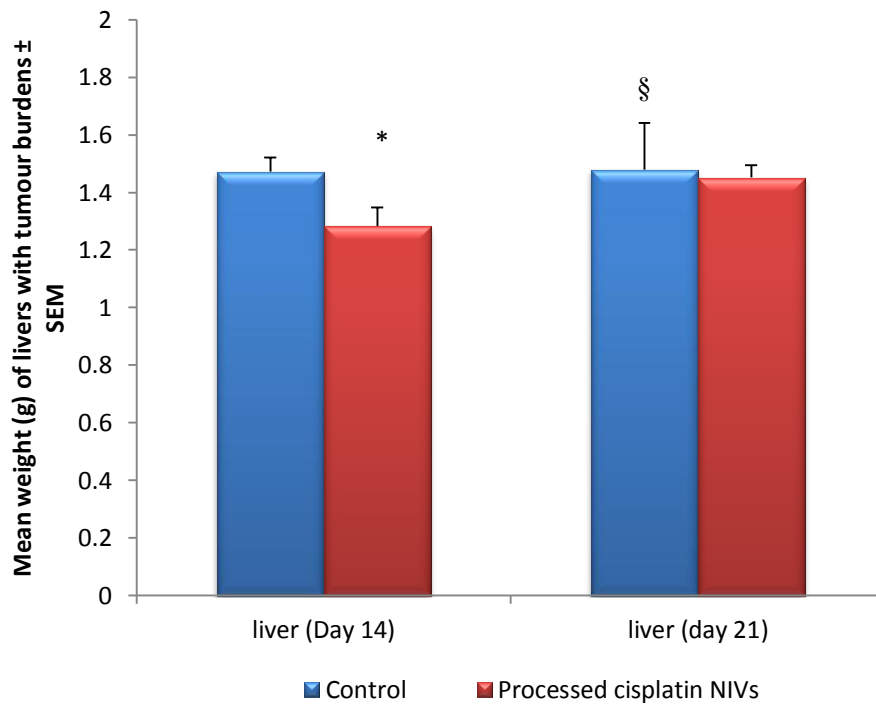


Figure 7.4. Tumour burdens in livers of BALB/c mice inoculated with 1×10^5 B16-F0 cells and administered 7 days post-inoculation by inhalation a single dose of control (0.9% w/v NaCl) solution or processed cisplatin NIVs (n=6). Dose of administered NIVs contained 0.81mg cisplatin. Mice were sacrificed 14 and 21 days post-inoculation. . § indicates n=5 where an animal died during the study before reaching the end point. * indicates significant differences in comparison to the control group in reducing tumour burdens ($p \leq 0.05$).

7.2.2. *In vivo* tissue uptake of cisplatin

This study was aimed at studying the distribution of cisplatin NIVs *in vivo* and its levels in organs of the MPS and the kidneys, which is the site of nephrotoxicity, in comparison with cisplatin solution.

Healthy mice were administered a single dose of the drug by intravenous or inhalation routes. Mice were sacrificed 5min post-dosing for organs of interest to be dissected and serum and lung lavages to be separated as described (Section 2.2.9.3) Stored samples were prepared for analysis as described (Section 2.2.9.3) and analysed by HPLC (Section 2.2.5.1) using method I as described (Section 2.2.5.2).

7.2.2.1. Comparison between cisplatin solution and non-processed cisplatin NIVs

Male BALB/c mice were divided into six groups of five. Every three groups were administered 0.2ml by intravenous injection or 0.5ml by inhalation of either 0.5mg/ml cisplatin solution, non-processed cisplatin NIVs hydrated with 0.5mg/ml cisplatin or non-processed cisplatin NIVs hydrated with 6mg/ml cisplatin then diluted to 0.5mg/ml. The dose of cisplatin solution given by intravenous and inhalation routes was 0.1mg and 0.25mg, respectively. The entrapment efficiency of the NIVs was not determined.

Following a single intravenous injection (Figure 7.5), no platinum levels could be detected in the lungs following the administration of cisplatin solution. The only sites that showed platinum levels were the serum, kidneys and liver with mean values of (\pm SEM) $2.2 \pm 1.9\mu\text{g/ml}$, $1.7 \pm 1.1\mu\text{g/g}$ and $2.4 \pm 2.4\mu\text{g/g}$, respectively. The levels obtained at these sites were not significantly different for both non-processed NIVs formulations. Non-processed NIVs hydrated with 0.5mg/ml cisplatin also failed to accumulate in the lungs and low levels were detected in the serum, spleens and kidneys with levels of $0.3 \pm 0.2\mu\text{g/ml}$, $0.5 \pm 0.5\mu\text{g/g}$ and $0.7 \pm 0.5\mu\text{g/g}$, respectively. Non-processed NIVs hydrated with 6mg/ml cisplatin and diluted to 0.5mg/ml prior to dosing showed detectable levels in the lungs ($0.3 \pm 0.3\mu\text{g/g}$) as well as the spleens ($0.4 \pm 0.4\mu\text{g/g}$) and the serum ($0.3 \pm 0.1\mu\text{g/ml}$) with no detectable levels in the kidneys. Although uptake in the lungs was achieved, no significance was observed.

Large variations in the results were due to an inability to detect platinum in some samples, which contributed to high SEM values.

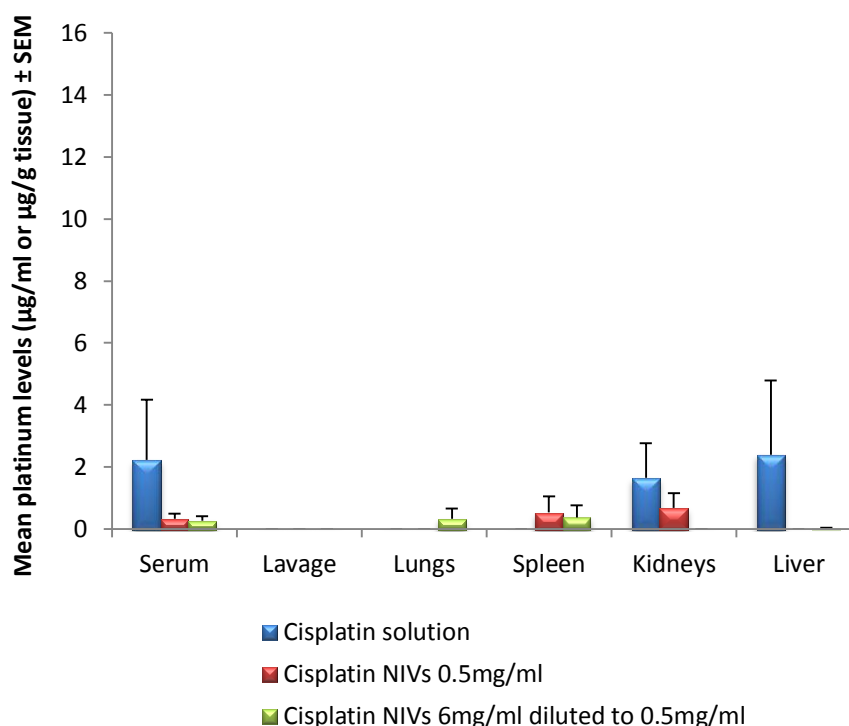


Figure 7.5. The accumulation of cisplatin solution, non-processed cisplatin NIVs hydrated with 0.5mg/ml and non-processed NIVs hydrated with 6mg/ml and diluted to 0.5mg/ml following a single intravenous injection to BALB/c mice (n=5). Dose of cisplatin solution administered was 0.1mg. No significant difference was observed between treatments.

Inhalation therapy showed a different trend with platinum levels detected in the lung lavages ($0.4 \pm 0.2 \mu\text{g/ml}$) rather than the lung tissues following administration of non-processed cisplatin NIVs hydrated with 6mg/ml cisplatin and diluted to 0.5mg/ml. Other sites of platinum accumulation included the spleens ($0.4 \pm 0.2 \mu\text{g/g}$) and the kidneys ($0.8 \pm 0.03 \mu\text{g/g}$). Non-processed cisplatin NIV hydrated with 0.5mg/ml cisplatin showed greater accumulation in the kidneys ($1.2 \pm 0.3 \mu\text{g/g}$) with lower levels in the spleens ($0.3 \pm 0.1 \mu\text{g/g}$), lung lavage ($0.2 \pm 0.002 \mu\text{g/ml}$) and serum (0.2

$\pm 0.2\mu\text{g/ml}$). Platinum levels following administration of cisplatin solution also showed greater levels in the kidneys ($0.8 \pm 0.04\mu\text{g/g}$) and less accumulation in the spleens ($0.2 \pm 0.1\mu\text{g/g}$) and lung lavage ($0.1 \pm 0.1\mu\text{g/ml}$). Platinum levels from the different formulations did not significantly differ from each other (Figure 7.6).

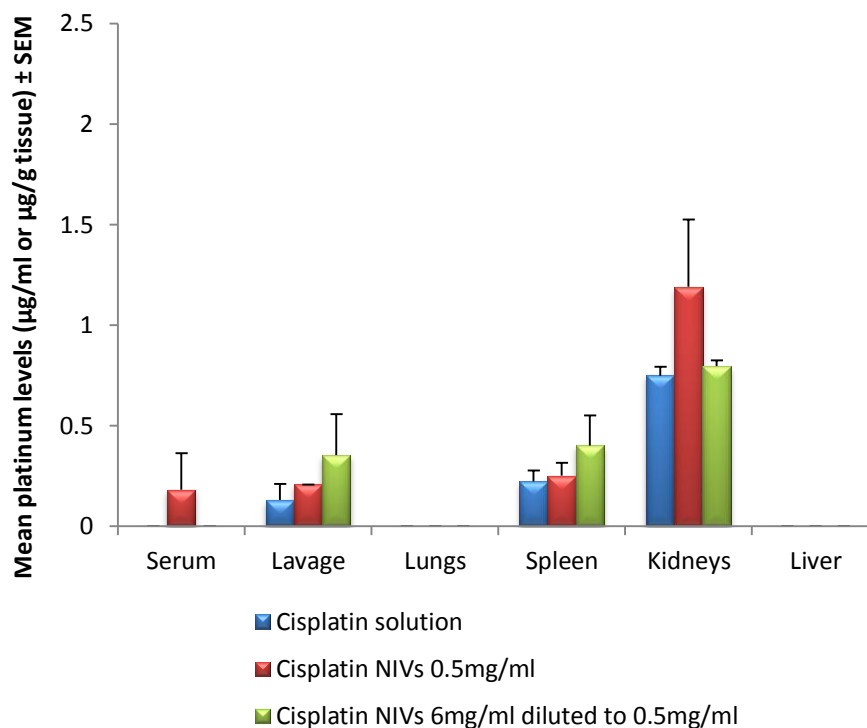


Figure 7.6. The accumulation of cisplatin solution, non-processed cisplatin NIVs hydrated with 0.5mg/ml and non-processed NIVs hydrated with 6mg/ml and diluted to 0.5mg/ml following inhalation treatment of BALB/c mice (n=5). Dose of cisplatin solution administered was 0.25mg. No significant difference between any of the formulations was observed.

7.2.2.2. Comparison between cisplatin solution and processed cisplatin NIVs

Male BALB/c mice in four groups of five were administered cisplatin solution or processed cisplatin NIVs either by a 0.2ml single intravenous injection or 0.5ml inhalation of either formulation. The amount of cisplatin administered in the cisplatin solution and processed NIVs, in 0.2ml and 0.5ml doses, is indicated (Table 7.6).

Table 7.6. Amount of cisplatin contained in 0.2ml and 0.5ml dose of cisplatin solution and processed NIVs administered by intravenous injection and inhalation, respectively.

Formulation composition	Concentration of cisplatin		
	In formulation	In 0.2ml dose	In 0.5ml dose
Cisplatin solution	0.5mg/ml	0.10mg	0.25mg
Processed NIVs hydrated with 6mg/ml cisplatin	0.92mg/ml (entrapped)	0.18mg	0.46mg

Following a single intravenous injection (Figure 7.7), processed cisplatin NIVs showed preferential uptake into the lungs reaching (\pm SEM) $13.1 \pm 2.0\mu\text{g/g}$ tissue whereas cisplatin solution showed significant lower levels $0.6 \pm 0.2\mu\text{g/g}$ ($p=0.004$). Cisplatin solution failed to accumulate in the serum and livers and showed very low levels in the spleens $0.1 \pm 0.1\mu\text{g/g}$. In contrast, processed cisplatin NIVs managed to accumulate significantly in the liver, spleen and serum reaching $5.4 \pm 2.4\mu\text{g/g}$, $7.1 \pm 1.4\mu\text{g/g}$ and $0.5 \pm 0.1\mu\text{g/ml}$, respectively ($p=0.01$, 0.01 and 0.014 , respectively). As will be discussed later, significant higher levels of platinum from processed cisplatin NIVs were found in the kidneys than from cisplatin solution $7.6 \pm 3.7\mu\text{g/g}$ and $1.0 \pm 0.6\mu\text{g/g}$, respectively ($p=0.03$). However by comparing free and entrapped drug levels in lung and kidney, levels of processed cisplatin NIVs in the lungs were about 24 times greater than its solution counterpart, whereas in the kidneys platinum levels from the NIVs were about 7 times greater than solution.

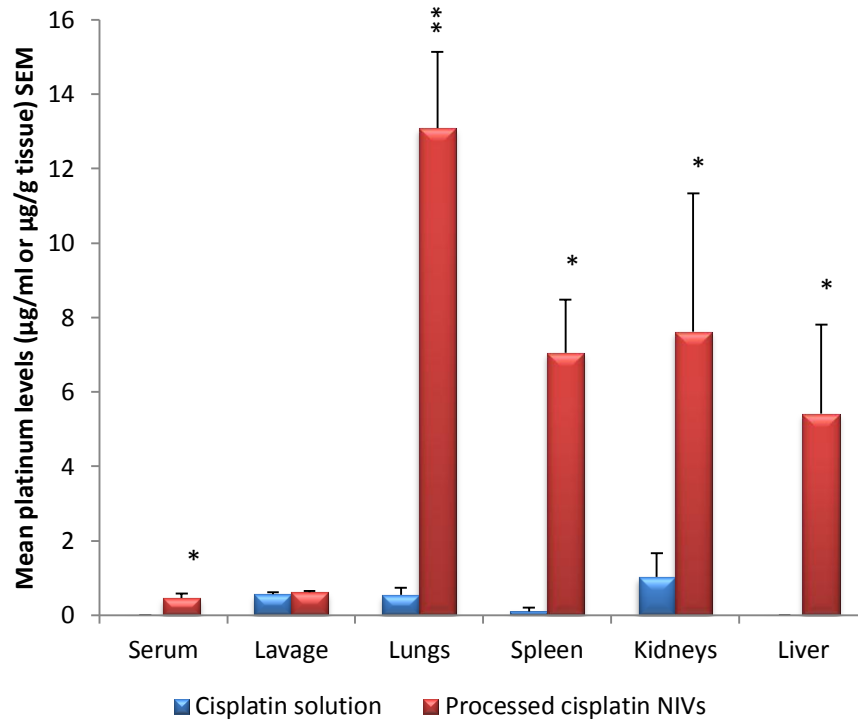


Figure 7.7. The accumulation of cisplatin solution and processed cisplatin following single intravenous injection to BALB/c mice (n=5). Doses of solution and NIVs contained 0.1mg and 0.18mg cisplatin, respectively. * indicates significant levels of cisplatin from processed NIVs in comparison to cisplatin solution ($p \leq 0.05$), ** indicates ($p \leq 0.005$).

Tissue levels following inhalation therapy (Figure 7.8) did not demonstrate much accumulation of processed cisplatin NIVs compared to intravenous delivery (Figure 7.7). Platinum levels post-administration of processed NIVs by inhalation were found to accumulate in the spleens and the livers to a lesser extent in comparison with intravenous administration of the same formulation. No significant difference in platinum levels post-administration following inhalation between cisplatin solution and processed NIVs in either tissue was observed. Spleen levels of cisplatin processed NIVs following inhalation therapy reached $1.6 \pm 0.4 \mu\text{g/g}$, which is about half the level achieved following intravenous administration, and for cisplatin solution was $1.7 \pm 0.5 \mu\text{g/g}$. Liver levels after inhalation therapy for processed cisplatin NIVs and cisplatin solution were $0.06 \pm 0.03 \mu\text{g/g}$ and $0.04 \pm 0.02 \mu\text{g/g}$,

respectively. As will be discussed later, many factors are associated with pulmonary delivery, which have a direct influence on drug deposition.

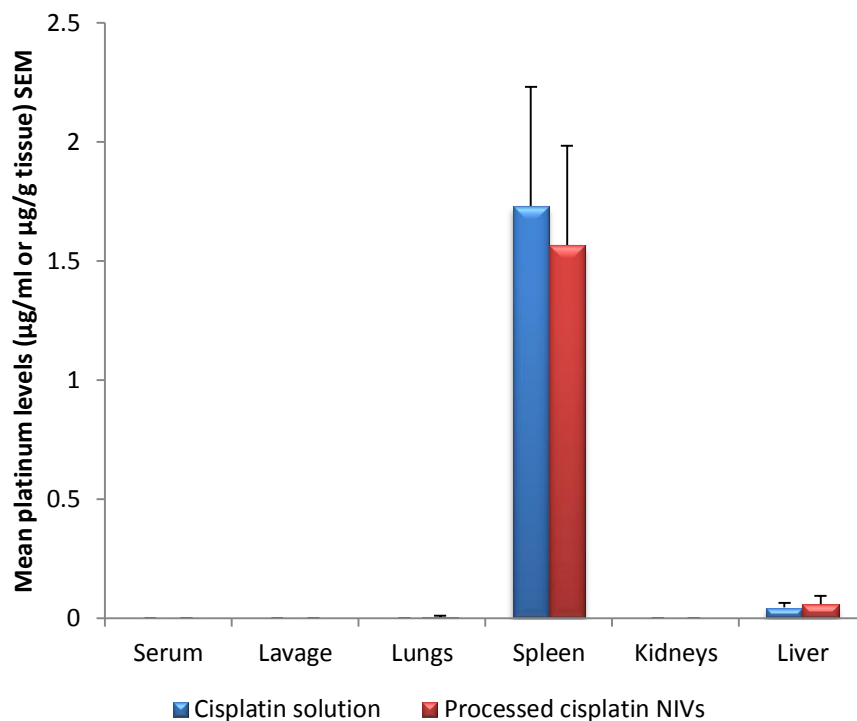


Figure 7.8. The accumulation of cisplatin solution and processed cisplatin administered by inhalation to BALB/c mice (n=5). Doses of solution and NIVs contained 0.25mg and 0.46mg cisplatin, respectively. No significant difference was observed between the formulations.

7.2.3. Preliminary pharmacokinetic study

Male Sprague Dawley rats were divided into two groups of twelve and administered 0.2ml by intravenous injection of a cisplatin solution or 0.5ml by inhalation processed cisplatin NIVs. At different time points post dosing 3 rats were taken from each treatment group and sacrificed as described (Section 2.2.9.4). The amount of cisplatin administered from cisplatin solution in a 0.2ml dose and from processed cisplatin NIVs in a 0.5ml dose is indicated (Table 7.7). Platinum levels for the pharmacokinetic study were determined by ICP-MS as described (Section 2.2.9.4).

Table 7.7. Amount of cisplatin contained in 0.2ml of cisplatin solution administered by intravenous injection and 0.5ml of processed cisplatin NIVs administered by inhalation.

Formulation composition	Concentration of cisplatin		
	In formulation	In 0.2ml dose	In 0.5ml dose
Cisplatin solution	1.0mg/ml	0.20mg	-
Processed NIVs hydrated with 6mg/ml cisplatin	0.72mg/ml (entrapped)	-	0.38mg

Plasma platinum levels (Figure 7.9) following intravenous delivery of cisplatin solution was at the highest 5min after dosing (\pm SEM) reaching 742 ± 142 ppb w/v then decreased significantly 30min post-dosing 278 ± 7 ppb w/v and maintained a stable level thereafter. Following inhalation with processed cisplatin NIVs stable platinum level was achieved throughout all the time periods. Intravenous delivery showed significantly higher levels of platinum than inhalation therapy at 5, 240 and 480min post-dosing. A different trend was observed in the lungs (Figure 7.10) where inhaled NIVs showed higher levels than injected drug that was significantly higher at 240 and 480min post-dosing. The maximum level with each formulation was obtained 5min post-dosing reaching 782 ± 153 ppb w/w for cisplatin solution and 1400 ± 159 ppb w/w for processed cisplatin NIVs.

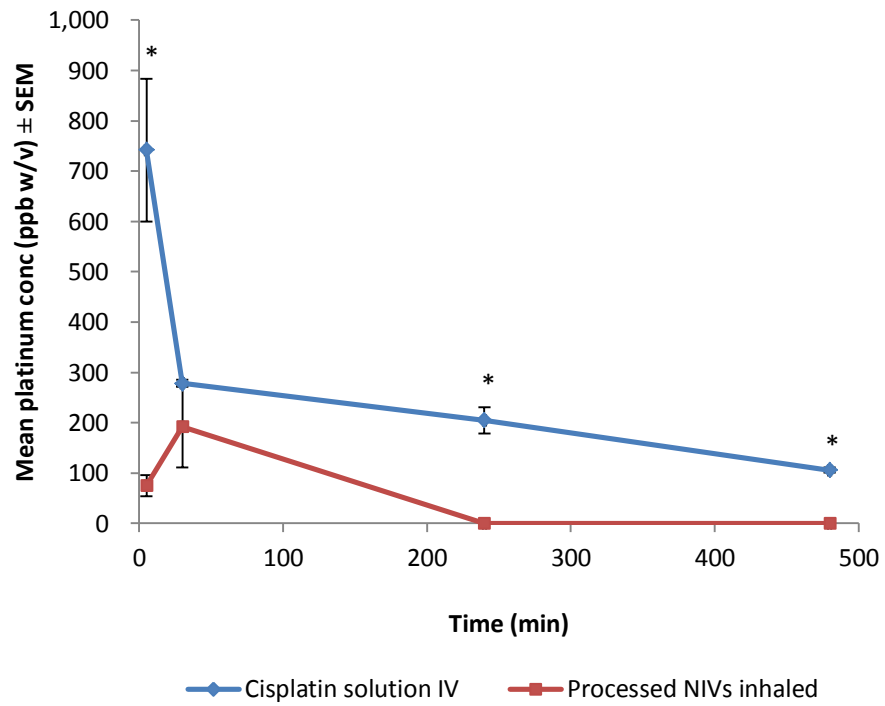


Figure 7.9. Pharmacokinetic profile of platinum in plasma of Sprague-Dawley rats following a single intravenous injection of cisplatin solution or inhalation administration of processed cisplatin NIVs (n=3). Doses of solution and NIVs contained 0.20mg and 0.38mg cisplatin, respectively. * indicates significant difference in platinum levels between injected solution and inhaled NIVs.

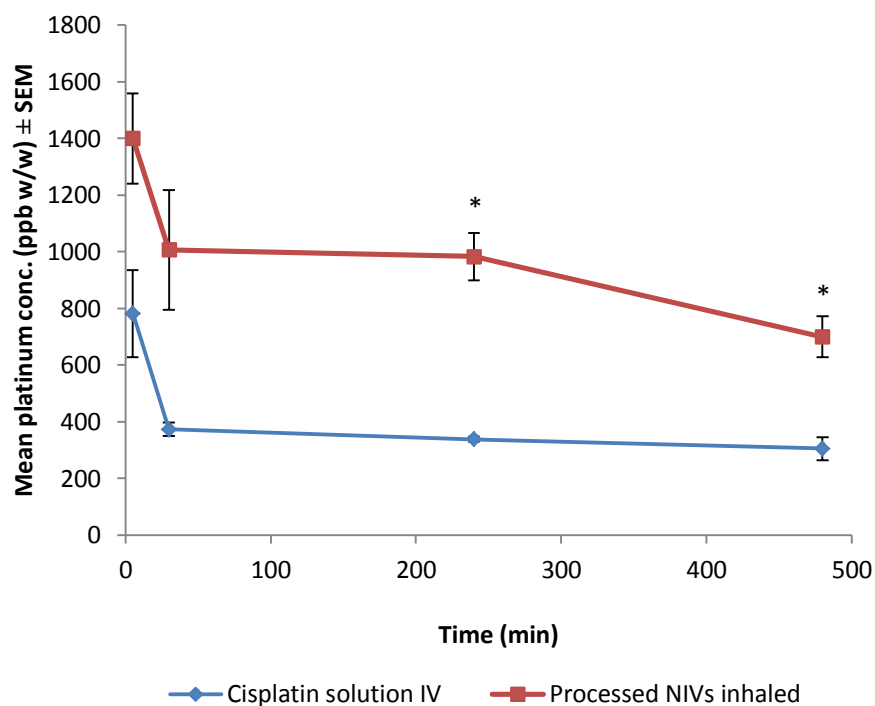


Figure 7.10. Pharmacokinetic profile of platinum in lungs of Sprague-Dawley rats following a single intravenous injection of cisplatin solution or inhalation administration of processed cisplatin NIVs (n=3). Doses of solution and NIVs contained 0.20mg and 0.38mg cisplatin, respectively. * indicates significant difference in platinum levels between injected solution and inhaled NIVs.

7.3. Discussion

Preclinical *in vivo* studies are crucial before the clinical use of a new drug or formulation (Talmadge *et al.*, 2007). This indicates that even though cisplatin is already an established anticancer drug that has been approved since 1978, formulating cisplatin into lipid vesicles as a novel drug delivery system requires preclinical studies to demonstrate improved efficacy and/or safety over the solution form before any approval for clinical use. In the present chapter, a small-scale preliminary *in vivo* study was carried out to compare the different cisplatin NIVs formulations to conventional cisplatin solution and determine whether NIVs have the potential to enhance the therapeutic effectiveness of cisplatin.

Talmadge *et al.* (2007) indicated that preclinical studies should involve anti-tumour activity studies in addition to absorption, elimination, metabolism, excretion (ADME) and toxicity studies. The first part of the present study was the study of the anti-tumour effects of different cisplatin NIVs formulations in comparison with cisplatin solution and control treatment. Among the different criteria reported by Talmadge *et al.* (2007) to assess anticancer efficacy are tumour burden and incidence of metastasis by weighing the organ and counting tumour nodes in the organs. These were chosen as endpoint criteria for the chosen tumour model. Hollingshead *et al.* (2008) suggested initiating preclinical studies with an evaluation using a tumour model known to be sensitive to the anticancer drug. Accordingly, the tumour model chosen was the metastatic murine melanoma B16-F0 cell line, which has known sensitivity to cisplatin and been used as a tumour model for cisplatin in many studies (Zamboni *et al.*, 2004, Hwang *et al.*, 2007). The B16 melanoma has been reported to metastasise primarily in the lungs (Fidler *et al.*, 1975). B16-F0 metastasises greatly in the lungs and to a lesser extent in liver (Nakamura *et al.*, 2002). This was observed during the extraction of lungs and livers from inoculated mice in the present studies where visible black tumour nodes were present in all the lungs and some of the livers. Despite the significant increase in the incidence of lung tumour nodes with successive tumour lines of B16-F0 (Fidler *et al.*, 1975), Nakamura *et al.* (2002) have shown that the malignant aggressiveness between the cell lines was not different and that B16-F0 cells inoculated in numbers of 1×10^5 were sufficient enough to produce metastatic lung nodes and result in cancer related death.

BALB/c mice were used as the host for studying the effect of cisplatin on the murine melanoma cancer cell model of B16-F0. However, it has been emphasised that syngeneic hosts should be used whenever possible to overcome the likelihood of tumour rejection (Welch, 1997). Therefore, the use of allogeneic BALB/c mice as a host for the metastatic B16-F0 model instead of syngeneic C57BL/6 mice may be argued. In fact, many studies have used syngeneic C57BL/6 where B16 melanoma was studied as a tumour model (Fidler 1975; Lavi *et al.*, 2007; Hyoudou *et al.*, 2009). Nonetheless, studies have also indicated that B16 cells tend to lower the expression of the major histocompatibility complex (MHC) class I, which impedes their identification by CD8⁺ T cells. Therefore the low MHC class I expression on

the surface of B16 cells makes them poorly immunogenic and able to evade identification and most anti-tumour responses (Seliger *et al.*, 2001; Merritt *et al.*, 2004; Becker *et al.*, 2010). Older studies have also supported the poor immunogenic properties of the B16 melanoma cells obtained through *in vitro* passage. These cells were as capable of inducing tumours in allogeneic BALB/c mice as they were in syngeneic C57BL/6 mice (Ashman *et al.*, 1980; Ashman, 1987). Prior to the present PhD project, preliminary studies confirmed that B16-F0 exhibited low expression of MHC class I and that BALB/c mice had a higher incidence of lung and liver metastasis than C57BL/6 (results not shown, personal communication, Dr Katharine Carter, University of Strathclyde). This demonstrated the suitability of using BALB/c mice as a host for the B16-F0 tumour model.

Tumour burden studies showed equivalent anti-tumour effects from cisplatin solution and non-processed cisplatin NIVs (Figure 7.1) in comparison with the control group 7 days post-treatment. Tumour burdens of both cisplatin treated groups were reduced by approximately half in comparison with the control group. A similar reduction in tumour burdens was observed with groups treated with processed NIVs (Figure 7.3) 7 days post-treatment. Therefore, from the rate of tumour reduction in the lungs it seemed that non-processed cisplatin NIVs had no therapeutic advantage over cisplatin solution. Although processed cisplatin NIVs were evaluated in a separate study in comparison to a control group, it also seemed to show equal ability to reduce tumour growth as non-processed NIVs and cisplatin solution, thereby showing no therapeutic advantage to conventional cisplatin. Unfortunately, tumours were not counted in both these studies to provide further evaluation of the anti-tumour effects.

However, an interesting observation was the exclusive ability of processed cisplatin NIVs following inhalation treatment to significantly reduce liver tumour burdens in comparison with the control group (Figure 7.4), in contrast to the groups treated with cisplatin solution and non-processed NIVs (Figure 7.1). This could be due to the higher concentration of cisplatin contained in the processed NIVs dose administered to the mice in comparison to cisplatin solution and non-processed NIVs. The anti-tumour effect in the liver demonstrated the possibility of systemic absorption through pulmonary delivery.

Another observation was the extent of processed NIVs in maintaining an anti-tumour effect. The ability of processed cisplatin NIVs to reduce tumour burdens on day 7 post-treatment was not observed by day 14 post-treatment (Figures 7.3 and 7.4). Tumour burdens on day 14 post-treatment with processed cisplatin NIVs did not differ significantly from the control group. This could indicate reduced anti-tumour activity of processed cisplatin NIVs beyond 7 days where tumours start to grow. Similarly, another study showed that tumour burdens measured 14 days post-treatment with processed cisplatin NIVs and cisplatin solution showed no significant difference to the control group (Figure 7.2). The incidence of metastasis determined in the lungs and livers of these treatment groups were not significantly different (Tables 7.3 and 7.4). These observations could possibly suggest that anti-tumour activity of processed NIVs is limited to a week where afterwards another dose, or a maintenance dose, will be needed. If proven this could offer a great advantage over conventional therapy where a single dose by inhalation can replace a 6-8h intravenous infusion. Nonetheless, processed NIVs need to demonstrate enhanced anti-tumour effectiveness over the solution form. As will be discussed later, there are factors that affect pulmonary delivery and by optimising these factors successful pulmonary delivery can be achievable.

The second part of the present study involved studying the absorption and distribution profile of different cisplatin formulations by two routes of administration. The uptake of cisplatin in the lungs; which is the target organ; livers, spleens and kidneys in addition to its availability in serum and lung lavages was determined. Using the described HPLC method in platinum analysis, it is anticipated that detection will be limited to active platinum species which are unbound to proteins (Bannister *et al.*, 1979; Drummer *et al.*, 1984; Andrews *et al.*, 1984; Goel *et al.*, 1990; Lopez-Flores *et al.*, 2005). This is the reason why animals were sacrificed 5min post-dosing as previous studies showed difficulty in detecting platinum levels when animals were left for longer times following cisplatin solution administration (results not shown, personal communication, Dr Katharine Carter, University of Strathclyde). This is possibly due to binding of cisplatin with proteins thereby hindering detection by the adapted HPLC method.

The first route of administration investigated was the intravenous route. Following a single intravenous administration, non-processed cisplatin NIVs whether hydrated with 0.5mg/ml cisplatin or 6mg/ml cisplatin then diluted to 0.5mg/ml, did not show significant uptake by target tissues when compared to cisplatin solution (Figure 7.5). In contrast, significant tissue uptake from a single intravenous dose of processed cisplatin NIVs was observed in comparison with cisplatin solution (Figure 7.7), particularly in the lungs, exploiting their uptake by the MPS. The high accumulation of cisplatin in the lungs delivered by processed NIVs is most likely because of the lungs being the initial site of particle clearance through the pulmonary circulation following intravenous injection (Washington *et al.*, 2001). This could lead to most of the vesicles being taken into the lungs by the MPS and those evading pulmonary uptake being taken up by the MPS in the liver and spleens, which could explain the high platinum levels observed there as well. Such an uptake mechanism is primarily controlled by vesicle size and charge. As mentioned previously, the larger the size of a vesicular delivery system the greater the uptake by such a mechanism with the presence of a surface charge further enhancing uptake in the order of negative, positive then neutral charge (Drummond *et al.*, 2008). Fidler *et al.* (1980) indicated that enhanced pulmonary uptake of liposomes administered intravenously can be achieved by incorporating a negative charge and increasing vesicle size. In their study they reported enhanced pulmonary uptake of negatively charged MLVs by alveolar macrophages. Accordingly, this would mean that non-processed cisplatin NIVs should also be taken up as they are large in size, even larger than processed NIVs, and they also bear a negative charge (Section 3.2.1.1). However, the failure of cisplatin delivered by non-processed NIVs to accumulate significantly in the lungs could be due to low drug entrapment in case of NIVs hydrated with 0.5mg/ml or the low number of vesicles/dose in case of NIVs hydrated with 6mg/ml. Non-processed NIVs hydrated with 6mg/ml cisplatin would require subsequent dilution to 0.5mg/ml to avoid precipitation of untrapped cisplatin, as mentioned previously.

Even though the intravenously administered dose of processed cisplatin NIVs was almost double the concentration of that of cisplatin solution (0.18mg versus 0.10mg, respectively), more than double the levels of platinum were observed in all organs following treatment with processed cisplatin NIVs while still maintaining low serum

levels. This could indicate rapid opsonisation of the vesicles in blood followed by MPS uptake. However, as previously reported, cisplatin greatly binds to serum proteins with about 90% of the dose being protein bound (Prestayko, 1981a). This could be a logical explanation for the absence of platinum in the serum of the cisplatin solution treated group, where the HPLC method is specific for detecting active platinum species and incapable of detecting protein bound platinum species. The binding of cisplatin solution to serum proteins could also explain the low accumulation of cisplatin in tissues in comparison to processed cisplatin NIVs. This would suggest that the lipid vesicles were able to protect cisplatin from binding to plasma proteins thereby enhancing cisplatin delivery to other organs. As mentioned previously, one of the problems with conventional cisplatin treatment is that even though cisplatin is given as an infusion, not enough cisplatin reaches the required sites contributing to chemoresistance (Kelland, 2007). The use of lipid vesicles can provide the means of enhancing or targeting the delivery of cisplatin to the required sites in sufficient amounts thereby enhancing efficacy. This can allow a reduction in dose and frequency of cisplatin administration without compromising efficiency.

Although kidney levels were also significantly higher for the processed NIVs in comparison to solution, a preferential selectivity was obtained in the lungs for the processed NIVs compared to free drug solution. This may indicate the possibility of achieving therapeutic levels with lower risk of nephrotoxicity. However, the high kidney levels after administration of NIVs could just be a consequence of blood flow through the kidney vasculature rather than extravasation of renal tissue. Nonetheless, lack of nephrotoxicity in the present study will need to be confirmed by histological studies. In a study by Júnior *et al.* (2007a) using stealth pH sensitive liposomal cisplatin injected intravenously as a single dose of 6mg/kg to mice, higher kidney levels from liposomal cisplatin were observed over the free solution of the same dose. Nonetheless, their findings indicated that cisplatin solution had partitioned to a greater extent in renal tissues than liposomal cisplatin, which can be an indication of lower nephrotoxic effect. Devarajan *et al.* (2004) reported that when an equivalent dose of 5mg/kg of cisplatin solution and Lipoplatin[®] were administered intraperitoneally to rats, the same high levels were obtained in the kidneys.

Afterwards cisplatin solution showed a 5 times greater steady state accumulation of platinum up to 160h

post dosing in comparison to Lipoplatin[®] in the kidneys. Further histological studies showed that in contrast to cisplatin solution no sign of nephrotoxicity was observed from Lipoplatin[®] (Devarajan *et al.*, 2004).

One of the many benefits of using liposomes is their ability to avoid disposition in specific sites such as the kidney and heart, thereby minimising site related toxicity (Lasic, 1995). This was evidenced in the reduced nephrotoxicity with liposomal amphotericin B (Goyal *et al.*, 2005) and reduced cardiotoxicity with liposomal doxorubicin (Park, 2002).

The second route of administration investigated was the pulmonary route. In pulmonary delivery, the advantage of offering a non-invasive route of therapy over parenteral administration is achieved with the benefit of locally targeting lung diseases and minimising undesirable side effects with possible dose reduction (Kellaway and Farr, 1990). The high absorptive surface area of the lungs, membrane permeability and the rich vascularisation can also provide the benefit of systemic treatment (Huang and Wang, 2006). Using lipid vesicles in inhalation therapy offers further advantage over conventional drugs, where they can facilitate intracellular delivery of the entrapped drug such as targeting the alveolar macrophages (Schreier *et al.*, 1993).

The main requirement in inhalation therapy is for the drug to achieve therapeutic levels of peripheral deposition where absorption is likely to occur (Taylor and Kellaway, 2001). Peripheral deposition of inhaled particles is size dependent, which is measured by the aerodynamic diameter. The aerodynamic diameter is defined as the diameter of a spherical particle with a unit density of one that settles with the same velocity in still air as the drug particle regardless of its shape or density (de Boer *et al.*, 2002; Ali, 2010). Based on the aerodynamic diameter, the deposition of an inhaled spherical particle follows one of the three major mechanisms; inertial impaction, gravitational sedimentation or diffusion (Carvalho *et al.*, 2011b). Sedimentation is the mechanism through which successful peripheral deposition can

be achieved. It has been reported that particles ranging in size between 1-5 μm are more likely to sediment in the smaller airways and alveoli. Larger particles on the other hand have the possibility of impaction on the walls of the conducting airways leading to their clearance by the mucociliary escalator. Particles 0.5 μm or less are able to reach the alveoli but because they are too small they are constantly in Brownian motion, or diffuse, and not able to become deposited and therefore are eventually exhaled (O'Callaghan and Barry, 1997; Washington *et al.*, 2001; Martini and Nath, 2009c).

Based on this information, drug delivery systems in the nano-size range are too small to achieve the required deposition profile (Roa *et al.*, 2011). Therefore pulmonary delivery devices are designed to deliver drugs in the required aerodynamic diameter range of 1-5 μm (Azarmi *et al.*, 2008). When vesicles are inhaled using nebulisation, the particle size distribution becomes dependent on the aerosol droplets produced by the nebuliser rather than vesicles themselves (Kellaway and Farr, 1990). The droplet size is usually expressed as mass median aerodynamic diameter (MMAD), which is defined as the aerodynamic diameter where the aerosol mass is distributed evenly into droplets of either larger or smaller aerodynamic diameters (Jaafer-Maalej *et al.*, 2009). Several studies have reported a MMAD of nebulised lipid vesicles within the size range required for peripheral deposition (Desai *et al.*, 2002; Desai and Finlay, 2002; Terzano *et al.*, 2005; Wittgen *et al.*, 2007).

Regardless of the site of deposition or the particle nature (Geiser *et al.*, 2003), once the droplets are deposited they are immersed in the lining fluids of the respiratory tract whether it was the mucous layer of the conducting airways or the surfactant-lining fluid layer of the respiratory airways (Yang *et al.*, 2008). Depending on the site of deposition and the nature of the particle/droplet, clearance mechanism will differ. Particles/droplets deposited in the conducting airway are predominantly cleared via the mucociliary escalator with lower chances of systemic, bronchial or lymphatic absorption (Labiris and Dolovich, 2003a; Groneberg *et al.*, 2003). This is because absorption mainly takes place in the alveoli of the lungs (Yang *et al.*, 2008) and any chances of absorption from the conducting airways is hindered by the lining mucous layer and the underlying epithelium (Smola *et al.*, 2008). The thickness of

the epithelial layer and lining mucous in the conducting airways have been estimated to be 50-60 μm and 5-10 μm , respectively (Patton, 1996). Moreover, the surface velocity of the mucociliary escalator is estimated between 1-10mm/min (Patton, 1996) indicating particles are cleared in a relatively short time (Kellaway and Farr, 1990; Seikmeier and Scheuh, 2008). A study by Geiser *et al.* (1990) on hamsters showed that within 24h an average of 87% of inhaled polystyrene microsphere particles were cleared by the mucociliary escalator. Another study by Farr *et al.* (1985) on humans showed that the fraction retained (\pm SEM) 6h post-dosing by inhalation of $^{99\text{m}}\text{Tc}$ -labelled dipalmitoylphosphatidylcholine MLVs and SUVs as an indication of mucociliary clearance was $87.5 \pm 2.1\%$ and $76.8 \pm 5.1\%$, respectively.

Particles/droplets deposited in the alveolar region are cleared by two mechanisms. Phagocytosis by alveolar macrophages, where phagocytosed material is carried to the lymphatic system or slowly transported to the mucociliary clearance, or absorption of deposited material by epithelial cells into the systemic circulation (Labiris and Dolovich, 2003a). Yang *et al.* (2008) have cited Chono *et al.* (2006) suggesting that with alveolar macrophages about 15-22 μm in diameter, particles with a size range of 1-3 μm are taken up very easily. The most likely clearance scenario for lipid vesicles deposited in the alveolar region is phagocytosis by alveolar macrophages (Oberdörster, 1993; Schreier *et al.*, 1993). Furthermore, because of the lipid nature of vesicles a unique clearance mechanism could also be achieved. Lipid vesicles can be incorporated into the endogenous surfactant pool in the alveolar region and taken up by alveolar type II cells where processing, uptake and recycling of lung surfactant occurs (Labiris and Dolovich, 2003b; Schreier *et al.*, 1993). Lung surfactant consists of 90% lipids and 10% proteins (Yu and Possmayer, 2003). The lipid portion consists of 3% neutral lipids and 97% phospholipids (Yu *et al.*, 1983). The neutral lipid portion mainly consists of cholesterol with traces of triglycerides and free fatty acids (Goerke *et al.*, 1998). The phospholipid portion consists of 79% phosphatidylcholine with dipalmitoylphosphatidylcholine the most abundant, 11% phosphatidylglycerol (Yu *et al.*, 1983) and low amounts of phosphatidylethanolamine, phosphatidylinositol and phosphatidylserine (Goerke *et al.*, 1998). In a study by Huang and Wang (2006), liposomal insulin administered by inhalation in a dose of 0.5IU/ml was able to significantly reduce blood glucose levels of diabetic BALB/c

mice in comparison to a control saline solution and insulin mixed with empty liposomes. It was suggested that liposomal insulin enhanced insulin absorption by incorporation into the surfactant pool. It is thought that exogenous liposomes enhance surfactant recycling process thereby enhancing liposomal uptake (Hussein *et al.*, 2004; Seikmeier and Scheuh, 2008).

However, from the inhalation treatment results in the present chapter, tissue uptake levels did not show favourable results, where accumulation sites of both non-processed NIVs did not differ significantly from cisplatin solution (Figure 7.6). However this would be expected since intravenous results also did not demonstrate any significance of non-processed NIVs over cisplatin solution. No platinum was detected in the lung tissues themselves from any of the formulations although significant levels were found in the spleens and kidneys, but platinum was detected in the lung lavages. Lung lavages contain airway and alveolar fluids combined which make it difficult to interpret results (Patton, 1996). Platinum detected in the lung lavages could be representative of drug portion trapped in the mucociliary clearance or drug portion in the alveolar region that had been phagocytosed and/or had not been absorbed yet. The detection of platinum in the serum following administration of non-processed NIVs hydrated with 0.5mg/ml cisplatin can further support the hypothesis of systemic absorption. In a study using liposomal all-*trans*-retinoic acid (ATRA) administered by inhalation to mice, the absence of ATRA in the livers and serum was suggested to be due to local absorption of the drug in the lungs, which did show high levels. This was confirmed by microscopic images showing the adherence of fluorescently labelled liposomes to alveolar epithelial cells (Parthasarathy *et al.*, 1999).

Inhalation of processed cisplatin NIVs also showed unfavourable results, where similar levels as cisplatin solution were found in spleens and livers (Figure 7.8). Although delivery was via inhalation, platinum levels that could not even be quantified were found in the lung tissues following inhalation. No platinum was detected in lung lavages from either formulation. This however raises a question why processed cisplatin NIVs failed to significantly accumulate in lung tissue when administered by inhalation but was observed to accumulate following intravenous

delivery. It was also anomalous why processed cisplatin NIVs were not able to accumulate significantly in comparison to the solution form following inhalation as they were following intravenous administration.

One possible reason is that solution viscosity can affect nebulisation rates (Labiris and Dolovich, 2003b) and the higher viscosity of the NIVs formulation could impede the complete aerosolisation of the NIVs in the fixed nebulisation time period. This could affect subsequent tissue levels and anti-tumour effects if cisplatin solution or NIVs were administered in equal doses and the NIVs were incompletely nebulised. From the 0.5ml suspension dosed for nebulisation a measured volume (\pm SEM) of 0.24 ± 0.03 ml was found to be nebulised. In the case of mice dosed with processed cisplatin NIVs (0.96mg/ml) that would mean that only 0.22mg of cisplatin was nebulised from the 0.46mg that was contained in 0.5ml, in comparison to 0.25mg cisplatin solution. As mentioned (Section 7.1.2), the nebulisation technology used employs no pressure and propellant, thus dose will be aerosolised in the available volume. By taking into consideration the volume of the spacer and the breathing rate and tidal volume of the mouse, an estimate of amount inhaled in a fixed time can be calculated. The breathing rate and tidal volume (\pm SEM) of unrestrained 69 day old BALB/c mice in a double chamber plethysmograph were measured to be 572 ± 17 breaths per minute and 0.22 ± 0.1 ml, respectively (DeLorme and Moss. 2002). The volume of the spacer used in the present study was approximately 800ml. Therefore, in a 6.5min nebulisation period, it would be expected that one mouse would inhale approximately 818ml. That indicates the whole 800ml of aerosol containing 0.22mg cisplatin would be inhaled completely before completing the fixed time period. Furthermore, even with that dose delivered from cisplatin processed NIVs or any other formulation, not all the dose will be inhaled as the use of the spacer results in complete body exposure of the mouse to the aerosol. This could lead to partial loss of the dose by absorption onto the fur coat which was observed to become wet from aerosol exposure in the present study. Phalen and Mendez (2009) have explained the inability of whole-body inhalation systems to allow complete inhalation of an administered dose and their unsuitability for short exposure times. They indicated that absorption of drug on the animal fur and the possible ingestion of absorbed drug during grooming as well as eye irritation and the behaviour of the animal during

inhalation such as burying its nose in its fur could all limit complete inhalation. In addition to the partial loss of the 0.22mg nebulised, the presence of 2-3 mice in the spacer would mean that the available dose for inhalation would be further divided among the mice with 2 mice/spacer inhaling larger portions than 3 mice/spacer. This suggests that whole-body exposure systems along with the experimental design may not be suitable for interpretation of inhalation results.

Therefore, such low doses inhaled could explain the very low levels of cisplatin in tissues in comparison to intravenous injection. That is of course if the inhaled dose actually deposits in the alveolar region and is then absorbed into the systemic circulation. If that is not the case and lymphatic clearance has been reported to be negligible in mice and rats (Snipes *et al.*, 1983), then the inhaled dose would probably have been swallowed after clearance from the upper respiratory tract resulting in systemic absorption from the gastrointestinal tract. Despite suggestions that swallowed particles following clearance from inhalation contribute minimally if at all to systemic absorption (Labiris and Dolovich, 2003a), a study by Sakagami *et al.* (2003) suggested otherwise. It was found that the contribution of pulmonary, nasal and gastrointestinal absorption to the total systemic absorption of fluorescein following inhalation by nose-only exposure system with MMAD of 3.7 μ m in rats was 24.2%, 12.5% and 63.3%, respectively. The study also showed that rats pre-treated orally with activated charcoal, to minimise gastrointestinal absorption of fluorescein, exhibited significantly lower plasma levels of fluorescein than the charcoal-untreated group. This indicated the clearance of inhaled material from the nasopharyngeal and tracheobronchial regions by the mucociliary escalator following inhalation to the gastrointestinal tract where absorption occurred (Sakagami *et al.*, 2003). However this will depend on whether the inhaled drug reaching the gastrointestinal tract can be absorbed or not. Nonetheless, it has been suggested that niosomes have the potential for gastrointestinal absorption (Rentel *et al.*, 1999; Bayinder and Yuksil, 2010). Moreover, cisplatin has been shown to be absorbed across the gastrointestinal tract by passive diffusion (Binks and Dobrota, 1990).

Other than the exposure mode used for inhalation delivery, site of deposition and the size of the aerosol produced; there are other factors that control the fate of an inhaled

particle such as animal species and even interspecies variability (Méndez *et al.*, 2010). Although deposition mechanisms are the same in all mammalian species, variability in particle size, lung morphology, tidal volume and breathing rate will affect deposition (Méndez *et al.*, 2010). The volume of breathed air per unit time as a function of body weight increases for smaller mammals thus leading to inhalation of greater volumes than larger ones, which can play a role in enhancing deposition (Phalen and Mendez, 2009; Méndez *et al.*, 2010). However, the nasal anatomy and mode of bronchial branching is different between mammalian species, thereby also playing a role in affecting the deposition of inhaled particles (Phalen and Mendez, 2009). Because of the complicated nasal anatomy in smaller mammalian species, they are more effective in trapping inhaled particles (Phalen and Mendez, 2009). In BALB/c mice, it has been estimated that particles larger than 1.5 μm in diameter are less likely to deposit in the peripheral regions as they are trapped in the extrathoracic region then cleared (Oldham and Robinson, 2007). When BALB/c mice were administered fluorescent monodisperse polystyrene latex particles of three different particle sizes through a nose-only exposure system; the number of particles deposited in the lungs decreased with increasing size. It was found that for particle sizes 0.5, 1 and 2 μm administered by inhalation; the number of particles deposited in the lungs (\pm SEM) was 593 ± 65 , 324 ± 41 and 5 ± 1 , respectively (Oldham *et al.*, 2009). Furthermore, the amount that actually does reach the pulmonary region in mice and rats is expected to deposit at a faster rate than in humans due to the absence of respiratory bronchioles, where terminal bronchioles are connected directly to the alveoli thereby providing a shorter travelling distance for the aerosol to deposit in the alveoli (Phalen and Mendez, 2009). Nevertheless, the rapid clearance of inhaled particles in mice and rats could also be associated with mechanical clearance resulting in significant amounts being swallowed and entering into the GIT (Snipes *et al.*, 1983).

Therefore, from the different factors affecting pulmonary delivery and the physiological considerations in mice it appears that the unfavourable results obtained following inhalation treatment, especially using processed cisplatin NIVs, could be a result of low dose administered, incomplete nebulisation because of viscosity, mode of exposure, exposure time and the droplet size produced by the nebuliser. By

optimising these factors and verifying deposition using inert tracers of same particle size or biomarkers such as radioactive or fluorescently labelled NIVs can help in obtaining better estimates of pulmonary delivery. Foster *et al.* (2001) evaluated the deposition profile of radiolabeled particles following three inhalation techniques using gamma scintigraphy. Pulmonary deposition (\pm SEM) was estimated to be $77 \pm 7\%$ following a $40\mu\text{l}$ dose administered intratracheally, $81 \pm 2\%$ following a $50\mu\text{l}$ dose administered by oropharyngeal aspiration and $32 \pm 2\%$ following administration by nose-only aerosol inhalation. However, the dose administered by the nose-only method was not specified although the size of the nebulised particles was reported to be $0.65\mu\text{m}$.

The third part of the present study involved a pharmacokinetic study of cisplatin in a rat model. Inhaled processed cisplatin NIVs were compared to intravenously administered cisplatin solution. This time, ICP-MS was used as a highly sensitive non-specific method for detecting total platinum. The non-selectivity of ICP-MS could explain the ability to detect platinum in rat plasma (Figure 7.9) 5min post-dosing following a single intravenous injection unlike the inability to detect platinum in mouse serum (Figure 7.7) 5min post-dosing following a single intravenous dose using HPLC. This could further endorse the fact that cisplatin does actually bind rapidly to plasma proteins. This could also demonstrate the selectivity of the adapted HPLC method to unbound species of platinum.

The pharmacokinetic profile of cisplatin has been previously described by DeConti *et al.* (1973) to follow a biphasic model when administered as a single intravenous dose ranging from $0.066\text{-}3.15\text{mg/kg}$. In the present pharmacokinetic study, the pharmacokinetic profile of both formulations in plasma (Figure 7.9) and lungs (Figure 7.10) when administered as a single intravenous injection or inhalation followed first-order kinetics. Cisplatin solution achieved T_{max} 5min post dosing in both the plasma and lungs, indicating an immediate effect. Inhalation delivery of cisplatin NIVs also achieved T_{max} 5min post dosing in the lungs indicating rapid uptake of cisplatin in the lungs, whereas T_{max} in plasma was 30min indicating time required for drug to be absorbed from the lungs into the systemic circulation. Following inhalation therapy of processed cisplatin NIVs, exposure in the lungs

based on the $AUC_{(0-\infty)}$ was approximately 41 times higher than $AUC_{(0-\infty)}$ in the plasma. This could indicate optimum delivery of cisplatin to lung tissue with minimal systemic exposure by inhalation therapy. The breathing rate and tidal volume of Sprague-Dawley rats was found to be 95 ± 4 breaths/min and 2.22ml, respectively (Walker *et al.*, 1997a). Therefore in a 6.5min nebulisation period using the same 800ml spacer, one rat is expected to inhale approximately 1371ml. That indicates that by approximately 4min the whole nebulised dose would be inhaled. Based on the measured concentration of the processed NIVs (0.75mg/ml) and assuming complete inhalation and deposition of the nebulised dose, 0.20mg of cisplatin would be available for inhalation if 0.27ml of the NIVs were actually nebulised. This would mean that the resultant percentage bioavailability of the inhaled NIVs would be approximately 19%. This could further indicate the preferential localisation of niosomal cisplatin in the lungs with reduced threat of systemic exposure. However as mentioned previously, there is still the possibility of incomplete inhalation of the nebulised dose because of the whole body exposure system which can affect the resultant bioavailability. Unfortunately, no studies regarding pharmacokinetic profile of vesicular cisplatin in rats or mice following inhalation have been reported that can be compared to the present study.

It is evident that additional work is still needed to elucidate the potential of cisplatin NIVs as a successful candidate for targeting lung cancer. It seems that there are many points in this study that require reconsideration before future studies. Financial and time constraints have limited the repetition of such studies for further assessment within the scope of the current research. Points that should be considered include:

- Better standardisation of the model in terms of tumour induction, dosing methodology and formulation dose.
- Standardisation of end-point criteria in anti-tumour assessment where all samples are more rigorously evaluated for tumour burdens and incidence of metastases.

- Processed cisplatin NIVs in the anti-tumour studies should probably be compared to a solution treated group of the same cisplatin concentration, instead of just a comparison to a control group, to provide a more reliable comparison.
- Due to viscosity issue of cisplatin NIVs in dose administration by inhalation, studies comparing different formulations can start by administration of NIVs first and then administration of the same concentration of cisplatin solution.
- Intravenous delivery could probably also be evaluated for anti-tumour activity and compared to inhalation as in tissue uptake studies, especially if processed cisplatin NIVs were found to accumulate significantly in the lung following intravenous administration.
- If processed cisplatin NIVs in these studies are administered without separating the untrapped from entrapped cisplatin, concentration of NIVs should probably be determined for entrapped and untrapped cisplatin as a total.
- It would also be interesting to conduct additional histological studies to evaluate toxicity of cisplatin NIVs in comparison to solution form in the kidneys.
- Optimisation of inhalation delivery would probably play a role in understanding results obtained by such method. By knowing the exact MMAD of the nebulised formulations a decision can be made whether that size is suitable for pulmonary deposition in the chosen animal model or not. Once this has been optimised then suitable mode of exposure should be chosen and the dose accordingly. Whole-body exposure systems are suitable for long dosing times whereas specific site exposure systems can be suitable for short dosing times such as the nose-only or head-only exposure systems. The pulmonary deposition profiles using these systems may be indicated but further evaluation of deposition profile can be done. For instance, deposition

using inert tracers of same particle size or biomarkers such as radioactive or fluorescently labelled NIVs may be useful and allow supplemental imaging to be performed. Such studies could indicate the likelihood of local uptake or systemic absorption. Analysis of susceptible organs and plasma can further endorse the findings.

- Performance of lungs in diseased state should also be taken into consideration in the optimisation of pulmonary delivery as delivery is intended for patients with lung cancer.
- ICP-MS can also be used to compare injected cisplatin solution with cisplatin NIVs and inhaled cisplatin solution with cisplatin NIVs.

7.4. Conclusion

The success of a novel drug in achieving enhanced therapeutic efficacy and/or safety in comparison to conventional therapy is vital for clinical approval. From this preliminary *in vivo* study it can be concluded that processed NIVs show some promise and may prove to be a better candidate than non-processed NIVs in enhancing cisplatin delivery. Intravenous delivery of processed cisplatin NIVs may have additional potential to enhance cisplatin bioavailability. Inhalation therapy may however offer advantageous local targeting. This was supported by the ICP-MS studies of processed cisplatin NIVs that showed greater accumulation of platinum in the lungs than intravenously administered cisplatin solution. However, further studies will need to be done to verify such potential prior to clinical studies being carried out.

General Conclusions and Future work

The aim of the present project was to study the potential of NIVs to provide stable and reliable carriers for the anti-cancer drug cisplatin. This can be achieved through sufficient and sustainable entrapment efficiency and stability as a colloidal system. Entrapment efficiency can be enhanced by preparing NIVs at high drug concentrations. However, this is impeded by the limited aqueous solubility of cisplatin at room temperature. The inclusion of heating enhanced the solubility limit of cisplatin which could subsequently improve entrapment efficiency. However, upon cooling untrapped cisplatin would precipitate which would necessitate the dilution of NIVs. Therefore, the incorporation of ultrafiltration to the preparation steps of NIVs allowed preparation of NIVs (processed NIVs) using high cisplatin concentrations whilst maintaining low untrapped concentrations hence preventing cisplatin precipitation. This was more convenient than diluting the NIVs (non-processed NIVs) which would compromise the number of vesicles per volume in an administered dose. Characterisation studies showed that the size and surface negative charge of the vesicles could be exploited in targeting MPS rich organs, particularly the lungs. Characterisation studies also showed stability of the vesicular delivery system over the short term in terms of entrapment efficiency, size, absence of signs of aggregation through sufficient electrostatic repulsion and absence of precipitated cisplatin. Preliminary *in vitro* studies showed the ability of NIVs to enhance the cytotoxic effect of cisplatin against B16-F0 murine melanoma cancer cells in comparison to cisplatin solution. The characterisation and *in vitro* findings encouraged the investigation of NIVs *in vivo*. A preliminary *in vivo* study of tissue accumulation and anti-tumour activity of cisplatin solution and cisplatin NIVs in a murine model of metastatic lung cancer via intravenous and pulmonary delivery routes was compared. It was also interesting to compare the pharmacokinetic profile of cisplatin NIVs following inhalation as opposed to intravenous cisplatin solution. The preliminary *in vivo* study showed the negative impact of diluting NIVs without ultrafiltration. Non-processed NIVs failed to accumulate efficiently in target tissues unlike its processed counterpart, despite the higher entrapment efficiency obtained with the former. Intravenous administration demonstrated the enhanced accumulation of cisplatin delivered by processed NIVs in the lungs as opposed to cisplatin

solution. Intravenous delivery of processed cisplatin NIVs may have additional potential to enhance cisplatin bioavailability where it provided a better reflection of the *in vivo* fate of processed cisplatin NIVs as demonstrated by their favourable accumulation in the lungs in comparison to inhalation delivery. In the preliminary pharmacokinetic study a more sensitive analytical method was used for detecting platinum levels. Favourable accumulation of cisplatin in the lungs delivered in processed NIVs following inhalation as opposed to intravenous delivery of cisplatin solution was shown. This indicated the possibility of using inhalation therapy to locally target lung tumours. The low local lung concentrations observed in this work could be countered, to some degree, by perhaps increasing the frequency of dosing to compensate for low drug delivery within a vesicle. This indicated the complications associated with pulmonary delivery by nebulisation and the requirement of its optimisation depending on the animal model used, physiological variabilities associated with inhalation therapy and variabilities associated with diseased state of the respiratory tract.

Further evaluation of cisplatin NIVs characteristics prepared in a large scale were investigated over a long-term stability study in comparison with empty NIVs. The study proved the ability of NIVs composed of surfactant VIII, cholesterol and DCP to provide a stable colloidal system on their own. Stable vesicle size with sufficient repulsion and stable content of all lipids was obtainable with no physical signs of sedimentation or flocculation for the whole time period at 4°C and up to the time point empty NIVs were available at 25°C/60% RH and 40°C/75% RH. This indicated the requirement to repeat the stability study at these two storage conditions for empty NIVs to elucidate their stability over a prolonged time period. Utilisation of these NIVs as delivery vehicles for cisplatin showed considerable stability in terms of size, sufficient repulsion with no physical signs of sedimentation or flocculation and overall lipid stability. However, cisplatin NIVs did not meet required stability standards in terms of entrapment efficiency. Using a high cisplatin concentration to enhance entrapment efficiency could be achieved but stability could not be maintainable over the long term as demonstrated by visible precipitation of cisplatin. Lowering the cisplatin concentration solved the problem of unwanted drug precipitation when 1mg/ml cisplatin was used in preparing the NIVs compared with

3 and 6mg/ml cisplatin in a larger scale production. However, this was associated with difficulties in characterising these NIVs in terms of entrapment efficiency. Furthermore, although there is a possibility that cisplatin may react with DCP in a concentration dependant manner, the present research showed that this interaction was negligible and insignificant to jeopardise overall colloidal stability but its effects on anticancer activity still have to be established. This indicates that more studies investigating possible cisplatin and DCP interactions would be advisable. The stability of cisplatin NIVs over the long term requires further optimisation. If cisplatin NIVs were to be stored in suspension form then low concentrations of cisplatin would have to be used in the preparation of NIVs and 25°C would be the appropriate storage condition for cisplatin. However, this would contradict the objective of achieving high entrapment efficiency. If cisplatin NIVs were to be stored in lyophilised forms then probably high cisplatin concentrations may be used in the preparation. However, further studies in optimising the lyophilised formulation will need to be performed.

Future studies could start with addressing the various problems that were reported to be associated with the present research and then expand research.

In characterisation studies, batch to batch variability in entrapment efficiency as a result of heterogeneous vesicle size distribution may be reduced by minimising size heterogeneity. The use of an alternative size reduction method such as sonication or size extrusion may be a mechanism to achieve this. However, this may not be completely overcome because of the heterogeneity of cisplatin in solution form itself in affecting vesicle size and resultant entrapment efficiency.

It would be interesting to study cisplatin particles in solution form and the extent of size heterogeneity and if this heterogeneity is concentration dependant.

Visualisation using FFEM of the different NIVs formulations were not conclusive in defining the structure and lamellarity of the vesicles studied. Perhaps better quality images would be helpful or using other imaging techniques in combination with FFEM would be of greater assistance. Cryo-electron microscopy could endorse images obtained by FFEM by giving a 2-dimensional image of the NIVs to verify

lamellarity. Confocal laser scanning microscopy is also another imaging technique that could be suitable for the NIVs used in the present research.

Lyophilisation may enable the preparation of NIVs using high cisplatin concentrations. However studies will be required to determine the effect of lyophilisation on cisplatin itself and what implications will lyophilisation have on the solubility of cisplatin upon hydration. The vesicle structure can be maintained by adding lyoprotectants, but it would be advisable to perform characterisation studies on cisplatin NIVs before and after lyophilisation for comparison.

If using a high cisplatin concentration in preparation of the NIVs proves impossible perhaps a lower cisplatin may be used. However other methods to separate entrapped from unentrapped drug will need to be performed in order to characterise the NIVs based on entrapment efficiency. Once the entrapment efficiency of NIVs prepared with low cisplatin concentrations can be established then *in vitro* and *in vivo* evaluations can be performed.

Stability studies can be performed on the optimised cisplatin NIVs formulation to investigate its physicochemical characteristics over the long term. Stability studies performed on cisplatin NIVs could also include *in vitro* and *in vivo* evaluation of cisplatin NIVs at each time point in addition to the evaluation of their physicochemical characteristics.

Once physical characteristics of cisplatin NIVs have been optimised, further studies investigating their benefit *in vitro* and *in vivo* can be undertaken. Preliminary *in vitro* studies were performed on a cancer cell line sensitive to cisplatin in the present research. Additional repeat studies can be performed and even *in vitro* studies using cancer cell lines resistant to cisplatin could be considered.

The preliminary *in vivo* study has shown several points that require reconsideration for better *in vivo* evaluation of cisplatin NIVs (Chapter 7). *In vivo* studies can be repeated with these aforementioned points taken into consideration. If results showed a therapeutic potential for cisplatin NIVs as an effective anti-cancer agent then perhaps preclinical studies can be performed on cisplatin resistant cancer models or other animal models.

Cisplatin NIVs may also be evaluated in combination with other chemotherapeutic drugs known to be used with cisplatin whether these drugs were also encapsulated in NIVs or used through their conventional dosing routes. Novel molecular targeting agents may also be considered for use in combination with cisplatin NIVs.

If above highlighted barriers are successfully addressed there is an exciting opportunity for the therapeutic profile of cisplatin to be extended by the use of a drug delivery device to the benefit of a patient population who at present are poorly catered for and who have significant mortality and morbidity. It may also provide a template for the optimisation of new and existing drugs in the oncology field by the utilisation of NIVs.

References

- Abrams, M. (1990). The chemistry of platinum antitumour agents. In D. E. Wilman (Ed.), *The chemistry of platinum antitumour agents* (pp. 331-339): Blackie and Son Ltd., Glasgow, UK.
- Aebi, S., KurdiHaidar, B., Gordon, R., Cenni, B., Zheng, H., Fink, D., *et al.* (1996). Loss of DNA mismatch repair in acquired resistance to cisplatin. *Cancer Research*, 56(13), 3087-3090.
- Aerogen (2010). Aeroneb Lab Retrieved 29-09-2011, from <http://www.aerogen.com/>
- Agilent (2011). The principles of ICP-MS: take a close look at the agilent 7500 ORS Retrieved 29-09-2011, from <http://www.chem.agilent.com/en-US/Products/Instruments/atomicspectroscopy/icp-ms/Pages/gp39983.aspx>
- Ahmed, S. A., Gogal, R. M. and Walsh, J. E. (1994). A new rapid and simple nonradioactive assay to monitor and determine the proliferation of lymphocytes - an alternative to [H-3] thymidine incorporation assay. *Journal of Immunological Methods*, 170(2), 211-224.
- Ahuja, S. (2005). Overview: Handbook of pharmaceutical analysis by HPLC. In S. Ahuja & M. W. Dong (Eds.), *Handbook of pharmaceutical analysis by HPLC* (pp. 1-17): Elsevier Inc.
- Al-Nasiry, S., Geusens, N., Hanssens, M., Luyten, C. and Pijnenborg, R. (2007). The use of Alamar Blue assay for quantitative analysis of viability, migration and invasion of choriocarcinoma cells. *Human Reproduction*, 22(5), 1304-1309.
- Ali, M. (2010). Pulmonary drug delivery. In V. S. Kulkarni (Ed.), *Handbook of non-invasive drug delivery systems* (pp. 209-246): Elsevier Inc.
- Allen, T. M. and Chonn, A. (1987). Large unilamellar liposomes with low uptake into the reticuloendothelial system. *FEBS Letters*, 223(1), 42-46.
- Alley, M. C., Scudiero, D. A., Monks, A., Hursey, M. L., Czerwinski, M. J., Fine, D. *et al.* (1988). Feasibility of drug screening with panels of human-tumor cell-lines using a microculture tetrazolium assay. *Cancer Research*, 48(3), 589-601.
- Almeida, C. A. and Barry, S. A. (2010a). The basics of cancer. In C. A. Almeida & S. A. Barry (Eds.), *Cancer basic science and clinical aspects* (pp. 1-25): John Wiley & Sons Ltd, UK.

- Almeida, C. A. and Barry, S. A. (2010b). Lung Cancer. In C. A. Almeida & S. A. Barry (Eds.), *Cancer basic science and clinical aspects* (pp. 293-311): John Wiley & Sons Ltd., UK.
- Andersson, A. and Ehrsson, H. (1994). Determination of cisplatin and cis-diammineaqua-chloroplatinum (II) ion by liquid-chromatography using postcolumn derivatization with diethyldithiocarbamate. *Journal of Chromatography B-Biomedical Applications*, 652(2), 203-210.
- Andersson, A., Fagerberg, J., Lewensohn, R. and Ehrsson, H. (1996). Pharmacokinetics of cisplatin and its monohydrated complex in humans. *Journal of Pharmaceutical Sciences*, 85(8), 824-827.
- Andrews, P. A., Mann, S. C., Huynh, H. H. and Albright, K. D. (1991). Role of the Na^+, K^+ -adenosine triphosphatase in the accumulation of cis-diamminedichloroplatinum (II) in human ovarian-carcinoma cells. *Cancer Research*, 51(14), 3677-3681.
- Andrews, P. A., Wung, W. E. and Howell, S. B. (1984). A high-performance liquid-chromatographic assay with improved selectivity for cisplatin and active platinum (II) complexes in plasma ultrafiltrate. *Analytical Biochemistry*, 143(1), 46-56.
- Ang, W. H., Myint, M. and Lippard, S. J. (2010). Transcription inhibition by platinum-DNA cross-links in live mammalian cells. *Journal of the American Chemical Society*, 132(21), 7429-7435.
- Anoopkumar-Dukie, S., Carey, J. B., Conere, T., O'Sullivan, E., van Pelt, F. N. and Allshire, A. (2005). Resazurin assay of radiation response in cultured cells. *British Journal of Radiology*, 78(934), 945-947.
- Anthony, D. A., McIlwrath, A. J., Gallagher, W. M., Edlin, A. R. M. and Brown, R. (1996). Microsatellite instability, apoptosis, and loss of p53 function in drug-resistant tumor cells. *Cancer Research*, 56(6), 1374-1381.
- Appleton, T. G. (1997). Donor atom preferences in complexes of platinum and palladium with amino acids and related molecules. *Coordination Chemistry Reviews*, 166, 313-359.

- Arčon, I., Kodre, A., Abra, R. M., Huang, A., Vallner, J. J. and Lasic, D. D. (2004). EXAFS study of liposome-encapsulated cisplatin. *Colloids and Surfaces B-Biointerfaces*, 33(3-4), 199-204.
- Arentsen, H. C., Hendricksen, K., Oosterwijk, E. and Witjes, J. A. (2009). Experimental rat bladder urothelial cell carcinoma models. *World Journal of Urology*, 27(3), 313-317.
- Armstrong, D. K., Bundy, B., Wenzel, L., Huang, H. Q., Baergen, R., Lele, S., *et al.* (2006). Intraperitoneal cisplatin and paclitaxel in ovarian cancer. *New England Journal of Medicine*, 354(1), 34-43.
- Arriagada, R., Le Pechoux, C. and Baeza, M. R. (2003). Prophylactic cranial irradiation in high-risk non-small cell lung cancer patients. *Lung Cancer*, 42, S41-S45.
- Arunothayanun, P., Bernard, M. S., Craig, D. Q. M., Uchegbu, I. F. and Florence, A. T. (2000). The effect of processing variables on the physical characteristics of non-ionic surfactant vesicles (niosomes) formed from a hexadecyl diglycerol ether. *International Journal of Pharmaceutics*, 201(1), 7-14.
- Arunothayanun, P. and Florence, A. T. (2000). Rheology of niosome dispersions. In I. F. Uchegbu (Ed.), *Synthetic surfactant vesicles: niosomes and other non-phospholipid vesicular systems* (pp. 25-48): Overseas Publishers Association.
- Ashman, L. K. (1987). The immunogenicity of tumor-cells. *Immunology and Cell Biology*, 65, 271-277.
- Ashman, L. K., Goh, D. H. B. and Kotlarski, I. (1980). Involvement of donor lymphoreticular cells in the rejection of B16 melanoma by allogeneic mice. *Australian Journal of Experimental Biology and Medical Science*, 58(APR), 159-166.
- Athanasiadis, I., Kies, R. S., Miller, M., Ganzenko, N., Joob, A., Marymont, M., Rademaker, A. and Gradishar, W. J. (1995). Phase II study of all-trans-retinoic acid and alpha-interferon in patients with advanced non-small cell lung cancer. *Clinical Cancer Research*, 1(9), 973-979.
- Augey, V., Cociglio, M., Galtier, M., Yearoo, R., Pinsani, V. and Bressolle, F. (1995). High-performance liquid-chromatographic determination of cis-

- dichlorodiammineplatinum (II) in plasma ultrafiltrate. *Journal of Pharmaceutical and Biomedical Analysis*, 13(9), 1173-1178.
- Auperin, A., Arriagada, R., Pignon, J. P., Le Pechoux, C., Gregor, A., Stephens, R., *et al.* (1999). Prophylactic cranial irradiation for patients with small-cell lung cancer in complete remission. *New England Journal of Medicine*, 341(7), 476-484.
- Azarmi, S., Roa, W. H. and Loebenberg, R. (2008). Targeted delivery of nanoparticles for the treatment of lung diseases. *Advanced Drug Delivery Reviews*, 60(8), 863-875.
- Bailey, M. M. and Berkland, C. J. (2009). Nanoparticle formulations in pulmonary drug delivery. *Medicinal Research Reviews*, 29(1), 196-212.
- Banduwardene, R., Mullen, A. B. and Carter, K. C. (1997). Immune responses of *Leishmania donovani* infected BALB/c mice following treatment with free and vesicular sodium stibogluconate formulations. *International Journal of Immunopharmacology*, 19(4), 195-203.
- Bangham, A. D., Standish, M. M. and Watkins, J. C. (1965). Diffusion of univalent ions across lamellae of swollen phospholipids. *Journal of Molecular Biology*, 13(1), 238-252.
- Bannister, S. J., Chang, Y., Sternson, L. A. and Repta, A. J. (1978). Atomic-absorption spectrophotometry of free circulating platinum species in plasma derived from cis-dichlorodiammineplatinum (II). *Clinical Chemistry*, 24(6), 877-880.
- Bannister, S. J., Sternson, L. A. and Repta, A. J. (1979). Urine analysis of platinum species derived from cis-dichlorodiammineplatinum (II) by high-performance liquid-chromatography following derivatization with sodium diethyldithiocarbamate. *Journal of Chromatography*, 173(2), 333-342.
- Bannister, S. J., Sternson, L. A., Repta, A. J. and James, G. W. (1977). Measurement of free-circulating cis-dichlorodiammineplatinum (II) in plasma. *Clinical Chemistry*, 23(12), 2258-2262.
- Barbeau, J., Cammas-Marion, S., Auvray, P. and Benvegnu, T. (2011). Preparation and characterization of stealth archaeosomes based on a synthetic pegylated archaeal tetraether lipid. *Journal of drug delivery*, 2011, 396068.

- Barenholz, Y. (2001). Liposome application: problems and prospects. *Current Opinion in Colloid & Interface Science*, 6(1), 66-77.
- Barth, H. G. and Sun, S. T. (1991). Particle-size analysis. *Analytical Chemistry*, 63(12), R1-R10.
- Bassett, E., Vaisman, A., Tropea, K. A., McCall, C. M., Masutani, C., Hanaoka, F. and Chaney, S. G. (2002). Frameshifts and deletions during *in vitro* translesion synthesis past Pt-DNA adducts by DNA polymerases beta and eta. *DNA Repair*, 1(12), 1003-1016.
- Bayindir, Z. S. and Yuksel, N. (2010). Characterization of niosomes prepared with various non-ionic surfactants for paclitaxel oral delivery. *Journal of Pharmaceutical Sciences*, 99(4), 2049-2060.
- Becker, J. C., Houben, R., Schrama, D., Voigt, H., Ugurel, S. and Reisfeld, R. A. (2010). Mouse models for melanoma: a personal perspective. *Experimental Dermatology*, 19(2), 157-164.
- Bell, D. N., Liu, J. J., Tingle, M. D. and McKeage, M. J. (2006). Specific determination of intact cisplatin and monohydrated cisplatin in human plasma and culture medium ultrafiltrates using HPLC on-line with inductively coupled plasma mass spectrometry. *Journal of Chromatography B-Analytical Technologies in the Biomedical and Life Sciences*, 837(1-2), 29-34.
- Beretta, G. L., Gatti, L., Tinelli, S., Corna, E., Colangelo, D., Zunino, F. and Perego, P. (2004). Cellular pharmacology of cisplatin in relation to the expression of human copper transporter CTR1 in different pairs of cisplatin-sensitive and -resistant cells. *Biochemical Pharmacology*, 68(2), 283-291.
- Bergh, M., Shao, L. P., Hagelthorn, G., Gafvert, E., Nilsson, J. L. G. and Karlberg, A. T. (1998). Contact allergens from surfactants: Atmospheric oxidation of polyoxyethylene alcohols, formation of ethoxylated aldehydes, and their allergenic activity. *Journal of Pharmaceutical Sciences*, 87(3), 276-282.
- Berne, B. J. and Pecora, R. (1976). Light scattering and fluctuations. In B. J. Berne & R. Pecora (Eds.), *Dynamic light scattering with applications to chemistry, biology and physics* (pp. 10-23): John Wiley and Sons, Inc.

- Berners-Price, S. J. and Appleton, T. G. (2000). The chemistry of cisplatin in aqueous solution. In L. Kelland & N. P. Farrell (Eds.), *Platinum-based drugs in cancer therapy* (pp. 3-35): Humana Press Inc., NJ, USA.
- Bibi, S., Kaur, R., Henriksen-Lacey, M., McNeil, S. E., Wilkhu, J., Lattmann, E., Christensen, D., Mohammed, A. R. and Perrie, Y. (2011). Microscopy imaging of liposomes: from coverslips to environmental SEM. *International Journal of Pharmaceutics*, 417(1-2), 138-150.
- Bidlingmeyer, B. A. (1992a). Overview of modern liquid chromatography. In B. A. Bidlingmeyer (Ed.), *Practical HPLC methodology and applications* (pp. 1-26): John Wiley and Sons, Inc., NY, USA.
- Bidlingmeyer, B. A. (1992b). Gradient elution chromatography. In B. A. Bidlingmeyer (Ed.), *Practical HPLC methodology and applications* (pp. 284-317): John Wiley and Sons, Inc., NY, USA.
- Binks, S. P. and Dobrota, M. (1990). Kinetics and mechanism of uptake of platinum-based pharmaceuticals by the rat small intestine. *Biochemical Pharmacology*, 40(6), 1329-1336.
- Bodin, A., Linnerborg, M., Nilsson, J. L. G. and Karlberg, A. T. (2003). Structure elucidation, synthesis, and contact allergenic activity of a major hydroperoxide formed at autoxidation of the ethoxylated surfactant C12E5. *Chemical Research in Toxicology*, 16(5), 575-582.
- Bosch, M. E., Sanchez, A. J. R., Rojas, F. S. and Ojeda, C. B. (2008). Analytical methodologies for the determination of cisplatin. *Journal of Pharmaceutical and Biomedical Analysis*, 47(3), 451-459.
- Boughattas, N. A., Levi, F., Fournier, C., Hecquet, B., Lemaigre, G., Roulon, A., Mathe, G. and Reinberg, A. (1990). Stable circadian mechanisms of toxicity of 2 platinum analogs (cisplatin and carboplatin) despite repeated dosages in mice. *Journal of Pharmacology and Experimental Therapeutics*, 255(2), 672-679.
- Boyer, C. and Zasadzinski, J. A. (2007). Multiple lipid compartments slow vesicle contents release in lipases and serum. *ACS Nano*, 1(3), 176-182.

- Brabec, V. (2000). Chemistry and structural biology of 1,2-interstrand adducts of cisplatin. In L. Kelland & N. P. Farrell (Eds.), *Platinum-based drugs in cancer therapy* (pp. 37-61): Humana Press Inc., NJ, USA.
- Brabec, V. and Leng, M. (1993). DNA interstrand cross-links of trans-diamminedichloroplatinum (II) are preferentially formed between guanine and complementary cytosine residues. *Proceedings of the National Academy of Sciences of the United States of America*, 90(11), 5345-5349.
- Brambilla, E., Travis, W. D., Colby, T. V., Corrin, B. and Shimosato, Y. (2001). The new World Health Organization classification of lung tumours. *European Respiratory Journal*, 18(6), 1059-1068.
- Brière, K. M., Goel, R., Shirazi, F. H., Stewart, D. J. and Smith, I. C. P. (1996). The integrity of cisplatin in aqueous and plasma ultrafiltrate media studied by Pt-195 and N-15 nuclear magnetic resonance. *Cancer Chemotherapy and Pharmacology*, 37(6), 518-524.
- Brouwers, E. E. M., Tibben, M., Rosing, H., Schellens, J. H. M. and Beijnen, J. H. (2008a). The application of inductively coupled plasma mass spectrometry in clinical pharmacological oncology research. *Mass Spectrometry Reviews*, 27(2), 67-100.
- Brouwers, E. E. M., Tibben, M. M., Plum, D., Rosing, H., Boot, H., Cats, A., Schellens, J. H. M. and Beijnen, J. H. (2008b). Inductively coupled plasma mass spectrometric analysis of the total amount of platinum in DNA extracts from peripheral blood mononuclear cells and tissue from patients treated with cisplatin. *Analytical and Bioanalytical Chemistry*, 391(2), 577-585.
- Brouwers, E. E. M., Huitema, A. D. R., Beijnen, J. H. and Schellens, J. H. M. (2008c). Long-term platinum retention after treatment with cisplatin and oxaliplatin. *BMC clinical pharmacology*, 8, 7.
- Bruhn, S. L., Pil, P. M., Essigmann, J. M., Housman, D. E. and Lippard, S. J. (1992). Isolation and characterization of human cDNA clones encoding a high mobility group box protein that recognizes structural distortions to DNA caused by binding of the anticancer agent cisplatin. *Proceedings of the National Academy of Sciences of the United States of America*, 89(6), 2307-2311.

- Burger, K. N. J., Staffhorst, R. and De Kruijff, B. (1999). Interaction of the anti-cancer drug cisplatin with phosphatidylserine in intact and semi-intact cells. *Biochimica Et Biophysica Acta-Biomembranes*, 1419(1), 43-54.
- Burger, K. N. J., Staffhorst, R., de Vijlder, H. C., Velinova, M. J., Bomans, P. H., Frederik, P. M. and de Kruijff, B. (2002). Nanocapsules: lipid-coated aggregates of cisplatin with high cytotoxicity. *Nature Medicine*, 8(1), 81-84.
- Carvalho, T. C., Carvalho, S. R. and McConville, J. T. (2011a). Formulations for pulmonary administration of anticancer agents to treat lung malignancies. *Journal of Aerosol Medicine and Pulmonary Drug Delivery*, 24(2), 61-80.
- Carvalho, T. C., Peters, J. I. and Williams, R. O., III (2011b). Influence of particle size on regional lung deposition - What evidence is there? *International Journal of Pharmaceutics*, 406(1-2), 1-10.
- Carver, B. S. and Pandolfi, P. P. (2006). Mouse modeling in oncologic preclinical and translational research. *Clinical Cancer Research*, 12(18), 5305-5311.
- Cevc, G. and Richardsen, H. (1999). Lipid vesicles and membrane fusion. *Advanced Drug Delivery Reviews*, 38(3), 207-232.
- Chaney, S. G. and Sancar, A. (1996). DNA repair: Enzymatic mechanisms and relevance to drug response. *Journal of the National Cancer Institute*, 88(19), 1346-1360.
- Chang, A. (2010). Chemotherapy, chemoresistance and the changing treatment landscape for NSCLC. *Lung cancer*.
- Chang, Y. H., Abdalla, D. S. P. and Sevanian, A. (1997). Characterization of cholesterol oxidation products formed by oxidative modification of low density lipoprotein. *Free Radical Biology and Medicine*, 23(2), 202-214.
- Chen, C., Han, D., Zhang, Y., Yuan, Y. and Tang, X. (2010). The freeze-thawed and freeze-dried stability of cytarabine-encapsulated multivesicular liposomes. *International Journal of Pharmaceutics*, 387(1-2), 147-153.
- Chono, S., Tanino, T., Seki, T. and Morimoto, K. (2006). Influence of particle size on drug delivery to rat alveolar macrophages following pulmonary administration of ciprofloxacin incorporated into liposomes. *Journal of Drug Targeting*, 14(8), 557-566.

- Choy, H., Park, C. and Yao, M. (2008). Current status and future prospects for satraplatin, an oral platinum analogue. *Clinical Cancer Research*, 14(6), 1633-1638.
- Christian, G. D. (1994). Chromatographic methods. In G. D. Christian (Ed.), *Analytical chemistry* (5th ed., pp. 505-561): John Wiley and Sonc, Inc., USA.
- Ciuleanu, T., Samarzjia, M., Demidchik, Y., Beliakouski, V., Rancic, M., *et al.* (2010). Randomized phase III study (SPEAR) of picolatin plus best supportive care (BSC) or BSC alone in patients (pts) with SCLC refractory or progressive within 6 months after first-line platinum-based chemotherapy. *Journal of Clinical Oncology*, 28(Suppl: abstr 7002), 15s.
- Cortesi, R., Esposito, E., Corradini, F., Sivieri, E., Drechsler, M., Rossi, A., Scatturin, A. and Menegatti, E. (2007). Non-phospholipid vesicles as carriers for peptides and proteins: Production, characterization and stability studies. *International Journal of Pharmaceutics*, 339(1-2), 52-60.
- Crommelin, D. J. A., Hennink, W. E. and Storm, G. (2001). Drug targeting systems: fundamentals and applications to parenteral drug delivery. In A. M. Hillery, A. W. Lloyd & J. Swarbrick (Eds.), *Drug delivery and targeting for pharmacists and pharmaceutical scientists* (pp. 118-144): CRC Press, Florida, USA.
- Crommelin, D. J. A. and Schreier, H. (1994). Liposomes. In J. Kreuter (Ed.), *Colloidal drug delivery systems* (pp. 73-190): Marccel Dekker, Inc., NY, USA.
- CRUK (2010). CancerStats-Key Facts on lung cancer and smoking Retrieved 29-09-2010, from <http://info.cancerresearchuk.org/cancerstats/types/lung/index.htm?script=true>
- Cui, Y. H., Konig, J., Buchholz, U., Spring, H., Leier, I. and Keppler, D. (1999). Drug resistance and ATP-dependent conjugate transport mediated by the apical multidrug resistance protein, MRP2, permanently expressed in human and canine cells. *Molecular Pharmacology*, 55(5), 929-937.
- Cullis, P. R., Hope, M. J., Bally, M. B., Madden, T. D., Mayer, L. D. and Fenske, D. B. (1997). Influence of pH gradients on the transbilayer transport of drugs,

- lipids, peptides and metal ions into large unilamellar vesicles. *Biochimica Et Biophysica Acta-Reviews on Biomembranes*, 1331(2), 187-211.
- Dabrowiak, J. C. and Bradner, W. T. (1987). Platinum antitumour agents. *Progress in medicinal chemistry*, 24, 129-158.
- Daleyates, P. T. and McBrien, D. C. H. (1983). Cisplatin metabolites: a method for their separation and for measurement of their renal clearance invivo. *Biochemical Pharmacology*, 32(1), 181-184.
- Daleyates, P. T. and McBrien, D. C. H. (1984). Cisplatin metabolites in plasma: a study of their pharmacokinetics and importance in the nephrotoxic and antitumour activity of cisplatin. *Biochemical Pharmacology*, 33(19), 3063-3070.
- Dancey, J. E. (2007). Epidermal growth factor receptor inhibitors in non-small cell lung cancer. *Drugs*, 67(8), 1125-1138.
- de Boer, A. H., Gjaltema, D., Hagedoorn, P. and Frijlink, H. W. (2002). Characterization of inhalation aerosols: a critical evaluation of cascade impactor analysis and laser diffraction technique. *International Journal of Pharmaceutics*, 249(1-2), 219-231.
- DeConti, R. C., Toftness, B. R., Lange, R. C. and Creasey, W. A. (1973). Clinical and pharmacological studies with cis-diamminedichloroplatinum (II). *Cancer Research*, 33(6), 1310-1315.
- DeLorme, M. P. and Moss, O. R. (2002). Pulmonary function assessment by whole-body plethysmography in restrained versus unrestrained mice. *Journal of Pharmacological and Toxicological Methods*, 47(1), 1-10.
- Derjaguin, B. and Landau, L. (1941). Theory of the stability of strongly charged lyophobic sols and of the adhesion of strongly charged particles in solution of electrolytes. *Acta Physico Chimica (USSR)*(14), 633-662.
- Desai, T. R. and Finlay, W. H. (2002). Nebulization of niosomal all-trans-retinoic acid: an inexpensive alternative to conventional liposomes. *International Journal of Pharmaceutics*, 241(2), 311-317.
- Desai, T. R., Hancock, R. E. W. and Finlay, W. H. (2002). A facile method of delivery of liposomes by nebulization. *Journal of Controlled Release*, 84(1-2), 69-78.

- Deschamps, F. S., Chaminade, P., Ferrier, D. and Baillet, A. (2001a). Assessment of the retention properties of poly(vinyl alcohol) stationary phase for lipid class profiling in liquid chromatography. *Journal of Chromatography A*, 928(2), 127-137.
- Deschamps, F. S., Gaudin, K., Lesellier, E., Tchaplal, A., Ferrier, D., Baillet, A. and Chaminade, P. (2001b). Response enhancement for the evaporative light scattering detection for the analysis of lipid classes and molecular species. *Chromatographia*, 54(9-10), 607-611.
- Devarajan, P., Tarabishi, R., Mishra, J., Ma, Q., Kourvetaris, A., Vougiouka, M. and Boulikas, T. (2004). Low renal toxicity of lipoplatin compared to cisplatin in animals. *Anticancer Research*, 24(4), 2193-2200.
- DeVita, V. T., Jr. and Chu, E. (2008). A history of cancer chemotherapy. *Cancer Research*, 68(21), 8643-8653.
- Di Costanzo, F., Mazzoni, F., Mela, M. M., Antonuzzo, L., Checcacci, D., Saggese, M. and Di Costanzo, F. (2008). Bevacizumab in non-small cell lung cancer. *Drugs*, 68(6), 737-746.
- Di Marzio, L., Marianecchi, C., Petrone, M., Rinaldi, F. and Carafa, M. (2011). Novel pH-sensitive non-ionic surfactant vesicles: comparison between Tween 21 and Tween 20. *Colloids and Surfaces B-Biointerfaces*, 82(1), 18-24.
- Dolan, J. W. (1986). LC troubleshooting: Separation artifacts I - sample overload and injection-solvent problems. *LC*, 4, 16-20.
- Dolan, J. W. (1992). LC troubleshooting: pump shutdown, sparging problems, double peaks. *LC-GC*, 10, 84-86.
- Dolan, J. W. (2004). LC troubleshooting: system suitability. *LC-GC*, 22, 430-435.
- Dong, M. W. (2006a). Introduction. In M. W. Dong (Ed.), *Modern HPLC for practicing scientists* (pp. 1-14): John Wiley and Sons, Inc., NJ, USA.
- Dong, M. W. (2006b). HPLC instrumentation and trends. In M. W. Dong (Ed.), *Modern HPLC for practicing scientists* (pp. 77-110): John Wiley and Sons, Inc., NJ, USA.
- Drummer, O. H., Proudfoot, A., Howes, L. and Louis, W. J. (1984). High-performance liquid-chromatographic determination of platinum (II) in plasma

- ultrafiltrate and urine: comparison with a flameless atomic-absorption spectrometric method. *Clinica Chimica Acta*, 136(1), 65-74.
- Drummond, D. C., Noble, C. O., Hayes, M. E., Park, J. W. and Kirpotin, D. B. (2008). Pharmacokinetics and *in vivo* drug release rates in liposomal nanocarrier development. *Journal of Pharmaceutical Sciences*, 97(11), 4696-4740.
- du Plessis, J., Ramachandran, C., Weiner, N. and Muller, D. G. (1996). The influence of lipid composition and lamellarity of liposomes on the physical stability of liposomes upon storage. *International Journal of Pharmaceutics*, 127(2), 273-278.
- Eastman, A. (1999). The mechanism of action of cisplatin: from adducts to apoptosis. In B. Lippert (Ed.), *Cisplatin: chemistry and biochemistry of a leading anticancer drug* (pp. 111-134): Zurich: Verlag Helvetica Chimica Acta; Weinham; NY: Wiley-VCH.
- Eckardt, J. R., Bentsion, D. L., Lipatov, O. N., Polyakov, I. S., MacKintosh, F. R., Karlin, D. A., Baker, G. S. and Breitz, H. B. (2009). Phase II study of picoplatin as second-line therapy for patients with small-cell lung cancer. *Journal of Clinical Oncology*, 27(12), 2046-2051.
- Edwards, K. A. and Baeumner, A. J. (2006). Analysis of liposomes. *Talanta*, 68(5), 1432-1441.
- Eksteen, R. (1996). Column selection in high performance liquid chromatography. In E. D. Katz (Ed.), *High performance liquid chromatography: principles and methods*: John Wiley and Sons, Ltd., West Sussex, UK.
- Elmi, M. M. and Sarbolouki, M. N. (2001). A simple method for preparation of immuno-magnetic liposomes. *International Journal of Pharmaceutics*, 215(1-2), 45-50.
- eMC (2011). The electronic Medicines Compendium Retrieved 22-09-2011, from www.medicines.org.uk/EMC/searchresults.aspx?term=Cisplatin&searchtype=QuickSearch
- Erdogan, S., Ozer, A. Y., Ercan, M. T., Eryilmaz, M. and Hincal, A. A. (1996). *In vivo* studies on iopromide radiopaque niosomes. *STP Pharma Sciences*, 6(1), 87-93.

- Espinosa, E., Feliu, J., Zamora, P., Baron, M. G., Sanchez, J. J., Ordonez, A. and Espinosa, J. (1995). Serum-albumin and other prognostic factors related to response and survival in patients with advanced non-small cell lung cancer. *Lung Cancer*, 12(1-2), 67-76.
- Falta, T., Heffeter, P., Mohamed, A., Berger, W., Hann, S. and Koellensperger, G. (2011). Quantitative determination of intact free cisplatin in cell models by LC-ICP-MS. *Journal of Analytical Atomic Spectrometry*, 26(1), 109-115.
- Falter, R. and Wilken, R. D. (1999). Determination of carboplatinum and cisplatinum by interfacing HPLC with ICP-MS using ultrasonic nebulisation. *Science of the Total Environment*, 225(1-2), 167-176.
- Fang, F., Balch, C., Schilder, J., Breen, T., Zhang, S., Shen, C. Y., Li, L., Kulesavage, C., Snyder, A. J., Nephew, K. P. and Matei, D. E. (2010). A Phase 1 and pharmacodynamic study of decitabine in combination with carboplatin in patients with recurrent, platinum-resistant, epithelial ovarian cancer. *Cancer*, 116(17), 4043-4053.
- Farr, S. J., Kellaway, I. W., Parryjones, D. R. and Woolfrey, S. G. (1985). Technetium ^{99m} as a marker of liposomal deposition and clearance in the human lung. *International Journal of Pharmaceutics*, 26(3), 303-316.
- Felnerova, D., Viret, J. F., Gluck, R. and Moser, C. (2004). Liposomes and virosomes as delivery systems for antigens, nucleic acids and drugs. *Current Opinion in Biotechnology*, 15(6), 518-529.
- Ferlay, J., Shin, H. R., Bray, F., Forman, D., Mathers, C. and Parkin, D. M. (2010). GLOBOCAN 2008, Cancer Incidence and Mortality Worldwide. Retrieved 24-08-2011, from International Agency for Research on Cancer, Lyon, France: <http://globocan.iarc.fr>
- Ferry, K. V., Hamilton, T. C. and Johnson, S. W. (2000). Increased nucleotide excision repair in cisplatin-resistant ovarian cancer cells - Role of ERCC1-XPF. *Biochemical Pharmacology*, 60(9), 1305-1313.
- Fidler, I. J. (1975). Biological behaviour of malignant-melanoma cells correlated to their survival *in vivo*. *Cancer Research*, 35(1), 218-224.

- Fidler, I. J., Raz, A., Fogler, W. E., Kirsh, R., Bugelski, P. and Poste, G. (1980). Design of liposomes to improve delivery of macrophage-augmenting agents to alveolar macrophages. *Cancer Research*, 40(12), 4460-4466.
- Fink, D., Nebel, S., Aebi, S., Zheng, H., Cenni, B., Nehme, A., Christen, R. D. and Howell, S. B. (1996). The role of DNA mismatch repair in platinum drug resistance. *Cancer Research*, 56(21), 4881-4886.
- Florence, A. T. (1993a). New drug delivery systems. *Chemistry & Industry*(24), 1000-1004.
- Florence, A. T. (1993b). Non-ionic surfactant vesicle preparation and characterisation. In G. Gregordias (Ed.), *Liposomes Technology* (Vol. 2, pp. 157-176): CRC Press, Florida, USA.
- Fonseca, M., vanWinden, E. C. A. and Crommelin, D. J. A. (1997). Doxorubicin induces aggregation of small negatively charged liposomes. *European Journal of Pharmaceutics and Biopharmaceutics*, 43(1), 9-17.
- Foster, W. M., Walters, D. M., Longphre, M., Macri, K. and Miller, L. M. (2001). Methodology for the measurement of mucociliary function in the mouse by scintigraphy. *Journal of Applied Physiology*, 90(3), 1111-1117.
- Fransen, G. J., Salemink, P. J. M. and Crommelin, D. J. A. (1986). Critical parameters in freezing of liposomes. *International Journal of Pharmaceutics*, 33(1-3), 27-35.
- Freshney, R. I. (1994a). Introduction. In R. I. Freshney (Ed.), *Culture of animal cells: a manual of basic techniques* (3rd ed., pp. 1-7): Wiley-Liss, Inc., NY, USA.
- Freshney, R. I. (1994b). Quantitation of experimental design. In R. I. Freshney (Ed.), *Culture of animal cells: a manual of basic techniques* (3rd ed., pp. 267-286): Wiley-Liss, Inc., NY, USA.
- Fresta, M., Villari, A., Puglisi, G. and Cavallaro, G. (1993). 5-Fluorouracil - various kinds of loaded liposomes - encapsulation efficiency, storage stability and fusogenic properties. *International Journal of Pharmaceutics*, 99(2-3), 145-156.
- Froudarakis, M. E., Pataka, A., Pappas, P., Anevlavis, S., Argiana, E., Nikolaidou, M., *et al.* (2008). Phase 1 trial of lipoplatin and gemcitabine as a second-line

- chemotherapy in patients with non-small cell lung carcinoma. *Cancer*, 113(10), 2752-2760.
- Gadducci, A., Cosio, S., Muraca, S. and Genazzani, A. R. (2002). Molecular mechanisms of apoptosis and chemosensitivity to platinum and paclitaxel in ovarian cancer: biological data and clinical implications. *European Journal of Gynaecological Oncology*, 23(5), 390-396.
- García Sar, D., Montes-Bayon, M., Blanco-Gonzalez, E. and Sanz-Medel, A. (2010). Quantitative methods for studying DNA interactions with chemotherapeutic cisplatin. *Trac-Trends in Analytical Chemistry*, 29(11), 1390-1398.
- Gately, D. P. and Howell, S. B. (1993). Cellular accumulation of the anticancer agent cisplatin - a review. *British Journal of Cancer*, 67(6), 1171-1176.
- Gaumet, M., Vargas, A., Gurny, R. and Delie, F. (2008). Nanoparticles for drug delivery: The need for precision in reporting particle size parameters. *European Journal of Pharmaceutics and Biopharmaceutics*, 69(1), 1-9.
- Gazzano-Santoro, H., Ralph, P., Ryskamp, T. C., Chen, A. B. and Mukku, V. R. (1997). A non-radioactive complement-dependent cytotoxicity assay for anti-CD20 monoclonal antibody. *Journal of Immunological Methods*, 202(2), 163-171.
- Geiser, M., Schurch, S. and Gehr, P. (2003). Influence of surface chemistry and topography of particles on their immersion into the lung's surface-lining layer. *Journal of Applied Physiology*, 94(5), 1793-1801.
- Giaccone, G., O'Brien, M. E. R., Byrne, M. J., Bard, M., Kaukel, E. and Smit, B. (2002). Phase II trial of ZD0473 as second-line therapy in mesothelioma. *European Journal of Cancer*, 38, S19-S24.
- Gianasi, E., Cociancich, F., Uchegbu, I. F., Florence, A. T. and Duncan, R. (1997). Pharmaceutical and biological characterisation of a doxorubicin-polymer conjugate (PK1) entrapped in sorbitan monostearate Span 60 niosomes. *International Journal of Pharmaceutics*, 148(2), 139-148.
- Gilpin, R. K. and Gilpin, C. S. (2009). Pharmaceuticals and Related Drugs. *Analytical Chemistry*, 81(12), 4679-4694.
- Glavas-Dodov, M., Fredro-Kumbaradzi, E., Goracinova, K., Simonoska, M., Calis, S., Trajkovic-Jolevskaa, S. and Hincal, A. A. (2005). The effects of

- lyophilization on the stability of liposomes containing 5-FU. *International Journal of Pharmaceutics*, 291(1-2), 79-86.
- Gloeckner, H., Jonuleit, T. and Lemke, H. D. (2001). Monitoring of cell viability and cell growth in a hollow-fiber bioreactor by use of the dye Alamar Blue (TM). *Journal of Immunological Methods*, 252(1-2), 131-138.
- Goel, R., Andrews, P. A., Pfeifle, C. E., Abramson, I. S., Kirmani, S. and Howell, S. B. (1990). Comparison of the pharmacokinetics of ultrafilterable cisplatin species detectable by derivatization with diethyldithiocarbamate or atomic-absorption spectroscopy. *European Journal of Cancer*, 26(1), 21-27.
- Goerke, J. (1998). Pulmonary surfactant: functions and molecular composition. *Biochimica Et Biophysica Acta-Molecular Basis of Disease*, 1408(2-3), 79-89.
- Gore, M. E., Atkinson, R. J., Thomas, H., Cure, H., Rischin, D., Beale, P., Bougnoux, P., Dirix, L. and Smit, W. M. (2002). A phase II trial of ZD0473 in platinum-pretreated ovarian cancer. *European Journal of Cancer*, 38(18), 2416-2420.
- Goyal, P., Goyal, K., Kumar, S. G. V., Singh, A., Katare, O. P. and Mishra, D. N. (2005). Liposomal drug delivery systems: clinical applications. *Acta Pharmaceutica (Zagreb)*, 55(1), 1-25.
- Gralla, R. J., Osoba, D., Kris, M. G., Kirkbride, P., Hesketh, P. J., Chinnery, L. W., et al. (1999). Recommendations for the use of antiemetics: evidence-based, clinical practice guidelines. *Journal of Clinical Oncology*, 17(9), 2971-2994.
- Gray, A. and Morgan, J. (1991). Liposomes in hematology. *Blood Reviews*, 5(4), 258-271.
- Grit, M. and Crommelin, J. A. (1993). Chemical-stability of liposomes - implications for their physical stability. *Chemistry and Physics of Lipids*, 64(1-3), 3-18.
- Groneberg, D. A., Witt, C., Wagner, U., Chung, K. F. and Fischer, A. (2003). Fundamentals of pulmonary drug delivery. *Respiratory Medicine*, 97(4), 382-387.
- Gude, R. P., Jadhav, M. G., Rao, S. G. A. and Jagtap, A. G. (2002). Effects of niosomal cisplatin and combination of the same with theophylline and with

- activated macrophages in murine B16-F10 melanoma model. *Cancer Biotherapy and Radiopharmaceuticals*, 17(2), 183-192.
- Guerin, T. F., Mondido, M., McClenn, B. and Peasley, B. (2001). Application of resazurin for estimating abundance of contaminant-degrading microorganisms. *Letters in Applied Microbiology*, 32(5), 340-345.
- Gullo, J. J., Litterst, C. L., Maguire, P. J., Sikic, B. I., Hoth, D. F. and Woolley, P. V. (1980). Pharmacokinetics and protein-binding of cis-dichlorodiammine platinum (II) administered as a one-hour or as a 20-hour infusion. *Cancer Chemotherapy and Pharmacology*, 5(1), 21-26.
- Hajdu, S. I. (2011a). A note from history: Landmarks in history of cancer, part 1. *Cancer*, 117(5), 1097-1102.
- Hajdu, S. I. (2011b). A Note From History: Landmarks in History of Cancer, Part 2. *Cancer*, 117(12), 2811-2820.
- Hajdu, S. I. (2011c). A note from history: Landmarks in history of cancer, part 3. *Cancer*, n/a-n/a.
- Hamid, R., Rotshteyn, Y., Rabadi, L., Parikh, R. and Bullock, P. (2004). Comparison of Alamar Blue and MTT assays for high through-put screening. *Toxicology in vitro*, 18(5), 703-710.
- Hammond, E. W. (1993). High performance liquid chromatography. In E. W. Hammond (Ed.), *Chromtography for the analysis of lipids* (pp. 113-153): CRC Press, Inc., Florida, USA.
- Hanahan, D. and Weinberg, R. A. (2000). The hallmarks of cancer. *Cell*, 100(1), 57-70.
- Hanai, T. (1999). Basic concepts of HPLC. In T. Hanai (Ed.), *HPLC a practical guide* (pp. 1-10): The Royal Society of Chemistry, Cambridge, UK.
- Handjani-Vila, R. M., Ribier, A., Rondot, B. and Vanlerberghie, G. (1979). Dispersions of lamellar phases of nonionic lipids in cosmetic products. *International Journal of Cosmetic Science*, 1(5), 303-314.
- Hann, S., Koellensperger, G., Stefanka, Z., Stingeder, G., Furrhacker, M., Buchberger, W. and Mader, R. M. (2003). Application of HPLC-ICP-MS to speciation of cisplatin and its degradation products in water containing

- different chloride concentrations and in human urine. *Journal of Analytical Atomic Spectrometry*, 18(11), 1391-1395.
- Hann, S., Stefanka, Z., Lenz, K. and Stinger, G. (2005). Novel separation method for highly sensitive speciation of cancerostatic platinum compounds by HPLC-ICP-MS. *Analytical and Bioanalytical Chemistry*, 381(2), 405-412.
- Hansson, J. and Wood, R. D. (1989). Repair synthesis by human cell-extracts in DNA damaged by cis-diamminedichloroplatinum (II) and trans-diamminedichloroplatinum (II). *Nucleic Acids Research*, 17(20), 8073-8091.
- Harrington, K. J., Lewanski, C. R., Northcote, A. D., Whittaker, J., Wellbank, H., Vile, R. G., Peters, A. M. and Stewart, J. S. W. (2001). Phase I-II study of pegylated liposomal cisplatin (SPI-077TM) in patients with inoperable head and neck cancer. *Annals of Oncology*, 12(4), 493-496.
- Harrington, K. J., Lewanski, C. R. and Stewart, J. S. W. (2000a). Liposomes as vehicles for targeted therapy of cancer. Part 1: Preclinical development. *Clinical Oncology*, 12(1), 2-15.
- Harrington, K. J., Rowlinson-Busza, G., Syrigos, K. N., Vile, R. G., Uster, P. S., Peters, A. M. and Stewart, J. S. W. (2000b). Pegylated liposome-encapsulated doxorubicin and cisplatin enhance the effect of radiotherapy in a tumour xenograft model. *Clinical Cancer Research*, 6(12), 4939-4949.
- Hartmann, J. T., Kollmannsberger, C., Kanz, L. and Bokemeyer, C. (1999). Platinum organ toxicity and possible prevention in patients with testicular cancer. *International Journal of Cancer*, 83(6), 866-869.
- Haxton, K. J. and Burt, H. M. (2009). Polymeric drug delivery of platinum-based anticancer agents. *Journal of Pharmaceutical Sciences*, 98(7), 2299-2316.
- Heindryckx, B., Vanden Meerschaut, F., Lierman, S., Qian, C., O'Leary, T., Gerris, J. and De Sutter, P. (2010). Comparison of three artificial activating stimuli using a mouse model deficient for oocyte activation. *Human Reproduction*, 25, I199-I200.
- Helleman, J., van Staveren, I. L., Dinjens, W. N. M., van Kuijk, P. F., Ritstier, K., Ewing, P. C., *et al.* (2006). Mismatch repair and treatment resistance in ovarian cancer. *Bmc Cancer*, 6.

- Hemström, P., Nygren, Y., Bjorn, E. and Irgum, K. (2008). Alternative organic solvents for HILIC separation of cisplatin species with on-line ICP-MS detection. *Journal of Separation Science*, 31(4), 599-603.
- Herbst, R. S., Heymach, J. V. and Lippman, S. M. (2008). Molecular origins of cancer: Lung cancer. *New England Journal of Medicine*, 359(13), 1367-1380.
- Heudi, O., Cailleux, A. and Allain, P. (1997). Interactions between cisplatin derivatives and mobile phase during chromatographic separation. *Chromatographia*, 44(1-2), 19-24.
- Heurtault, B., Saulnier, P., Pech, B., Proust, J. E. and Benoit, J. P. (2003). Physico-chemical stability of colloidal lipid particles. *Biomaterials*, 24(23), 4283-4300.
- Hillery, A. M. (2001). Drug delivery: the basic concepts. In A. M. Hillery, A. W. Lloyd & J. Swarbrick (Eds.), *Drug delivery and targeting for pharmacists and pharmaceutical scientists* (pp. 1-48): CRC Press, Florida, USA.
- Hirai, M., Minematsu, H., Hiramatsu, Y., Kitagawa, H., Otani, T., Iwashita, S., *et al.* (2010). Novel and simple loading procedure of cisplatin into liposomes and targeting tumor endothelial cells. *International Journal of Pharmaceutics*, 391(1-2), 274-283.
- Hoffman, P. C., Mauer, A. M. and Vokes, E. E. (2000). Lung cancer. *Lancet*, 355(9202), 479-485.
- Holding, J. D., Lindup, W. E., Bowdler, D. A., Siodlak, M. Z. and Stell, P. M. (1991). Disposition and tumor concentrations of platinum in hypoalbuminemic patients after treatment with cisplatin for cancer of the head and neck. *British Journal of Clinical Pharmacology*, 32(2), 173-179.
- Hollingshead, M. G. (2008). Antitumor efficacy testing in rodents. *Journal of the National Cancer Institute*, 100(21), 1500-1510.
- Holzer, A. K., Samimi, G., Katano, K., Naerdemann, W., Lin, X. J., Safaei, R. and Howell, S. B. (2004). The copper influx transporter human copper transport protein 1 regulates the uptake of cisplatin in human ovarian carcinoma cells. *Molecular Pharmacology*, 66(4), 817-823.

- Hong, M., Zhu, S., Jiang, Y., Tang, G. and Pei, Y. (2009). Efficient tumour targeting of hydroxycamptothecin loaded PEGylated niosomes modified with transferrin. *Journal of Controlled Release*, 133(2), 96-102.
- Hood, E., Gonzalez, M., Plaas, A., Strom, J. and VanAuker, M. (2007). Immuno-targeting of non-ionic surfactant vesicles to inflammation. *International Journal of Pharmaceutics*, 339(1-2), 222-230.
- Horlick, G. and Shao, Y. (1992). Inductively coupled plasma-mass spectroscopy for elemental analysis. In A. Montaser & D. W. Golightly (Eds.), *Inductively coupled plasmas in analytical atomic spectroscopy* (2nd ed., pp. 551-612): VCH publishers, Inc.
- Howell, S. B. (2009). The design and development of the tumour-targeting nanopolymer DACH platinum conjugate AP5346 (Prolindac). In A. Bonetti, R. Leone, F. M. Muggia & S. B. Howell (Eds.), *Platinum and other heavy metal compounds in cancer chemotherapy: molecular mechanisms and clinical applications* (pp. 33-39): Humana Press Inc., NY, USA.
- Howell, S. B., Safaei, R., Larson, C. A. and Sailor, M. J. (2010). Copper transporters and the cellular pharmacology of the platinum-containing cancer drugs. *Molecular Pharmacology*, 77(6), 887-894.
- Huang, Y.-Y. and Wang, C.-H. (2006). Pulmonary delivery of insulin by liposomal carriers. *Journal of Controlled Release*, 113(1), 9-14.
- Huang, Y., Chen, J., Chen, X., Gao, J. and Liang, W. (2008). PEGylated synthetic surfactant vesicles (Niosomes): novel carriers for oligonucleotides. *Journal of Materials Science: Materials in Medicine*, 19(2), 607-614.
- Huang, Z., Timerbaev, A. R., Keppler, B. K. and Hirokawa, T. (2006). Determination of cisplatin and its hydrolytic metabolite in human serum by capillary electrophoresis techniques. *Journal of Chromatography A*, 1106(1-2), 75-79.
- Hull, D. A., Muhammad, N., Lanese, J. G., Reich, S. D., Finkelstein, T. T. and Fandrich, S. (1981). Determination of platinum in serum and ultrafiltrate by flameless atomic-absorption spectrophotometry. *Journal of Pharmaceutical Sciences*, 70(5), 500-502.

- Hussain, A., Arnold, J. J., Khan, M. A. and Ahsan, F. (2004). Absorption enhancers in pulmonary protein delivery. *Journal of Controlled Release*, 94(1), 15-24.
- Hvattum, E., Uran, S., Sandbaek, A. G., Karlsson, A. A. and Skotland, T. (2006). Quantification of phosphatidylserine, phosphatidic acid and free fatty acids in an ultrasound contrast agent by normal-phase high-performance liquid chromatography with evaporative light scattering detection. *Journal of Pharmaceutical and Biomedical Analysis*, 42(4), 506-512.
- Hwang, T. L., Lee, W. R., Hua, S. C. and Fang, J. Y. (2007). Cisplatin encapsulated in phosphatidylethanolamine liposomes enhances the *in vitro* cytotoxicity and *in vivo* intratumour drug accumulation against melanomas. *Journal of Dermatological Science*, 46(1), 11-20.
- Hyoudou, K., Nishikawa, M., Ikemura, M., Kobayashi, Y., Mendelsohn, A., Miyazaki, N., *et al.* (2009). Prevention of pulmonary metastasis from subcutaneous tumours by binary system-based sustained delivery of catalase. *Journal of Controlled Release*, 137(2), 110-115.
- Ishida, S., Lee, J., Thiele, D. J. and Herskowitz, I. (2002). Uptake of the anticancer drug cisplatin mediated by the copper transporter CTR1 in yeast and mammals. *Proceedings of the National Academy of Sciences of the United States of America*, 99(22), 14298-14302.
- Israelachvili, J. N. (1973). Theoretical considerations on asymmetric distribution of charged phospholipid molecules on inner and outer layers of curved bilayer membranes. *Biochimica Et Biophysica Acta*, 323(4), 659-663.
- Izutsu, K.-I., Yomota, C. and Kawanishi, T. (2011). Stabilization of liposomes in frozen solutions through control of osmotic flow and internal solution freezing by trehalose. *Journal of Pharmaceutical Sciences*, 100(7), 2935-2944.
- Jaafar-Maalej, C., Andrieu, V., Elaissari, A. and Fessi, H. (2009). Assessment methods of inhaled aerosols: technical aspects and applications. *Expert Opinion on Drug Delivery*, 6(9), 941-959.
- Jackman, D. M. and Johnson, B. E. (2005). Small-cell lung cancer. *Lancet*, 366(9494), 1385-1396.

- Jacobs, C., Bertino, J. R., Goffinet, D. R., Fee, W. E. and Goode, R. L. (1978). 24-Hour infusion of cis-platinum in head and neck cancers. *Cancer*, 42(5), 2135-2140.
- Jadon, P. S., Gajbhiye, V., Jadon, R. S., Gajbhiye, K. R. and Ganesh, N. (2009). Enhanced oral bioavailability of griseofulvin via niosomes. *Aaps Pharmscitech*, 10(4), 1186-1192.
- Jahn, A., Vreeland, W. N., DeVoe, D. L., Locascio, L. E. and Gaitan, M. (2007). Microfluidic directed formation of liposomes of controlled size. *Langmuir*, 23(11), 6289-6293.
- Jain, C. P. and Vyas, S. P. (1995a). Preparation and characterization of niosomes containing rifampicin for lung targeting. *Journal of Microencapsulation*, 12(4), 401-407.
- Jain, C. P. and Vyas, S. P. (1995b). Lymphatic delivery of niosome encapsulated methotrexate. *Pharmazie*, 50(5), 367-368.
- Jensen, M. and Nerdal, W. (2008). Anticancer cisplatin interactions with bilayers of total lipid extract from pig brain: a C¹³, P³¹ and N¹⁵ solid-state NMR study. *European Journal of Pharmaceutical Sciences*, 34(2-3), 140-148.
- Johnson, S. W., Ferry, K. V. and Hamilton, T. C. (1998). Recent insights into platinum drug resistance in cancer. *Drug Resistance Updates*, 1(4), 243-254.
- Jones, A. H. (1976). Determination of platinum and palladium in blood and urine by flameless atomic-absorption spectrophotometry. *Analytical Chemistry*, 48(11), 1472-1474.
- Jones, J. C., Zhen, W. P., Reed, E., Parker, R. J., Sancar, A. and Bohr, V. A. (1991). Gene-specific formation and repair of cisplatin intrastrand adducts and interstrand cross-links in Chinese-hamster ovary cells. *Journal of Biological Chemistry*, 266(11), 7101-7107.
- Judson, I. and Kelland, L. R. (2000). New developments and approaches in the platinum arena. *Drugs*, 59, 29-36.
- Júnior, A. D. C., Mota, L. G., Nunan, E. A., Wainstein, A. J. A., Wainstein, A., Leal, A. S., Cardoso, V. N. and De Oliveira, N. C. (2007a). Tissue distribution evaluation of stealth pH-sensitive liposomal cisplatin versus free cisplatin in Ehrlich tumour-bearing mice. *Life Sciences*, 80(7), 659-664.

- Júnior, A. D. C., Vieira, F. P., De Melo, V. J., Lopes, M. T. P., Silveira, J. N., Ramaldes, G. A., *et al.* (2007b). Preparation and cytotoxicity of cisplatin-containing liposomes. *Brazilian Journal of Medical and Biological Research*, 40(8), 1149-1157.
- Junyaprasert, V. B., Teeranachaideekul, V. and Supaperm, T. (2008). Effect of charged and non-ionic membrane additives on physicochemical properties and stability of niosomes. *Aaps Pharmscitech*, 9(3), 851-859.
- Kalemkerian, G. P., Jasti, R. K., Celano, P., Nelkin, B. D. and Mabry, M. (1994). All-trans-retinoic acid alters myc gene-expression and inhibits *in vitro* progression in small-cell lung-cancer. *Cell Growth & Differentiation*, 5(1), 55-60.
- Kato, K., Walde, P., Koine, N., Ichikawa, S., Ishikawa, T., Nagaharna, R., *et al.* (2008). Temperature-sensitive non-ionic vesicles prepared from Span 80 (sorbitan monooleate). *Langmuir*, 24(19), 10762-10770.
- Kavanagh, J. J., Levenback, C. F., Ramirez, P. T., Wolf, J. L., Moore, C. L., Jones, *et al.*, (2010). Phase 2 study of canfosfamide in combination with pegylated liposomal doxorubicin in platinum and paclitaxel refractory or resistant epithelial ovarian cancer. [Article]. *Journal of Hematology & Oncology*, 3, 11.
- Kayes, J. B. (1988). Disperse systems. In M. E. Aulton (Ed.), *Pharmaceutics: the science of dosage form design* (pp. 81-118): Churchill Livingstone, NY, USA.
- Kelland, L. (2007). The resurgence of platinum-based cancer chemotherapy. *Nature Reviews Cancer*, 7(8), 573-584.
- Kelland, L. R. (2000). Preclinical perspectives on platinum resistance. *Drugs*, 59, 1-8.
- Kellaway, I. W. and Farr, S. J. (1990). Liposomes as drug delivery systems to the lung. *Advanced Drug Delivery Reviews*, 5(1-2), 149-161.
- Kelley, S. L., Basu, A., Teicher, B. A., Hacker, M. P., Hamer, D. H. and Lazo, J. S. (1988). Overexpression of metallothionein confers resistance to anticancer drugs. *Science*, 241(4874), 1813-1815.

- Kepler, D. (1999). Export pumps for glutathione S-conjugates. *Free Radical Biology and Medicine*, 27(9-10), 985-991.
- Khuhawar, M. Y. and Arain, G. M. (2005). Liquid chromatographic determination of cisplatin as platinum (II) in pharmaceutical preparation, serum and urine samples of cancer patients. *Talanta*, 66(1), 34-39.
- Khuhawar, M. Y. and Lanjwani, S. N. (1998). High performance liquid chromatographic separation and UV determination of cobalt, copper iron and platinum in pharmaceutical preparations using Bis(isovalerylacetone)ethylenediimine as complexing reagent. *Mikrochimica Acta*, 129(1-2), 65-70.
- Khuhawar, M. Y., Lanjwani, S. N. and Memon, S. A. (1997). High-performance liquid chromatographic determination of cisplatin as platinum (II) in a pharmaceutical preparation and blood samples of cancer patients. *Journal of Chromatography B*, 693(1), 175-179.
- Khuhawar, M. Y., Memon, A. A. and Bhangar, M. I. (1999). The GC determination of cisplatin as platinum (II) from pharmaceutical preparations and blood sample of cancer patients. *Chromatographia*, 49(5-6), 249-252.
- Kim, E. S., Lu, C., Khuri, F. R., Tonda, M., Glisson, B. S., Liu, D., *et al.* (2001). A phase II study of STEALTH cisplatin (SPI-77) in patients with advanced non-small cell lung cancer. *Lung Cancer*, 34(3), 427-432.
- Kim, Y. H. and Mishima, M. (2011). Second-line chemotherapy for small-cell lung cancer (SCLC). *Cancer Treatment Reviews*, 37(2), 143-150.
- Kisak, E. T., Coldren, B., Evans, C. A., Boyer, C. and Zasadzinski, J. A. (2004). The vesosome: a multicompartement drug delivery vehicle. *Current Medicinal Chemistry*, 11(2), 199-219.
- Kisak, E. T., Coldren, B. and Zasadzinski, J. A. (2002). Nanocompartments enclosing vesicles, colloids, and macromolecules via interdigitated lipid bilayers. *Langmuir*, 18(1), 284-288.
- Kraker, A. J. and Moore, C. W. (1988). Accumulation of cis-diamminedichloroplatinum (II) and platinum analogues by platinum-resistant murine leukemia-cells invitro. *Cancer Research*, 48(1), 9-13.

- Kralchevsky, P. A., Danov, K. D. and Denkov, N. D. (2009). Chemical physics of colloid systems and interfaces. In K. S. Birdi (Ed.), *Handbook of surface and colloid chemistry* (3rd ed., pp. 197-377): Taylor and Francis Group, Florida, USA.
- Krieger, M. L., Eckstein, N., Schneider, V., Koch, M., Royer, H.-D., Jaehde, U. and Bendas, G. (2010). Overcoming cisplatin resistance of ovarian cancer cells by targeted liposomes *in vitro*. *International Journal of Pharmaceutics*, 389(1-2), 10-17.
- Labiris, N. R. and Dolovich, M. B. (2003a). Pulmonary drug delivery. Part I: Physiological factors affecting therapeutic effectiveness of aerosolized medications. *British Journal of Clinical Pharmacology*, 56(6), 588-599.
- Labiris, N. R. and Dolovich, M. B. (2003b). Pulmonary drug delivery. Part II: The role of inhalant delivery devices and drug formulations in therapeutic effectiveness of aerosolized medications. *British Journal of Clinical Pharmacology*, 56(6), 600-612.
- Laghari, A. J., Khuhawar, M. Y., Zardari, L. A. and Bhatti, A. G. (2008). GC determination of cisplatin in serum and urine of cancer patients after chemotherapy as platinum (II) pyrrolidinedithiocarbamate chelate. *Chromatographia*, 67(9-10), 748-753.
- Lanjwani, S. N., Zhu, R. K., Khuhawar, M. Y. and Ding, Z. F. (2006). High performance liquid chromatographic determination of platinum in blood and urine samples of cancer patients after administration of cisplatin drug using solvent extraction and N,N'-bis(salicylidene)-1,2-propanediamine as complexation reagent. *Journal of Pharmaceutical and Biomedical Analysis*, 40(4), 833-839.
- Lasic, D. D. (1995). Applications of liposomes. In R. Lipowsky & E. Sackmann (Eds.), *Handbook of biological physics* (Vol. 1, pp. 491-519): Elsevier Science B.V.
- Lasic, D. D. (1998). Novel applications of liposomes. *Trends in Biotechnology*, 16(7), 307-321.
- Lasic, D. D., Ceh, B., Stuart, M. C. A., Guo, L., Frederik, P. M. and Barenholz, Y. (1995). Transmembrane gradient driven phase-transitions within vesicles:

- lessons for drug-delivery. *Biochimica Et Biophysica Acta-Biomembranes*, 1239(2), 145-156.
- Lasic, D. D. and Needham, D. (1995). The "Stealth" liposome: A prototypical biomaterial. *Chemical Reviews*, 95(8), 2601-2628.
- Lasic, D. D. and Papahadjopoulos, D. (1995). Liposomes revisited. *Science*, 267(5202), 1275-1276.
- Lavi, G., Voronov, E., Dinarello, C. A., Apte, R. N. and Cohen, S. (2007). Sustained delivery of IL-1Ra from biodegradable microspheres reduces the number of murine B16 melanoma lung metastases. *Journal of Controlled Release*, 123, 123-130.
- Leite, E. A., Giuberti, C. D., Alberto, J. A. W., Wainstein, A., Coelho, L. G. V., Lana, A. M. Q., Savassi-Rocha, P. R. and De Oliveira, M. C. (2009). Acute toxicity of long-circulating and pH-sensitive liposomes containing cisplatin in mice after intraperitoneal administration. *Life Sciences*, 84(19-20), 641-649.
- Levi, F. (2006). Chronotherapeutics: The relevance of timing in cancer therapy. *Cancer Causes & Control*, 17(4), 611-621.
- Levi, F., Focan, C., Karaboue, A., de la Valette, V., Focan-Henrard, D., Baron, B., Kreutz, F. and Giacchetti, S. (2007). Implications of circadian clocks for the rhythmic delivery of cancer therapeutics. *Advanced Drug Delivery Reviews*, 59(9-10), 1015-1035.
- Levin, R. D., Daehler, M. A., Grutsch, J. F., Quiton, J., Lis, C. G., Peterson, C., *et al.* (2005). Circadian function in patients with advanced non-small cell lung cancer. *British Journal of Cancer*, 93(11), 1202-1208.
- Lewis, A. D., Hayes, J. D. and Wolf, C. R. (1988). Glutathione and glutathione-dependent enzymes in ovarian adenocarcinoma cell-lines derived from a patient before and after the onset of drug-resistance: intrinsic differences and cell-cycle effects. *Carcinogenesis*, 9(7), 1283-1287.
- Li, X. M., Tanaka, K., Sun, J., Filipski, E., Kayitalire, L., Focan, C. and Levi, F. (2005). Preclinical relevance of dosing time for the therapeutic index of gemcitabine-cisplatin. *British Journal of Cancer*, 92(9), 1684-1689.
- Lian, T. and Ho, R. J. Y. (2001). Trends and developments in liposome drug delivery systems. *Journal of Pharmaceutical Sciences*, 90(6), 667-680.

- Lokshin, A., Zhang, H. F., Mayotte, J., Lokshin, M. and Levitt, M. L. (1999). Early effects of retinoic acid on proliferation, differentiation and apoptosis in non-small cell lung cancer cell lines. *Anticancer Research*, 19(6B), 5251-5254.
- Lopez-Flores, A., Jurado, R. and Garcia-Lopez, P. (2005). A high-performance liquid chromatographic assay for determination of cisplatin in plasma, cancer cell, and tumour samples. *Journal of Pharmacological and Toxicological Methods*, 52(3), 366-372.
- Maitani, Y., Igarashi, S., Sato, M. and Hattori, Y. (2007). Cationic liposome (DC-Chol/DOPE=1: 2) and a modified ethanol injection method to prepare liposomes, increased gene expression. *International Journal of Pharmaceutics*, 342(1-2), 33-39.
- Malmsten, M. (2002). Liposomes. In M. Malmsten (Ed.), *Surfactants and polymers in drug delivery* (pp. 87-132): Marcel Dekker Inc., NY, USA.
- Malvern (2004). Zetasizer Nano Series: User Manual (Issue 2.1): Malvern Instruments Ltd., Worcestershire, UK.
- Manosroi, J., Khositsuntiwong, N., Manosroi, W., Goetz, F., Werner, R. G. and Manosroi, A. (2010). Enhancement of Transdermal Absorption, Gene Expression and Stability of Tyrosinase Plasmid (pMEL34)-Loaded Elastic Cationic Niosomes: Potential Application in Vitiligo Treatment. *Journal of Pharmaceutical Sciences*, 99(8), 3533-3541.
- Mantripragada, S. (2002). A lipid based depot (DepoFoam[®] technology) for sustained release drug delivery. *Progress in Lipid Research*, 41(5), 392-406.
- Marsh, K. C., Sternson, L. A. and Repta, A. J. (1984). Post-column reaction detector for platinum (II) antineoplastic agents. *Analytical Chemistry*, 56(3), 491-497.
- Martin, A., Swarbrick, J. and Cammarata, A. (1983a). Colloids. In A. Martin, J. Swarbrick & A. Cammarata (Eds.), *Physical pharmacy: physical chemical principles in the pharmaceutical sciences* (3rd ed., pp. 469-491): Lea and Febiger, Philadelphia, USA.
- Martin, A., Swarbrick, J. and Cammarata, A. (1983b). Interfacial Phenomena. In A. Martin, J. Swarbrick & A. Cammarata (Eds.), *Physical Pharmacy: physical chemical principles in the pharmaceutical sciences* (3rd ed., pp. 445-468): Lea and Febiger, Philadelphia, USA.

- Martini, F. and Nath, J. L. (2009a). The heart. In F. Martini & J. L. Nath (Eds.), *Fundamentals of anatomy and physiology* (8th ed., pp. 681-718): Pearson Education, Inc., California, USA.
- Martini, F. and Nath, J. L. (2009b). Blood vessels and circulation. In F. Martini & J. L. Nath (Eds.), *Fundamentals of anatomy and physiology* (8th ed., pp. 719-775): Pearson Education, Inc., California, USA.
- Martini, F. and Nath, J. L. (2009c). The respiratory system. In F. Martini & J. L. Nath (Eds.), *Fundamentals of anatomy and physiology* (8th ed., pp. 825-873): Pearson Education, Inc., California, USA.
- Mattison, J., van der Weyden, L., Hubbard, T. and Adams, D. J. (2009). Cancer gene discovery in mouse and man. *Biochimica Et Biophysica Acta-Reviews on Cancer*, 1796(2), 140-161.
- Mattison, K., Morfesis, A. and Kaszuba, M. (2003). A primer on particle sizing using dynamic light scattering. *American Biotechnology Laboratory*, 21(13), 20-22.
- McKeage, M. (2007). Satraplatin in hormone-refractory prostate cancer and other tumour types: pharmacological properties and clinical evaluation. *Drugs*, 67(6), 859-869.
- McMaster, M. C. (2007a). Advantages and disadvantages of HPLC. In M. C. McMaster (Ed.), *HPLC: a practical user's guide* (2nd ed., pp. 3-13): John Wiley and Sons, Inc., NJ, USA.
- McMaster, M. C. (2007b). Column aging, diagnosis and healing. In M. C. McMaster (Ed.), *HPLC a practical user's guide* (2nd ed., pp. 73-87): John Wiley and Sons, Inc., NJ, USA.
- McMaster, M. C. (2007c). Separation models. In M. C. McMaster (Ed.), *HPLC a practical user's guide* (2nd ed., pp. 45-60): John Wiley and Sons, Inc., NJ, USA.
- McMillian, M. K., Li, L., Parker, J. B., Patel, L., Zhong, Z., Gunnett, J. W., Powers, W. J. and Johnson, M. D. (2002). An improved resazurin-based cytotoxicity assay for hepatic cells. *Cell Biology and Toxicology*, 18(3), 157-173.
- Meerum Terwogt, J. M., Groenewegen, G., Pluim, D., Maliepaard, M., Tibben, M. M., Huisman, A., *et al.* (2002). Phase I and pharmacokinetic study of SPI-77,

- a liposomal encapsulated dosage form of cisplatin. *Cancer Chemother Pharmacol*, 49(3), 201-210.
- Memon, S. A. and Dalziel, J. A. W. (2001). Elution of copper (II), nickel (II), cobalt (II) and zinc (II) and the separation of nickel (II), palladium (II) and platinum (II) complexes of quinoxaline-2,3-dithiol, using reversed phase ion-pair HPLC. *Journal of the Chemical Society of Pakistan*, 23(4), 234-237.
- Méndez, L. B., Gookin, G. and Phalen, R. F. (2010). Inhaled aerosol particle dosimetry in mice: A review. *Inhalation Toxicology*, 22(12), 1032-1037.
- Merritt, R. E., Yamada, R. E., Crystal, R. G. and Korst, R. J. (2004). Augmenting major histocompatibility complex class I expression by murine tumours *in vivo* enhances antitumor immunity induced by an active immunotherapy strategy. *Journal of Thoracic and Cardiovascular Surgery*, 127(2), 355-364.
- Meyer, H. W. and Richter, W. (2001). Freeze-fracture studies on lipids and membranes. *Micron*, 32(6), 615-644.
- Michaelson, D. M., Horwitz, A. F. and Klein, M. P. (1973). Transbilayer asymmetry and surface homogeneity of mixed phospholipids in cosonicated vesicles. *Biochemistry*, 12(14), 2637-2645.
- Mistry, P., Kelland, L. R., Abel, G., Sidhar, S. and Harrap, K. R. (1991). The relationships between glutathione, glutathione-s-transferase and cytotoxicity of platinum drugs and melphalan in 8 human ovarian-carcinoma cell lines. *British Journal of Cancer*, 64(2), 215-220.
- Mohammed, A. R., Bramwell, V. W., Coombes, A. G. A. and Perrie, Y. (2006). Lyophilisation and sterilisation of liposomal vaccines to produce stable and sterile products. *Methods*, 40(1), 30-38.
- Montaser, A., McLean, J. A. and Liu, H. (1998). Introduction to ICP spectrometries for elemental analysis. In A. Montaser (Ed.), *Inductively coupled plasma mass spectrometry* (pp. 1-32): Wiley-VCH, Inc.
- Montes-Bayón, M., DeNicola, K. and Caruso, J. A. (2003). Liquid chromatography-inductively coupled plasma mass spectrometry. *Journal of Chromatography A*, 1000(1-2), 457-476.
- Morgan, A. S., Sanderson, P. E., Borch, R. F., Tew, K. D., Niitsu, Y., Takayama, T., *et al.* (1998). Tumour efficacy and bone marrow-sparing properties of

- TER286, a cytotoxin activated by glutathione S-transferase. *Cancer Research*, 58(12), 2568-2575.
- Mormont, M. C. and Levi, F. (2003). Cancer chronotherapy: Principles, applications, and perspectives. *Cancer*, 97(1), 155-169.
- Muggia, F. M. (2009). Platinum compounds: the culmination of the era of cancer chemotherapy. In A. Bonetti, R. Leone, F. M. Muggia & S. B. Howell (Eds.), *Platinum and other heavy metal compounds in cancer chemotherapy: molecular mechanisms and clinical applications* (pp. 1-10): Humana Press Inc., NY, USA.
- Mullen, A. B., Baillie, A. J. and Carter, K. C. (1998). Visceral leishmaniasis in the BALB/c mouse: A comparison of the efficacy of a non-ionic surfactant formulation of sodium stibogluconate with those of three proprietary formulations of amphotericin B. *Antimicrobial Agents and Chemotherapy*, 42(10), 2722-2725.
- Mullen, A. B., Baillie, A. J. and Carter, K. C. (2000). Non-ionic surfactant vesicles for the treatment of Visceral Leishmaniasis. In I. F. Uchegbu (Ed.), *Synthetic surfactant vesicles: niosomes and other non-phospholipid vesicular systems* (pp. 97-113): Overseas Publishers Association, Amsterdam, The Netherlands.
- Mullen, A. B., Carter, K. C. and Baillie, A. J. (1997). Comparison of the efficacies of various formulations of amphotericin B against murine visceral leishmaniasis. *Antimicrobial Agents and Chemotherapy*, 41(10), 2089-2092.
- Mylonakis, N., Athanasiou, A., Ziras, N., Angel, J., Rapti, A., Lampaki, S., *et al.* (2009). Phase II study of liposomal cisplatin (Lipoplatin™) plus gemcitabine versus cisplatin plus gemcitabine as first line treatment in inoperable (Stage IIIB/IV) non-small cell lung cancer. *Lung Cancer*, 68(2), 240-247.
- Nair, A., Klusmann, M. J., Jogeessvaran, K. H., Grubnic, S., Green, S. J. and Vlahos, I. (2011). Revisions to the TNM staging of non-small cell lung cancer: rationale, clinicoradiologic implications, and persistent limitations. *Radiographics*, 31(1), 215-U284.
- Nakamura, K., Yoshikawa, N., Yamaguchi, Y., Kagota, S., Shinozuka, K. and Kunitomo, M. (2002). Characterization of mouse melanoma cell lines by their

- mortal malignancy using an experimental metastatic model. *Life Sciences*, 70(7), 791-798.
- Nakayama, G. R., Caton, M. C., Nova, M. P. and Parandoosh, Z. (1997). Assessment of the Alamar Blue assay for cellular growth and viability *in vitro*. *Journal of Immunological Methods*, 204(2), 205-208.
- Naresh, R. A. R. and Udupa, N. (1996). Niosome encapsulated bleomycin. *Stp Pharma Sciences*, 6(1), 61-71.
- Newman, M. S., Colbern, G. T., Working, P. K., Engbers, C. and Amantea, M. A. (1999). Comparative pharmacokinetics, tissue distribution, and therapeutic effectiveness of cisplatin encapsulated in long-circulating, pegylated liposomes (SPI-077) in tumour-bearing mice. *Cancer Chemotherapy and Pharmacology*, 43(1), 1-7.
- NICE (2008). Erlotinib for the treatment of non-small cell lung cancer. *NICE technology appraisal guidance 162* Retrieved 25-08-2011, from www.nice.org.uk/guidance/TA162
- NICE (2010a). Pemetrexed for the maintenance treatment of non-small-cell lung cancer. *NICE technology appraisal guidance 190* Retrieved 25-08-2011, from www.nice.org.uk/guidance/TA190
- NICE (2010b). Gefitinib for the first-line treatment of locally advanced or metastatic non-small-cell lung cancer. *NICE technology appraisal guidance 192* Retrieved 25-08-2011, from www.nice.org.uk/guidance/TA192
- NICE (2011). Lung cancer: the diagnosis and treatment of lung cancer. *NICE clinical guideline 121* Retrieved 25-08-2011, from www.nice.org.uk/guidance/CG121
- Nikolaychik, V. V., Samet, M. M. and Lelkes, P. I. (1996). A new method for continual quantitation of viable cells on endothelialized polyurethanes. *Journal of Biomaterials Science-Polymer Edition*, 7(10), 881-891.
- Nowotnik, D. P. and Cvitkovic, E. (2009). ProLindacTM (AP5346): A review of the development of an HPMA DACH platinum Polymer Therapeutic. *Advanced Drug Delivery Reviews*, 61(13), 1214-1219.
- O'Brien, J., Wilson, I., Orton, T. and Pognan, F. (2000). Investigation of the Alamar Blue (resazurin) fluorescent dye for the assessment of mammalian cell cytotoxicity. *European Journal of Biochemistry*, 267(17), 5421-5426.

- O'Callaghan, C. and Barry, P. W. (1997). The science of nebulised drug delivery. *Thorax*, 52, S31-S44.
- O'Dwyer, P. J., Stevenson, J. P. and Johnson, S. W. (1999). Clinical status of cisplatin, carboplatin and other platinum-based antitumour drugs. In B. Lippert (Ed.), *Cisplatin: chemistry and biochemistry of a leadign anticancer drug* (pp. 29-69): Zurich: Verlag Helvetica Chimica Acta; Weinheim; Wiley-VCH.
- O'Dwyer, P. J., Stevenson, J. P. and Johnson, S. W. (2000). Clinical pharmacokinetics and administration of established platinum drugs. *Drugs*, 59, 19-27.
- Oberdörster, G. (1993). Lung dosimetry - pulmonary clearance of inhaled particles. *Aerosol Science and Technology*, 18(3), 279-289.
- Oldham, M. J., Phalen, R. F. and Budiman, T. (2009). Comparison of predicted and experimentally measured aerosol deposition efficiency in BALB/c mice in a new nose-only exposure system. *Aerosol Science and Technology*, 43(10), 970-977.
- Oldham, M. J. and Robinson, R. J. (2007). Predicted tracheobronchial and pulmonary deposition in a murine asthma model. *Anatomical Record-Advances in Integrative Anatomy and Evolutionary Biology*, 290(10), 1309-1314.
- Ornaph, R. M. and Dong, M. W. (2005). Key concepts of HPLC in pharmaceutical analysis. In S. Ahuja & M. W. Dong (Eds.), *Handbook of pharmaceutical analysis by HPLC* (pp. 19-46): Elsevier, Inc.
- Ozer, A. Y., Hincal, A. A. and Bouwstra, J. A. (1991). A novel drug delivery system: non-ionic surfactant vesicles. *European Journal of Pharmaceutics and Biopharmaceutics*, 37(2), 75-79.
- Ozer, A. Y. and Talsma, H. (1989). Preparation and stability of liposomes containing 5-fluorouracil. *International Journal of Pharmaceutics*, 55(2-3), 185-191.
- Pagano, J. S., Blaser, M., Buendia, M.-A., Damania, B., Khalili, K., Raab-Traub, N. and Roizman, B. (2004). Infectious agents and cancer: criteria for a causal relation. *Seminars in Cancer Biology*, 14(6), 453-471.

- Park, J. W. (2002). Liposome-based drug delivery in breast cancer treatment. *Breast Cancer Res*, 4(3), 95-99.
- Parthasarathi, G., Udupa, N., Umadevi, P. and Pillai, G. K. (1994). Niosome encapsulated of vincristine sulfate - improved anticancer activity with reduced toxicity in mice. *Journal of Drug Targeting*, 2(2), 173-182.
- Parthasarathy, R., Gilbert, B. and Mehta, K. (1999). Aerosol delivery of liposomal all-trans-retinoic acid to the lungs. *Cancer Chemotherapy and Pharmacology*, 43(4), 277-283.
- Patrick, G. L. (2009). Anticancer agents. In G. L. Patrick (Ed.), *An introduction to medicinal chemistry* (4th ed., pp. 519-578): Oxford University Press Inc., NY, USA.
- Patton, J. S. (1996). Mechanisms of macromolecule absorption by the lungs. *Advanced Drug Delivery Reviews*, 19(1), 3-36.
- Pecorino, L. (2008a). Introduction. In L. Pecorino (Ed.), *Molecular biology of cancer: mechanisms, targets and therapeutics* (2nd ed., pp. 1-19): Oxford University Press Inc., NY, USA.
- Pecorino, L. (2008b). Growth factor signaling and oncogenes. In L. Pecorino (Ed.), *Molecular biology of cancer: mechanisms, targets, and therapeutics* (2nd ed., pp. 69-94): Oxford University Press, Inc., NY, USA.
- Peleg-Shulman, T., Gibson, D., Cohen, R., Abra, R. and Barenholz, Y. (2001). Characterization of sterically stabilized cisplatin liposomes by nuclear magnetic resonance. *Biochimica Et Biophysica Acta-Biomembranes*, 1510(1-2), 278-291.
- Pencer, J. and Hallett, F. R. (2003). Effects of vesicle size and shape on static and dynamic light scattering measurements. *Langmuir*, 19(18), 7488-7497.
- Pera, M. F. and Harder, H. C. (1977). Analysis for platinum in biological material by flameless atomic-absorption spectrometry. *Clinical Chemistry*, 23(7), 1245-1249.
- Pereira-Lachataignerais, J., Pons, R., Panizza, P., Courbin, L., Rouch, J. and Lopez, O. (2006). Study and formation of vesicle systems with low polydispersity index by ultrasound method. *Chemistry and Physics of Lipids*, 140(1-2), 88-97.

- Pereira-Maia, E. and Garnier-Suillerot, A. (2003). Impaired hydrolysis of cisplatin derivatives to aquated species prevents energy-dependent uptake in GLC4 cells resistant to cisplatin. *Journal of Biological Inorganic Chemistry*, 8(6), 626-634.
- Perez-Soler, R. (1989). Liposomes as carriers of antitumor agents - toward a clinical reality. *Cancer Treatment Reviews*, 16(2), 67-82.
- Perez, R. P., Hamilton, T. C. and Ozols, R. F. (1990). Resistance to alkylating-agents and cisplatin: insights from ovarian-carcinoma model systems. *Pharmacology & Therapeutics*, 48(1), 19-27.
- Phalen, R. F. and Mendez, L. B. (2009). Dosimetry considerations for animal aerosol inhalation studies. *Biomarkers*, 14, 63-66.
- Pil, P. M. and Lippard, S. J. (1992). Specific binding of chromosomal protein-HMG1 to DNA damaged by the anticancer drug cisplatin. *Science*, 256(5054), 234-237.
- Plumb, J. A., Strathdee, G., Sludden, J., Kaye, S. B. and Brown, R. (2000). Reversal of drug resistance in human tumour xenografts by 2'-deoxy-5-azacytidine-induced demethylation of the hMLH1 gene promoter. [Article]. *Cancer Research*, 60(21), 6039-6044.
- Pratten, M. K. and Lloyd, J. B. (1986). Pinocytosis and phagocytosis: the effect of size of a particulate substrate on its mode of capture by rat peritoneal-macrophages cultured *in vitro*. *Biochimica Et Biophysica Acta*, 881(3), 307-313.
- Prestayko, A. W. (1981a). Clinical pharmacology of cisplatin. In S. T. Crooke & A. W. Prestayko (Eds.), *Cancer and chemotherapy* (Vol. 3, pp. 351-356): Academic Press, Inc., NY, USA.
- Prestayko, A. W. (1981b). Molecular pharmacology of cisplatin. In S. T. Crooke & A. W. Prestayko (Eds.), *Cancer and chemotherapy* (Vol. 3, pp. 303-309): Academic Press, Inc., NY, USA.
- Pullman, A. and Pullman, B. (1981). Molecular electrostatic potential of the nucleic-acids. [Review]. *Quarterly Reviews of Biophysics*, 14(3), 289-380.
- Rabinovich-Guilatt, L., Dubernet, C., Gaudin, K., Lambert, G., Couvreur, P. and Chaminade, P. (2005). Phospholipid hydrolysis in a pharmaceutical emulsion

- assessed by physicochemical parameters and a new analytical method. *European Journal of Pharmaceutics and Biopharmaceutics*, 61(1-2), 69-76.
- Ramachandran, S., Quist, A. P., Kumar, S. and Lal, R. (2006). Cisplatin nanoliposomes for cancer therapy: AFM and fluorescence imaging of cisplatin encapsulation, stability, cellular uptake, and toxicity. *Langmuir*, 22(19), 8156-8162.
- Ranade, V. V. (1989). Drug delivery systems .1. Site-specific drug delivery using liposomes as carriers. *Journal of Clinical Pharmacology*, 29(8), 685-694.
- Ranson, M., Howell, A., Cheeseman, S. and Margison, J. (1996). Liposomal drug delivery. *Cancer Treatment Reviews*, 22(5), 365-379.
- Rentel, C. O., Bouwstra, J. A., Naisbett, B. and Junginger, H. E. (1999). Niosomes as a novel peroral vaccine delivery system. *International Journal of Pharmaceutics*, 186(2), 161-167.
- Ricart, A. D., Sarantopoulos, J., Calvo, E., Chu, Q. S., Greene, D., Nathan, F. E., *et al.* (2009). Satraplatin, an oral platinum, administered on a five-day every-five-week schedule: a pharmacokinetic and food effect study. *Clinical Cancer Research*, 15(11), 3866-3871.
- Richardson, R. (2005). Scattering and reflection techniques. In T. Cosgrove (Ed.), *Colloid science: principles, methods and applications* (pp. 228-254): Blackwell Publishing Ltd.
- Riley, C. M. (1988). Bioanalysis of cisplatin analogues: a selective review. *Journal of Pharmaceutical and Biomedical Analysis*, 6(6-8), 669-676.
- Riley, J. (2005). Charge in colloidal systems. In T. Cosgrove (Ed.), *Colloid science: principles, methods and applications* (pp. 14-35): Blackwell Publishing Ltd.
- Risbo, J., Jorgensen, K., Sperotto, M. M. and Mouritsen, O. G. (1997). Phase behavior and permeability properties of phospholipid bilayers containing a short-chain phospholipid permeability enhancer. *Biochimica Et Biophysica Acta-Biomembranes*, 1329(1), 85-96.
- Roa, W. H., Azarmi, S., Al-Hallak, M. H. D. K., Finlay, W. H., Magliocco, A. M. and Loebenberg, R. (2011). Inhalable nanoparticles, a non-invasive approach to treat lung cancer in a mouse model. *Journal of Controlled Release*, 150(1), 49-55.

- Robenek, H. and Severs, N. J. (2008). Recent advances in freeze-fracture electron microscopy: the replica immunolabeling technique. *Biological procedures online*, 10, 9-19.
- Rogerson, A., Cummings, J. and Florence, A. T. (1987). Adriamycin-loaded niosomes : drug entrapment, stability and release. *Journal of Microencapsulation*, 4(4), 321-328.
- Rosenberg, B., Vancamp, L. and Krigas, T. (1965). Inhibition of cell division in escherichia coli by electrolysis products from a platinum electrode. *Nature*, 205(4972), 698-&.
- Rosenberg, B., Vancamp, L., Trosko, J. E. and Mansour, V. H. (1969). Platinum compounds: a new class of potent antitumour agents. *Nature*, 222(5191), 385-&.
- Rosti, G., Bevilacqua, G., Bidoli, P., Portalone, L., Santo, A. and Genestreti, G. (2006). Small cell lung cancer. *Annals of Oncology*, 17, 5-10.
- Rothschild, B. M., Tanke, D. H., Helbling, M. and Martin, L. D. (2003). Epidemiologic study of tumours in dinosaurs. *Naturwissenschaften*, 90(11), 495-500.
- Roy, M. T., Gallardo, M. and Estelrich, J. (1997). Bilayer distribution of phosphatidylserine and phosphatidylethanolamine in lipid vesicles. *Bioconjugate Chemistry*, 8(6), 941-945.
- Roy, M. T., Gallardo, M. and Estelrich, J. (1998). Influence of size on electrokinetic behavior of phosphatidylserine and phosphatidylethanolamine lipid vesicles. *Journal of Colloid and Interface Science*, 206(2), 512-517.
- Safaei, R. and Howell, S. B. (2005). Copper transporters regulate the cellular pharmacology and sensitivity to Pt drugs. *Critical Reviews in Oncology Hematology*, 53(1), 13-23.
- Safaei, R., Katano, K., Samimi, G., Naerdemann, W., Stevenson, J. L., Rochdi, M. and Howell, S. B. (2004). Cross-resistance to cisplatin in cells with acquired resistance to copper. *Cancer Chemotherapy and Pharmacology*, 53(3), 239-246.
- Sakagami, M., Kinoshita, W., Sakon, K. and Makino, Y. (2003). Fractional contribution of lung, nasal and gastrointestinal absorption to the systemic

- level following nose-only aerosol exposure in rats: a case study of 3.7 μ m fluorescein aerosols. *Archives of Toxicology*, 77(6), 321-329.
- Samimi, G., Safaei, R., Katano, K., Holzer, A. K., Rochdi, M., Tomioka, M., Goodman, M. and Howell, S. B. (2004). Increased expression of the copper efflux transporter ATP7a mediates resistance to cisplatin, carboplatin, and oxaliplatin in ovarian cancer cells. *Clinical Cancer Research*, 10(14), 4661-4669.
- Sancar, A. (1996). DNA excision repair. *Annual Review of Biochemistry*, 65, 43-81.
- Sanchez, J. M., Obrezkov, O. and Salvado, V. (2000). Separation of some platinum group metal chelates with 8-hydroxyquinoline by various high-performance liquid chromatographic methods. *Journal of Chromatography A*, 871(1-2), 217-226.
- Sanford, M. and Scott, L. J. (2009). Gefitinib: a review of its use in the treatment of locally advanced/metastatic non-small cell lung cancer. *Drugs*, 69(16), 2303-2328.
- Santos Giuberti, C. d., de Oliveira Reis, E. C. s., Ribeiro Rocha, T. G., Leite, E. A., Lacerda, R. G., Ramaldes, G. A. and de Oliveira, M. n. C. (2011). Study of the pilot production process of long-circulating and pH-sensitive liposomes containing cisplatin. *Journal of Liposome Research*, 21(1), 60-69.
- Sapra, P. and Allen, T. M. (2003). Ligand-targeted liposomal anticancer drugs. *Progress in Lipid Research*, 42(5), 439-462.
- Sarker, S. D., Nahar, L. and Kumarasamy, Y. (2007). Microtitre plate-based antibacterial assay incorporating resazurin as an indicator of cell growth, and its application in the *in vitro* antibacterial screening of phytochemicals. *Methods*, 42(4), 321-324.
- Sas, B., Peys, E. and Helsen, M. (1999). Efficient method for (lyso)phospholipid class separation by high-performance liquid chromatography using an evaporative light-scattering detector. *Journal of Chromatography A*, 864(1), 179-182.
- Schnitzer, E., Pinchuk, I., Bor, A., Leikin-Frenkel, A. and Lichtenberg, D. (2007). Oxidation of liposomal cholesterol and its effect on phospholipid peroxidation. *Chemistry and Physics of Lipids*, 146(1), 43-53.

- Schreier, H., Gonzalezrothi, R. J. and Stecenko, A. A. (1993). Pulmonary delivery of liposomes. *Journal of Controlled Release*, 24(1-3), 209-223.
- Schroeder, A., Honen, R., Turjeman, K., Gabizon, A., Kost, J. and Barenholz, Y. (2009). Ultrasound triggered release of cisplatin from liposomes in murine tumours. *Journal of Controlled Release*, 137(1), 63-68.
- Scott, R. P. W. (1996). The principles of separation by high liquid chromatography. In E. D. Katz (Ed.), *High performance liquid chromatography: principles and methods*: John Wiley and Sons, Inc., West Sussex, UK.
- Seliger, B., Wollscheid, U., Momburg, F., Blankenstein, T. and Huber, C. (2001). Characterization of the major histocompatibility complex class I deficiencies in B16 melanoma cells. *Cancer Research*, 61(3), 1095-1099.
- Serova, M., Ghoul, A., Rezai, K., Lokiec, F., Cvitkovic, E., Nowotnik, D., Faivre, S. and Raymond, E. (2009). *In vitro* anti-proliferative effects of ProLindac, a novel DACH-platinum-linked polymer compound, as a single agent and in combination with other anticancer drugs. In A. Bonetti, R. Leone, F. M. Muggia & S. B. Howell (Eds.), *Platinum and other heavy metal compounds in cancer chemotherapy: molecular mechanisms and clinical applications* (pp. 41-47): Humana Press Inc., NY, USA.
- Severs, N. J. (2007). Freeze-fracture electron microscopy. *Nature Protocols*, 2(3), 547-576.
- Shabbits, J. A., Chiu, G. N. C. and Mayer, L. D. (2002). Development of an *in vitro* drug release assay that accurately predicts *in vivo* drug retention for liposome-based delivery systems. *Journal of Controlled Release*, 84(3), 161-170.
- Sharma, A. and Sharma, U. S. (1997). Liposomes in drug delivery: progress and limitations. *International Journal of Pharmaceutics*, 154(2), 123-140.
- Sher, T., Dy, G. K. and Adjei, A. A. (2008). Small cell lung cancer. *Mayo Clinic Proceedings*, 83(3), 355-367.
- Sherman, S. E. and Lippard, S. J. (1987). Structural aspects of platinum anticancer drug-interactions with DNA. *Chemical Reviews*, 87(5), 1153-1181.
- Shi, B., Fang, C. and Pei, Y. (2006). Stealth PEG-PHDCA niosomes: Effects of chain length of PEG and particle size on niosomes surface properties, *in vitro*

- drug release, phagocytic uptake, *in vivo* pharmacokinetics and antitumor activity. *Journal of Pharmaceutical Sciences*, 95(9), 1873-1887.
- Siekmeier, R. and Scheuch, G. (2008). Systemic treatment by inhalation of macromolecules: principles, problems, and examples. *Journal of Physiology and Pharmacology*, 59, 53-79.
- Simões, S., Moreira, J. N., Fonseca, C., Duzgunes, N. and de Lima, M. C. P. (2004). On the formulation of pH-sensitive long circulation times. *Advanced Drug Delivery Reviews*, 56(7), 947-965.
- Slaughter, M. R., Bugelski, P. J. and O'Brien, P. J. (1999). Evaluation of Alamar Blue reduction for the *in vitro* assay of hepatocyte toxicity. *Toxicology in vitro*, 13(4-5), 567-569.
- Slotman, B., Faivre-Finn, C., Kramer, G., Rankin, E., Snee, M., Hatton, M., *et al.* (2007). Prophylactic cranial irradiation in extensive small-cell lung cancer. *New England Journal of Medicine*, 357(7), 664-672.
- Smola, M., Vandamme, T. and Sokolowski, A. (2008). Nanocarriers as pulmonary drug delivery systems to treat and to diagnose respiratory and non respiratory diseases. *International Journal of Nanomedicine*, 3(1), 1-19.
- Snipes, M. B., Boecker, B. B. and McClellan, R. O. (1983). Retention of monodisperse or polydisperse aluminosilicate particles inhaled by dogs, rats, and mice. *Toxicology and Applied Pharmacology*, 69(3), 345-362.
- Spector, M. S., Zasadzinski, J. A. and Sankaram, M. B. (1996). Topology of multivesicular liposomes, a model biliquid foam. *Langmuir*, 12(20), 4704-4708.
- Speelmans, G., Sips, W., Grisel, R. J. H., Staffhorst, R., Fichtinger-Schepman, A. M. J., Reedijk, J. and deKruijff, B. (1996). The interaction of the anti-cancer drug cisplatin with phospholipids is specific for negatively charged phospholipids and takes place at low chloride ion concentration. *Biochimica Et Biophysica Acta-Biomembranes*, 1283(1), 60-66.
- Stensrud, G., Sande, S. A., Kristensen, S. and Smistad, G. (2000). Formulation and characterisation of primaquine loaded liposomes prepared by a pH gradient using experimental design. *International Journal of Pharmaceutics*, 198(2), 213-228.

- Sternberg, C. N., Petrylak, D., Witjes, F., Ferrero, J., Eymard, J., Falcon, S., *et al.* (2007). Satraplatin (S) demonstrates significant clinical benefits for the treatment of patients with HRPC: Results of a randomized phase III trial. *ASCO Meeting Abstracts*, 25(18_suppl), 5019.
- Sternberg, C. N., Petrylak, D. P., Sartor, O., Witjes, J. A., Demkow, T., Ferrero, J.-M., *et al.* (2009). Multinational, double-blind, phase III study of prednisone and either satraplatin or placebo in patients with castrate-refractory prostate cancer progressing after prior chemotherapy: the SPARC trial. *Journal of Clinical Oncology*, 27(32), 5431-5438.
- Sullivan, S. M. and Huang, L. (1986). Enhanced delivery to target cells by heat-sensitive immunoliposomes. *Proceedings of the National Academy of Sciences of the United States of America*, 83(16), 6117-6121.
- Szoka, F. and Papahadjopoulos, D. (1978). Procedure for preparation of liposomes with large internal aqueous space and high capture by reverse-phase evaporation. *Proceedings of the National Academy of Sciences of the United States of America*, 75(9), 4194-4198.
- Talmadge, J. E., Singh, R. K., Fidler, I. J. and Raz, A. (2007). Murine models to evaluate novel and conventional therapeutic strategies for cancer. *American Journal of Pathology*, 170(3), 793-804.
- Tandon, V., Bhagavatula, S. K., Nelson, W. C. and Kirby, B. J. (2008). Zeta potential and electroosmotic mobility in microfluidic devices fabricated from hydrophobic polymers: 1. The origins of charge. *Electrophoresis*, 29(5), 1092-1101.
- Taylor, G. and Kellaway, I. (2001). Pulmonary drug delivery. In A. M. Hillery, A. W. Lloyd & J. Swarbrick (Eds.), *Drug delivery and targeting for pharmacists and pharmaceutical scientists* (pp. 269-300). Boca Raton, Florida: CRC Press.
- Terzano, C., Allegra, L., Alhaique, F., Marianecchi, C. and Carafa, M. (2005). Non-phospholipid vesicles for pulmonary glucocorticoid delivery. *European Journal of Pharmaceutics and Biopharmaceutics*, 59(1), 57-62.

- Timmer-Bosscha, H., Mulder, N. H. and Devries, E. G. E. (1992). Modulation of cis-diamminedichloroplatinum (II) resistance - a review. *British Journal of Cancer*, 66(2), 227-238.
- Toney, J. H., Donahue, B. A., Kellett, P. J., Bruhn, S. L., Essigmann, J. M. and Lippard, S. J. (1989). Isolation of cDNAs encoding a human protein that binds selectively to DNA modified by the anticancer drug cis-diamminedichloroplatinum (II). *Proceedings of the National Academy of Sciences of the United States of America*, 86(21), 8328-8332.
- Transave (2010). Sustained release Liposomal Inhalation Therapy (SLIT) Retrieved 22-10-2010, from <http://www.transaveinc.com>
- Treat, J., Schiller, J., Quoix, E., Mauer, A., Edelman, M., Modiano, M., *et al.* (2002). ZD0473 treatment in lung cancer: an overview of the clinical trial results. *European Journal of Cancer*, 38, S13-S18.
- Triano, L. R., Deshpande, H. and Gettinger, S. N. (2010). Management of patients with advanced non-small cell lung cancer current and emerging options. *Drugs*, 70(2), 167-179.
- Tyrrell, C., Bullard, S., Barber, J. and Graham, J. (2001). Open-label phase II study of ZD0473 in patients with metastatic hormone refractory prostate cancer. *European Journal of Cancer*, 37(Supplement 6), S222.
- Uchegbu, I. F., Double, J. A., Turton, J. A. and Florence, A. T. (1995). Distribution, metabolism and tumoricidal activity of doxorubicin administered in sorbitan monostearate (Span-60) niosomes in the mouse. *Pharmaceutical Research*, 12(7), 1019-1024.
- Uchegbu, I. F. and Duncan, R. (1997). Niosomes containing N-(2-hydroxypropyl)methacrylamide copolymer-doxorubicin (PK1): effect of method of preparation and choice of surfactant on niosome characteristics and a preliminary study of body distribution. *International Journal of Pharmaceutics*, 155(1), 7-17.
- Uchegbu, I. F. and Florence, A. T. (1995). Non-ionic surfactant vesicles (niosomes): Physical and pharmaceutical chemistry. *Advances in Colloid and Interface Science*, 58(1), 1-55.

- Uchegbu, I. F. and Vyas, S. P. (1998). Non-ionic surfactant based vesicles (niosomes) in drug delivery. *International Journal of Pharmaceutics*, 172(1-2), 33-70.
- Vail, D. M., Kurzman, I. D., Glawe, P. C., O'Brien, M. G., Chun, R., Garrett, L. D., *et al.* (2002). STEALTH liposome-encapsulated cisplatin (SPI-77) versus carboplatin as adjuvant therapy for spontaneously arising osteosarcoma (OSA) in the dog: a randomized multicenter clinical trial. *Cancer Chemotherapy and Pharmacology*, 50(2), 131-136.
- Velinova, M. J., Staffhorst, R., Mulder, W. J. M., Dries, A. S., Jansen, B. A. J., de Kruijff, B. and de Kroon, A. (2004). Preparation and stability of lipid-coated nanocapsules of cisplatin: anionic phospholipid specificity. *Biochimica Et Biophysica Acta-Biomembranes*, 1663(1-2), 135-142.
- Vemuri, S. and Rhodes, C. T. (1995). Preparation and characterization of liposomes as therapeutic delivery systems: a review. *Pharmaceutica acta Helvetiae*, 70(2), 95-111.
- Verschraagen, M., van der Born, K., Zwiers, T. H. U. and van der Vijgh, W. J. F. (2002). Simultaneous determination of intact cisplatin and its metabolite monohydrated cisplatin in human plasma. *Journal of Chromatography B-Analytical Technologies in the Biomedical and Life Sciences*, 772(2), 273-281.
- Verwey, E. J. W. and Overbeek, J. T. G. (1948). Theory of the stability of lyophobic colloids. Elsevier, Amsterdam.
- Voinea, M. and Simionescu, M. (2002). Designing of 'intelligent' liposomes for efficient delivery of drugs. *Journal of Cellular and Molecular Medicine*, 6(4), 465-474.
- Völkel, T., Holig, P., Merdan, T., Muller, R. and Kontermann, R. E. (2004). Targeting of immunoliposomes to endothelial cells using a single-chain Fv fragment directed against human endoglin (CD105). *Biochimica Et Biophysica Acta-Biomembranes*, 1663(1-2), 158-166.
- Wagner, A., Vorauer-Uhl, K. and Katinger, H. (2002). Liposomes produced in a pilot scale: production, purification and efficiency aspects. *European Journal of Pharmaceutics and Biopharmaceutics*, 54(2), 213-219.

- Walker, J. K. L., Lawson, B. L. and Jennings, D. B. (1997a). Breath timing, volume and drive to breathe in conscious rats: Comparative aspects. *Respiration Physiology*, 107(3), 241-250.
- Walker, S. A., Kennedy, M. T. and Zasadzinski, J. A. (1997b). Encapsulation of bilayer vesicles by self-assembly. *Nature*, 387(6628), 61-64.
- Wang, X., Yin, X. and Cheng, H. (2010). Microflow injection chemiluminescence system with spiral microchannel for the determination of cisplatin in human serum. *Analytica Chimica Acta*, 678(2), 135-139.
- Washington, N., Washington, C. and Wilson, C. G. (2001a). Parenteral drug delivery. In N. Washington, C. Washington & C. G. Wilson (Eds.), *Physiological pharmaceuticals barriers to drug absorption* (2nd ed., pp. 19-35): CRC Press, Florida, USA.
- Washington, N., Washington, C. and Wilson, C. G. (2001b). Pulmonary drug delivery. In N. Washington, C. Washington & C. G. Wilson (Eds.), *Physiological pharmaceuticals barriers to drug absorption* (2nd ed., pp. 221-248): CRC Press, Florida, USA.
- Wasungu, L. and Hoekstra, D. (2006). Cationic lipids, lipoplexes and intracellular delivery of genes. *Journal of Controlled Release*, 116(2), 255-264.
- Watwe, R. M. and Bellare, J. R. (1995). Manufacture of liposomes - a review. *Current Science*, 68(7), 715-724.
- Weinberg, R. A. (2007). The nature of cancer. In R. A. Weinberg (Ed.), *The biology of cancer* (pp. 25-56): Garland Science, Taylor and Francis Group, LLC, NY, USA.
- Weiss, R. B. and Christian, M. C. (1993). New cisplatin analogues in development - a review. *Drugs*, 46(3), 360-377.
- Welch, D. R. (1997). Technical considerations for studying cancer metastasis *in vivo*. *Clinical & Experimental Metastasis*, 15(3), 272-306.
- Wheate, N. J., Walker, S., Craig, G. E. and Oun, R. (2010). The status of platinum anticancer drugs in the clinic and in clinical trials. *Dalton Transactions*, 39(35), 8113-8127.
- White, S. C., Lorigan, P., Margison, G. P., Margison, J. M., Martin, F., Thatcher, N., Anderson, H. and Ranson, M. (2006). Phase II study of SPI-77 (sterically

- stabilised liposomal cisplatin) in advanced non-small-cell lung cancer. *British Journal of Cancer*, 95(7), 822-828.
- WHO (2011). Cancer Fact Sheet No. 297 Retrieved 25-08-2011, from <http://www.who.int/mediacentre/factsheets/fs297/en.index.html>
- Williams, D. M., Carter, K. C. and Baillie, A. J. (1995). Visceral leishmaniasis in the BALB/c mouse: a comparison of the in-vivo activity of 5 non-ionic surfactant vesicle preparations of sodium stibogluconate. *Journal of Drug Targeting*, 3(1), 1-7.
- Wilson, A. P. (1992). Cytotoxicity and bioavailability assays. In R. I. Freshney (Ed.), *Animal cell culture: a practical approach* (2nd ed., pp. 263-303): Oxford University Press, NY, USA.
- Wittgen, B. P. H., Kunst, P. W. A., van der Born, K., van Wijk, A. W., Perkins, W., Pilkiewicz, F. G., *et al.* (2007). Phase I study of aerosolized SLIT cisplatin in the treatment of patients with carcinoma of the lung. *Clinical Cancer Research*, 13(8), 2414-2421.
- Woo, J., Chiu, G. N. C., Karlsson, G., Wasan, E., Ickenstein, L., Edwards, K. and Bally, M. B. (2008). Use of a passive equilibration methodology to encapsulate cisplatin into preformed thermo sensitive liposomes. *International Journal of Pharmaceutics*, 349(1-2), 38-46.
- Xiao, C. J., Qi, X. R., Maitani, Y. and Nagai, T. (2004). Sustained release of cisplatin from multivesicular liposomes: Potentiation of antitumor efficacy against S180 murine carcinoma. *Journal of Pharmaceutical Sciences*, 93(7), 1718-1724.
- Yang, W., Peters, J. I. and Williams, R. O. (2008). Inhaled nanoparticles: A current review. *International Journal of Pharmaceutics*, 356(1-2), 239-247.
- Yu, S., Harding, P. G. R., Smith, N. and Possmayer, F. (1983). Bovine pulmonary surfactant, chemical composition and physical properties. *Lipids*, 18(8), 522-529.
- Yu, S. H. and Possmayer, F. (2003). Lipid compositional analysis of pulmonary surfactant monolayers and monolayer-associated reservoirs. *Journal of Lipid Research*, 44(3), 621-629.

- Zamboni, W. C., Gervais, A. C., Egorin, M. J., Schellens, J. H. M., Zuhowski, E. G., Pluim, D., *et al.* (2004). Systemic and tumour disposition of platinum after administration of cisplatin or STEALTH liposomal-cisplatin formulations (SPI-077 and SPI-077B103) in a preclinical tumour model of melanoma. *Cancer Chemotherapy and Pharmacology*, 53(4), 329-336.
- Zhang, L., Liu, L., Qian, Y. and Chen, Y. (2008). The effects of cryoprotectants on the freeze-drying of ibuprofen-loaded solid lipid microparticles (SLM). *European Journal of Pharmaceutics and Biopharmaceutics*, 69(2), 750-759.
- Zhang, W., vanWinden, E. C. A., Bouwstra, J. A. and Crommelin, D. J. A. (1997). Enhanced permeability of freeze-dried liposomal bilayers upon rehydration. *Cryobiology*, 35(3), 277-289.
- Zhong, H. J., Deng, Y. J., Wang, X. M. and Yang, B. H. (2005). Multivesicular liposome formulation for the sustained delivery of breviscapine. *International Journal of Pharmaceutics*, 301(1-2), 15-24.
- Zhong, Z., Ji, Q. and Zhang, J. A. (2010). Analysis of cationic liposomes by reversed-phase HPLC with evaporative light-scattering detection. *Journal of Pharmaceutical and Biomedical Analysis*, 51(4), 947-951.